Structural and Functional Studies of OmpA from *Salmonella enterica* Typhimurium: A Novel B-cell Immunomodulator and Therapeutic Target

Ph.D. Thesis

By
RAHUL CHAUDHARI

MEHTA FAMILY SCHOOL OF BIOSCIENCES AND BIOMEDICAL ENGINEERING
INDIAN INSTITUTE OF TECHNOLOGY INDORE
AUGUST 2025

Structural and Functional Studies of OmpA from *Salmonella enterica* Typhimurium: A Novel B-cell Immunomodulator and Therapeutic Target

A THESIS

Submitted in partial fulfillment of the
requirements for the award of the degree
of
DOCTOR OF PHILOSOPHY

by

RAHUL CHAUDHARI

MEHTA FAMILY SCHOOL OF BIOSCIENCES AND BIOMEDICAL ENGINEERING
INDIAN INSTITUTE OF TECHNOLOGY INDORE
AUGUST 2025

INDIAN INSTITUTE OF TECHNOLOGY INDORE

I hereby certify that the work which is being presented in the thesis entitled **"Structural and Functional Studies of OmpA from *Salmonella enterica* Typhimurium: A Novel B-cell Immunomodulator and Therapeutic Target"** in the partial fulfillment of the requirements for the award of the degree of **Doctor of Philosophy** and submitted in the **Mehta Family School of Biosciences and Biomedical Engineering, Indian Institute of Technology Indore**, is an authentic record of my own work carried out during the time period from August 2020 to August 2025 under the supervision of **Dr. Prashant Kodgire**, Professor, BSBE, IIT Indore.

The matter presented in this thesis has not been submitted by me for the award of any other degree of this or any other institute.

Rahul 09/01/2026

Signature of the student with date

(RAHUL CHAUDHARI)

This is to certify that the above statement made by the candidate is correct to the best of my knowledge.

P.V. Kodgire 09/01/2026

Signature of Thesis Supervisor with date

(Prof. PRASHANT KODGIRE)

RAHUL CHAUDHARI has successfully given his Ph.D. Oral Examination held on .

P.V. Kodgire 09/01/2026

Signature of Thesis Supervisor with date

(Prof. PRASHANT KODGIRE)

ACKNOWLEDGEMENTS

The journey of a PhD has been many things—demanding, enlightening, often unpredictable, but above all, it has been a shared journey. This thesis is not just the result of my academic efforts; it reflects the constant encouragement, helpful advice, and kind gestures I received throughout the journey. Every part of this work carries the influence of people who helped me grow, not only as a researcher but also as a person.

First and foremost, I would like to express my heartfelt thanks to my thesis supervisor and mentor, Prof. Prashant Kodgire. Your knowledge, patience, and constant support have been the foundation of this research. From our early discussions on how to start experiments, write emails, prepare presentations, and deliver them effectively, to the final steps of this thesis, your guidance has been consistent and thoughtful. You have taught me to think deeply, work independently, and stay true to the core values of good science. Your belief in me gave me the confidence to explore new ideas and grow through every challenge. I am truly grateful for your mentorship; it has shaped not only my work but also the way I view science and approach life.

I would like to express my gratitude to the members of my doctoral PSPC committee: Prof. Amit Kumar and Dr. Abhijeet Joshi. Your invaluable feedback, suggestions, and encouragement over the years have significantly shaped my research. The advice you provided during our meetings always inspired new ideas and helped me enhance my experiments and presentations. Your continuous support motivated me to do my best at every stage of this journey. I also want to thank the Head of the Mehta Family School of Biosciences and Biomedical Engineering and the DPGC Convener for their ongoing reinforcement and motivation throughout my thesis work.

I would like to express my sincere gratitude to the Head of the Mehta Family School of Biosciences and Biomedical Engineering at the Indian Institute of Technology Indore for providing a supportive academic environment, excellent research facilities, and a community that has inspired me throughout my journey. I extend special thanks to Mr. Arif Patel, Mr. Gaurav Singh, and Mr. Amit Mishra for their efficient management of day-to-day activities, as well as their tremendous support

in maintaining the instrument facilities and handling invoice processing. Their assistance allowed me to stay focused on my research. Furthermore, I would like to acknowledge the Director of IIT Indore for his vision in making the institute one of the best research institutions and a beautiful campus in the country. I am also grateful to the Dean of Academic Affairs for serving as the structural and organizational backbone of the research program. Additionally, I would like to express my heartfelt appreciation to IIT Indore for providing world-class research facilities, comfortable hostel accommodations, and sports facilities. I am thankful for the opportunities to attend various conferences, lectures, and events that have enriched my PhD journey. I also thank the institute's library, Sophisticated Instrumentation Center, and IT support services for their resources and assistance.

I would like to express my gratitude to the Council of Scientific and Industrial Research (CSIR) for awarding me the Junior and Senior Research Fellowship (JRF/SRF), which provided crucial financial support for my PhD research. I also thank the Department of Science and Technology (DST), the Department of Biotechnology (DBT), and the Indian Council of Medical Research (ICMR) for their funding contributions that created a productive research environment.

I sincerely thank my lab mates for being an essential part of my PhD journey. I'm especially grateful to Dr. Ankit Jaiswal and Dr. Anubhav Tamrakar for their inspiring support and guidance in molecular biology experiments. I would also like to thank my current lab mates, Surbhi, Brijeshwar, Kritika, Bindu, and Saurav, for creating a supportive and collaborative lab environment. Additionally, I am grateful to Vinay, Kanika, and Sayali for their invaluable support during my early PhD journey. I want to thank Kanika, Sushma, Mallar, and Deveish for their support on my project. Kanika taught me effective writing for my first review paper, and I'm seeing the positive impact of our work on antibiotic resistance in *Salmonella*. Sushma is clever and goal-focused, while Mallar is smart and asks insightful questions that aid my research. Deveish is hardworking and quickly learns new experiments, which inspires me. I'm also grateful to Dr. Saumya Jaiswal, Dr. Rajshree Roy, Dr. Satyam Singh, Dr. Sayan Poddar, Kapil Ursal, Khandu Wadhonkar, Suman Koirala, and Aritra for their

support. We've had a great time together, both in research and during our enjoyable picnics throughout our PhD journeys.

In addition to my research journey, I would like to express my gratitude to my friends who have been my greatest support during my PhD. I am especially thankful for Krishna Singh, Vikas Munia, Ravindar Goyal, Akash Jena, and Loknath Mohapatra. Together, we have shared valuable experiences, cooked together, and created a positive environment during tough times. I am also grateful to Lokesh Yadav, my Navodayan mate. With his encouragement, I pursued playing in the Inter IIT games, and I thoroughly enjoyed participating in water polo, basketball, athletics, and other sports alongside him.

None of this would have been possible without my family's support. I deeply express my love and gratitude to my parents for their unwavering support and belief in me throughout my PhD journey and my life.

RAHUL CHAUDHARI

"I dedicate this thesis to my parents, my greatest source of inspiration and strength, and to my mentor, whose guidance and passion for science have profoundly shaped my research journey."

SYNOPSIS

Abstract

Salmonella enterica serovar Typhimurium is a Gram-negative bacterium that causes gastrointestinal infections and is associated with rising antibiotic resistance worldwide. Increasing antibiotic resistance necessitates the exploration of alternative therapeutic approaches that target the virulence mechanisms of *Salmonella*. Among these, outer membrane proteins (OMPs) and outer membrane vesicles (OMVs) play a crucial role in mediating host-pathogen interaction, immune invasion, and pathogenesis. Notably, OmpA plays a significant role in these processes; however, its structure-function relationship and potential for immunomodulation are still not fully understood.

To investigate the structural analysis of OmpA, we initially conducted a computational analysis that revealed a conserved β-barrel architecture of OmpA within the Enterobacteriaceae family. Furthermore, due to its β-sheet-rich structure, recombinant OmpA tends to form inclusion bodies during overexpression. To mitigate this, we used a high pH buffer for solubilization followed by refolding with LDAO. This approach effectively preserved the protein's native structure, which was confirmed through CD spectroscopy and tryptophan fluorometry. Additionally, immunoinformatic analysis identified multiple conserved B- and T-cell epitopes, further supporting OmpA's potential as a subunit vaccine.

To explore the functional role of OmpA in receptor interactions, both *in silico* docking studies and *in vitro* cell-based assays, including pull-down, co-immunoprecipitation, and co-localization analyses, revealed that OmpA specifically interacts with Toll-like receptor 2 (TLR2) on HEp-2 epithelial cells and Raji human B-cells. Furthermore, stimulation of B-cells with OmpA activated NF-κB signaling, which subsequently increased the expression of pro-inflammatory cytokines, such as TNFα, and led to the upregulation of activation-induced cytidine deaminase (AID).

Furthermore, our key findings demonstrate that OmpA is crucial for inducing AID expression in B-cells, leading to increased class switch recombination (CSR). Interestingly, the increased AID expression was likely due to overexpression of cMYC, an activator for AID expression. Not only was the expression of cMYC elevated, but its occupancy on the *aicda* locus was also raised. Notably, the increased AID expression resulted in CSR events,

particularly switching to IgA.

To enhance antigen presentation and cellular uptake, we engineered recombinant OmpA-OMVs (rOmpA-OMVs). These vesicles retained their native morphology, as confirmed through ATR-FTIR, dynamic light scattering (DLS), and scanning electron microscopy (SEM). Furthermore, treatment of B-cells with rOmpA-OMVs resulted in TLR2 activation, increased expression of AID, and enhanced switching of IgA production, indicating functional CSR.

Collectively, this work reveals a novel immunomodulatory role of OmpA in B-cell biology by linking its interaction with TLR2 to enhanced AID expression and CSR. These findings enhance our understanding of OmpA's structure-function relationship but also suggest the potential application of OmpA and rOmpA-OMVs in the development of targeted vaccines or immunotherapies against drug-resistant *Salmonella* infections.

Introduction

Salmonella enterica serovar Typhimurium (*S.* Typhimurium) is a Gram-negative bacterium known to cause gastrointestinal infection globally, largely due to antibiotic resistance [1]. It is estimated that non-typhoidal *Salmonella* causes around 93.8 million illnesses and 1,55,000 deaths each year worldwide [2]. The improper and excessive use of antibiotics for this infection makes it more challenging to treat and contributes significantly to the emergence of multidrug-resistant (MDR) *Salmonella* strains [3]. Among the various factors contributing to *Salmonella* pathogenesis, outer membrane proteins (OMPs) and outer membrane vesicles (OMVs) play crucial roles in host-pathogen interactions, immune evasion, and bacterial survival.

Background of Work and Objectives

OMPs are involved in various crucial processes such as nutrient transport across the membrane, host-pathogen interactions, and maintaining the structural integrity of the bacterial envelope. Among these, OmpA plays an important role in *Salmonella* pathogenesis due to its high abundance and multifaceted roles in adhesion, biofilm formation, antibiotic resistance, and immune evasion [4]. Despite their significance, complete information regarding immune cell activation upon OmpA stimulation remains limited. Therefore, elucidating the structural characteristics of OmpA and uncovering its functional role in immunomodulation are essential for developing it as a potential

therapeutic target.

In parallel, OMVs are spherical, lipid bilayer nanoparticles ranging from 10 to 300 nm in diameter, secreted by Gram-negative bacteria. They naturally carry adjuvant-specific cargo molecules, like OMPs, lipopolysaccharides (LPS), flagellin, and peptidoglycans, aiding in a delivery system for various functions, including virulence factor delivery, horizontal gene transfer, biofilm formation, and immune evasion [5]. Recent advances suggest that the recombinant OMVs can serve as delivery platforms for engineered antigens, including OMPs such as OmpA. They offer a promising platform for vaccine development due to their natural adjuvant properties and ability to mimic pathogen-associated molecular patterns (PAMPs).

Functionally, OmpA is not only useful for bacterial survival but also actively involved in host-cell interactions, particularly in immunomodulation by interacting with host pattern recognition receptors (PRRs), like Toll-like receptor 2 (TLR2). Interestingly, the OmpA protein from multidrug-resistant *Acinetobacter baumannii* activates both the NF-κB pathway and the NOD-, LRR- and pyrin domain-containing protein 3 (NLRP3) inflammasome, resulting in the release of pro-inflammatory cytokines such as IL-1β, IL-18, and TNFα, thereby promoting inflammation. Additionally, findings from Duan *et al*. indicate that cytokines like TNFα are vital for inflammation and stimulate the expression of activation-induced cytidine deaminase (AID) via NF-κB signaling [6]. AID is a crucial enzyme that belongs to the cytidine deaminase family, responsible for converting cytosine nucleotides into uracil in single-stranded DNA. It plays a pivotal role in inducing somatic hypermutation (SHM) for antibody affinity maturation and class switch recombination (CSR), allowing the switching of antibody isotypes from IgM to IgG, IgA, or IgE in adaptive immunity. These processes are essential for improving antibody affinity and helping the immune system combat a variety of pathogens [7]. Therefore, utilizing OmpA from *S*. Typhimurium alongside natural adjuvants like OMVs is significant for the development of therapeutic vaccine candidates.

This thesis work investigates the structural relationship of OmpA from *S*. Typhimurium, explores its functional role in B-cell immunomodulation, and highlights its potential as a target for novel therapeutics.

The main objectives of this study are as follows:

1. To investigate the structural features of OmpA from *S.* Typhimurium through computational and biophysical analysis, highlighting its refolding dynamics, secondary structure, and immunoinformatic assessment for therapeutic potential.
2. To investigate the interaction of OmpA from *S.* Typhimurium with TLR2 in host cells and its role in modulating immune responses.
3. To investigate the OmpA-induced AID expression and its role in modulating class switch recombination in human B-cells.
4. To engineer and evaluate OMVs carrying OmpA from *S.* Typhimurium for targeted modulation of human B-cell function through AID expression and class switch recombination.

Chapter 1.

Computational and biophysical characterization of OmpA, a major outer membrane protein from *S.* Typhimurium.

In *S.* Typhimurium, OmpA has an N-terminal domain with 8 transmembrane β-barrel motifs in the outer membrane and a C-terminal domain in the periplasm, connected by a 15-amino-acid linker. While the crystal structure of the C-terminal domain is available (PDB ID: 5VES), the N-terminal domain remains unsolved. Addressing this structural gap is important as β-barrel domains are crucial for membrane integration, immune recognition, and therapeutic target development.

Interestingly, computational analysis shows a high conservation of OmpA in the *Enterobacteriaceae* family. On the other hand, due to its β-sheet-rich structure, OmpA forms inclusion bodies during overexpression. To address this, we used a high pH buffer for solubilization and refolding with LDAO, which effectively preserves its native structure. OmpA forms a dimer, confirmed by semi-native SDS-PAGE and size exclusion chromatography. Additionally, secondary structures assessment via ATR-FTIR indicated a mixed α-helices, β-sheet, and coiled structures. In addition, CD spectroscopy confirmed that OmpA is rich in β-sheets. We also evaluated various detergents and lipids for refolding and revealed that LDAO is the most effective candidate, as demonstrated through tryptophan fluorimetry and CD spectroscopy.

Additionally, we conducted the immunoinformatic analysis and identified the B-cell and T-cell epitopes within OmpA's extracellular domain, which highlights its potential

as a vaccine candidate. Notably, immune simulations demonstrate that OmpA enhances both innate and adaptive immune responses, thereby facilitating the generation of memory cells and contributing to the elimination of bacterial infections. Overall, this study provides a foundation for developing novel therapeutics against *S.* Typhimurium pathogenesis **(Fig. 1).**

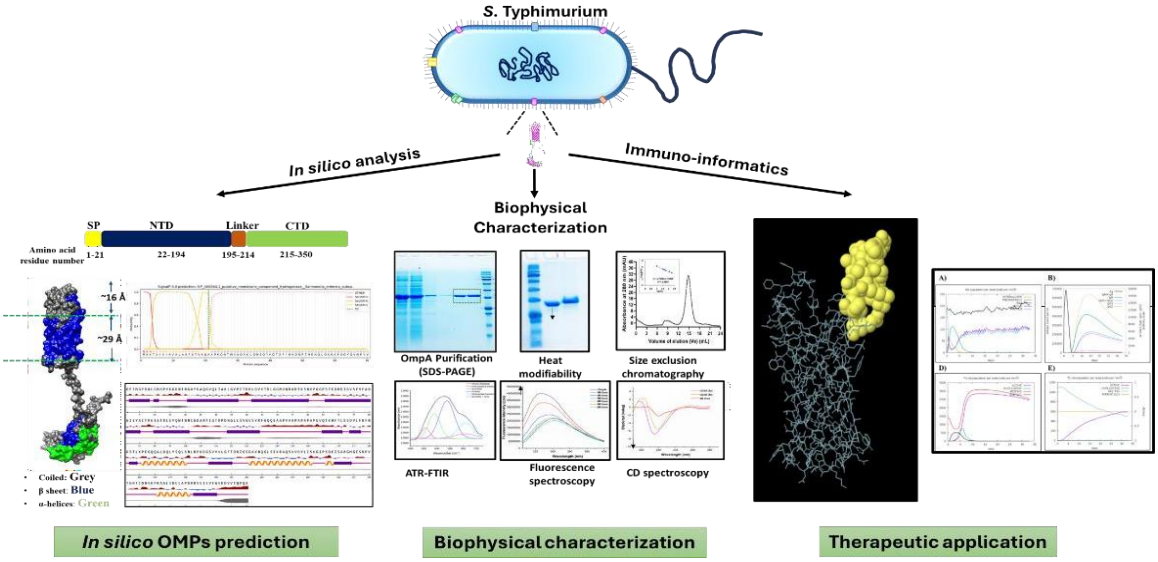

Fig. 1 Schematic representation of the computational and biophysical characterization of OmpA from *S.* Typhimurium, integrating *in silico* prediction of OMP features, structural validation through biophysical methods, and immunoinformatic epitope analysis.

Chapter 2.

Unravelling the role of OmpA from *S.* Typhimurium in host TLR2 interaction and its impact on immune modulation.

To investigate the interaction of OmpA from *S.* Typhimurium with the host cells, we explored its interaction with TLR2, a receptor involved in recognizing bacterial outer membrane components and mediating immune responses [8]. We initially conducted an *in silico* docking analysis focused on the extracellular domain of OmpA and selected TLR2 for this study. The analysis revealed that the extracellular region of OmpA plays a crucial role in interacting with the host cell surface receptor.

Furthermore, we have experimentally validated the interaction between OmpA and TLR2 and investigated how OmpA interacts with host cells using two different cell line models. The HEp-2 cell line, which is derived from human laryngeal carcinoma, serves as a model for studying pathogen-epithelial interactions. Meanwhile, Raji cells, a B-cell line derived from human Burkitt lymphoma, were used to investigate immune modulation. We

validated this interaction using pulldown assays, co-immunoprecipitation, and co-localization studies. Furthermore, our findings revealed that OmpA stimulation enhances TLR2 expression and induces pro-inflammatory cytokine production, like TNFα, through NF-κB activation in Raji human B-cells, contributing to inflammation. Additionally, we observed that OmpA plays a role in inducing AID expression, which is essential for generating antibody diversity in immunoglobulins. Thus, in this study, OmpA serves a dual purpose: it links innate immune activation through TLR2/NF-κB signaling with the adaptive immune response via the upregulation of AID expression **(Fig. 2)**.

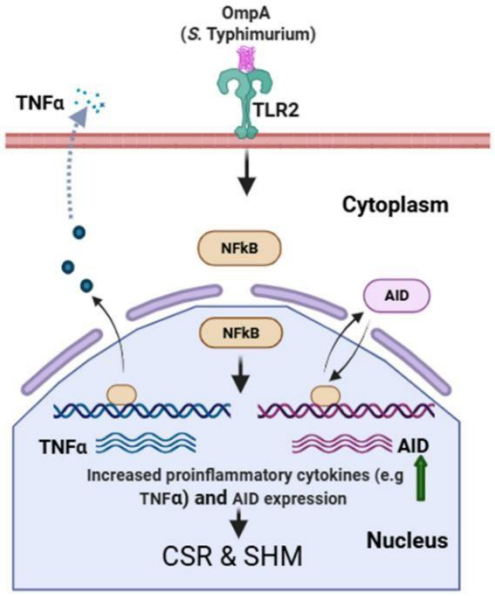

Fig. 2 Schematic illustration showing how OmpA interacts with TLR2 on the B-cell surface, leading to the activation of NF-κB signaling and the induction of pro-inflammatory cytokines like TNFα, as well as the upregulation of AID expression.

Chapter 3.

Unraveling the impact of OmpA, from *S.* Typhimurium, on inducing AID expression and class switch recombination in human B-cells.

In this study, we explored the impact of OmpA on AID expression in B-cells, which are essential for the class switching of immunoglobulins by initiating the process of CSR. We purified and characterized recombinantly cloned OmpA and ensured endotoxin removal. Stimulation of B-cells with endotoxin-free OmpA resulted in altered cell morphology and reduced viability, as confirmed by MTT and Trypan blue exclusion assays. Our findings show that OmpA activates TLR2 and enhances AID expression at both mRNA and protein levels within 24 hours. Several transcription factors, including cMYC, Pax5, SMAD3, and

STAT6, promote AID expression, while cMYB and E2F1 inhibit it [9]. In our study, OmpA enhances the expression of activators such as cMYC, Pax5, and STAT6. Concurrently, OmpA reduces the binding of repressors like E2F1 and cMYB to the AID promoter. This suggests that OmpA transcriptionally regulates AID by enhancing the recruitment of activators and decreasing the binding of repressors. Interestingly, in our study, we found that increased AID expression was likely due to cMYC overexpression, which acts as an activator for AID. Indeed, ChIP assays confirmed elevated cMYC occupancy at the *aicda* locus.

Additionally, we found that increased AID expression is involved in CSR events, specifically in switching to IgA **(Fig. 3)**. In summary, our study suggests that OmpA may modulate B-cell regulation and the adaptive immune system, highlighting its potential as a therapeutic target against *S.* Typhimurium pathogenesis.

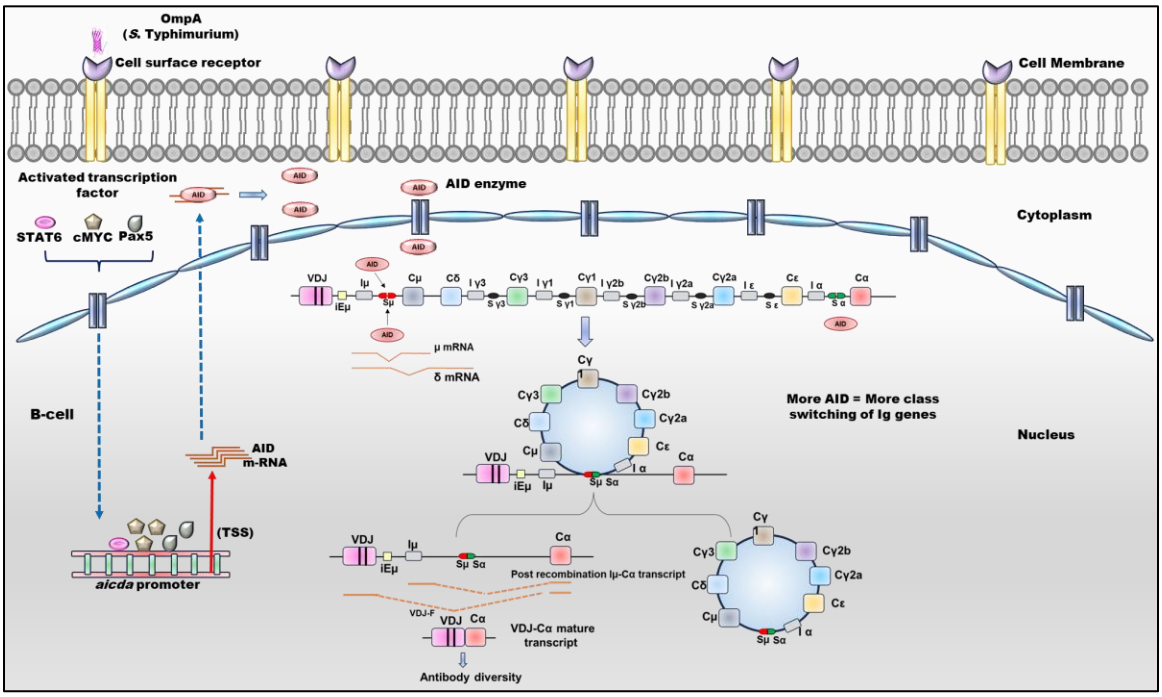

Fig. 3 Schematic representation of stimulation of OmpA in B-cells, resulting in increased AID expression within B-cells participating in SHM and CSR.

Chapter 4.

Engineering OMVs carrying OmpA from *S.* Typhimurium for targeted modulation of human B-cell function through AID expression and CSR.

In this study, we demonstrate that OMVs enriched with recombinant OmpA (rOmpA-OMVs) activate TLR2 and induce NF-κB expression, resulting in the activation of

downstream signaling. Notably, this B-cell activation by OmpA-OMVs significantly upregulated AID expression, a key enzyme in CSR and antibody diversification (Fig. 4). This upregulation is accompanied by transcription activators of AID such as cMYC, PAX5, STAT6, and SMAD3. At the same time, there was a downregulation of the repressor cMYB, as analyzed at the mRNA level. Protein-level confirmation via immunoblotting showed elevated expression of cMYC and PAX5. Moreover, we also observed increased cMYC occupancy at the nuclear level over time through chromatin immunoprecipitation analysis. This indicates that OmpA transcriptionally regulates AID by enhancing the recruitment of activators and reducing the binding of repressors.

Functionally, OmpA-OMVs promoted IgA expression within 24 h, indicating active isotype switching from IgM. This suggests that OmpA-OMVs enhance the immunogenic properties of OmpA and improve vesicular-mediated delivery, boosting immune activation compared to purified OmpA protein. These findings support the potential use of OmpA-OMVs in targeted immunotherapies or vaccines against *Salmonella* infections.

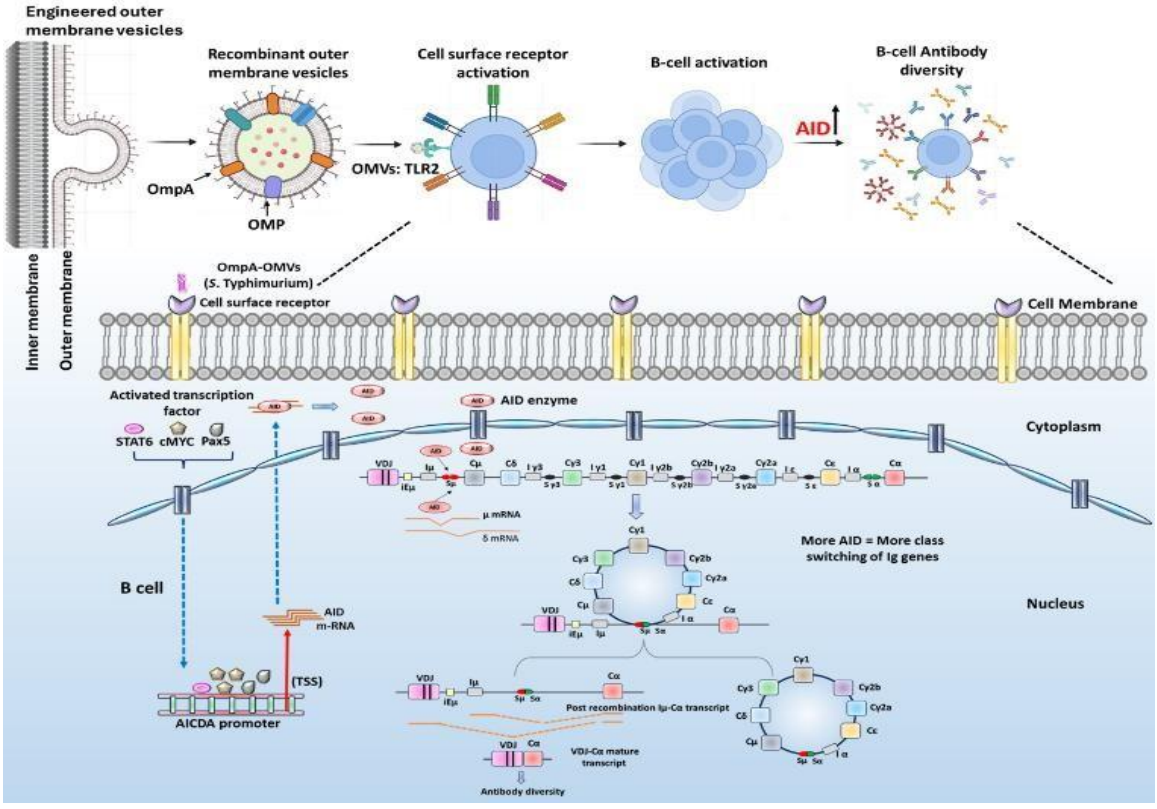

Fig. 4 A graphical illustration represents the activation of B-cells by OmpA-OMVs, leading to increased AID expression in B-cells involved in SHM and CSR.

Scope of the thesis

The thesis is broadly divided into seven chapters. The introduction and review of the literature lead towards the objectives, making Chapter 1. Chapter 2 outlines the experimental methodologies and materials used to achieve these objectives. Subsequently, Chapter 3 represents the results from the analysis of the computational and biophysical characterization of OmpA. Chapter 4 talks about the role of OmpA in interaction with TLR2 and immune modulation. Furthermore, in Chapter 5, we explored the outcomes of OmpA's role in the induced expression of AID and the class switching of immunoglobulin from IgM to IgA in human B-cells. Chapter 6 explores the use of engineered OMVs enriched with recombinant OmpA (rOmpA-OMVs) to target and modulate the human B-cell function by inducing AID expression and promoting CSR. Finally, Chapter 7 concludes the Ph.D. work by providing a summary and outlining the scope for future research **(Fig. 5)**, offering insights into a better understanding of OmpA in *Salmonella* pathogenesis and its potential for therapeutic applications.

In summary, our work represents a better understanding of OmpA's role in *S.* Typhimurium pathogenesis. We explored the refolding dynamics of OmpA and further examined its role in host cell modulation by studying its interaction with the cell surface receptor TLR2. This activates NF-κB signaling and induces B-cell activation. Notably, OmpA was involved in increased AID expression and promoted class switching from IgM to IgA. We also demonstrated that recombinant OmpA-containing OMVs induce AID expression and enhance IgA class switching, suggesting that OmpA-OMVs improve immunogenicity and vesicular delivery compared to purified OmpA. These findings highlight the potential of OmpA-OMVs in immunotherapy or vaccines against *Salmonella* infections.

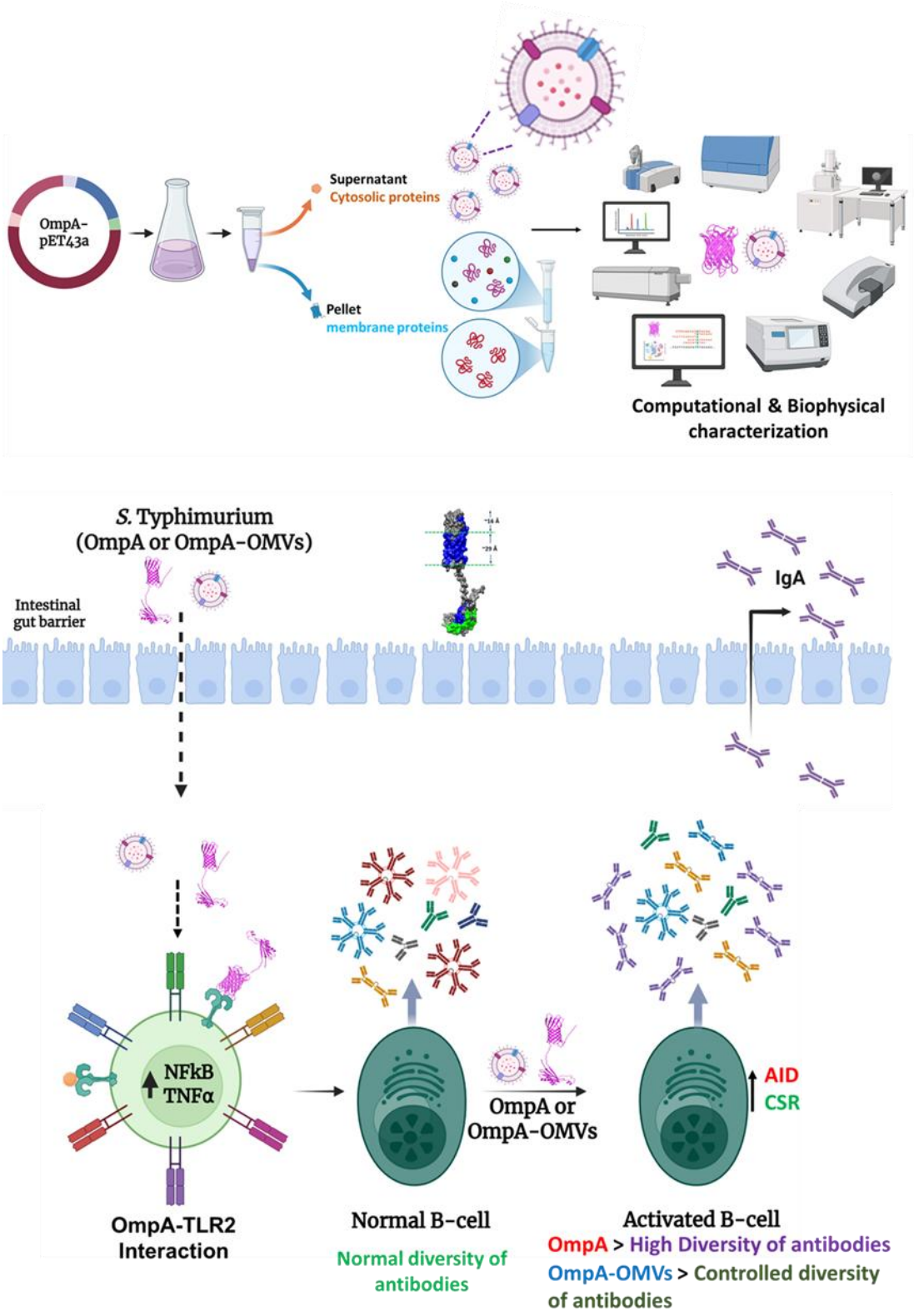

Fig. 5 Schematic overview summarizing the objectives 1, 2, 3, and 4 of the study.

References

[1] D. Kaur, A. Mukhopadhaya, Outer membrane protein OmpV mediates *Salmonella enterica* serovar typhimurium adhesion to intestinal epithelial cells via fibronectin and α1β1 integrin, Cellular Microbiology 22 (2020) e13172. https://doi.org/10.1111/cmi.13172.

[2] S.E. Majowicz, J. Musto, E. Scallan, F.J. Angulo, M. Kirk, S.J. O'Brien, T.F. Jones, A. Fazil, R.M. Hoekstra, International Collaboration on Enteric Disease "Burden of Illness" Studies, The global burden of nontyphoidal *Salmonella* gastroenteritis, Clin Infect Dis 50 (2010) 882–889. https://doi.org/10.1086/650733.

[3] S.M. Jajere, A review of *Salmonella enterica* with particular focus on the pathogenicity and virulence factors, host specificity and antimicrobial resistance including multidrug resistance, Vet World 12 (2019) 504–521. https://doi.org/10.14202/vetworld.2019.504-521.

[4] M.L. Ortiz-Suarez, F. Samsudin, T.J. Piggot, P.J. Bond, S. Khalid, Full-Length OmpA: Structure, Function, and Membrane Interactions Predicted by Molecular Dynamics Simulations, Biophys J 111 (2016) 1692–1702. https://doi.org/10.1016/j.bpj.2016.09.009.

[5] L. Fantappiè, M. de Santis, E. Chiarot, F. Carboni, G. Bensi, O. Jousson, I. Margarit, G. Grandi, Antibody-mediated immunity induced by engineered *Escherichia coli* OMVs carrying heterologous antigens in their lumen, Journal of Extracellular Vesicles 3 (2014) 24015. https://doi.org/10.3402/jev.v3.24015.

[6] Z. Duan, H. Zheng, H. Liu, M. Li, M. Tang, X. Weng, W. Yi, A.M. Bode, Y. Cao, AID expression increased by TNF-α is associated with class switch recombination of Igα gene in cancers, Cell Mol Immunol 13 (2016) 484–491. https://doi.org/10.1038/cmi.2015.26.

[7] M. Choudhary, A. Tamrakar, A.K. Singh, M. Jain, A. Jaiswal, P. Kodgire, AID Biology: A pathological and clinical perspective, International Reviews of Immunology 37 (2018) 37–56. https://doi.org/10.1080/08830185.2017.1369980.

[8] I. Bekeredjian-Ding, G. Jego, Toll-like receptors--sentries in the B-cell response, Immunology 128 (2009) 311–323. https://doi.org/10.1111/j.1365-2567.2009.03173.x.

[9] A. Tamrakar, P. Kodgire, HomA and HomB, outer membrane proteins of *Helicobacter pylori* down-regulate activation-induced cytidine deaminase (AID) and Ig switch germline transcription and thereby affect class switch recombination (CSR) of Ig genes in human B-cells, Molecular Immunology 142 (2022) 37–49. https://doi.org/10.1016/j.molimm.2021.12.014.

LIST OF PUBLICATIONS

[1] **R. Chaudhari**, K. Singh, P. Kodgire, Biochemical and molecular mechanisms of antibiotic resistance in *Salmonella* spp., Research in Microbiology 174 (2023) 103985. https://doi.org/10.1016/j.resmic.2022.103985. **(Impact Factor: 3.4)**

[2] **R. Chaudhari**, M. Dasgupta, P. Kodgire, Unravelling the Impact of Outer Membrane Protein, OmpA, From *S.* Typhimurium on Aberrant AID Expression and IgM to IgA Class Switching in Human B-Cells, Immunology 175 (2025) 359–372. https://doi.org/10.1111/imm.13938. **(Impact Factor: 5)**

[3] **R. Chaudhari**, M. Dasgupta, D. Nigam, P. Kodgire, Engineering outer membrane vesicles (OMVs) carrying OmpA from *S.* Typhimurium for targeted modulation of human B-cell function through AID expression and class switch recombination, Microbial Pathogenesis 207 (2025) 107918. https://doi.org/10.1016/j.micpath.2025.107918. **(Impact Factor: 3.5)**

[4] **R. Chaudhari**, D. Nigam, M. Dasgupta, K. Chandravanshi, K. Malik, P. Kodgire, Unraveling the refolding dynamics, TLR2 interaction, and immunomodulatory role of OmpA from *Salmonella* Typhimurium, Microbial Pathogenesis (2025). **Under Review**

[5] K. Malik, S. Ahirwar, **R. Chaudhari**, P. Kodgire, Biophysical and functional insights into YchP, a putative invasin outer membrane protein of *Salmonella* Typhimurium, and its role in virulence, International Journal of Biological Macromolecules 337 (2026) 149337. https://doi.org/10.1016/j.ijbiomac.2025.149337**. (Impact Factor: 8.5)**

TABLE OF CONTENTS

ACKNOWLEDGEMENTS ..... **I**

SYNOPSIS ..... **VII**

LIST OF PUBLICATIONS ..... **XIX**

TABLE OF CONTENTS ..... **XXI**

LIST OF FIGURES ..... **XXV**

LIST OF TABLES ..... **XXIX**

ABBREVIATIONS ..... **XXXI**

CHAPTER 1 ..... **1**

1. INTRODUCTION AND REVIEW OF LITERATURE **1**

1.1 *Salmonella* **1**

1.2 Molecular Mechanism of *Salmonella* Infection **1**

1.3 Molecular Mechanism of Antibiotic Resistance in *Salmonella* **2**

1.4 Structural and Functional Insights into the OMPs **3**

1.5 The Structural and Functional Insights into the OmpA **7**

1.6 Insights into the Formation Mechanism and Functional role of OMVs **9**
1.6.1 Biogenesis of OMVs 10
1.6.2 Functional role of OMVs 10

1.7 B-cell Immunomodulation and Antibody Diversity Generation **12**
1.7.1 Somatic Hypermutation (SHM) 12
1.7.2 Class Switch Recombination (CSR) 13
1.7.3 Aberrant AID Expression: Implications for Immunodeficiency and Cancer 14

1.8 Background of Work and Objectives **16**

CHAPTER 2 ..... **19**

2. MATERIALS, METHODS, AND INSTRUMENTATION **19**

2.1 Materials **19**

2.1.1 Genomic DNA, Cloning Vectors, and Competent Cells 19
2.1.2 Primers, Enzymes, and Antibodies 19
2.1.3 Chemicals 19
2.1.4 Reagents and Kits 20

2.2 Methods and Instrumentation 20
2.2.1 Bioinformatics Analysis of OmpA 20
2.2.1.1 *In silico* analysis of OmpA to Characterize the Structural Features of OmpA 20
2.2.1.2 Interaction of OmpA Protein with TLR2 21
2.2.1.3 Screening of OmpA Protein as a Vaccine Target and Immune-Simulation 21
2.2.2 PCR Amplification and Cloning of OmpA 22
2.2.3 Expression, Solubilization, and Purification Strategy of OmpA Protein 22
2.2.4 Size Exclusion Chromatography (SEC) 24
2.2.5 Heat Modifiability Assay 24
2.2.6 Trypsin Digestion Assay 24
2.2.7 Attenuated Total Reflection-Fourier Transform Infrared (ATR-FTIR) 25
2.2.8 Secondary Structure Analysis of OmpA by CD Spectroscopy 25
2.2.9 Tryptophan Fluorescence Spectroscopy 26
2.2.10 Expression and Isolation of OMVs 26
2.2.11 OMVs Characterization 27
2.2.12 Cell Culture 27
2.2.13 Endotoxin Removal from Purified OmpA Protein 28
2.2.14 B-Cell Morphology and Viability Following Stimulation with OmpA and OMVs 28
2.2.15 RNA Isolation and cDNA Synthesis 29
2.2.16 Reverse Transcriptase-Quantitative Polymerase Chain Reaction (RT-qPCR) 30
2.2.17 Protein Isolation and Western Immunoblotting 30
2.2.18 Pull-Down Assay 31
2.2.19 Co-Immunoprecipitation (Co-IP) Assay 32
2.2.20 Immunofluorescence Assay 32
2.2.21 Chromatin Immunoprecipitation (ChIP) Assay 33
2.2.22 Quantification of TNF-α secretion by Enzyme-linked immunosorbent assay (ELISA) 34
2.2.23 Statistical Analysis 34

CHAPTER 3 37

3. COMPUTATIONAL AND BIOPHYSICAL CHARACTERIZATION OF OMPA, A MAJOR OUTER MEMBRANE PROTEIN FROM *S.* TYPHIMURIUM 37

3.1 Introduction 37

3.2 Results 39
3.2.1 *In silico* analysis of OmpA protein: Signal peptide, physicochemical properties, and structural features 39
3.2.2 Expression, purification, and identification of OmpA 43
3.2.3 Characterization of OmpA revealed dimer formation 44
3.2.4 OmpA is rich in β-sheet structure 47
3.2.5 Structural assessment of OmpA protein: Effects of pH, temperature, detergent, and lipids on topology studied using fluorescent spectroscopy 53
3.2.6 Immuno-informatics for prediction of multi-epitopes 56
3.2.7 Immune simulation reveals the potential of OmpA as a vaccine candidate. 60

3.3 Summary 62

CHAPTER 4 65

4. UNRAVELLING THE ROLE OF OMPA FROM *S.* TYPHIMURIUM IN HOST TLR2 INTERACTION AND ITS IMPACT ON IMMUNE MODULATION. 65

4.1 Introduction 65

4.2 Results 67
4.2.1 Interaction between OmpA with TLR2 using *In Silico* Analysis 67
4.2.2 Biochemical and Cellular Validation of OmpA–TLR2 Interaction in HEp-2 and Raji Human B-cells 68
4.2.3 OmpA Stimulation Enhances TLR2 Expression and Activates the NF-κB–AID axis in B-cells 71

4.3 Summary 76

CHAPTER 5 79

5. UNRAVELING THE IMPACT OF OUTER MEMBRANE PROTEIN, OMPA, FROM *S.* TYPHIMURIUM ON ABERRANT AID EXPRESSION AND IGM TO IGA CLASS SWITCHING IN HUMAN B-CELLS. 79

5.1 Introduction 79

5.2 Results 81
5.2.1 Cell Morphology, Cell Viability, Proliferation Marker Expression, and Cell Surface Receptor Activation in Response to OmpA-Stimulation 81
5.2.2 OmpA Upregulates AID Expression 82
5.2.3 Involvement of AID Transcription Regulators in Response to OmpA Stimulation 82
5.2.4 OmpA affects the CSR of the immunoglobulin gene 89

5.3 Summary 92

CHAPTER 6 93

6. ENGINEERING OUTER MEMBRANE VESICLES (OMVS) CARRYING OMPA FROM *S.* TYPHIMURIUM FOR TARGETED MODULATION OF HUMAN B-CELL FUNCTION THROUGH AID EXPRESSION AND CLASS SWITCH RECOMBINATION. 93

6.1 Introduction 93

6.2 Results 95
6.2.1 Construction and Characterization of Recombinant OMVs 95
6.2.2 Cell Cytotoxicity and Cell Surface Receptor Activation in Response to OMV Stimulation 97
6.2.3 OmpA-OMVs Mediated Upregulation of AID Expression in B-cells 102
6.2.4 OmpA-OMV Influences the Transcriptional Regulation of AID Expression 102
6.2.5 OmpA-OMV Enhances the CSR of Ig Genes 109

6.3 Summary 112

CHAPTER 7 113

7. CONCLUSION AND SCOPE OF FUTURE PROSPECTS 113

7.1 Introduction 113

7.2 Computational and biophysical characterization of OmpA, a major outer membrane protein from *S.* Typhimurium. 114

7.3 Unravelling the role of OmpA from *S.* Typhimurium in host TLR2 interaction and its impact on immune modulation. 119

7.4 Unraveling the impact of Outer Membrane Protein, OmpA, from *S.* Typhimurium on aberrant AID expression and IgM to IgA class switching in human B-cells. 121

7.5 Engineering Outer Membrane Vesicles (OMVs) carrying OmpA from *S.* Typhimurium for targeted modulation of human B-cell function through AID expression and class switch recombination. 126

7.6 Conclusion 132

7.7 Future directions 133

APPENDIX A 137

pET43a vector map 137

APPENDIX B 139

List of primers used in the study 139

APPENDIX C 141

List of antibodies used in the study 141

REFERENCES 143

LIST OF FIGURES

Figures		Page no
Chapter 1. Introduction and Review of Literature		
Figure 1.1	Molecular mechanisms of antibiotic resistance in *Salmonella* spp.	4
Figure 1.2	Schematic representation of Gram-negative bacterial cell membrane structure.	5
Figure 1.3	Biogenesis pathway of OMP formation in the Gram-negative bacteria.	6
Figure 1.4	Schematic illustration of the OMVs generation from Gram-negative bacteria.	11
Figure 1.5	Molecular mechanism of SHM and CSR.	14
Chapter 2. Materials, Methods, and Instrumentation		
Figure 2.1	Schematic representation of the methodology used in the study.	35
Chapter 3. Computational and Biophysical Characterization of OmpA, a Major Outer Membrane Protein from *S.* Typhimurium.		
Figure 3.1	*In silico* analysis for OmpA.	40
Figure 3.2	Multiple sequence alignment of the OmpA	41
Figure 3.3	The 3D structure of the OmpA protein, excluding the signal peptide sequence.	42
Figure 3.4	The analysis of the structural features of the OmpA pore cavity includes the following aspects.	43
Figure 3.5	Cloning, solubilization, purification, and Western immunoblotting of OmpA	45
Figure 3.6	Standard for SEC and heat modifiability analysis for refolded OmpA.	46
Figure 3.7	Trypsin digestion analysis of OmpA and examining the secondary structure of the OmpA protein through ATR-FTIR, involving curve fitting in the amide-I region (1600–1700 cm^{-1}).	48
Figure 3.8	CD spectra analysis of refolded OmpA using different detergents and lipids.	50
Figure 3.9	CD spectra analysis of OmpA under varying conditions of urea concentration, pH, and temperature.	51

Figures		Page no
Figure 3.10	Tryptophan fluorescence analysis of refolded OmpA using different detergents and lipids.	54
Figure 3.11	Tryptophan fluorescence analysis of OmpA under varying conditions of urea concentration, pH, and temperature.	55
Figure 3.12	Predicted Discontinuous B-cell Epitopes of OmpA Using the ElliPro Server.	59
Figure 3.13	*In silico* immune simulation spectrum using C-ImmSim.	61

Chapter 4. Unravelling the Role of OmpA from *S.* Typhimurium in Host TLR2 Interaction and Its Impact on Immune Modulation.

Figure 4.1	Interaction between OmpA and TLR2 using *In Silico* Analysis.	67
Figure 4.2	Molecular dynamics simulation of OmpA-TLR2 complex by the iMODs server.	69
Figure 4.3	Analysis of the interaction between OmpA and TLR2 in HEp-2 and Raji human B-cells.	70
Figure 4.4	Analysis of the interaction between OmpA and TLR2 in HEp-2 and Raji human B-cells.	72
Figure 4.5	OmpA-induced TLR2-mediated cell activation in HEp-2 and Raji human B-cells.	73
Figure 4.6	TLR2-mediated NF-κB activation induces TNFα and AID expression, which is inhibited by MMG11 in Raji B-cells.	74
Figure 4.7	Effect of OmpA and TLR2 inhibitor on TLR2, NF-κB, and TNF-α expression in Raji human B-cells.	75

Chapter 5. Unraveling the Impact of Outer Membrane Protein, OmpA, from *S.* Typhimurium on Aberrant AID Expression and IgM to IgA Class Switching in Human B-cells.

Figure 5.1	Cell morphology, cell viability, and cell proliferation marker expression in OmpA-stimulated B-cells.	83
Figure 5.2	AID mRNA expression in OmpA-treated B-cells analyzed using RT-qPCR	84
Figure 5.3	AID protein expression in OmpA-treated B-cells was analyzed using Western immunoblotting.	85
Figure 5.4	Analysis of AID transcription activator and repressor expression.	86
Figure 5.5	AID transcription activator expression analysis.	87

Figures		Page

		no
Figure 5.6	Chromatin immunoprecipitation (ChIP) assay showing c-MYC occupancy at the promoter region in B-cells.	88
Figure 5.7	OmpA increases the induction of class switching to IgA.	90
Figure 5.8	Schematic representation of stimulation of OmpA in B-cells, resulting in increased AID expression within B-cells participating in SHM and CSR.	91

Chapter 6. Engineering Outer Membrane Vesicles (OMVs) Carrying OmpA from *S.* Typhimurium for Targeted Modulation of Human B-cell Function through AID Expression and Class Switch Recombination.

Figure 6.1	Analysis of protein content and phosphate levels in lipids extracted from isolated OMVs.	96
Figure 6.2	Characterization of OMVs by SDS-PAGE, Western Blot, and ATR-FTIR spectroscopy	98
Figure 6.3	Morphological characterization of OMVs by DLS, Zeta Potential, and SEM	99
Figure 6.4	Cell morphology and cell cytotoxicity in response to OMVs stimulated Raji human B-cells.	100
Figure 6.5	Cell surface receptor expression in response to OMVs stimulated Raji human B-cells.	101
Figure 6.6	AID expression in stimulated Raji human B-cells.	103
Figure 6.7	Examine the mRNA expression analysis of the AID transcription activator over 0, 4, 8, and 24 h.	104
Figure 6.8	Examine the mRNA expression analysis of the AID transcription repressor over 0, 4, 8, and 24 h.	106
Figure 6.9	Evaluation of cMYC expression as a transcriptional activator for AID using Western blotting, confocal microscopy, and ChIP analysis.	107
Figure 6.10	Evaluation of PAX5 expression as a transcriptional activator for AID using Western blotting and confocal microscopy.	108
Figure 6.11	Evaluation of CSR dynamics in stimulated Raji human B-cells.	110
Figure 6.12	A graphical illustration depicting the activation of OmpA-OMVs in B-cells, leading to abnormal AID expression in B-cells involved in SHM and CSR.	111

Chapter 7. Conclusion and Scope of Future Prospects

Figure 7.1	Schematic overview summarizing the chapters 3, 4, 5, and 6 of the research work.	135

Figures

		Page no
Appendix		
Appendix A	pET43a vector map	137

LIST OF TABLES

Tables		Page no
Chapter 1. Introduction and Review of Literature		
Table 1.1	Functional classification and characteristics of OMPs from Gram-negative bacteria.	8
Chapter 3. Computational and Biophysical Characterization of OmpA, a Major Outer Membrane Protein from *S.* Typhimurium.		
Table 3.1	The physicochemical properties of OmpA were analyzed using the ProtParam tool.	42
Table 3.2	Evaluation of OmpA concentration obtained through different approaches for solubilization, refolding, and purification of the OmpA protein.	46
Table 3.3	Evaluation of OmpA concentration obtained through different approaches for solubilization, refolding, and purification of the OmpA protein.	46
Table 3.4	Secondary structure content analysis of OmpA through ATR-FTIR second derivative spectrum of OmpA based on the selective region (1600-1700 cm^{-1}).	49
Table 3.5	Estimation of the secondary structure content of the OmpA protein in the presence of various lipids and detergents.	52
Table 3.6	Interaction of MHC-I interacting epitopes of OmpA protein through NetCTLpan server with class-I epitope immunogenicity, antigenicity, and toxicity analysis. Epitope residues highlighted are located in exposed loops of OmpA.	56
Table 3.7	Interaction of MHC-II interacting epitopes of OmpA protein predicted through the IEDB server with their interacting HLA alleles, percentile rank, antigenicity, and toxicity analysis. Epitope residues highlighted are located in exposed loops of OmpA.	57
Table 3.8	B-cell epitope prediction using the ABCpred tool with its antigenicity analysis. Epitope residues highlighted in red are located in exposed loops of OmpA.	58
Table 3.9	A list of the predicted discontinuous B-cell epitopes, along with their corresponding amino acid residues.	60
Table 3.10	Summary table of the biochemical and biophysical assays and their inferences.	63

	Tables	Page no
Appendix B	List of primers used in the study	139
Appendix C	List of antibodies used in the study	141

ABBREVIATIONS

Abbreviation	Full Form
AID	Activation-induced cytidine deaminase
ANOVA	Analysis of variance
AP Site	Apurinic/Apyrimidinic site
APE	Apurinic/Apyrimidinic endonuclease
APS	Ammonium persulfate
ATR-FTIR	Attenuated total reflection-Fourier transform infrared
BAM	β-barrel assembly machinery
BCRs	B-cell receptors
BER	Base excision repair
BSA	Bovine serum albumin
CD	Circular dichroism
CDC	Centers for disease control and prevention
cDNA	Complementary DNA
CSR	Class switch recombination
ChIP	Chromatin Immunoprecipitation
Co-IP	Co-Immunoprecipitation
DDM	n-Dodecyl β-D-maltoside
DEPC	Diethyl pyrocarbonate
DHL/THL	Double/triple-hit lymphoma
DLBCLs	Diffuse large B-cell lymphomas
DMPC	Dimyristoylphosphatidylcholine
DMSO	Dimethyl sulphoxide
DOPC	Dioleoyl phosphatidylcholine
DSB	Double-strand break
FBS	Fetal bovine serum
HGT	horizontal gene transfer
iGB	Induced germinal center phenotype B-cells
ILFs	Isolated lymphoid follicles
IPTG	Isopropyl β-D-1-thiogalactopyranoside
LDAO	Lauryl dimethylamine-N-oxide
LPS	Lipopolysaccharides
MDR	Multidrug resistant
MTT	3-(4,5-dimethylthiazol-2-yl)-2,5-diphenyltetrazolium bromide
NF-κB	Nuclear Factor kappa-light-chain-enhancer of activated B-cells
NFW	Nuclease-free water
NHEJ	Non-homologous end joining
NLRP3	NOD-, LRR-, and pyrin domain-containing protein 3

Abbreviation	Full Form
OMPs	Outer membrane proteins
OMVs	Outer membrane vesicles
PAMPs	Pathogen-associated molecular patterns
PBMCs	Peripheral blood mononuclear cells
PBS	Phosphate-buffer saline
PDB	Protein Data Bank
PMN	Polymorphonuclear leukocytes
PMSF	Phenylmethylsulfonylfluoride
PRRs	Pattern recognition receptors
RAG	Recombination-activating gene
RT-qPCR	Reverse transcription-quantitative polymerase chain reaction
SAXS	Small-angle X-ray scattering
SCV	*Salmonella*-containing vacuole
SDS	Sodium dodecyl sulfate
SEC	Size exclusion chromatography
SHM	Somatic hypermutation
SNAP	Spontaneous nanoliposome antigen particles
SPI-1	*Salmonella* pathogenicity island 1
SPI-2	*Salmonella* pathogenicity island 2
T3SS	Type III secretion system
T3SS2	Type III secretion system 2
TEMED	Tetramethyl ethylenediamine
TLR	Toll-like receptor
TNFα	Tumor necrosis factor alpha
UNG	Uracil DNA glycosylase
VLPs	Virus-like particles
XDR	Extensively drug-resistant
β-OG	n-Octyl-β-D-Thio glucopyranoside

Chapter 1

Introduction and Review of Literature

Chapter 1
1. Introduction and Review of Literature

1.1 *Salmonella*

Globally, *Salmonella* is a major foodborne pathogen responsible for gastroenteritis, posing a significant public health concern and contributing to economic burdens in both industrialized and developing countries [1,2]. It is a flagellated, facultative anaerobic Gram-negative bacterium that belongs to the Enterobacteriaceae family. It is divided into two main species: *Salmonella enterica* and *Salmonella bongori*. *Salmonella* species are classified into various serotypes based on surface antigens, including O (somatic), H (flagellar), and Vi (capsular) antigens. There are around 2,600 serovars, with some *S. enterica* serovars causing typhoidal and non-typhoidal complications.

S. enterica is a significant global health concern. Its typhoidal serovars, including *S. enterica* serovar Typhi and serovars Paratyphi A, B, and C, are specifically adapted to humans and are the primary causative agents of enteric fever. The disease spreads primarily due to a lack of clean water, inadequate sanitation, and pathogen transmission through the fecal-oral route. According to the Centers for Disease Control and Prevention (CDC), it is estimated that 11 to 21 million cases of typhoid fever occur worldwide each year, resulting in approximately 1,48,000–1,61,000 deaths [3,4]. On the other hand, nontyphoidal serovars of *S. enterica*, such as Typhimurium and Enteritidis, are prevalent and cause salmonellosis around the world, which can spread through animal-derived food, person-to-person contact, and interaction with animals such as cats, dogs, and rodents [5]. It has been estimated that close to 5,35,000 nontyphoidal infections occurred in 2017, causing approximately 77,500 deaths [6]. Salmonellosis is usually mild, but it can become life-threatening. Typically, the *Salmonella* serotype determines the magnitude of the disease. Improper or excessive use of antibiotics in treating this infection contributes to treatment challenges and promotes the development of antibiotic resistance [7].

1.2 Molecular Mechanism of *Salmonella* Infection

The journey of *Salmonella* infections can occur from consuming contaminated foods or water, as they can also survive in the acidic environment of the stomach. They use their flagella and chemotactic systems to navigate to the intestine, where they attach to

the cells of the intestinal epithelium [8]. Interaction with the intestinal epithelium activates the type III secretion system (T3SS) located in *Salmonella* pathogenicity island 1 (SPI-1). This system introduces various bacterial effector proteins that modulate various host cellular functions. When these effector proteins, specifically SopE, SopE2, and SopB, activate host Rho-family GTPases, especially RAC1, which results in rearrangement of the actin cytoskeleton and promotes micropinocytosis. These processes facilitate the uptake of bacteria into host cells and the formation of a *Salmonella*-containing vacuole (SCV). In addition, the intracellular environment allows *Salmonella* to activate a different type III secretion system 2 (T3SS2) found in its *Salmonella* pathogenicity island 2 (SPI-2). This system aids the pathogen in evading innate immune defense mechanisms and reproducing within the cells. Infected cells produce proinflammatory cytokines like IL-8, TNF, and IL-1β, triggering the recruitment of macrophages and neutrophils. This inflammatory response alters the intestinal lumen environment in the presence of immune cells and increases the level of antimicrobial peptides, which deplete resident microbiota. Furthermore, the resultant inflamed tissue provides nutrients and electron acceptors that support the growth of *Salmonella*. As a result of this inflammatory response, there is an infiltration of polymorphonuclear leukocytes (PMNs) into the intestinal lumen, leading to diarrhea [9,10]. Together, these coordinated events help *Salmonella* to cause infection, persist in the host, and enhance its transmission.

1.3 Molecular Mechanism of Antibiotic Resistance in *Salmonella*

Antibiotics are low-molecular-weight compounds that can inhibit or kill bacteria. Their synthesis is a boon to society in this invisible war against infectious bacterial diseases. However, widespread use of antibiotics led to the emergence of antibiotic resistance [11,12]. Bacteria, including *Salmonella* spp., evolve various mechanisms to overcome the effects of antibiotic exposure. This poses a significant threat to global health, as it increases the likelihood of drug ineffectiveness and leads to treatment failure [13]. In the case of *Salmonella* spp., the growing resistance to fluoroquinolones has led to the use of third-generation antibiotics, such as cephalosporins (cefixime and ceftriaxone) and azithromycin, in extensively drug-resistant (XDR) *Salmonella enterica* serovar Typhi [14,15].

Antibiotics mainly synthesize to target cellular processes, which include DNA replication, mRNA synthesis, protein synthesis, and cell wall synthesis [2]. Antibiotic resistance in bacteria develops mainly through intrinsic and acquired mechanisms. Intrinsic resistance is the innate ability of bacteria to survive within a specific antibiotic exposure due to inherent structural and functional characteristics, such as efflux pumps, enzymes that inactivate the antibiotics, modification in the antibiotic target site of the antibiotic, and decreased membrane permeability, all of which contribute to the bacteria's survival [16]. On the other hand, acquired resistance involves the uptake of an antibiotic resistance gene from different organisms via horizontal gene transfer (HGT). This transfer, in which antibiotic resistance genes are carried and transmitted *via* plasmids, integrins, transposons, and prophages. By acquiring this gene, bacteria can develop an antibiotic-resistant phenotype. HGT is accomplished *via* three main mechanisms: transformation, conjugation, and transduction [2]. **Fig. 1.1** shows the molecular mechanisms of antibiotic resistance in *Salmonella* spp.

Among the intrinsic resistance mechanisms, outer membrane proteins (OMPs) play a crucial role by regulating the permeability of the bacterial outer membrane. Some OMPs function as porins, enabling the passive passage of small hydrophilic molecules, including antibiotics. As a result, any changes in the expression or structure of these porins, like OmpA, OmpF, OmpC, and OmpW, may lead to decreased antibiotic absorption and contribute to antibiotic resistance and survival in adverse conditions [17,18].

1.4 Structural and Functional Insights into the OMPs

A key element of *S.* Typhimurium's ability to cause disease is its capacity to manipulate the host's immune responses. This allows the pathogen to establish an infection while evading immune clearance. This immune modulation is facilitated by a range of virulence factors, including type III secretion systems, lipopolysaccharides (LPS), fimbriae, flagella, OMPs, and outer membrane vesicles (OMVs). Among these, OMPs are particularly important as they contribute to structural integrity, nutrient acquisition, antibiotic resistance, and direct interactions with host cells [2,19,20]. Gram-negative bacteria have a distinctive cell envelope structure that comprises an inner membrane, a peptidoglycan layer, and an outer membrane **(Fig. 1.2)**.

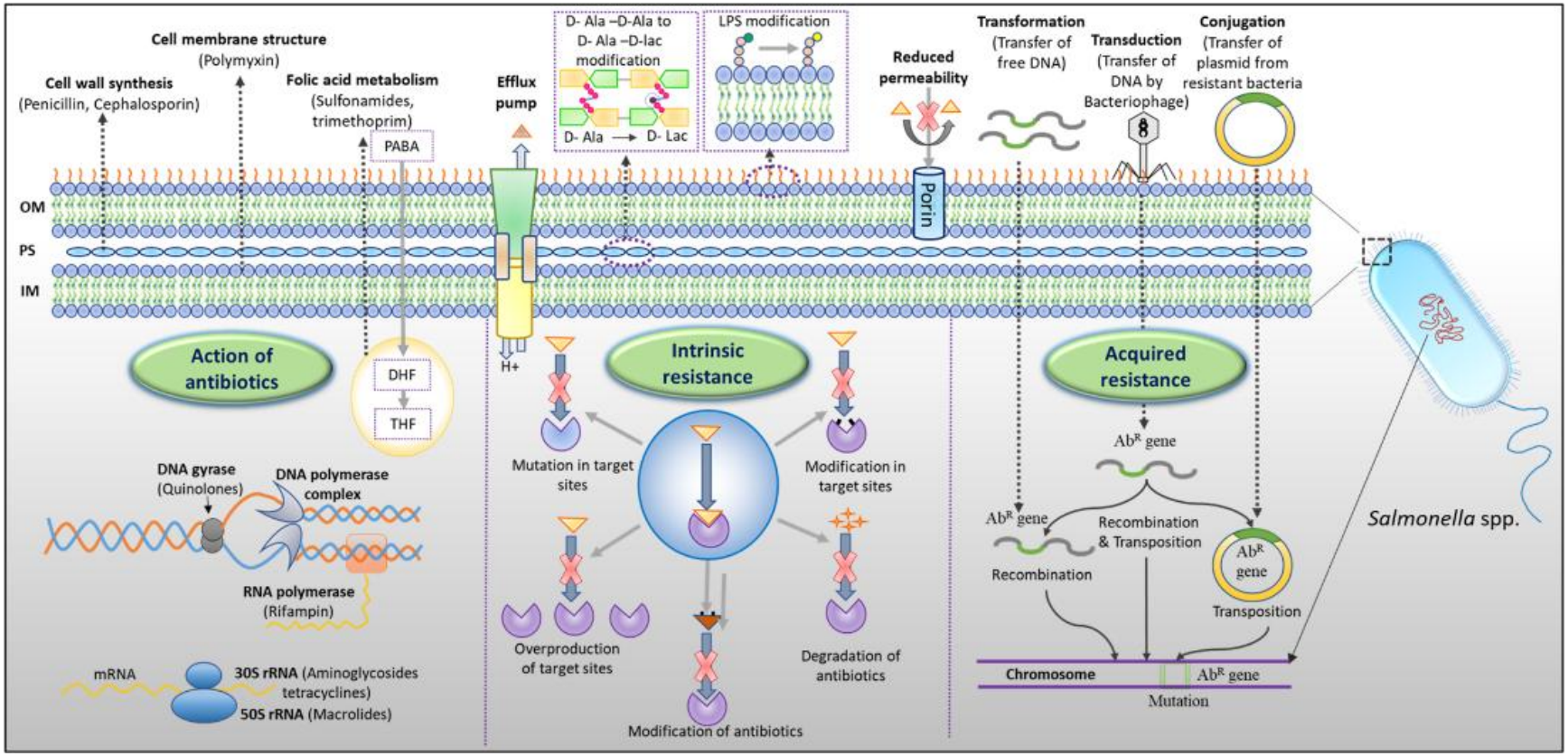

Fig. 1.1 Molecular mechanisms of antibiotic resistance in *Salmonella* spp., (i) the mode of action of antibiotics in *Salmonella* spp., (ii) the intrinsic mechanism of antibiotic resistance, and (iii) the acquired mechanism of antibiotic resistance.

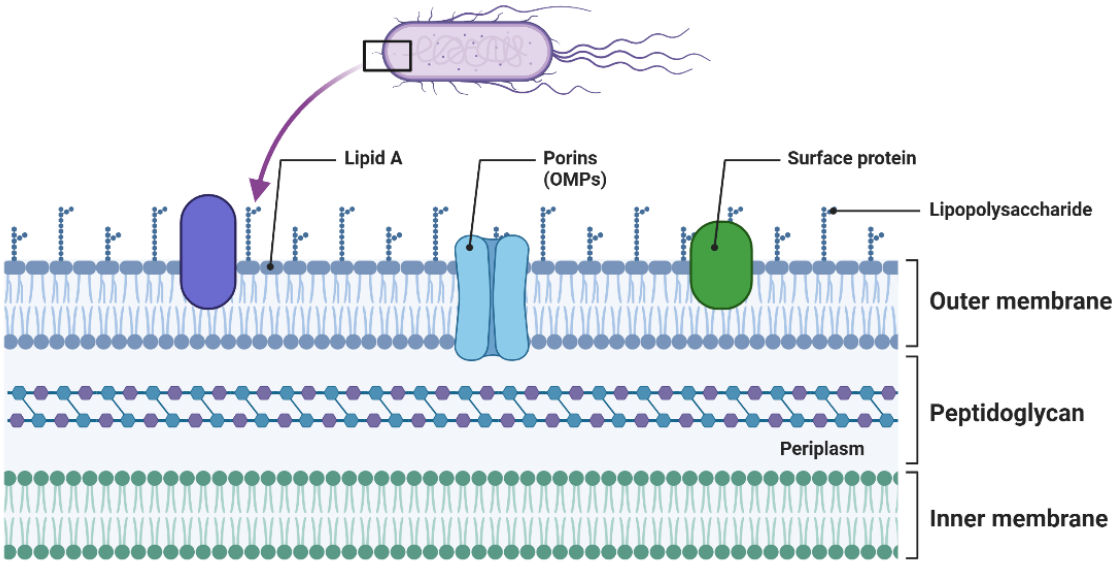

Fig. 1.2 Schematic representation of Gram-negative bacterial cell membrane structure. This figure was generated using Biorender.com.

The biogenesis of OMPs involves their journey from the cytoplasm to the outer membrane. Nascent OMPs are synthesized in the cytoplasm and are directed by chaperones such as SecA/SecB or the ribosome from the inner membrane to the periplasmic space via the Sec translocase. Once inside the periplasmic space, nascent OMPs with signal peptides are transported to the β-barrel assembly machinery (BAM complex) with the help of periplasmic chaperones like SurA or Skp. Any misfolded OMPs are degraded by proteases such as DegP to prevent aggregation. Ultimately, OMPs are inserted and properly folded into the outer membrane by the BAM complex, forming their functional β-barrel structures that are essential for membrane integrity, transport, and virulence functions **(Fig. 1.3)** [21].

The outer membrane contains OMPs, which are a class of β-barrel proteins crucial for maintaining membrane integrity and mediating the transport of diverse molecules. Based on their transport functions, OMPs are classified into specific and non-specific porins. Specific porins selectively permit the passage of particular substrates, for example, LamB, a sugar-specific channel, facilitates the transport of maltose [22]. In contrast, non-specific porins allow for the passive diffusion of small, hydrophilic molecules with low molecular weights [23]. Importantly, OMPs are characterized by unique antiparallel beta sheets, consisting of 8 to 26 beta strands that span the lipid bilayer, forming a pore or channel through which molecules can pass.

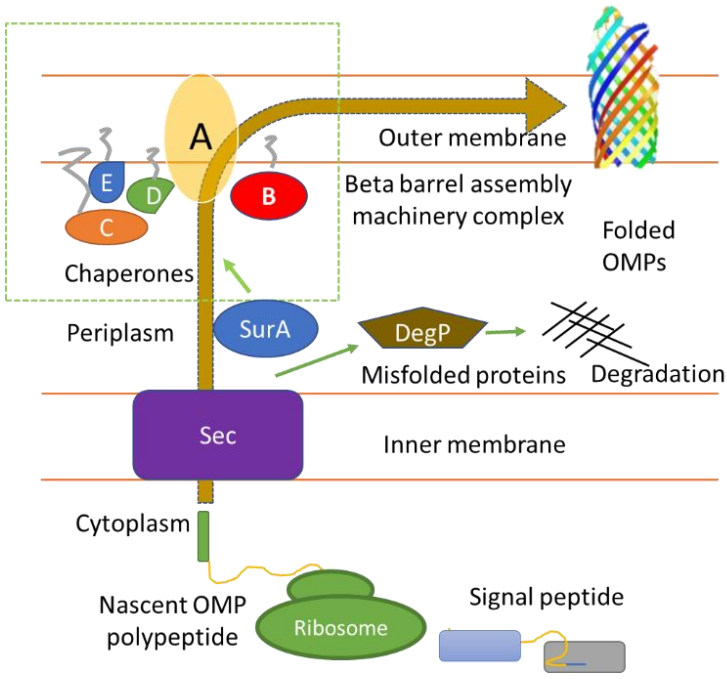

Fig. 1.3 Biogenesis pathway of OMP formation in the Gram-negative bacteria.

In the Gram-negative bacteria, approximately 2-3% of the genes encode for the OMPs [24]. Although the beta-barrel architecture of OMPs is conserved, many of these proteins also contain a domain that is localized in the periplasm, extracellular space, or within the barrel that includes a plug required for their function **(Fig. 1.4)**. The OMPs play diverse roles, including facilitating adhesion, nutrient transport, maintaining membrane integrity, enabling selective permeability to hydrophilic molecules, mediating protein secretion, and aiding in the efflux of toxic substances [25]. **Table 1.1** provides an overview of the roles and features of different OMPs.

Due to the structural diversity of OMPs, they perform a wide range of functions.

- **Porins:** OMPs such as OmpF and OmpC form trimeric complexes that create aqueous channels for the passive diffusion of small hydrophilic molecules (typically less than 600 Da). These channels serve as entry points for essential nutrients and metabolites [26,27].
- **Transporters:** Similarly, some OMPs function as transporters, such as FhuA and LamB, which have large plug domains within their barrels that facilitate the transport of iron-siderophore complexes or vitamin B12 through energy-coupled transport mechanisms [28].

- **Membrane integrity and Biogenesis:** OMPs play crucial roles in maintaining membrane integrity by anchoring to the peptidoglycan layer and supporting the asymmetric structure of the lipid bilayer, such as LptD [29,30]. Additionally, some OMPs, like BamA, are involved in the assembly and biogenesis of the outer membrane. BamA is a core component of the β-barrel assembly machinery (BAM complex), responsible for the proper folding and insertion of most OMPs into the outer membrane [21,30].
- **Antibiotic resistance:** It is also important to note that some OMPs participate in multidrug efflux systems, utilizing efflux pumps to expel antibiotics from the cells, thereby contributing to antibiotic resistance. For instance, TolC is involved in this process [31]. Additionally, some OMPs, such as OmpA, OmpF, OmpW, and OmpC, exhibit reduced expression, which limits the entry of antibiotics by acting as a barrier. Furthermore, some OMPs have evolved mechanisms to resist antibiotic action [32].
- **Adhesion and invasion:** Certain OMPs have extended extracellular loops that project above the outer membrane; examples include OmpA, OmpT, OmpV, and OmpW. These features assist in engaging with host receptors during infection, facilitating adhesion or invasion [1,2,33,34].

The most common members of OMPs include the OmpF, OmpC, OmpA, OmpD, PhoE, LamB, FhuA, and OmpW [18,35,36]. Among these OMPs, OmpA is particularly important due to its multifaceted role in structural integrity, immune modulation, and bacterial pathogenesis.

1.5 The Structural and Functional Insights into the OmpA

OmpA is the most abundant protein, with typically 1,00,000 copies per cell, and is highly conserved across multiple species of Gram-negative bacteria. It plays a multifaceted role in bacterial structural integrity and pathogenicity [20,37]. In *S.* Typhimurium, the N-terminal domain of OmpA contains 8 transmembrane β-barrel motifs residing within the outer membrane, while the C-terminal domain resides within the periplasm region. A 15-amino-acid residue linker region that connects the β-barrel protein to the soluble C-terminal domain [37]. Interestingly, the oligomeric state of OmpA is primarily dimeric. Marcoux et al. validated the static model of OmpA from *E. coli* using mass spectrometry data, confirming that OmpA predominantly forms dimers [38].

Table 1.1 Functional classification and characteristics of OMPs from Gram-negative bacteria.

Sr. No	OMPs	β-strands	Mol. weight (~kDa)	Category	Topology	Function	Applications	Ref
1	OmpW	8	19	Porins	Monomeric	Transport of small hydrophobic molecules is involved in antibiotic resistance	Potential efflux inhibitor target and vaccine candidate	[17, 39]
2	OmpX	8	19	Adhesin	Monomeric	Resistance to oxidative stress, Immunodominant, and immune evasion	Virulence factor studies.	[40, 41]
3	OmpA	8	38	Porin/Adhesin/ Invasin	Dimeric	Structural support, adhesion to host cells, protection from nitrosative stress, and immune modulation	Vaccine target, host-pathogen interaction studies	[42, 43]
4	PagC	8	20	invasin	Monomeric	Complement-resistant factor	Virulence factor research, serum antibody interactions, and diagnostics	[44, 45]
5	Rck	8	20	Invasin	Monomeric	Complement-resistant factor, resistant to serum, and zipper-like internalization	Vaccine and anti-virulence therapeutic target	[45, 46]
6	OmpV	10	33	Porin	Monomeric	Involved in adhesion and invasion	Model for bacterial pathogenic study, and vaccine candidate	[1]
7	OmpC	16	38	Porins	Trimeric	Non-specific porin for small hydrophilic solutes	Antibiotic resistance studies, diagnostic studies, and vaccine candidates	[47]
8	OmpF	16	38	Porins	Trimeric	General diffusion channel for small molecules	Antibiotic permeability and vaccine candidates	[26, 48]
9	OmpD	16	37	Porins	Trimeric	Major porin in *Salmonella* (homologous to OmpC/F)	Major role in permeability, vaccine candidate	[48]
10	LamB	18	48	Porins/ Receptor (phage λ)	Trimeric	Maltose and maltodextrin transport	Carbohydrate transport research	[49]
11	FepA	22	79	Transporters (TonB-dependent)	Monomeric	Enterobactin siderophore transporter	Iron acquisition studies	[50]
12	FhuA	22	78	Transporters (TonB-dependent)	Monomeric	Ferrichrome siderophore receptor	Siderophore-mediated iron uptake	[51, 52]
13	BtuB	22	66	Transporters (TonB-dependent)/ Phage receptors	Monomeric	Vitamin B12 (cobalamin) transporter	Cobalamin uptake studies, TonB-dependent transport research	[53, 54]

Furthermore, additional supporting evidence for the model was validated by low-resolution small-angle X-ray scattering (SAXS) studies, which indicated that OmpA from *E. coli* exists in an equilibrium between monomeric and dimeric states [55].

The functional aspect of OmpA in *Salmonella* and other Gram-negative bacteria is multifaceted, as it plays a crucial role in adhesion, biofilm formation, outer membrane permeability, and antibiotic resistance [20,37,56]. Given its multifaceted role, OmpA has emerged as a promising candidate for new drug and vaccine strategies in recent years. Notably, Nie et al. suggested that AbOmpA from *Acinetobacter baumannii* is a promising therapeutic target against drug-resistant *A. baumannii* infections due to its high degree of conservation, associated with virulence, and lacks homology to the human genome [57]. OmpA is recognized as a novel pathogen-associated molecular pattern (PAMP) due to its significant role in bacterial viability and pathogenicity, and it initiates adaptive immunity [58]. Similarly, OmpA from *Klebsiella pneumoniae* activates macrophages and dendritic cells along with binds to wide range of immune effector cells [42,59].

Importantly, a study by Ansari et al. revealed that mice administered a recombinant vector vaccine containing OmpA can effectively trigger both humoral and cellular immune responses [60]. Similarly, OmpA from *S.* Typhimurium also activates the dendritic cells and enhances Th1 polarization, which are crucial for developing effective vaccines and immunotherapy adjuvants for *S.* Typhimurium [42]. Notably, OmpA is a strong immunogen that can activate the adaptive immune response, particularly through B-cell modulation [20]. Interestingly, OMVs carrying OmpA are also gaining a potential role in enhancing the immunogenic characteristics of OmpA and suggest improvements in vesicle delivery [61,62].

1.6 Insights into the Formation Mechanism and Functional role of OMVs

OMVs from Gram-negative bacteria were first described in *E. coli* in 1965 [63]. OMVs are spherical nanoparticles composed of lipid bilayers, usually measuring between 10 and 300 nm in diameter. Gram-negative bacteria secrete these vesicles through various processes, such as outer membrane budding, peptidoglycan remodeling, and responses to bacterial stress [64–66]. OMVs inherently carry cargo molecules that are specific to

adjuvants, such as OMPs (OmpA, OmpC, and OmpF), LPS, flagellin, and peptidoglycan. Pathogenic bacteria utilize OMVs as tools to secrete and deliver various substances for multiple purposes. Functionally, OMVs facilitate several processes in bacteria, such as the transfer of virulence factors, horizontal gene transfer, biofilm formation, toxin delivery, and evasion of the immune response [19,67].

1.6.1 Biogenesis of OMVs

In Gram-negative bacteria, there are two membranes: the outer membrane and the inner membrane. Between these membranes lies a network of peptidoglycan and periplasmic space. The outer membrane contains LPS and is cross-linked by lipoproteins. The outer membrane also contains membrane proteins such as OmpA, OmpC, and OmpF. Both the inner and outer membranes are composed of phospholipids. In response to stress caused by misfolded proteins that accumulate between the outer phospholipid bilayer and the peptidoglycan layer, bacterial OMVs are formed **(Fig. 1.4)**. This process occurs through two mechanisms. The first mechanism involves a living extracellular membrane, the outer membrane bulges and eventually pinches off to secrete spherical OMVs. The second mechanism occurs during cell death, where the loss of membrane integrity leads to vesicle secretion as a result of explosive cell lysis [68,69].

1.6.2 Functional role of OMVs

OMVs serve as natural carriers for virulence factors and effectively deliver signaling molecules that can diffuse freely in complex environments and be taken up by host cells. *S.* Typhimurium utilizes a T3SS to introduce virulence factors into host cells. In addition to the traditional T3SS, *S.* Typhimurium employs OMVs to transfer virulence factors into the cytoplasm of host macrophages directly [70]. A study conducted by Yoon et al. revealed that *Salmonella* virulence factor translocated via OMVs, enriched with LPS and OMPs, function as alternative secretion vehicles, thereby highlighting a novel mechanism of bacterial pathogenesis [71]. Similarly, Balsalobre et al. reveal the alternative secretion pathway for alpha-haemolysin from *E. coli* via OMVs, complementing direct T1SS secretion. OMVs may act as delivery vehicles, protecting and transporting the toxin to host cells during infection [72].

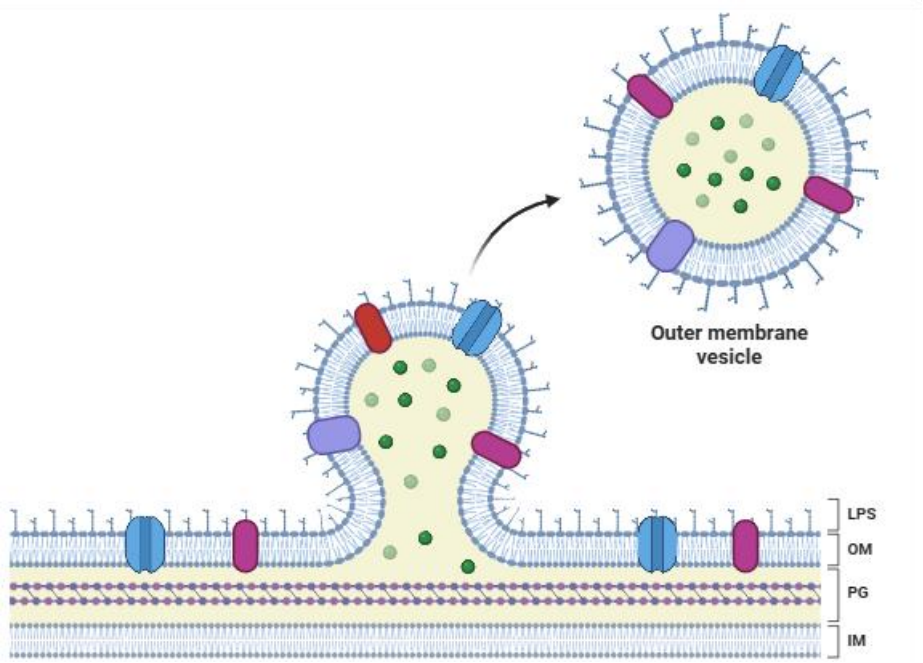

Fig. 1.4 Schematic illustration of the OMVs generation from Gram-negative bacteria. This figure was generated using Biorender.com.

Notably, adjuvants can enhance the immunogenicity of antigens. OMVs act as a natural adjuvant by acting as PAMPs that stimulate immunity via pathogen Pattern recognition receptors (PRRs) [73]. A report by Aghasadeghi showed that using OMVs in combination with HIV-1 virus-like particles (VLPs) and *Neisseria meningitidis* OMVs can induce strong humoral and cellular immune responses. This approach presents a promising strategy for the development of an HIV-1 vaccine, especially compared to traditional adjuvants [74]. Other receptors besides TLRs can also detect PAMPs carried by OMVs. For instance, when OMV-associated LPS enters immune cells through endocytosis, it is recognized by caspase-11 in the cytoplasm, which triggers cell death and the release of IL-1 during bacterial infections [75].

OMVs are increasingly being utilized in vaccine development. Avila-Calderón et al. reported that *Brucella melitensis* produces OMVs containing multiple immunogenic proteins, including SOD, GroES, Omp31, Omp25, Omp19, bp26, and Omp16. Their findings demonstrate that these OMVs elicit strong Th1 immune responses and offer protection compared to live vaccines Rev1, highlighting their potential as safe subunit vaccine candidates [76]. Weyant et al. developed the Avidin-based vaccine antigen crosslinking system, known as AvidVax. This universal platform

utilizes biotin-binding SNAP (Spontaneous nanoliposome antigen particles) proteins on OMVs to effectively attach a variety of biotinylated antigens. In studies with mice, SNAP-OMV vaccines elicited robust antigen-specific antibody responses, emphasizing their potential for rapid and customizable vaccine development [77]. Moreover, OMVs play a role in immune modulation. Chaudhari et al. found that OmpA-OMVs are involved in B-cell immunomodulation, leading to an increase in activation-induced cytidine deaminase (AID) expression and promoting class switch recombination (CSR) from IgM to IgA. Their study suggests that OmpA-OMVs could be a promising strategy for therapeutic use in immunodeficient candidates [61]. In summary, OMVs serve as a promising natural nanocarrier for the delivery of antigens and immune-stimulating agents, making them an effective platform for developing vaccines and therapies against *Salmonella* infection.

1.7 B-cell Immunomodulation and Antibody Diversity Generation

B-cells develop from hematopoietic stem cells in the liver during fetal life and in the bone marrow during adult life. During B-cell development in the bone marrow, each B-cell expresses a unique B-cell receptor (BCR), which results from the rearrangement of variable (V), diversity (D), and joining (J) gene segments mediated by recombination-activating gene (RAG) [78]. When B-cells encounter an antigen, they recognize it through BCRs, which results in B-cell proliferation and differentiation. Upon B-cell activation, it transforms into plasma cells that secrete antibodies or memory cells that offer long-lasting defense against secondary infections [79]. In addition to that, activated B-cells undergo somatic hypermutation (SHM) and CSR to further diversify antibodies when stimulated by antigens, which are crucial processes for generating high-affinity antibody production and further diversifying antibodies [80]. A key mediator of this crucial process is the essential enzyme known as AID, important for the SHM and CSR process [80].

1.7.1 Somatic Hypermutation (SHM)

SHM is a cellular mechanism which confined to point mutations in the variable regions of the light and heavy chains of immunoglobulin genes. This process primarily takes place in the dark zone of the germinal centers within secondary lymphoid organs during an immune response. SHM occurs in the dark zone and then transitions to the light zone

of the germinal center, where clonal selection of high-affinity antibodies and CSR take place [81,82].

This SHM process is mediated by the genome mutator enzyme known as an AID, which induces the point mutation through deamination of cytosine (C) to uracil (U) in the single-stranded DNA of the transcribed V region. The conversion of C: U creates a mismatch that is repaired through an error-prone repair pathway. If not corrected before replication, the U: G mismatch may pair with adenine, resulting in a C: G to T: A transition mutation. Additionally, if uracil DNA glycosylase (UNG) recognizes the U: G mismatch, it removes the uracil, creating an abasic (AP) site. This AP site is subsequently fixed through the involvement of error-prone DNA polymerase during the repair synthesis, which can cause point mutations. Additionally, if the U: G mismatch is addressed by either the base excision repair (BER) mechanism or the mismatch repair system, it may lead to deletion, insertion, or substitution mutations. In summary, the AID-mediated mutations in the V region of immunoglobulin genes are repaired unfaithfully, resulting in SHM **(Fig. 1.5)** [80,82,83].

1.7.2 Class Switch Recombination (CSR)

CSR is an AID-mediated process that occurs in the constant region of the IgH chain in activated B-cells. It is crucial for switching from IgM to other isotypes like IgG, IgA, or IgE without altering antigen specificity. CSR occurs in the light zone of the germinal center [81,82].

In the CSR process, AID induces deamination of cytosine in both the donor and acceptor switch regions. This results in the formation of a U: G mismatch specifically within the immunoglobulin heavy chain locus, particularly in the switch region. The switch region consists of repetitive G-rich DNA sequences located upstream of each constant region gene, except for IgD, which is rich in cytosine residues. This mismatch is processed by UNG (Uracil-N-glycosylase), which removes the uracil (U) residue, resulting in apurinic (AP) sites. These AP sites are then nicked by apurinic/apyrimidinic endonuclease (APE), creating single-strand nicks. If the opposing strand's nick is sufficiently close, this can lead to the formation of a double-strand break (DSB).

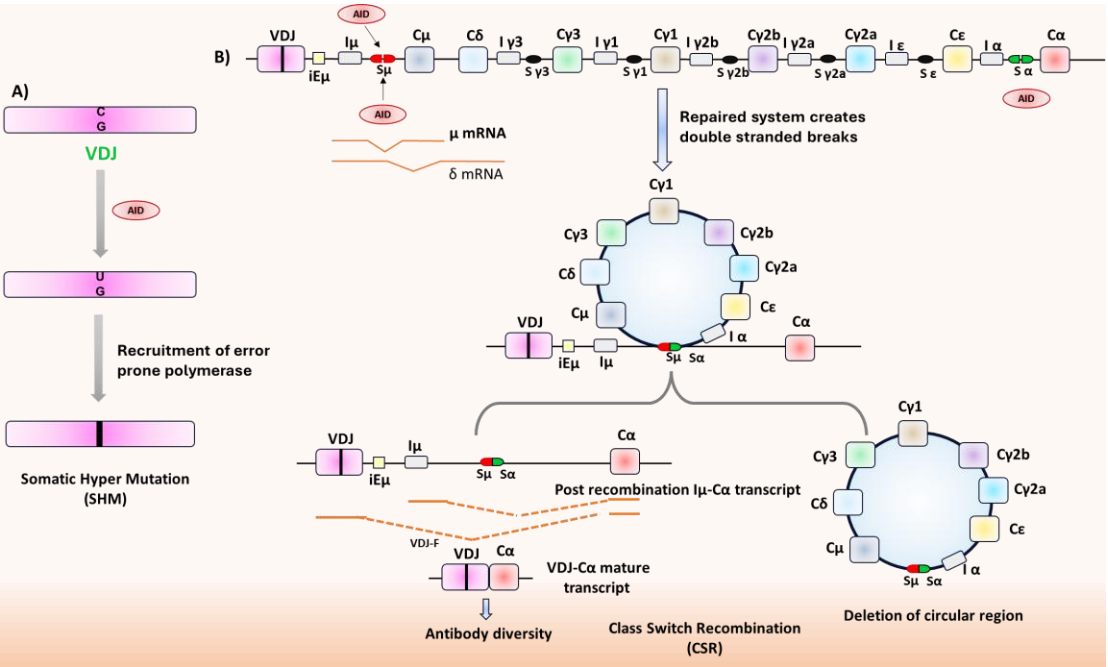

Fig. 1.5 Molecular mechanism of SHM and CSR: A) SHM, AID deaminates cytosine into uracil in the variable region of immunoglobulin genes. This creates a U: G mismatch, which is then repaired by an error-prone DNA polymerase that incorrectly repairs the uracil mismatch, leading to point mutations. **B)** CSR, the constant region of the immunoglobulin heavy (IgH) genes, is flanked by a switch region that is also deaminated by AID. The repair pathway involved creates double-stranded breaks, resulting in the deletion of the intervening sequence and enabling isotype switching from IgM to other isotypes such as IgA, IgG, and IgE.

The resulting DSB in both the donor and acceptor switch regions is repaired through the Non-Homologous End Joining (NHEJ) pathway, leading to the deletion of the intervening DNA sequence as a circular episome. This process ultimately results in the isotype switching of antibodies **(Fig. 1.5).** SHM and CSR are essential for adaptive immunity but must be tightly regulated to prevent genomic instability and off-target mutations [82,84,85].

1.7.3 Aberrant AID Expression: Implications for Immunodeficiency and Cancer

AID is a crucial enzyme involved in affinity maturation, a process that generates antibody diversity and drives the clonal selection necessary for the proliferation of B-cells producing high-affinity antibodies. However, despite its beneficial role in affinity maturation, AID also exhibits off-target activity that can lead to impaired affinity maturation, genomic instability, and further contribute to cancer progression

[79,80,86]. In B-cells, a deficiency in AID expression results in hyper-IgM syndrome. For instance, in humans, mutations affecting AID expression result in hyper-IgM syndrome type 2, a severe immunodeficiency characterized by elevated IgM levels, decreased SHM, and impaired CSR [87]. Similarly, a study by Tamrakar and Kodgire observed that OMPs from *Helicobacter pylori*, where the proteins HomA and HomB modulate B-cell responses, leading to reduced AID expression. This can potentially skew antibody production towards decreased isotype switching [79]. Furthermore, a study by Fagarasan et al. demonstrated that AID deficiency results in the hyperplasia of isolated lymphoid follicles (ILFs) and a significant expansion of anaerobic bacteria in the small intestine. This suggests that SHM of ILF B-cells plays a crucial role in regulating the intestinal microflora [88].

Importantly, induced AID expression may also contribute to the high frequency of malignancies [89,90]. A study by Kim et al. indicates that aberrant AID expression is induced through the NF-κB pathway, resulting in TP53 mutations in gastric cells, which contributes to *H. pylori*-associated gastric carcinogenesis [91]. Moreover, aberrant AID expression has been identified in various tumors originating from germinal centers, including Burkitt lymphomas, diffuse large B-cell lymphomas (DLBCLs), and follicular lymphomas [80]. Additionally, research by Miyaoka et al. found that AICDA and AID can serve as predictors of adverse clinical outcomes in double/triple-hit lymphoma (DHL/THL). Moreover, abnormal AID activity has been demonstrated to target multiple proto-oncogenes, including PIM1, MYC, RHOH/TTF, and PAX5, in over 50% of the DLBCL cases [89]. Notably, a study by Shinmura et al. suggests that aberrant AID expression increases mutation frequency, particularly in the p53 gene, contributing to lung cancer [92]. This highlights that dysregulation of AID expression results in impaired affinity maturation and genomic instability, which may further contribute to the development of cancer.

Notably, OMPs from Gram-negative bacteria act as immunomodulators, which may play a role in the modulation of AID expression, potentially leading to dysregulation of SHM and CSR. Therefore, understanding how OmpA and OmpA-OMVs influence AID expression is important for advancing immune defense strategies and addressing oncogenesis. By understanding the mechanisms by which OmpA and

its vesicular form regulate AID, we can better harness their therapeutic potential while minimizing associated oncogenic risks.

1.8 Background of Work and Objectives

OMPs are involved in various crucial processes such as nutrient transport across the membrane, host-pathogen interactions, antibiotic resistance, and maintaining the structural integrity of the bacterial envelope. Among these proteins, OmpA is particularly important in the pathogenesis of *Salmonella*. It is abundant, evolutionarily conserved among Gram-negative bacteria, and plays a multifaceted role in adhesion, biofilm formation, antibiotic resistance, and evasion of the immune system [37]. Despite their significance, complete information regarding immune cell activation and immune modulation upon OmpA stimulation remains limited. Therefore, elucidating the structural characteristics of OmpA and uncovering its functional role in immunomodulation are essential for developing it as a potential therapeutic target.

In parallel, OMVs are spherical, lipid bilayer nanoparticles ranging from 10 to 300 nm in diameter, secreted by Gram-negative bacteria. They naturally carry adjuvant-specific cargo molecules, like OMPs, LPS, flagellin, and peptidoglycans, aiding in a delivery system for various functions, including virulence factor delivery, horizontal gene transfer, biofilm formation, and immune evasion [67]. Recent advances suggest that the recombinant OMVs can serve as delivery platforms for engineered antigens, including OMPs such as OmpA. They offer a promising platform for vaccine development due to their natural adjuvant properties and ability to mimic PAMPs.

Functionally, OmpA is not only useful for bacterial survival but also actively involved in host-cell interactions, particularly in immunomodulation by interacting with host PRRs like TLR2. Interestingly, the OmpA from MDR *A. baumannii* activates the NF-κB and the NOD-, LRR-, and pyrin domain-containing protein 3 (NLRP3) inflammasome, leading to the release of pro-inflammatory cytokines such as IL-1β, IL-18, and TNFα, thus promoting inflammation. Additionally, findings from Duan et al. indicate that cytokines like TNFα are vital for inflammation and stimulate the expression of AID via NF-κB signaling [93]. AID is a crucial enzyme that belongs to the cytidine deaminase family, responsible for converting cytosine nucleotides into uracil in single-stranded DNA. It is predominantly expressed in the germinal centers of

activated B-cells and plays a pivotal role in inducing SHM and CSR. These processes are essential for improving antibody affinity and helping the immune system to combat a variety of pathogens [80]. Therefore, utilizing OmpA from *S*. Typhimurium alongside natural adjuvants like OMVs is significant for the development of therapeutic vaccine candidates.

This thesis work investigates the structural relationship of OmpA from *S*. Typhimurium, explores its functional role in B-cell immunomodulation, and highlights potential targets for novel therapeutics.

The main objectives of this study are as follows:

1) To investigate the structural features of OmpA from *S*. Typhimurium through computational and biophysical analysis, highlighting its refolding dynamics, secondary structure, and immunoinformatic assessment for therapeutic potential.

2) To investigate OmpA from *S*. Typhimurium interaction with TLR2 in host cells and its role in immune response modulation.

3) To explore the role of OmpA in inducing aberrant AID expression and modulating class switch recombination in human B-cells.

4) To engineer and evaluate OMVs carrying OmpA from *S.* Typhimurium for targeted modulation of human B-cell function through AID expression and class switch recombination.

Chapter 2

Materials, Methods, and Instrumentation

Chapter 2
2. Materials, Methods, and Instrumentation

2.1 Materials

2.1.1 Genomic DNA, Cloning Vectors, and Competent Cells

S. Typhimurium 14028s genomic DNA served as a template to amplify the *ompA* gene. The bacterial cloning and expression vector utilized in this study is pET43a (Novagen) **(Appendix A)**. For cloning, we used *E. coli* DH5α competent cells, while *E. coli* BL21(DE3) was employed for protein expression.

2.1.2 Primers, Enzymes, and Antibodies

All primers used in this study were obtained from Sigma Aldrich Pvt. Ltd. **(see Appendix B)**. All restriction enzymes utilized in this research were purchased from New England Biolabs (NEB) and Thermo Fisher. All antibodies used in this study were procured from Thermo Fisher (Invitrogen) and Santa Cruz **(Appendix C)**.

2.1.3 Chemicals

The following is a list of chemicals utilized in this research work: Tris base, Sodium hydroxide (NaOH), Hydrochloric acid (HCl), Ampicillin, Agarose, Luria-Bertani agar (LB- agar), Luria-Bertani broth (LB- broth), Ethylene diamine tetra acetic acid (EDTA), Sodium chloride (NaCl), Ethidium bromide (EtBr), Agarose, Calcium chloride ($CaCl_2$), Potassium dihydrogen phosphate (KH_2PO_4), Potassium hydrogen phosphate (K_2HPO_4), Sodium hydrogen phosphate (Na_2HPO_4), Sodium dihydrogen phosphate (NaH_2PO_4), Sodium carbonate (Na_2CO_3), Silver nitrate ($AgNO_3$), Methanol, Sodium dodecyl sulphate or Sodium lauryl sulphate (SDS), β- mercaptoethanol, Acrylamide, N, N′-Methylene bis-acrylamide (MBAA), Triethylenetetramine or Tetramethyl ethylene diamine (TEMED), Ammonium per sulphate (APS), Bovine serum albumin (BSA), Paraformaldehyde (PFA), Formaldehyde, Glycine, Imidazole, Isopropyl ß-D-1-thiogalactopyranoside (IPTG), Glycerol, Phenol, Chloroform, Methanol, N-lauroyl sarcosine, phenylmethylsulfonylfluoride (PMSF), Nonidet P-40, Triton X-100, Dimyristoyl phosphatidylcholine (DMPC), Dioleoyl phosphatidylcholine (DOPC), Lauryl dimethylamine oxide (LDAO), n-Dodecyl-beta-D-maltoside (DDM), n-Octyl-β-D-thioglucopyranoside (β-OG), Tween-20, Sodium

cacodylate, skimmed milk powder (SM powder), Bromophenol blue, Xylene cyanol, Fetal bovine serum (FBS), Dimethyl sulphoxide (DMSO), MMG-11, Protease inhibitor cocktail, 3-(4,5-dimethylthiazol-2-yl)-2,5-diphenyltetrazolium bromide (MTT), RNase A, DNases A. All the chemicals mentioned above are of molecular biology grade and procured from various suppliers, including Sigma Aldrich Chemical Pvt. Ltd., MP Biomedicals USA, Invitrogen Pvt. Ltd., HiMedia Pvt. Ltd., Otto Chemie Pvt. Ltd., and Sisco Research Labs Pvt. Ltd.

2.1.4 Reagents and Kits

Plasmid isolation kit, Gel/PCR purification kit procured from Favorgen Biotech Corporation, Taiwan, 1 kb DNA ladder (GeneDireX), KAPA *Taq* PCR kit (Merck), *Pfu* DNA polymerase (HiMedia), dNTP mix (HiMedia), T4 DNA ligase, *Nde*I (NEB), *Xho*I (NEB), 1kb DNA ladder, unstained protein marker (Bio-Rad), prestained protein marker (Genetix), Malachite green phosphate assay kit (Sigma-Aldrich), High capacity endotoxin removal resin, Chromogenic endotoxin quantification kit, DEPC-treated water, TRIzol reagents for RNA isolation, Verso cDNA Synthesis Kit, and PowerUp SYBR Green Master Mix were procured from Thermo Scientific. Protein A/G Plus-Agarose beads (sc2003, Santa Cruz Biotechnology).

2.2 Methods and Instrumentation

2.2.1 Bioinformatics Analysis of OmpA

2.2.1.1 *In silico* analysis of OmpA to Characterize the Structural Features of OmpA

The OmpA protein sequence was downloaded from the NCBI database (https://www.ncbi.nlm.nih.gov/), and multiple sequence alignment from different species was performed using Clustal Omega (https://www.ebi.ac.uk/jdispatcher/msa/clustalo) and analyzed using the ESPript 3.0 program (https://espript.ibcp.fr/ESPript/ESPript/) [94]. SignalP-6.0 (https://services.healthtech.dtu.dk/service.php?SignalP-6.0) was used to identify the presence of signal peptides based on the amino acid sequence of OmpA [95]. The predictions of the secondary structure of OmpA were carried out using NetSurfP-3.0, accessible at (https://services.healthtech.dtu.dk/services/NetSurfP-3.0/) [96]. Tertiary

structure prediction was performed using AlphaFold 2.0 [97,98] (https://deepmind.com/research/open-source/alphafold). Prediction of the OmpA protein pore was performed by PoreWalker, a tool that can identify and characterize membrane porin channels using their 3D structure, accessible at (https://www.ebi.ac.uk/thornton-srv/software/PoreWalker/) [99]. The physicochemical properties of the OmpA protein were analyzed using the ProtParam tool available at https://web.expasy.org/protparam/ [100].

2.2.1.2 Interaction of OmpA Protein with TLR2

To study the interaction analysis of the OmpA protein with the TLR2 receptor, the PDB ID for TLR2 (2Z81) was retrieved from the RCSB protein data bank. Interaction analysis was performed using the HADDOCK 2.4 server (https://wenmr.science.uu.nl/haddock2.4/) [101], and the top five complexes were refined, and their binding energy was determined using the PRODIGY server (https://wenmr.science.uu.nl/prodigy/run/3VUa1DEC) [102,103]. Normalized mode analysis (NMA) is a technique used to describe the flexible states that a protein can adopt around its equilibrium position. In our study, the OmpA-TLR2 complex was uploaded in PDB file format to the iMODS server (https://imods.iqf.csic.es/). The iMODS server utilizes NMA in internal (dihedral) coordinates to predict the collective movements of macromolecules, including proteins [104,105].

2.2.1.3 Screening of OmpA Protein as a Vaccine Target and Immune-Simulation

To identify the antigenic and immunogenic properties of OmpA for potential vaccine candidates, we employed an immuno-informatics approach for the design of a multi-epitope-based vaccine [106]. We have retrieved the amino acid sequence of OmpA (*S.* Typhimurium) from the NCBI web server. MHC class-I epitopes were identified using the NetCTL pan server (https://services.healthtech.dtu.dk/services/NetCTL-1.2/) [107], while MHC class-II epitopes were analyzed using the IEDB server (http://tools.iedb.org/tepitool/) [108]. B-cell epitopes were predicted using the Bepipred linear epitope prediction 2.0 (https://services.healthtech.dtu.dk/services/BepiPred-2.0/) [109]. The screened epitopes were further analyzed for class-I immunogenicity using the IEDB server (http://tools.iedb.org/immunogenicity/) [110]. The antigenicity property of OmpA was

assessed using the VaxiJen 2.0 server (https://www.ddg-pharmfac.net/vaxijen/VaxiJen/VaxiJen.html) [111], and toxicity analysis was performed using (https://webs.iiitd.edu.in/raghava/toxinpred/multi_submit.php) [112]. Moreover, the role of the OmpA protein in both humoral and cellular immune responses was examined using the C-ImmSim online server (https://kraken.iac.rm.cnr.it/C-IMMSIM/index.php) [113]. This comprehensive analysis was used to develop an effective multi-epitope-based vaccine against *S.* Typhimurium.

2.2.2 PCR Amplification and Cloning of OmpA

S. Typhimurium 14028s genomic DNA served as a template to amplify the *ompA* gene. The amplification of the *ompA* gene was carried out using *Pfu* DNA Polymerase with the forward primer and reverse primer **(Appendix B)**. The thermal cycling conditions for gene amplification were: initial denaturation at 95°C for 5 min, 30 cycles of denaturation at 92°C for 30 s, annealing at 60°C for 30 s, extension at 72°C for 90 s, followed by a final extension cycle at 72°C for 10 min. Subsequently, the amplified OmpA product was cloned into the pET43a plasmid at *Nde*I and *Xho*I restriction sites and ligated using T4 DNA ligase. The recombinant plasmid vector was transformed into *E. coli* DH5α competent cells. The presence of inserted DNA in the recombinant clone was confirmed through colony PCR, restriction digestion analysis, and DNA sequencing.

2.2.3 Expression, Solubilization, and Purification Strategy of OmpA Protein

The recombinant plasmid was first isolated and then transformed into *E. coli* BL21(DE3) competent cells and subsequently cultured in LB medium supplemented with 100 µg/mL ampicillin. Recombinant protein expression was induced by adding 0.5 mM IPTG at an optical density at 600 nm of 0.6, followed by further incubation for 4 h at 37°C. Cells were harvested by centrifugation at 5000 rpm for 15 min, and the resulting pellet was washed and resuspended in an ice-cold Tris-buffer containing 20 mM Tris-Cl at pH 8.0, 200 mM NaCl, and 1 mM PMSF at pH 8.0. The resuspended sample was sonicated at 65% amplitude, with 2 s on and 2 s off for 30 min. The resulting cell lysate was centrifuged at 10,000 rpm for 30 min at 4°C to

obtain the inclusion body. This inclusion body was washed with membrane washing buffer containing 20 mM Tris-Cl at pH 8.0, 200 mM NaCl, 1% Triton X-100, and 2M urea. The inclusion body was washed twice with membrane washing buffer without Triton X-100. Finally, the inclusion body was solubilized using the solubilizing buffer.

The solubilization of the cell pellet was performed using different solubilizing agents: 1% sodium dodecyl sulfate (SDS), 6M guanidinium hydrochloride (GnHCl), 6 M urea, 8 M urea, and high-pH Tris-buffer at pH 12.5. Denatured protein was purified using nickel-IMAC resin and refolded using a rapid dilution method with refolding buffer.

1) Denatured OmpA protein (6M urea in Tris-Buffer at pH 8.0) was purified using nickel-charged iminodiacetic acid-based chromatography (IMAC) resin (Bio-Rad) with the C-terminal 6X His-tag incorporated by pET-43a. A volume of 2 mL of nickel-IMAC resin was used per 10 mL of 6 M urea-dissolved denatured protein. The resin was equilibrated by adding 10 mL of equilibration buffer-I (10 mM Imidazole and 6M urea in Tris-buffer at pH 8.0). Resin washing was performed by sequentially adding 30 mL of 30 mM, 40 mM, and 60 mM imidazole in Tris-buffer containing 6 M urea, respectively. Bound OmpA was eluted using 300 mM imidazole in Tris-buffer containing 6 M urea. Purified OmpA protein was then refolded using the rapid dilution method with a 10X volume of refolding buffer (10% glycerol, 0.5% LDAO, and 0.01% Triton X-100 in Tris-buffer at pH 8.0) [1].

2) Denatured OmpA protein (6M urea in Tris-Buffer) was refolded first using refolding buffer and subsequently subjected to purification using nickel-IMAC resin. The resin was equilibrated by adding 10 mL of equilibration buffer-II (10 mM Imidazole in Tris-Buffer at pH 8.0). Resin washing was performed by sequentially adding 30 mL of 30 mM, 40 mM, and 60 mM imidazole in Tris-buffer at pH 8.0, respectively. Bound OmpA was eluted using 300 mM imidazole in Tris-buffer at pH 8.0.

3) The **s**olubilized OmpA protein in high pH Tris-buffer (200 mM NaCl, 2M urea, and 100 mM Tris-Cl at pH 12.5) was refolded using the rapid dilution method with a 10X volume of refolding buffer. The refolded protein was then subjected to purification using nickel-IMAC resin. The resin was equilibrated by adding 10 mL of

equilibration buffer-II (10 mM Imidazole in Tris-buffer at pH 8.0). Subsequently, resin washing was performed by sequentially adding 30 mL of Tris-buffer containing 30 mM, 40 mM, and 60 mM imidazole in Tris-buffer at pH 8.0, respectively. Elution of bound OmpA was achieved using 300 mM imidazole in Tris-buffer at pH 8.0 [1].

Finally, purified OmpA was then subjected to overnight dialysis against dialysis buffer (20 mM Tris-Cl at pH 8.0, 200 mM NaCl, 10% glycerol, 0.5% LDAO, 5 mM EDTA, and 20 mM Imidazole). The protein was concentrated following dialysis using a 10-kDa cutoff concentrator (Amicon ultra centrifugal filter). Subsequently, the protein purity was evaluated by SDS-PAGE analysis, while the protein concentration was determined using the Bradford assay.

2.2.4 Size Exclusion Chromatography (SEC)

The oligomeric state of the protein was determined via SEC with a Superdex 200 Increase 10/300 GL column from GE Healthcare. The column was equilibrated with a refolding buffer. Subsequently, the purified OmpA protein was loaded onto the column and eluted at a flow rate of 0.5 mL/min. The calibration of size exclusion chromatography was executed using standard proteins with known molecular weights, including 12 kDa Cytochrome C, 29 kDa Carbonic anhydrase, 66 kDa (albumin), 150 kDa (alcohol dehydrogenase), and 200 kDa (β-amylase) [114], while the void volume of the column was determined using blue dextran (2000 kDa).

2.2.5 Heat Modifiability Assay

The recombinant OmpA protein was dissolved in an SDS sample buffer containing 120 mM Tris-Cl at pH 6.8, 20% glycerol, 1% SDS, and 0.02% bromophenol blue. Subsequently, one portion of the sample was boiled at 95°C, while another portion of the sample was kept at room temperature. These samples were subsequently subjected to semi-native PAGE, with electrophoresis performed at 150 volts under cold conditions [114,115].

2.2.6 Trypsin Digestion Assay

Purified OmpA protein (1 mg/mL) was treated with trypsin at different protein-to-trypsin ratios at 1:50, 1:100, 1:200, 1:500, and 1:1000 for 1 h at 37°C. The trypsin digestion reactions were stopped by adding 5 mM PMSF, and then the samples were

analyzed using SDS-PAGE and semi-native PAGE [114].

2.2.7 Attenuated Total Reflection-Fourier Transform Infrared (ATR-FTIR)

The ATR-FTIR spectroscopy is a useful technique for determining the relative amounts of different secondary structures in proteins. The ATR-FTIR spectra for the OmpA protein (20 mM Tris-Cl at pH 8.0 and 200 mM NaCl) were recorded on a Tensor 27 (Bruker) FTIR spectrometer with a resolution of 2 cm^{-1}. The absorption spectra of the amide-I group were utilized to assess the secondary structure. Quantitative analysis was performed by obtaining the second derivative of the absorption spectra and conducting multiple fittings for each peak through deconvolution using OriginPro software [114].

2.2.8 Secondary Structure Analysis of OmpA by CD Spectroscopy

Circular dichroism spectroscopy conducted on a Jasco J-815 spectropolarimeter (Jasco, Easton, MD) was employed to determine the folding pattern and structural content (e.g., α-helix, β-sheet, random coil) of the OmpA protein. The analysis was conducted within a wavelength range of 190-260 nm for far ultraviolet CD spectrum measurements. A cuvette with a path length of 1 mm was used, along with a bandwidth of 1 nm and a scan rate of 50 nm/min. To correct for baseline effects, the spectra of each sample were normalized by subtracting the corresponding buffer spectra [114].

The influence of urea at different concentrations (1-6 M urea in Tris-buffer) as well as in the presence of various pH buffers ranging from 3.0–10.0 pH and different temperature intervals from 10–90°C on OmpA protein was examined. Similarly, to evaluate the refolding of the denatured protein in the presence of detergents and lipids, which facilitate its solubilization and reconstitution as a membrane protein. OmpA protein was refolded using a refolding buffer comprising 20 mM Tris-Cl at pH 8.0, 200 mM NaCl, and various detergents and lipids. The detergents included LDAO at concentrations of 2x and 4x the critical micelle concentration (CMC), as well as DDM, β-OG, and Tween-20 at their 4x and 10x CMC concentrations. Additionally, the buffer contained lipids, specifically DMPC at concentrations of 25 nM and 100 nM, and DOPC at concentrations of 0.2 mM and 0.5 mM [114]. The CD spectra were analyzed using the BeStSel tool to estimate the secondary structural content of the OmpA.

2.2.9 Tryptophan Fluorescence Spectroscopy

The tryptophan fluorescence spectra of OmpA were employed to determine the structural topology, folding, and conformation changes of OmpA. The spectra were recorded using a FluoroMax-4p spectrofluorometer from Horiba Jobin Yvon (model: FM100), with excitation at 295 nm and emission collected in the range of 310–400 nm. The structural integrity of the OmpA protein was evaluated under denaturing conditions with increasing concentrations of urea (1–6 M in Tris-buffer), temperature gradients (10–90 °C), and varying pH (3.0–10.0), providing insights into protein unfolding, conformational changes, and aggregation [1]. Similarly, the influence of detergents and lipids on the refolding of denatured OmpA was evaluated using a refolding buffer. The buffer was composed of the following components: 20 mM Tris-Cl at pH 8.0, 200 mM NaCl, and various detergents and lipids. The detergents included LDAO at concentrations of 2x and 4x the CMC, as well as DDM, β-OG, and Tween-20 at their 4x and 10x CMC concentrations. Additionally, the buffer contained lipids, specifically DMPC at concentrations of 25 nM and 100 nM, and DOPC at concentrations of 0.2 mM and 0.5 mM [114].

2.2.10 Expression and Isolation of OMVs

OMVs were isolated from the BL21(DE3) (OmpA) and BL21(DE3) strains using a modified method from Tang et al [116]. In brief, the bacterial strains were cultured overnight in 500 mL of LB broth with ampicillin (100 µg/mL) at 37°C and 220 rpm. Induction with 0.5 mM IPTG occurred when the OD at 600 nm reached approximately 0.6, followed by an additional 4 h of incubation. The BL21(DE3) strain served as a control in the experiments. After centrifugation at 10,000 g for 10 min at 4°C, the culture supernatant was filtered through a 0.22 µm filter and concentrated using a 100-kDa centrifugal concentrator (Amicon Ultra Centrifugal Filter, Millipore). OMVs were isolated by ultracentrifugation at 120,000 × g for 2 h at 4°C, washed with phosphate-buffered saline (PBS) at pH 7.4, and then resuspended in PBS and stored at -20°C until further use.

2.2.11 OMVs Characterization

The protein concentration of OMVs and the OmpA protein was quantified using the Bradford method. Additionally, the protein content from each sample was analyzed through SDS-PAGE. Similarly, the lipid content was determined by quantifying the total phosphate levels using a standard protocol from a malachite green phosphate assay kit (Sigma Aldrich, cat: MAK307), which measures phosphate present in phospholipids, proteins, and DNA [117]. The OmpA protein within the OMV preparation was detected using Western blotting with an anti-6x His-tag mouse monoclonal antibody (Invitrogen). Additionally, the chemical composition of OMVs was analyzed using ATR-FTIR spectroscopy (Tensor 27 FTIR spectrometer, Bruker). The analysis of FTIR spectra was conducted by applying the second derivative to the absorption spectra, and the resulting peaks were further analyzed to identify the various groups present in the OMV samples. Data analysis was carried out using the OriginPro software [118,119]. Furthermore, the size distribution and zeta potential of OMVs were measured with a Nano Plus particle size analyzer (NanoPlus-3 model). Finally, high-resolution imaging of OMV morphology was conducted with a field emission scanning electron microscope (FE-SEM) (ZEISS Supra55) [120,121].

2.2.12 Cell Culture

Raji human B-cells were cultured in RPMI-1640 medium (MP Biomedicals) supplemented with 10% fetal bovine serum (FBS) (Gibco), 50 µM 2-mercaptoethanol (Sigma Aldrich), and 1% antibiotic solution (Penicillin 100 IU/mL and Streptomycin 100 µg/mL) (Gibco, Life Technologies) at 37°C in 5% CO_2.

Similarly, HEp-2 cells, a human laryngeal epithelial carcinoma cell line, were cultured in RPMI 1640 medium (MP Biomedicals) supplemented with 10% FBS (Gibco), 50 µM 2-mercaptoethanol (Sigma Aldrich), and 1% antibiotic solution (Penicillin 100 IU/mL and Streptomycin 100 µg/mL) (Gibco, Life Technologies) at 37°C in 5% CO_2. For subculturing, the cells were detached using the 0.25% trypsin-EDTA (Gibco), then neutralized using the complete growth RPMI-1460 medium.

2.2.13 Endotoxin Removal from Purified OmpA Protein

The endotoxin from the OmpA protein was removed using an endotoxin removal column (Pierce, Thermo Fisher Scientific) following the manufacturer's instructions. After removal, the endotoxin-free product was filtered through a 0.22-micron syringe filter. We quantified the endotoxin levels using the Limulus Amoebocyte Lysate test with the Pierce LAL Chromogenic Endotoxin Quant Kit (Thermo Fisher Scientific). The concentration of the OmpA protein was determined using the Bradford assay.

2.2.14 B-Cell Morphology and Viability Following Stimulation with OmpA and OMVs

To investigate the impact of OmpA and OMVs on B-cell morphology and viability, Raji human B-cells were assessed using the combination of microscopy and viability assay, including MTT (3-(4,5-dimethylthiazol-2-yl)-2,5-diphenyltetrazolium bromide) assay and trypan blue exclusion method.

The objective of this study was to assess the impact of OmpA and OMVs on Raji human B-cell morphology and viability. The B-cells, at a density of 5×10^6 cells per plate, were cultured and allowed to grow overnight. The following day, the cells were exposed to varying concentrations of OmpA (0, 2.5, 5, 10, 20, and 40 µg/mL) and OMVs, such as OmpA-OMVs and BL21-OMVs, at concentrations of 0, 0.08, 0.15, 0.312, 0.625, 1.25, 2.5, and 5 µg/mL for 24 h. After treatment, cell morphology was observed using phase contrast microscopy. Furthermore, to evaluate cell viability, the Trypan blue exclusion method was employed. Trypan blue is a membrane-impermeable dye that selectively stains non-viable cells. The cell suspensions were collected and mixed with Trypan blue at a dilution of 1:4. This mixture was then loaded onto a hemocytometer to differentiate between viable (unstained) and non-viable (blue-stained) cells. Finally, percent cell viability was calculated by comparing the results to untreated B-cells, which served as a positive control, representing 100% viability [122].

Similarly, the cell viability was also determined using the MTT assay. B-cells were cultured in 96-well plates at a density of 2×10^4 cells per well. The cells were exposed to various concentrations of OmpA (0, 2.5, 5, 10, 20, 40, and 80 µg/mL) and OMVs, such as OmpA-OMVs and BL21-OMVs (0, 0.08, 0.15, 0.312, 0.625, 1.25, 2.5,

and 5 µg/mL) for 24 h. Following this, the formazan crystals formed in each well were dissolved in 100 µL of acid-isopropanol (0.04 N HCl in Isopropanol) and left to incubate in the dark at room temperature for 15 min. The absorbance of the resulting solution was measured at 550 nm using a microplate reader. Finally, the percent cell viability was calculated by comparing the results to untreated B-cells, which served as a positive control, representing 100% viability [123,124].

2.2.15 RNA Isolation and cDNA Synthesis

Raji human B-cells were cultured until they reached approximately 90% confluency. Subsequently, the culture medium was replaced, and the cells were allowed to grow overnight at a density of 5×10^6 cells per plate. The following day, cells were exposed to purified and endotoxin-free OmpA at different concentrations (0, 5, 10, and 20 µg/mL) or with OMVs at 1.25 µg/mL. PBS was added to a separate group of cells as a control. Cell samples were collected at different time points: 0, 2, 4, 8, and 24 h. After stimulation, the cells were washed three times using PBS and utilized for RNA and protein isolation.

Similarly, the Raji human B-cells at a density of 5×10^6 cells per plate were treated with OMVs, including OmpA-OMVs and BL21-OMVs (1.25 µg/mL) and endotoxin-free OmpA (20 µg/mL). PBS served as the control. Cell samples were taken at various time points: 0, 4, 8, and 24 h. After stimulation, the cells were washed three times using PBS and utilized for RNA and protein isolation.

The total RNA was extracted from the cells using TRIzol reagent (Invitrogen). Briefly, the cell pellet was resuspended in 500 µL of TRIzol reagent, and the lysate was homogenized by pipetting up and down, followed by a 5 min incubation at room temperature. Subsequently, 200 µL of chloroform was added, the mixture was vigorously shaken, and further incubated for 5 min at room temperature. The phase separation was achieved by centrifugation at 12,000 × g for 15 minutes at 4°C. The resultant upper colorless aqueous phase was carefully transferred to a new tube, and 250 µL of isopropanol was added to precipitate RNA. After gentle mixing by pipetting, the mixture was incubated at room temperature for 10 minutes and then centrifuged at 12,000 × g for 10 minutes at 4°C. The supernatant was discarded, and the RNA pellet

was washed with 75% ethanol, air-dried, and then resuspended in diethyl pyrocarbonate (DEPC)-treated nuclease-free water (NFW). After extraction, the total RNA samples were treated with the DNA-free DNA removal kit (Invitrogen) to eliminate any DNA contamination. The concentration and purity of the total RNA were then measured using a Nanodrop spectrophotometer (Thermo Scientific). For cDNA synthesis, 1 μg of total RNA was utilized, and the cDNA was prepared according to the manufacturer's instructions using the Verso cDNA synthesis kit (Thermo Scientific).

2.2.16 Reverse Transcriptase-Quantitative Polymerase Chain Reaction (RT-qPCR)

cDNA amplification was performed to evaluate the transcription levels of gene expression. To evaluate cell proliferation, the expression of proliferation markers Ki-67 and PCNA was analysed. The mRNA expression level of TLR2 was measured to investigate B-cell surface activation, while transcript levels of NF-κB and TNFα were assessed to understand their roles in modulating B-cell responses. The transcriptional regulators of AID include activators such as cMYC, PAX5, SMAD3, and STAT6, along with repressors such as cMYB and E2F1. Similarly, the transcript levels of CSR, such as matured Ig transcripts IgV-Cμ and IgV-Cα, as well as the heavy chain of IgG, are analysed to examine CSR activity **(Appendix B)**. This analysis was conducted using the SYBR Green qPCR master mix (Thermo Scientific) on QuantStudio-3 (Applied Biosystems). The PCR cycling conditions involved a 15 s denaturation phase at 95°C, followed by a 60 s annealing/extension phase at 60°C for a total of 40 cycles. The data normalization was executed using the housekeeping gene GAPDH as an internal reference [79].

2.2.17 Protein Isolation and Western Immunoblotting

Stimulated Raji human B-cells were washed twice with PBS and centrifuged at 1200 rpm at 4°C for 5 min. Following this, the cells were lysed in a lysis buffer comprising 20 mM Tris-Cl (pH 7.6), 150 mM NaCl, 1% Triton-X 100, 1 mM EDTA (HiMedia), and Protease inhibitor + DNase I (1 μg/mL) (HiMedia). Protein concentration was determined using the Bradford assay. An equal concentration of protein samples obtained from each treatment group was added to 5x sample loading buffer (0.25 M Tris-Cl at pH 6.8, 10% SDS, 50% glycerol, 10% β-mercaptoethanol, and 0.02%

bromophenol blue), boiled at 95°C, and separated by 12% SDS-PAGE in mini protean tetra cell (Bio-Rad). Subsequently, the gel was transferred onto a nitrocellulose membrane (Amersham, GE Healthcare). The membranes were blocked with blocking buffer (5% non-fat milk in Tris-buffered saline with 0.1% Tween 20, TBST) for 3 h at room temperature. The Western immunoblotting was performed using antibodies **(Appendix C)**. Protein bands were visualized using an ECL substrate (Bio-Rad), and chemiluminescence was detected using the Image Quant LAS 4000 Gel Doc system (GE Healthcare). Band intensities were quantified using ImageJ analysis software (ImageJ). The relative expression of protein was normalized to GAPDH (Santa Cruz Biotechnology, sc-47724) levels [79].

2.2.18 Pull-Down Assay

To investigate the interaction between OmpA and TLR2, a pull-down assay was performed. The Raji human B-cells and Hep-2 cells (1×10^8) were used for the assay. First, the cells were washed twice with PBS and then harvested by centrifugation at 1200 rpm for 5 min. The cell pellets were lysed using a lysis buffer containing 50 mM Tris-Cl at pH 8.0, 150 mM NaCl, 0.1% Triton X-100, 0.1% SDS, and a protease inhibitor cocktail (HiMedia), supplemented with 1 µg/mL DNase I (HiMedia). The purified OmpA protein was then incubated with the whole cell lysate at a 1:1 concentration ratio with mild agitation overnight at 4°C to allow for binding. The following day, the mixture was applied to a pre-equilibrated Ni-NTA column (Qiagen) in equilibration buffer (50 mM Tris-Cl at pH 8.0, 150 mM NaCl, and 10 mM Imidazole) and incubated for 2 h. After incubation, the column was centrifuged to remove unbound proteins. Next, the columns were washed with a washing buffer containing 50 mM Tris-Cl (pH 8.0), 150 mM NaCl, and 30 mM Imidazole. Finally, proteins containing the His-tag were eluted using an elution buffer (50 mM Tris-Cl at pH 8.0, 150 mM NaCl, and 300 mM Imidazole). The samples were then subjected to Western blotting using anti-His (Invitrogen, MA1-21315) or anti-TLR2 (Invitrogen, MA532787) antibodies.

2.2.19 Co-Immunoprecipitation (Co-IP) Assay

To investigate the interaction between OmpA and TLR2, a Co-IP assay was performed. The cell lysate was prepared from untreated Raji human B-cells and HEp-2 cells (2×10^7). Briefly, cells were washed with PBS twice and harvested by centrifuging at 1200 rpm for 5 min. Cell pellets were lysed with lysis buffer (50 mM Tris-Cl at pH 8.0, 150 mM NaCl, 0.1% TritonX-100, and 0.1% SDS, protease inhibitor cocktail (HiMedia) supplemented with 1 µg/mL DNase I (HiMedia). Further, the cell lysate was passed through a 22-gauge needle to shear the DNA and was centrifuged at 12000 rpm for 30 min. Lysate supernatant was incubated with OmpA (10 µg/mL) or buffer overnight. The following day, Protein-A/G Agarose beads were washed and equilibrated with 1 mL of equilibration buffer (50 mM Tris-Cl at pH 8.0, 150 mM NaCl, 5 mM $MgCl_2$, 5 mM $MnCl_2$, 0.1% TritonX-100, and 0.1% SDS. The cell lysate was mixed with agarose beads and incubated for 2 h at 4°C, and pelleted by centrifugation. The pellet was washed three times using washing buffer (20 mM Tris-Cl at pH 8.0, 750 mM NaCl, 5 mM $MgCl_2$, 5 mM $MnCl_2$, 0.1% Triton X-100, and 0.1% SDS). Finally, the protein of interest was pulled down using elution buffer (120 mM Tris-Cl, pH 6.8, 1.0% SDS) and boiled at 95°C for 5 min. Subsequently, the Western blot was performed using anti-His (Invitrogen, MA1-21315) or anti-TLR2 (Invitrogen, MA532787) antibodies [1,82].

2.2.20 Immunofluorescence Assay

Stimulated Raji human B-cells (5×10^6) were processed for immunostaining. For TLR2 inhibition studies, cells were pre-treated with MMG-11 at concentrations of 25 µM and 50 µM for 1 hour before stimulation. Following stimulation, the cells were washed three times with PBS and centrifuged at 1400 rpm for 5 min each time. Subsequently, the cells were fixed in 4% paraformaldehyde (HiMedia) for 20 min, followed by permeabilization with PBS-T (0.1% Triton-X in PBS) for 10 min. The cells were then blocked for 30 min in PBS-T containing 5% BSA (HiMedia) and subjected to primary antibodies, including anti-TLR2 (Invitrogen, MA532787, and dilution 1:200), NF-κB-p65 (Invitrogen, MA515181, and dilution 1:200), anti-His (Invitrogen, MA1-21315), anti-AID (Invitrogen, ZA001, and dilution 1:200), and anti-cMYC (Invitrogen, 27H46L35, and dilution 1:300), anti-Pax5 (Invitrogen, JJ08-87, and dilution 1:300) for overnight incubation at 4°C on a rotating platform. After incubating the cells with the

primary antibody, they were washed three times with PBS-T, with each wash taking 5 min. Following this, the cells were exposed to secondary antibodies, Goat anti-mouse Alexa Fluor 488 (Invitrogen, A-11001) or Goat anti-rabbit Alexa Fluor 594 (Invitrogen, A-11012) at a dilution of 1:400 in PBS-T with 2% BSA for 2 h at room temperature. After the secondary antibody incubation, the cells were washed three times with PBS-T. Finally, high-resolution images were taken at 60x magnification using an Olympus confocal laser scanning microscope (Olympus, FV1200MPE). Mean fluorescent intensity was calculated using ImageJ software [79].

2.2.21 Chromatin Immunoprecipitation (ChIP) Assay

Stimulated Raji human B-cells (7×10^6) were cross-linked with 1% formaldehyde at 37°C for 10 min. Subsequently, the reaction was quenched by adding 125 mM glycine for 5 min at room temperature. The samples were washed twice with ice-cold PBS containing a protease inhibitor cocktail, and the lysate was resuspended in cell lysis buffer comprised of 20 mM Tris-Cl, pH 7.6, 100 mM NaCl, 5 mM EDTA, 1% Triton X-100, 0.5% NP-40 (Sigma), and protease inhibitor cocktail. The lysate was sonicated for 30 min (30 s on/30 s off) to obtain DNA fragments ranging from 200 bp to 500 bp. Following this, 100 µg of chromatin was aliquoted, and the final volume was adjusted to 300 µL using dilution buffer (20 mM Tris-Cl, pH 8.0, 100 mM NaCl, 1.5 mM EDTA, 1% Triton X-100). The chromatin was precleared by adding 40 µL of Protein A/G agarose beads to the samples and rotating for 2 h at 4°C. The chromatin samples were centrifuged at 3000 rpm for 5 min at 4°C. The supernatant containing chromatin was incubated overnight with primary antibodies (c-Myc Recombinant Rabbit Monoclonal Antibody, Invitrogen (27H46L35) at 4°C, followed by a 2 h incubation with 40 µL of Protein A/G agarose beads (Santa Cruz Biotechnology, sc2003). Following this, the beads were washed three times with a series of 1 mL low-salt buffer (20 mM Tris-Cl, pH 8.0, 150 mM NaCl, 0.1% SDS, 2 mM EDTA, and 1% Triton X-100), high-salt buffer (20 mM Tris-Cl, pH 8.0, 500 mM NaCl, 0.1% SDS, 2 mM EDTA, and 0.1% Triton X-100), followed by LiCl wash buffer (10 mM Tris-Cl, pH 8.0, 0.25 M LiCl, 1 mM EDTA, and 1% sodium deoxycholate). Finally, the immune complex beads were washed twice with TE buffer (10 mM Tris-Cl, pH 8.0, and 1 mM EDTA). Afterwards, the resuspended beads and input samples were reverse cross-linked by adding 300 µL

of elution buffer (2% SDS, 0.1 M $NaHCO_3$) supplemented with 1 µL of Proteinase K (20 µg/mL) and RNase (20 µg/mL), and incubating the samples at 55°C for 2 h. The mixture was then incubated overnight at 65°C to reverse the cross-links and release the immunoprecipitated DNA. The total DNA was isolated using a PCR purification kit (Favorgen). Finally, the isolated DNA was diluted and subjected to real-time PCR analysis [79,125–127]. The primers used for RT-qPCR analysis are listed in **Appendix B**.

2.2.22 Quantification of TNF-α secretion by Enzyme-linked immunosorbent assay (ELISA)

The Raji human B-cells were cultured at a density of 3×10^6 cells in the cell culture dish and maintained at 37 °C in a 5% CO_2 incubator overnight. The following day, cells were treated with purified, endotoxin-free OmpA (10 µg/mL) or the TLR2 antagonist MMG-11 at concentrations of 25 µM and 50 µM for 1 hour before stimulation, and a separate group was treated with Tris buffer as a control. The level of TNF-α in the culture supernatant of stimulated Raji human B-cells was measured according to the manufacturer's protocol (Krishgen BioSystems, KB1145). TNF-α concentrations were determined from a standard curve, and all samples were analysed in technical duplicates.

2.2.23 Statistical Analysis

Statistical analysis was conducted using PRISM 8.0 (GraphPad Software, San Diego, CA). The statistical significance of differences between test groups was analysed using one-way analysis of variance (ANOVA). The data are presented as mean ± SD. Differences in the mean values were considered significant at $P < 0.05$.

The methodologies used in chapters 3, 4, 5, and 6 are illustrated in **Figure 2.1.**

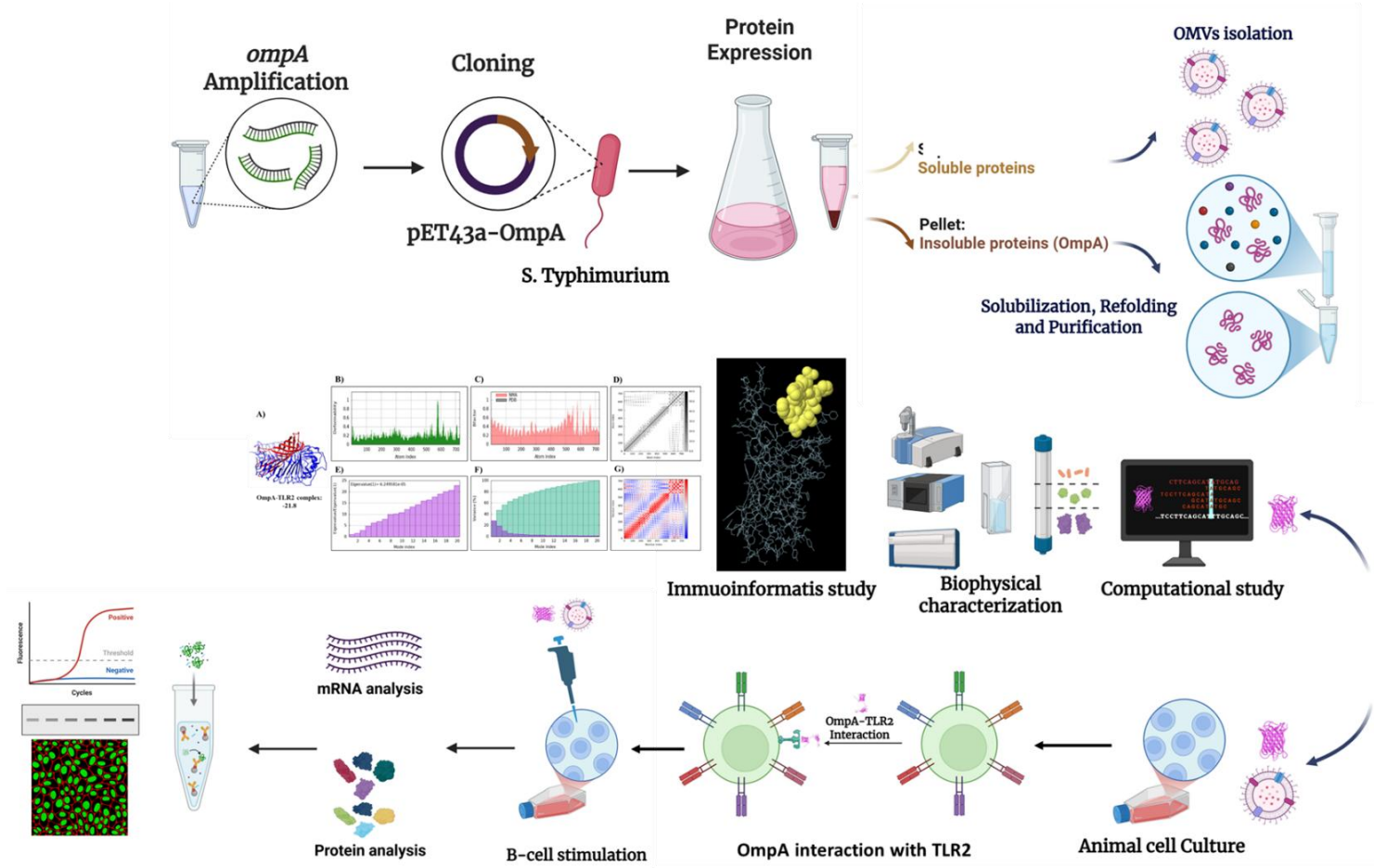

Fig. 2.1 Schematic representation of the methodology used in the study. The *ompA* gene was amplified and cloned into the pET43a vector for recombinant expression in *S.* Typhimurium. The resulting proteins were separated into soluble and insoluble fractions; the insoluble OmpA was solubilized, refolded, and purified. OMVs were isolated from the soluble fraction for functional studies. Immunoinformatic analyses predicted OmpA's structural and functional features, while computational modeling and biophysical characterization elucidated its attributes. Purified OmpA and OMVs were used to stimulate B-cells *in vitro*, with the interaction of OmpA and Toll-like receptor 2 (TLR2) evaluated through AID expression analysis via mRNA (qRT-PCR) and protein (Western blot). This approach connects OmpA's structural insights to its immunomodulatory effects on B-cells.

Chapter 3

Results for Objective 1

Chapter 3
3. Computational and Biophysical Characterization of OmpA, a Major Outer Membrane Protein from *S.* Typhimurium.

3.1 Introduction

Several factors contribute to the pathogenesis of *S.* Typhimurium, including adhesins, lipopolysaccharides, exotoxins, and outer membrane proteins (OMPs) [128]. OMPs are located in the outer membrane of Gram-negative bacteria and play crucial roles in various cellular functions, such as maintaining cell integrity, facilitating nutrient absorption, mediating import and export processes, promoting cell adhesion and invasion, and participating in cell signaling [21,129]. OMPs typically consist of β-barrel proteins, typically comprised of 8 to 24 anti-parallel β-strands connected by extracellular loops.

Among these OMPs, OmpA is the most abundant protein in Gram-negative bacteria, with typically 100,000 copies per cell, and is highly conserved across multiple species of Gram-negative bacteria. It plays a multifaceted role in bacterial structural integrity and pathogenicity [37]. In *S.* Typhimurium, the N-terminal domain of OmpA contains 8 transmembrane β-barrel motifs residing within the outer membrane, while the C-terminal domain resides within the periplasm region. A 15-amino-acid residue linker region that connects the β-barrel protein to the soluble C-terminal domain [37]. While the crystal structure of the C-terminal domain of OmpA is available in *S.* Typhimurium 14028s (PDB ID: 5VES), the three-dimensional structure of the N-terminal domain of OmpA in *S.* Typhimurium has not yet been solved. Therefore, addressing this structural gap is crucial, as β-barrel domains are essential for membrane integration and play a key role in immune recognition [130].

The functional aspect of OmpA in *Salmonella* and other Gram-negative bacteria is multifaceted, contributing significantly to virulence. OmpA plays a crucial role in adhesion, biofilm formation, and outer membrane permeability, and antibiotic resistance uncovers its potential as a therapeutic target. Numerous studies have explored the conserved OmpA protein found in different Gram-negative bacteria, such

as *E. coli* OmpA, *Francisella tularensis* FopA*, Chlamydia trachomatis* major outer membrane protein (MOMP), *Klebsiella pneumoniae* OmpA, and *Pseudomonas aeruginosa* OprF. These proteins are not only conserved but also crucial for pathogenesis and immune recognition [132]. Furthermore, OmpA also contributes to antibiotic resistance by stabilizing the outer membrane, thereby protecting *S.* Typhimurium from broad-spectrum β-lactam antibiotics such as ceftazidime and meropenem by stabilizing the outer membrane [133].

This study aims to examine the computational and biophysical characterization of OmpA from *S.* Typhimurium. Initially, to predict the structural features of OMPs, we conducted a computational analysis of OmpA to determine its secondary structure content. We then express and purify the OmpA protein for biophysical characterization. The structural characterization of OmpA, including SEC, was used to assess the oligomeric state of the OmpA protein. A heat modifiability assay was used to assess the distinctive migration pattern of the β-barrel protein, indicating the folding state of the native protein compared to the denatured protein [115]. Moreover, characterizing the OmpA by CD spectroscopy and ATR-FTIR provides information about the secondary structure content of the protein, such as the proportion of α-helices, β-sheets, and coiled structure [114]. Furthermore, tryptophan fluorescence spectroscopy was used to understand the folding topology and behavior of the protein from the denatured state to its native conformation. We employed various detergents and lipids. Detergents such as LDAO: Lauryl dimethylamine-N-oxide, DDM: n-Dodecyl β-D-maltoside, β-OG: n-Octyl-β-D-Thio glucopyranoside, and Tween-20 were utilized for solubilizing, facilitating refolding, and maintaining their stability in solution. Lipids, including DMPC: Dimyristoylphosphatidylcholine, and DOPC: Dioleoyl phosphatidylcholine, were selected to mimic the native membrane-like environment, thereby promoting proper folding and stability [134,135]. Furthermore, Immunoinformatic analysis was used to identify multi-epitopes from OmpA that interact with MHC class-I, MHC class-II, and B-cells. Immune simulation analysis was conducted to explore OmpA's potential as a therapeutic target.

In conclusion, this study provides insights into OmpA's structure and its

potential as a therapeutic target through various analyses, setting the stage for future research on its role in host-pathogen interactions and immune modulation.

3.2 Results

3.2.1 *In silico* analysis of OmpA protein: Signal peptide, physicochemical properties, and structural features

In silico analysis of the OmpA protein was used to predict the nature of the OMP characteristics. The OMP has the characteristics of having a signal peptide that will help bacteria transport the protein into the outer membrane via the BAM assembly complex. As a result, we looked at the amino acid sequence of OmpA in a SignalP-6.0 (**Fig. 3.1A**) to see if there was a signal peptide for the OmpA protein and observed that the OmpA protein contains the signal peptide that encodes for the outer membrane. Likewise, the analysis of the physicochemical properties of the OmpA protein without the signal peptide was predicted using the ProtParam analysis tool available on the Expasy website **(Table 3.1)**. The secondary structure analysis of OmpA protein using a NetSurfP-2.0 online tool showed a predominance of β-sheets as compared with the α-helices **(Fig. 3.1B)**. Additionally, when comparing the multiple sequence alignment of OmpA with various organisms, it reveals structural identity to the OmpA protein. It is also rich in β-sheets in other species **(Fig. 3.2A)**.

The 3D structure of the OmpA protein was predicted using the AlphaFold-2.0 server [97]. The top PTM score of the model revealed a signal peptide, a β-barrel-shaped domain rich in β-sheets, and a periplasmic domain containing α-helices **(Fig. 3.3A-B)**. Superimposition of the predicted model and the N-terminal domain of *E. coli* K12 (PDB ID: 1BXW) and the C-terminal domain of *S.* Typhimurium 14028s (PDB ID: 5VES) revealed the closeness to the Alphafold 2.0 generated structural model (RMSD=0.669 Å), **Fig. 3.3C**. Additionally, in **Fig. 3.3D**, the representation includes β-sheets (blue), α-helices (green), and coils (grey), displayed in side and bottom views for OmpA from left to right. Similarly, structure, charged residues, and the predicted dimension of the barrel part of OmpA, which is around ~29 Å embedded in the membrane, while the exposed loop is around ~16 Å. Visualization of the OmpA protein using the PoreWalker tool reveals a structure comprising a β-barrel-like protein, forming a pore-like cavity within the barrel. Thus, upon visualization of the OmpA

pore, cavity features, diameter, and shape, it was observed that the pore diameter of OmpA varied from 22 to 3 Å **(Fig. 3.4A-E)**.

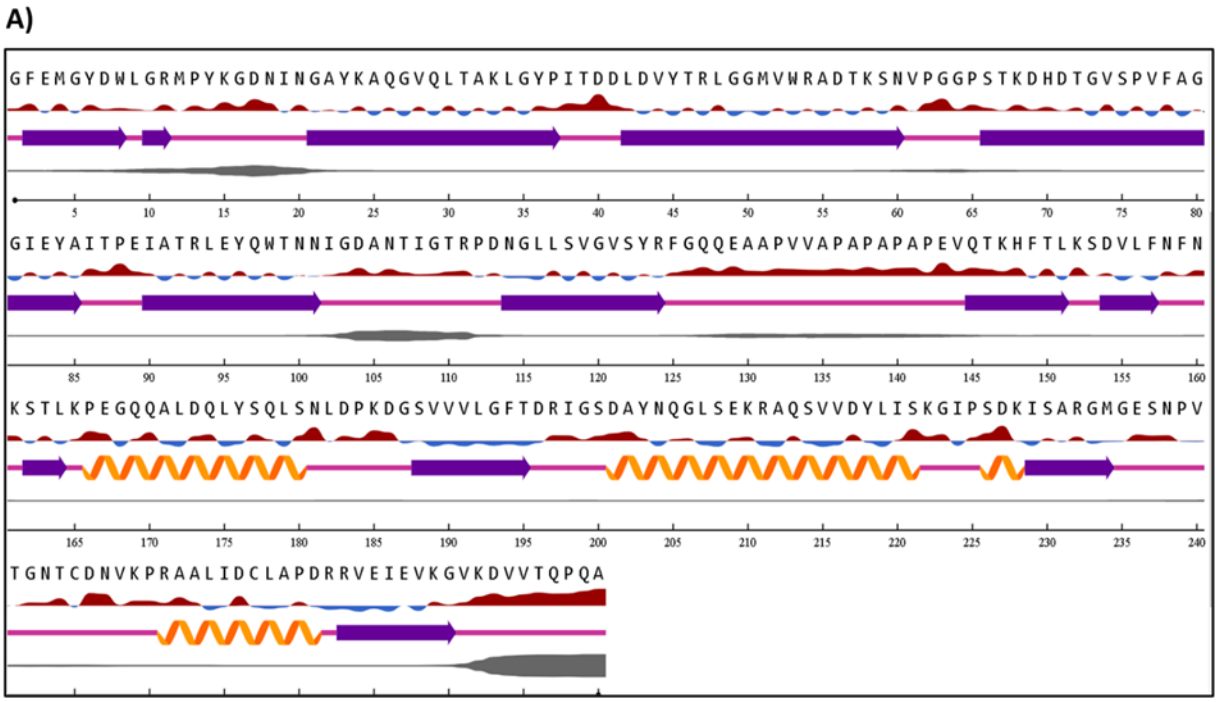

Fig. 3.1 *In silico* analysis for OmpA. A) Predicting the secondary structure contents of OmpA using NetSurfP-3.0.

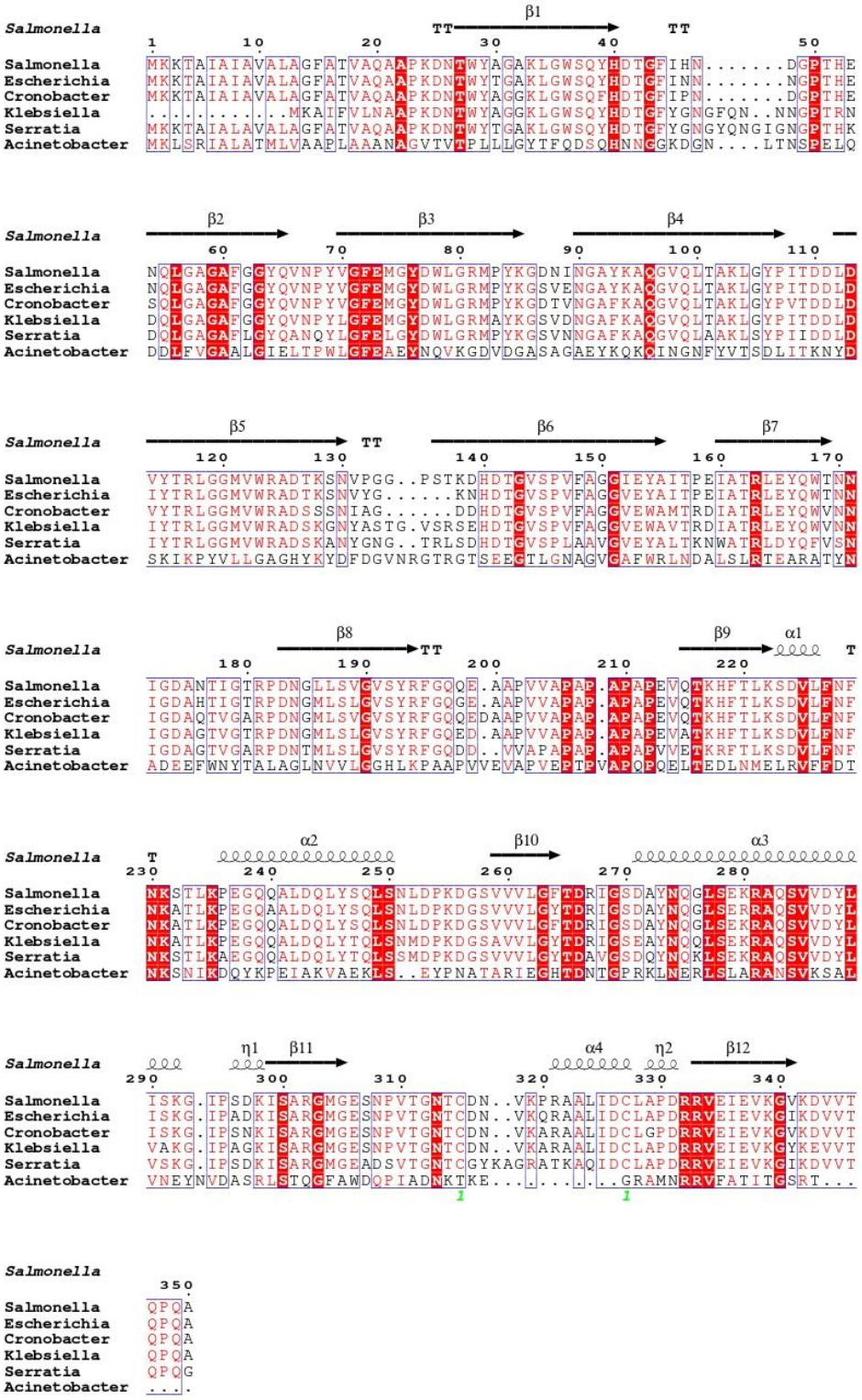

Fig. 3.2 A) Multiple sequence alignment of the OmpA protein with other species of Gram-negative bacteria.

Table 3.1 The physicochemical properties of OmpA were analyzed using the ProtParam tool.

Sr. no	Physicochemical properties	OmpA
1	Number of amino acids	350
2	Molecular weight	37515.04
3	Theoretical pI	5.60
4	Number of negative amino acids	37
5	Number of positive amino acids	32
6	Aliphatic index	76.66
8	Grand average hydropathicity	-0.360

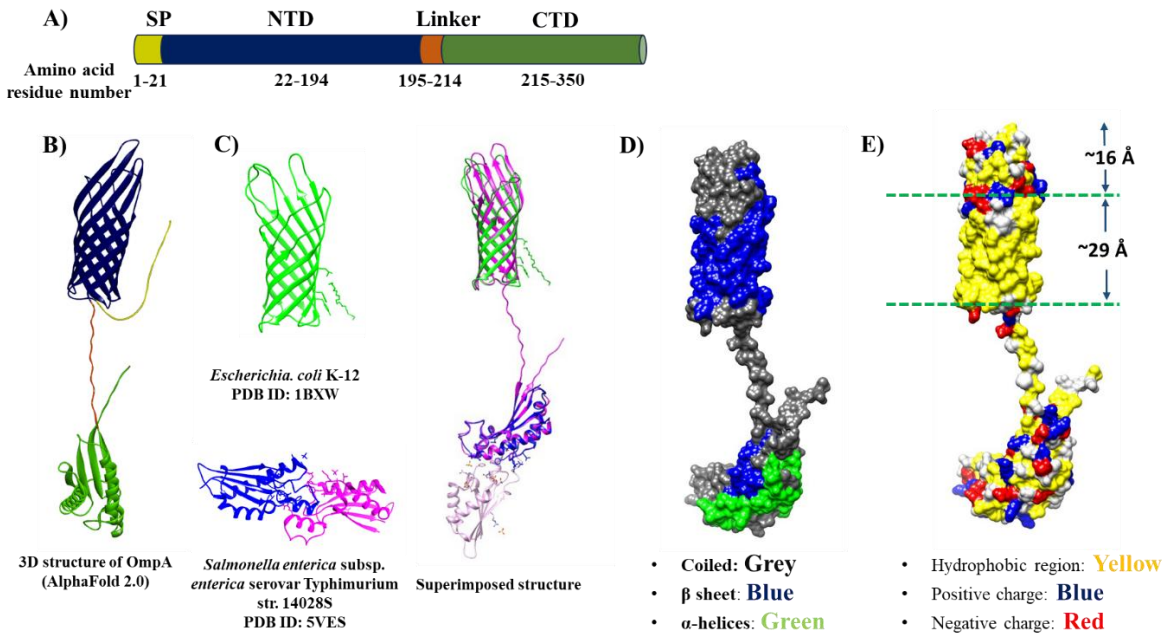

Fig. 3.3 The 3D structure of the OmpA protein, excluding the signal peptide sequence. A) Domain organization of OmpA. **B)** OmpA protein was predicted using AlphaFold 2.0. **C)** Predicted OmpA structure superimposed with the crystal structure of the N-terminal domain of *E. coli* K12 (PDB ID: 1BXW) and *S.* Typhimurium 14028s (PDB ID: 5VES). **D)** Tertiary structure representation of OmpA includes β-sheets (blue), α-helices (green), and coils (grey). **E**) A molecular surface view depicting the secondary structure and charged residues of OmpA is presented.

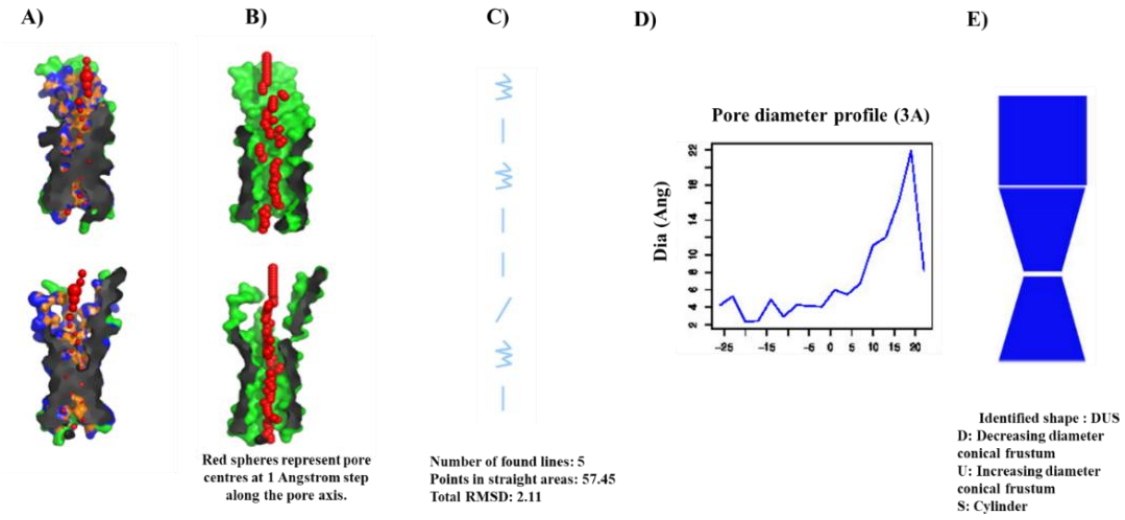

Fig. 3.4 The analysis of the structural features of the OmpA pore cavity includes the following aspects A) Visualization of the pore, **B)** Characteristics of the cavity, **C)** Straightness of the OmpA pore protein, **D)** Diameter of the OmpA pore, with the x-axis representing the pore depth, where position 0 corresponds to the center of the lipid bilayer, and **E)** The shape of the OmpA pore.

3.2.2 Expression, purification, and identification of OmpA

The *ompA* gene sequence from *S.* Typhimurium *OmpA* (accession no NC_003197.2) was obtained from the NCBI online server at (https://www.ncbi.nlm.nih.gov/). Primers were designed for the amplification of genes with the help of the *OmpA* gene sequence and inserting restriction sites for *Nde*I *and Xho*I in the forward and reverse primers, respectively **(Appendix B)**. The amplified *ompA* gene was successfully cloned into the pET43a vector at *Nde*I and *Xho*I restriction sites **(Fig. 3.5A)** and screened for recombinant clone through recombinant plasmid PCR, restriction digestion, and later successfully confirmed through DNA sequencing. The successful recombinant clone was transformed into *E. coli* BL21(DE3) cells to facilitate the expression and purification of OmpA.

The OmpA protein was purified using a Ni-IMAC resin (Bio-Rad). A C-terminal His-tag is present in the recombinant OmpA for affinity chromatography purification. OmpA expression tends to form inclusion bodies [136]; therefore, in our study, we used different solubilization buffers to solubilize the OmpA protein before purification. Notable differences were observed in solubilization depending on the

solubilizing agent used. Specifically, in our study, OmpA showed better solubilization in 6M and 8M urea and high pH buffer compared to 6M guanidine hydrochloride (GnHCl) and 1% SDS **(Fig. 3.5B)**. Solubilizing OmpA in a high pH buffer before refolding and purification resulted in a higher protein yield of 1.68 ± 0.12 mg/mL. In contrast, solubilization in 6M urea followed by purification and refolding yielded 0.8 ± 0.1 mg/mL, and solubilization in 6M urea followed by refolding and purification yielded 1.3 ± 0.07 mg/mL **(Table 3.2)**. As shown in **Fig. 3.5C**, the molecular weight of OmpA was determined to be approximately 38 kDa. A heat modifiability assay was performed to confirm the refolding condition of OmpA. This method serves as a key indicator for identifying integral OMPs with a β-barrel shape. To assess this, we conducted the heat modifiability assay by electrophoresing the OmpA protein and observed that the un-boiled sample moved slightly faster than the boiled one. This observation confirms that, in its native state, OmpA migrates slightly quicker than in its denatured state, which helps to identify its refolding condition **(Fig. 3.5D)**. Furthermore, the purity of OmpA was confirmed via Western blot analysis. The presence of the 6x His-tag was detected using an anti-His monoclonal antibody **(Fig. 3.5E)**.

3.2.3 Characterization of OmpA revealed dimer formation

In this study, size exclusion chromatography was performed to assess the oligomeric state of the OmpA protein, which revealed a dimeric form with an approximate molecular weight of 72 kDa **(Fig. 3.5F)** calculated through standard molecular weight markers **(Table 3.3),** and plotted a calibration curve **(Fig. 3.6A)**. Further analysis of the main peak from the SEC fraction was used for validation of dimer formation through semi-native SDS-PAGE and protease digestion assay.

Interestingly, we found that OmpA forms a dimer in semi-native SDS-PAGE at a molecular weight of around 75 kDa. While in the presence of β-mercaptoethanol (β-ME) and boiling the sample, we observed a band at around 38 kDa in monomeric form. However, neither β-ME alone nor boiling alone affected the dimer structure **(Fig. 3.5G)**. Further investigation involved refolding OmpA with various detergents and lipids, which are used to create a membrane-like environment and provide stability to a membrane protein.

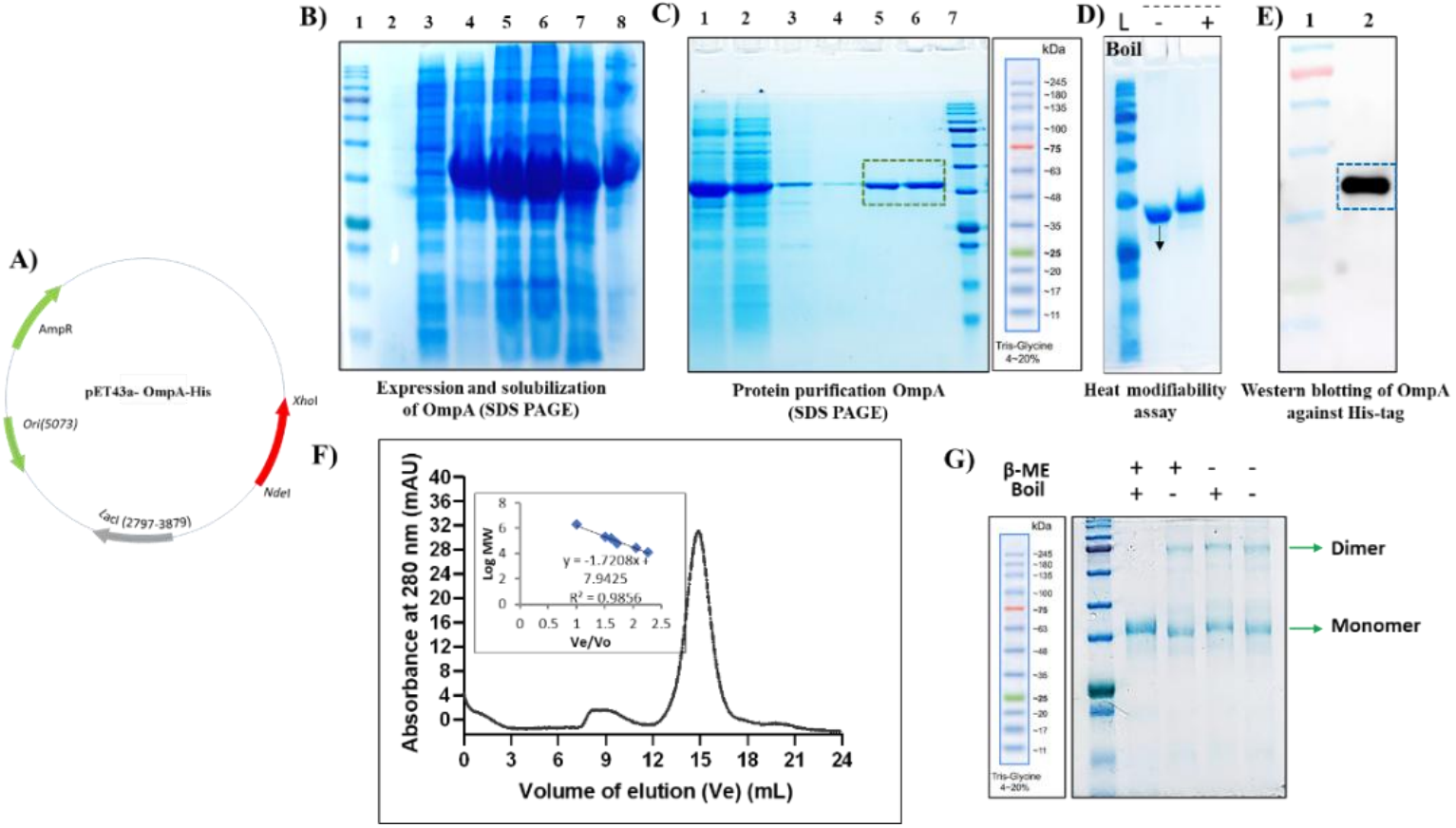

Fig. 3.5 Cloning, solubilization, purification, and Western immunoblotting of OmpA. A) Cloning strategy of OmpA in pET43a. **B)** SDS-PAGE of expression and solubilization of OmpA protein, Lane 1: protein marker, 2: Uninduced supernatant, 3: Uninduced pellet, 4: Induced pellet (1% SDS in Tris-buffer), 5: Induced pellet (8M urea in Tris-buffer), 6: Induced pellet (6M urea in Tris-buffer), 7: Induced pellet (2M urea in Tris-buffer, pH 12), 8: Induced pellet (6M GnHCl in Tris-buffer). **C)** SDS-PAGE of OmpA purification, Lane 1: Input sample, 2: Flowthrough, 3: Wash I, 4: Wash II, 5: Elution I, 6: Elution II, 7: protein marker. **D)** Heat modifiability assay of OmpA protein using SDS-PAGE. **E)** Western immunoblotting of OmpA against His-tag antibody, Lane 1: protein marker, 2: OmpA protein sample. **F)** Characterization of OmpA using size exclusion chromatography profile for OmpA protein on Superdex 200 Increase 10/300 GL column. **G)** Heat modifiability assay of OmpA protein using Semi-native SDS-PAGE.

Table 3.2 Evaluation of OmpA concentration obtained through different approaches for solubilization, refolding, and purification of the OmpA protein.

1L Culture	Solubilization (6M urea), purification, and refolding	Solubilization (6M urea), refolding, and purification	Solubilization (12.5 pH Tris-buffer), refolding, and purification
% Purity	93 ± 3	95 ± 1	94.5 ± 1.5
Concentration (mg/mL)	0.8 ± 0.1	1.3 ± 0.07	1.68 ± 0.12
Total protein (mg)	8 ± 1	13.3 ± 0.7	16.8 ± 1.2

Table 3.3 Evaluation of OmpA concentration obtained through different approaches for solubilization, refolding, and purification of the OmpA protein.

Proteins	MW (Da)	Ve	V0	Ve/V0	Log MW
Blue dextran	2000000	8.30	8.30	1.00	6.30
Beta amylase	200000	12.50	8.30	1.51	5.30
Alcohol Dehydrogenase	150000	13.45	8.30	1.62	5.18
Bovine Serum Albumin	66000	14.28	8.30	1.72	4.82
Carbonic Anhydrase	29000	17.10	8.30	2.06	4.46
Cytochrome C	12400	18.81	8.30	2.27	4.09
OmpA	Ve	V0	Ve/V0	Calculated MW	MW (kDa)
	14.9	8.30	1.79	71526.86	71.53

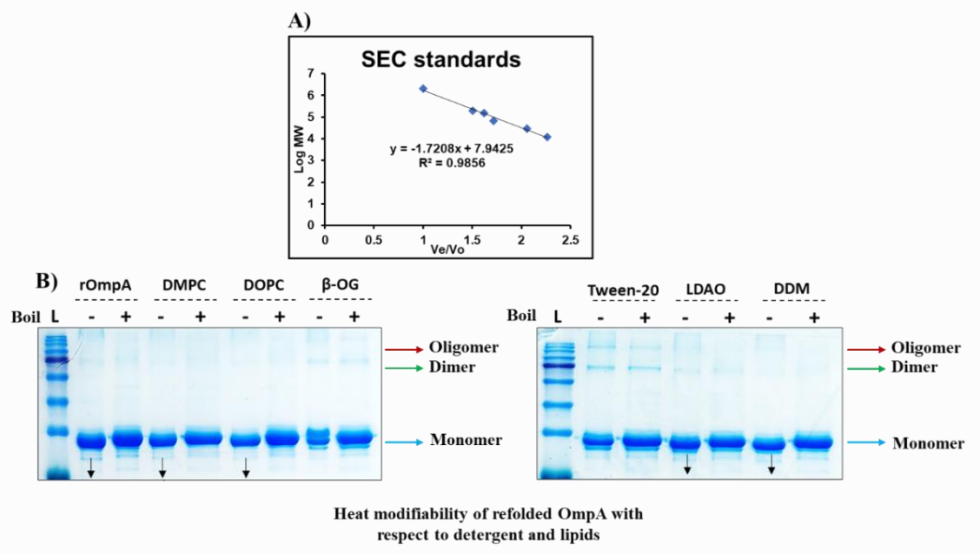

Fig. 3.6 Standard for SEC and heat modifiability analysis for refolded OmpA. A) Size exclusion chromatography calibration curve. The standard molecular weight markers for size exclusion chromatography were blue dextran (2000 kDa), β-amylase (200 kDa), Alcohol dehydrogenase (150 kDa), Bovine serum albumin (66 kDa), Carbonic anhydrase (29 kDa), and Cytochrome C (12 kDa). **B)** Heat modifiability of refolded OmpA in the presence of lipids and detergents.

We observed a slight migration difference with DMPC, DOPC, LDAO, and DDM, while β-OG and Tween-20 showed no migration difference between boiled and un-boiled samples **(Fig. 3.6B)**.

To further investigate the reliability of the predicted structure hypothesis, we conducted *in silico* studies that revealed the OmpA protein consists of a β-barrel. Interestingly, although trypsin has 27 cleavable sites across the OmpA sequence, the N-terminal transmembrane β-barrel domain appears to be resistant to proteolytic digestion. According to our *in-silico* analysis of the predicted OmpA model, there is a cleavable site at the 173rd amino acid residue (arginine) in the C-terminal β-barrel domain, which may facilitate the cleavage and separation of the two major domains: the N-terminal transmembrane domain and the C-terminal periplasmic domain, connected by a linker region **(Fig. 3.7A)**. To support this, we conducted a trypsin digestion assay. We observed that trypsin digestion at a 1:200 dilution for 60 min resulted in the presence of approximately 21 kDa and 17 kDa bands, which may correspond to the N-terminal β-barrel domain and the C-terminal periplasmic domain with linker region, respectively (as depicted in **Fig. 3.7B**). To differentiate the folded conformation of the β-barrel protein from the unfolded one, we performed semi-native PAGE. Interestingly, we observed a distinguishable band pattern, with higher band intensity in the un-boiled sample compared to the boiled sample, indicating the probable presence of the β-barrel protein **(Fig. 3.7C)**.

3.2.4 OmpA is rich in β-sheet structure

ATR-FTIR spectroscopy was employed to analyze the Amide-I region of the refolded OmpA protein, focusing on the spectral range from 1700 to 1600 cm^{-1}, which encompasses critical secondary structural components of the protein. In **Fig. 3.7D**, we illustrate the second derivative of the Amide-I band within this range for OmpA, and **Fig. 3.7E** represents the deconvolution of the amide-I spectra of OmpA for secondary structure content analysis. Our observations unveil that the OmpA protein is notably rich in β-sheets, evident from peaks at (1623-1633 cm^{-1}), (1633-1641 cm^{-1}), and (1672-1690 cm^{-1}). Likewise, peaks at (1649-1662 cm^{-1}) indicate α-helix structures. Furthermore, peaks at (1642-1649 cm^{-1}) suggest the presence of random coils, while

peaks at (1662-1690 cm^{-1}) indicate a mixture of β-sheets and random coils [137] (as depicted in **Table 3.4**).

We used far-ultraviolet CD spectroscopy to assess the secondary structure of OmpA. The spectrum showed a broad negative ellipticity maximum around 220 nm, indicating a β-sheet-rich structure. Analysis with the BeStSel tool revealed that β-sheets made up 48.1%, α-helices 12.5%, turns 6%, and other structures 33.4%. Membrane proteins are not soluble in aqueous solution; therefore, membrane proteins are reconstituted in the presence of detergents and lipids to create an amphipathic environment suitable for membrane proteins, which exhibit distinct physical properties compared to an aqueous environment, leading to unique spectral measurements [114,135]. Mimicking an outer membrane-like environment, detergents and lipids are used to refold denatured OMP within detergent and lipid micelles.

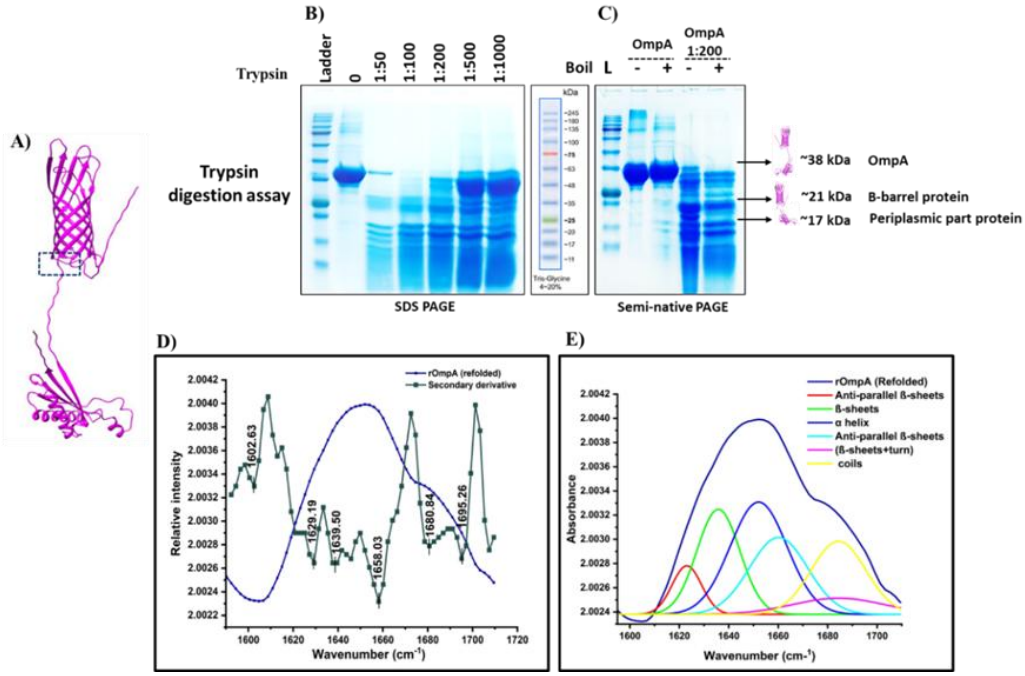

Fig. 3.7 Trypsin digestion analysis of OmpA and examining the secondary structure of the OmpA protein through ATR-FTIR, involving curve fitting in the amide-I region (1600–1700 cm−1). A) Prediction of trypsin cleavage sites present in the predicted OmpA model. **B)** SDS-PAGE analysis of trypsin-digested OmpA at different protein-to-trypsin ratios (1:50, 1:100, 1:200, 1:500, and 1:1000) analyzed by SDS-PAGE. **C)** Analysis of trypsin-digested OmpA in boiled and unboiled conditions using semi-native PAGE. **D)** IR absorbance spectra of OmpA alongside their second derivatives. **E)** Deconvolution of the amide-I spectra of OmpA to analyze the secondary structure content of the protein.

Table 3.4 Secondary structure content analysis of OmpA through ATR-FTIR second derivative spectrum of OmpA based on the selective region (1600-1700 cm^{-1}).

Sr no	Secondary structure content	Peak position (cm^{-1}) for OmpA
1	Sidechain	1616.25
2	Anti-parallel β-sheets	1623-1633
3	Parallel β-sheets	1633-1641
4	α-Helix	1649-1662
5	β-sheets	1672-1690
6	Random coil	1642-1649
8	β-sheets and random coils	1662-1690

In our study, we refolded denatured OmpA using a refolding buffer containing detergents and lipids. The inclusion of detergents (LDAO, DDM, β-OG, and Tween-20) and lipids (DMPC and DOPC) during the refolding process induces a hypochromic shift, notably increasing the β-sheets in the secondary structure of OmpA by analyzing the CD spectrum. This process may play a crucial role in preserving the integrity and stability of the secondary structure of OmpA **(Fig. 3.8A-F)**. Notably, compared to the denatured OmpA and the control without lipids or detergents, the best refolding results were observed in LDAO, followed by DMPC and DOPC, respectively. **Table 3.5** provides an estimation of the secondary structure of the OmpA protein in the presence of various lipids and detergents.

We further investigated the impact of varying concentrations of urea (0-6 M), pH buffer ranges from 3.0 to 10, and the presence of different temperature intervals on the secondary structure of OmpA. Interestingly, we observed that increasing the urea concentration resulted in the unfolding and destabilization of OmpA's secondary structure. This suggests that the native OmpA protein maintains greater integrity and stability compared to the urea-denatured sample **(Fig. 3.9A)**. **Fig. 3.9B** shows the far-UV CD spectra of OmpA during denaturation with varying urea concentrations. A decrease in ellipticity at 220 nm indicated denaturation, with OmpA stable up to 60°C **(Fig. 3.9C-D)**. Additionally, optimal stability was found at pH 7.0 to 10.0 **(Fig. 3.9E-F).**

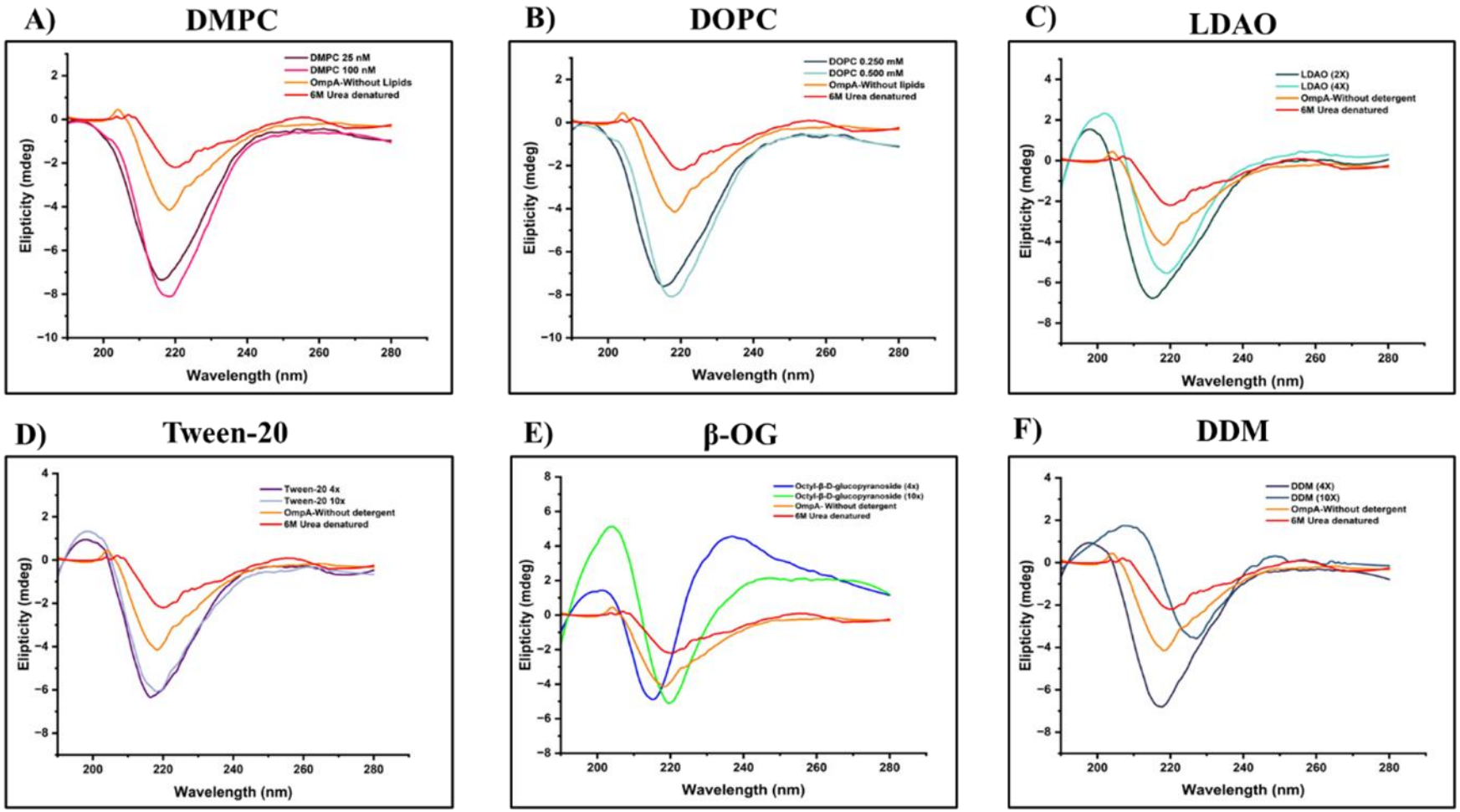

Fig. 3.8 CD spectra analysis of refolded OmpA using different detergents and lipids. (A-B) CD spectra for refolded OmpA by lipids, with a 10-fold dilution into a buffer containing DMPC at concentrations of 25 nM and 100 nM, and DOPC at 0.2 mM and 0.5 mM CMC concentrations. **(C-F)** CD spectra for refolded OmpA by detergents, 10-fold dilution into a buffer containing LDAO at 2x and 4x CMC concentrations, and Tween-20, β-OG, and DDM 4x and 10x CMC concentrations, respectively.

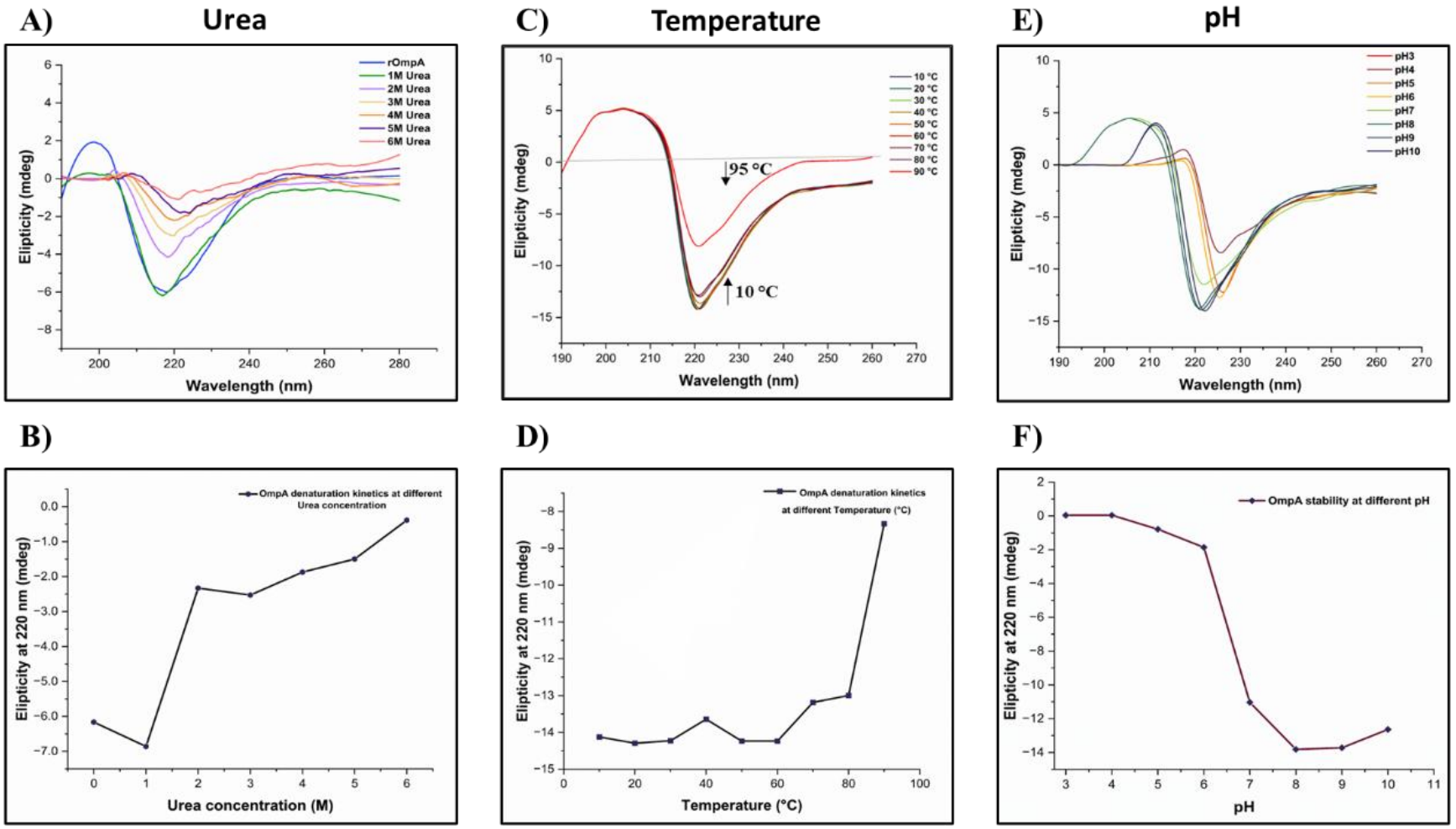

Fig. 3.9 CD spectra analysis of OmpA under varying conditions of urea concentration, pH, and temperature. A) Analysis of the effect of urea on OmpA. **B)** Denaturation kinetics of OmpA with increasing urea concentration. **C)** Analysis of the effect of different temperature conditions on OmpA. **D)** Denaturation kinetics of OmpA with increasing temperature interval. **E)** Analysis of the effect of different pH buffers on OmpA. **F)** Denaturation kinetics of OmpA with varying pH buffers.

Table 3.5 Estimation of the secondary structure content of the OmpA protein in the presence of various lipids and detergents.

Lipids and Detergent (CMC)	Helix	Anti-Parallel	Parallel	Turn	Other	Sparkline	Folding ranking
DMPC (25 nM)	6	24	32.5	2.3	35.2		3
DMPC (100 nM)	0	31.5	36.2	0	32.3		
DOPC (0.200 mM)	11.2	23	30.8	5.2	29.7		2
DOPC (0.500 mM)	0	31.3	36.5	0	32.2		
LDAO (2X)	18.2	27.3	25.5	6.7	32.3		1
LDAO (4X)	0	32.2	36.1	3.4	28.2		
Tween-20 (4X)	0.5	19	38.5	1.4	40.6		
Tween-20 (10X)	0	25.9	33.8	2.9	37.4		
Beta OG (4X)	0	78.2	0	0	21.8		
Beta OG (10X)	0	74.2	0	6.2	19.6		
DDM (4X)	0	21.4	37.7	0.6	40.2		
DDM (10X)	0	35	0	25.3	39.7		
OmpA Without Detrgent/Lipids	0	27.5	27.3	5.9	39.3		

3.2.5 Structural assessment of OmpA protein: Effects of pH, temperature, detergent, and lipids on topology studied using fluorescent spectroscopy

We employed the tryptophan fluorimetry assay to predict the structural arrangement of the OmpA protein. Initially, we identified a total of 5 tryptophan residues within the amino acid sequence of OmpA **(Fig. 3.10A)**. Subsequently, we observed that under its native conditions, the OmpA protein gives maximum emission peaks at 326 nm, called blue-shift, as the tryptophan residues present in the folded OmpA move from aqueous to the hydrophobic environment [138]. Furthermore, we have investigated the folding pattern of folded and denatured proteins in the presence of different concentrations of urea, and the presence of various detergents and lipids.

To investigate the refolding pattern of denatured OmpA, we refold denatured OmpA (6 M urea) by a 10-fold dilution in a Tris-buffer containing protein, detergents (CHAPS, LDAO, and Tween-20), and lipids (DOPC and DMPC). We observed that the refolded protein in the presence of 25 nM exhibited enhanced fluorescence intensity and a blue shift in emission maxima compared to the urea-denatured sample and lipid-free control, indicating successful refolding into a more hydrophobic environment, characteristic of native-like folding (**Fig. 3.10B**). However, when using DOPC at 25 nM and 500 nM, the fluorescence intensity was lower than that observed with DMPC, indicating that DOPC is less effective in stabilizing the native structure of OmpA (**Fig. 3.10C)**. Additionally, when OmpA was refolded in the presence of detergents such as LDAO, Tween-20, β-OG, and DDM **(Fig. 3.10D-G)**, both tested CMC concentrations give higher fluorescence intensities, indicating environments close to native-like conditions. Among these, LDAO and DDM demonstrated the best refolding efficiency, as evidenced by higher fluorescence intensities in comparison to the denatured OmpA and detergent-free control.

Furthermore, we checked the effect of urea on OmpA by incubating the protein in the presence of urea, resulting in a redshift in fluorescence emission peaks from 326 nm to 342 nm with an increase in urea concentration up to 6M **(Fig. 3.11A-B)**. Similarly, a decrease in fluorescence intensity with increasing temperature indicated OmpA denaturation, which remained stable up to 60°C before losing secondary structure stability **(Fig. 3.11C-D)**. Additionally, pH levels between 7.0 and 8.0 were found to be optimal for OmpA stability **(Fig. 3.11E-F)**.

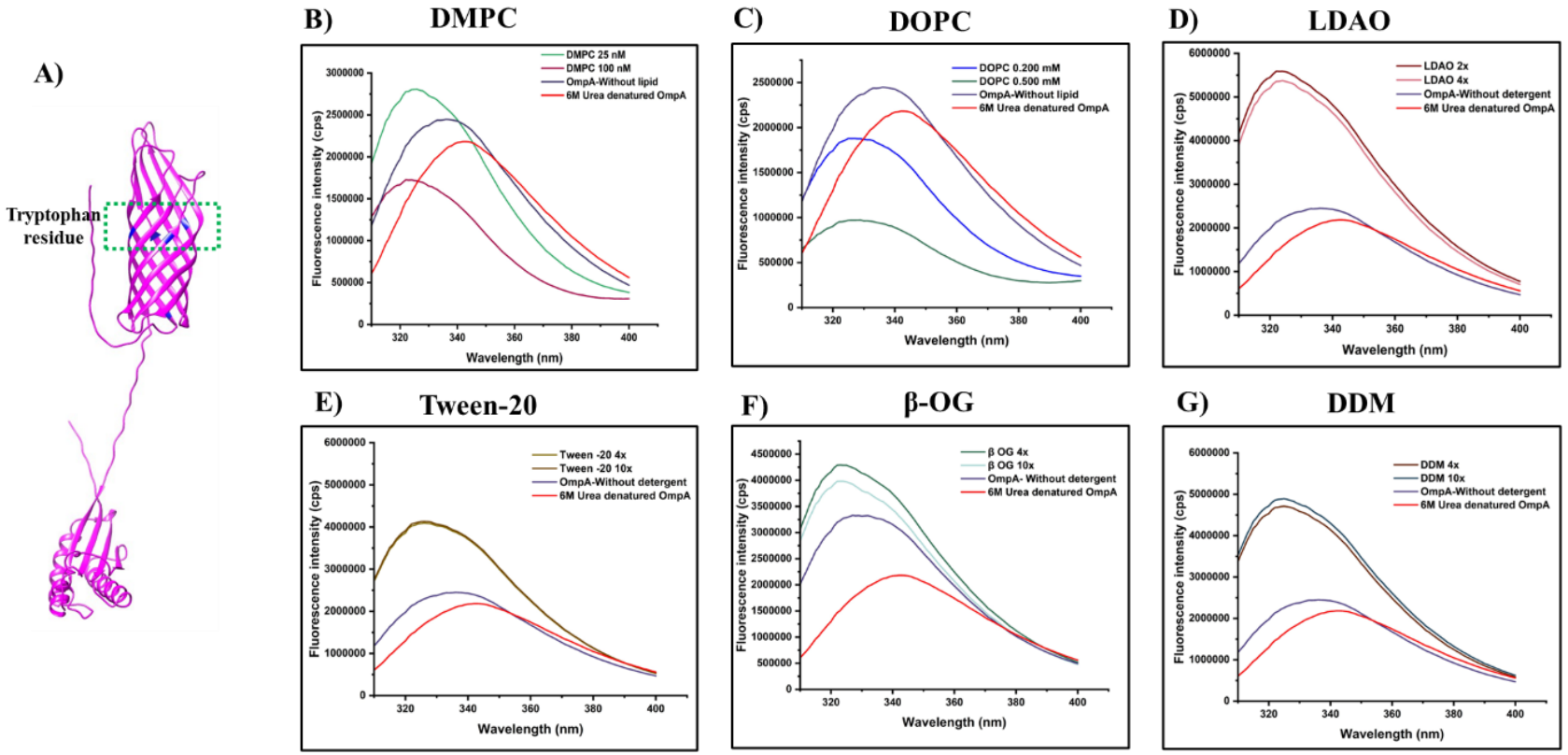

Fig. 3.10 Tryptophan fluorescence analysis of refolded OmpA using different detergents and lipids. A) Prediction of tryptophan residues present in the predicted OmpA model. **(B-C)** Tryptophan fluorescence analysis for refolded OmpA by lipids, with a 10-fold dilution into a buffer containing concentrations of 25 nM and 100 nM, and DOPC at 0.2 mM and 0.5 mM CMC concentrations. **(D-G)** Tryptophan fluorescence analysis for refolded OmpA by detergents, 10-fold dilution into a buffer containing LDAO at 2x and 4x CMC concentrations, and Tween-20, β-OG, and DDM 4x and 10x CMC concentrations, respectively.

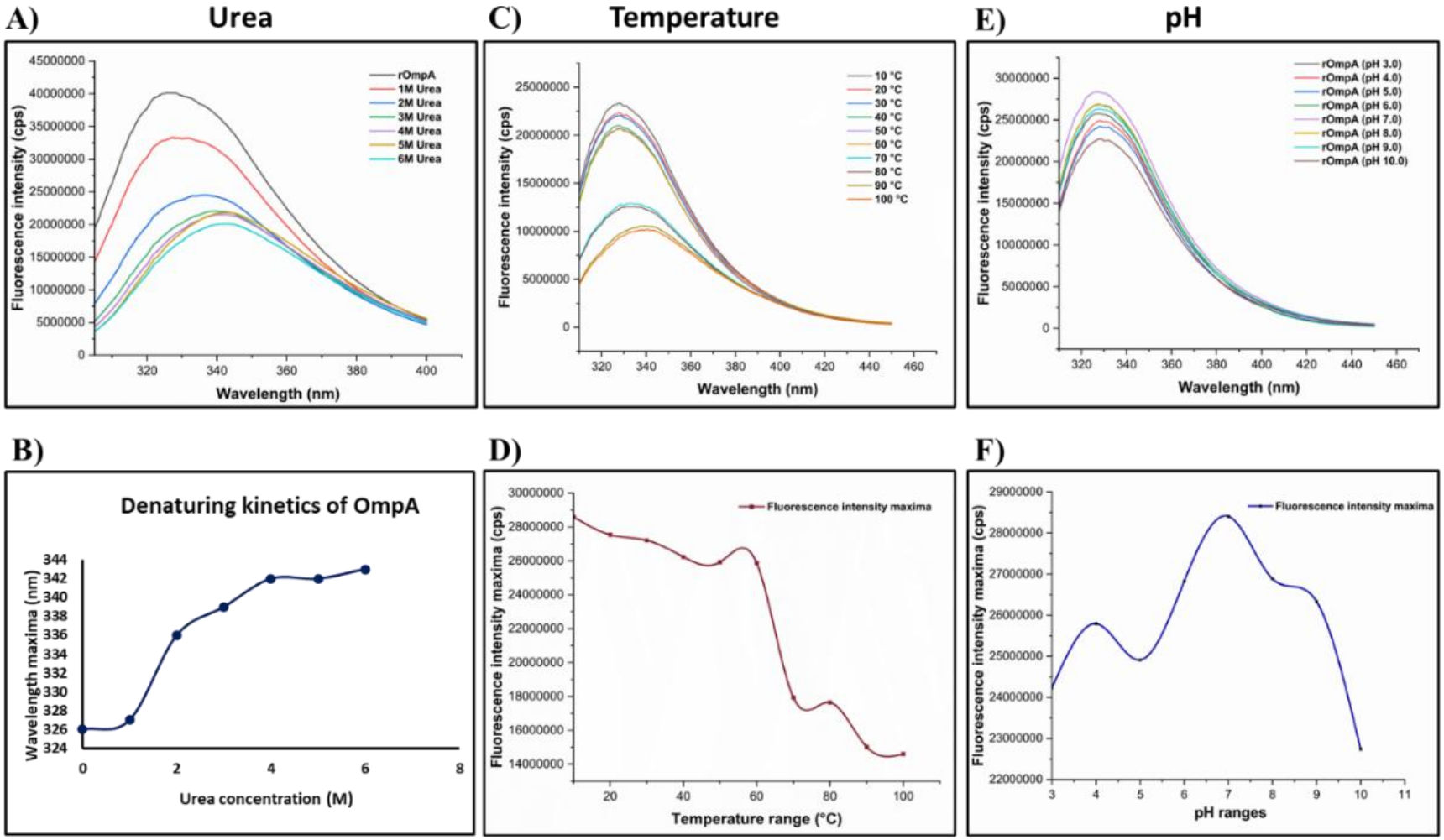

Fig. 3.11 Tryptophan fluorescence analysis of OmpA under varying conditions of urea concentration, pH, and temperature. A) Analysis of the effect of urea on OmpA. **B)** Denaturation kinetics of OmpA with increasing urea concentration. **C)** Analysis of the effect of different temperature conditions on OmpA. **D)** Denaturation kinetics of OmpA with increasing temperature interval. **E)** Analysis of the effect of different pH buffers on OmpA. **F)** Denaturation kinetics of OmpA with varying pH buffers.

3.2.6 Immuno-informatics for prediction of multi-epitopes

Through immuno-informatics analysis, the epitopes of OmpA were identified and screened. In this analysis, we identified 7 MHC class-I **(Table 3.5)**, 7 MHC class-II (**Table 3.6)**, and 19 B-cell **(Table 3.7)** interacting epitopes that were short-listed. The MHC class-I epitopes were further evaluated for class-I immunogenicity, with positive immunogenicity scores were selected. Additionally, the MHC class-I, MHC class-II, and B-cell epitopes were screened for antigenicity, toxicity, and the loop region of OmpA.

In this MHC class-I (KGDNINGAY), MHC class-II (RMPYKGDNINGAYKA, INGAYKAQGVQLTAK, and EYQWTNNIGDANTIG), and B-cell (TAKLGYPITDDLDVYT, GDANTIGTRPDNGLLS, VPGGPSTKDHDTGVSP, GFIHNDGPTHENQLGA, RLEYQWTNNIGDANTI, and DNINGAYKAQGVQLTA) epitopes were selected. A total of 4 conformational extracellular epitopes have been predicted from the OmpA **(Fig. 3.12)** and have a higher score of 0.806 **(Table 3.8)**. The selected epitopes can trigger the host immune response without toxicity, suggesting OmpA as a promising vaccine candidate against *S.* Typhimurium through immuno-informatics screening.

Table 3.6 Interaction of MHC-I interacting epitopes of OmpA protein through NetCTLpan server with class-I epitope immunogenicity, antigenicity, and toxicity analysis. Epitope residues highlighted are located in exposed loops of OmpA.

Sr. no	Start	Epitope sequence	Class-I immunogenicity	Antigenicity	Toxicity
1	21	AAPKDNTWY	-0.04291	Probable non-antigen	Non-toxin
2	85	**KGDNINGAY**	**0.17566**	Probable antigen	Non-toxin
3	98	VQLTAKLGY	-0.119	Probable antigen	Non-toxin
4	219	FTLKSDVLF	-0.33246	Probable antigen	Non-toxin
5	238	GQQALDQLY	-0.09239	Probable antigen	Non-toxin
6	264	FTDRIGSDA	0.09412	Probable antigen	Non-toxin
7	269	GSDAYNQGL	-0.04108	Probable antigen	Non-toxin

Table 3.7 Interaction of MHC-II interacting epitopes of OmpA protein predicted through the IEDB server with their interacting HLA alleles, percentile rank, antigenicity, and toxicity analysis. Epitope residues highlighted are located in exposed loops of OmpA.

Sr. no	HLA alleles	Start	Epitope sequence	Score	Percentile rank	Antigenicity	Toxicity
1	HLA-DRB3*02:02, HLA-DRB3*02:02, HLA-DRB3*02:02, HLA-DRB3*02:02	41	**DTGFIHNDG PTHENQ**	0.9522	0.01	Probable non-antigen	Non-toxin
2	HLA-DRB1*15:01, HLA-DRB1*15:01, HLA-DRB1*15:01,	63	**GYQVNPYVG FEMGYD**	0.9349	0.06	Probable antigen	Non-toxin
3	HLA-DRB3*01:01, HLA-DRB3*01:01, HLA-DRB3*02:02, HLA-DRB3*02:02,	81	**RMPYKGDNI NGAYKA**	0.5884	0.69	Probable antigen	Non-toxin
4	HLA-DRB3*02:02, HLA-DRB3*02:02, HLA-DRB3*02:02, HLA-DRB3*02:02	89	**INGAYKAQG VQLTAK**	0.2314	4.5	Probable antigen	Non-toxin
5	HLA-DRB3*01:01, HLA-DRB3*01:01, HLA-DRB3*01:01	120	**GMVWRADT KSNVPGG**	0.7341	0.31	Probable antigen	Non-toxin
6	HLA-DRB1*07:01, HLA-DRB1*15:01, HLA-DRB1*07:01, HLA-DRB1*07:01	149	**AGGIEYAIT PEIATR**	0.7522	0.76	Probable antigen	Non-toxin
7	HLA-DRB3*02:02, HLA-DRB3*02:02, HLA-DRB3*02:02	165	**EYQWTNNI GDANTIG**	0.5344	0.8	Probable antigen	Non-toxin

Table 3.8 B-cell epitope prediction using the ABCpred tool with its antigenicity analysis. Epitope residues highlighted in red are located in exposed loops of OmpA.

Rank	Sequence	Start position	Score	Antigenicity
1	GMVWRADTKSNVPGGP	120	0.95	Probable antigen
2	TPEIATRLEYQWTNNI	157	0.93	Probable antigen
3	GWSQYHDTGFIHNDGP	35	0.92	Probable non-antigen
4	TAKLG**YPITDDLDVYT**	101	0.88	Probable antigen
5	DWLGRMPYKGDNINGA	77	0.87	Probable antigen
6	**GDANTIGTRPD**NGLLS	173	0.87	Probable antigen
7	TVAQAAPKDNTWYAGA	17	0.87	Probable non-antigen
8	**VPGGPS**TKDHDTGVSP	131	0.86	Probable antigen
9	**GFIHNDGPTHE**NQLGA	43	0.83	Probable antigen
10	TWYAGAKLGWSQYHDT	27	0.83	Probable non-antigen
11	NGLLSVGVSYRFGQQE	184	0.83	Probable antigen
12	HENQLGAGAFGGYQVN	52	0.82	Probable antigen
13	AGGIEYAITPEIATRL	149	0.81	Probable antigen
14	LDVYTRLGGMVWRADT	112	0.81	Probable non-antigen
15	GGYQVNPYVGFEMGYD	62	0.79	Probable antigen
16	HDTGVSPVFAGGIEYA	140	0.75	Probable antigen
17	AIAIAVALAGFATVAQ	5	0.67	Probable non-antigen
18	RLEYQW**TNNIGDANTI**	163	0.67	Probable antigen
19	**DNIN**GAYKAQGVQLTA	87	0.62	Probable antigen

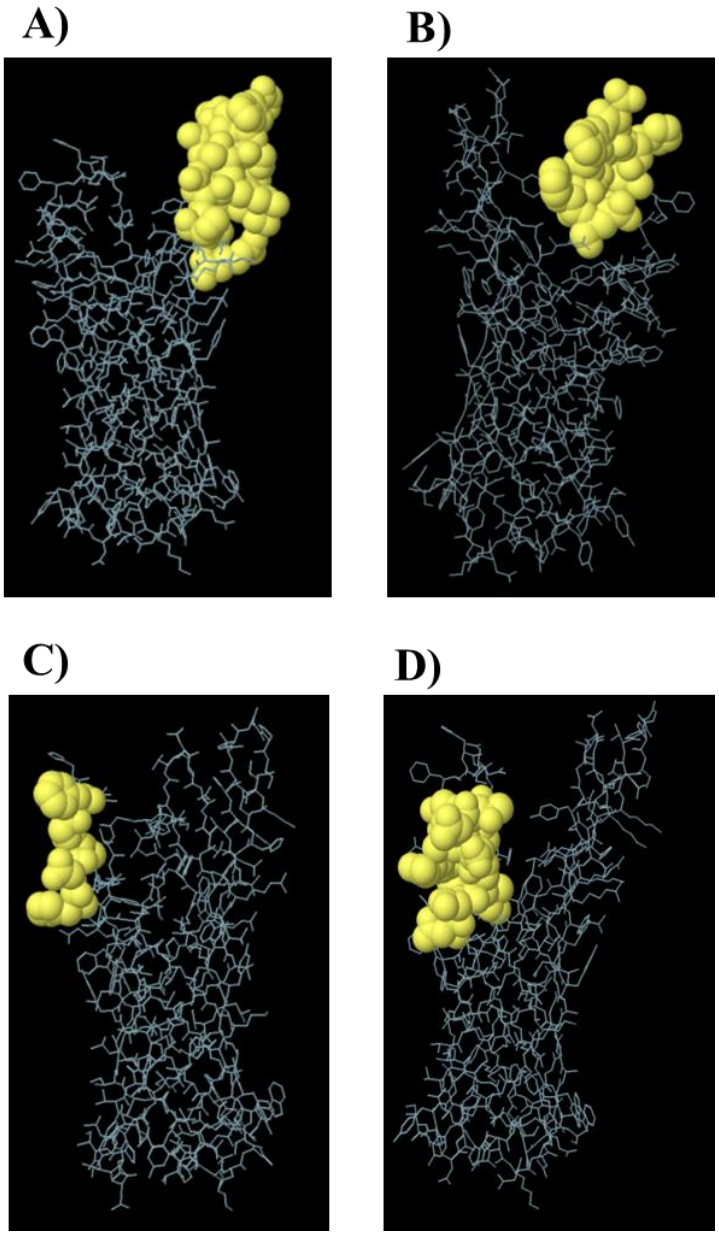

Fig. 3.12 Predicted Discontinuous B-cell Epitopes of OmpA Using the ElliPro Server. (A-D) The three-dimensional representations of the four top-predicted discontinuous B-cell epitopes from the exposed loops of OmpA. The protein backbone is displayed as a blue wireframe, while the residues that compose the epitopes are highlighted as yellow spheres.

Table 3.9 A list of the predicted discontinuous B-cell epitopes, along with their corresponding amino acid residues. Residues located in exposed loop regions are indicated in bold and highlighted in red to represent surface-accessible residues, as shown in **Fig. 3.12A–D.**

Sr. no.	Residues	No. of residues	Score
1	A:R60, A:P62, A:K64, **A:G65, A:D66, A:N67, A:I68**, A:N69, A:G70, A:K107, A:S108, A:N109, A:V110, A:P111, A:G112, A:G113, A:P114, A:S115, A:T116, A:K117, A:D118, A:H119	22	0.806
2	**A:I24, A:H25, A:N26, A:D27, A:G28, A:P29, A:T30, A:H31, A:E32**	9	0.797
3	**A:H19, A:D20, A:T21, A:G22, A:F23**	5	0.771
4	**A:N149, A:N150, A:I151, A:G152, A:D153, A:A154, A:N155, A:T156, A:I157, A:G158, A:T159, A:R160, A:P161**	13	0.665

3.2.7 Immune simulation reveals the potential of OmpA as a vaccine candidate.

Immune simulation using C-ImmSim was used to predict the potential role of OmpA in immune system activation. During an *S.* Typhimurium infection, the activation of the innate immune system contributes to the first line of defense against infection clearance. The innate immune system triggers the activation of various lymphocytes, including dendritic cells, macrophages, T-cells, and B-cells, thereby regulating the inflammatory response to bacteria and antigens that penetrate the intestinal barrier [139]. In our immune simulation study, the OmpA protein was used to predict the activation of the innate immune response by lymphocytes, revealing a predicted increase in macrophage activation after 5 days **(Fig. 3.13A)**. Similarly, there was an increase in immunoglobulin expression (IgM+IgG, IgM, IgG1+IgG2, and IgG2) after 10 days of OmpA stimulation, resulting in a decrease in antigen concentration **(Fig. 3.13B-C)**. There was also a predicted increase in activation of T-helper cells and T-cytotoxic cells with memory development **(Fig. 3.13D-E)**. Elevated levels of cytokines (IFN- and TGF-β) and interleukins (IL-10, IL-2, and IL-12) were predicted following OmpA exposure **(Fig. 3.13F)**.

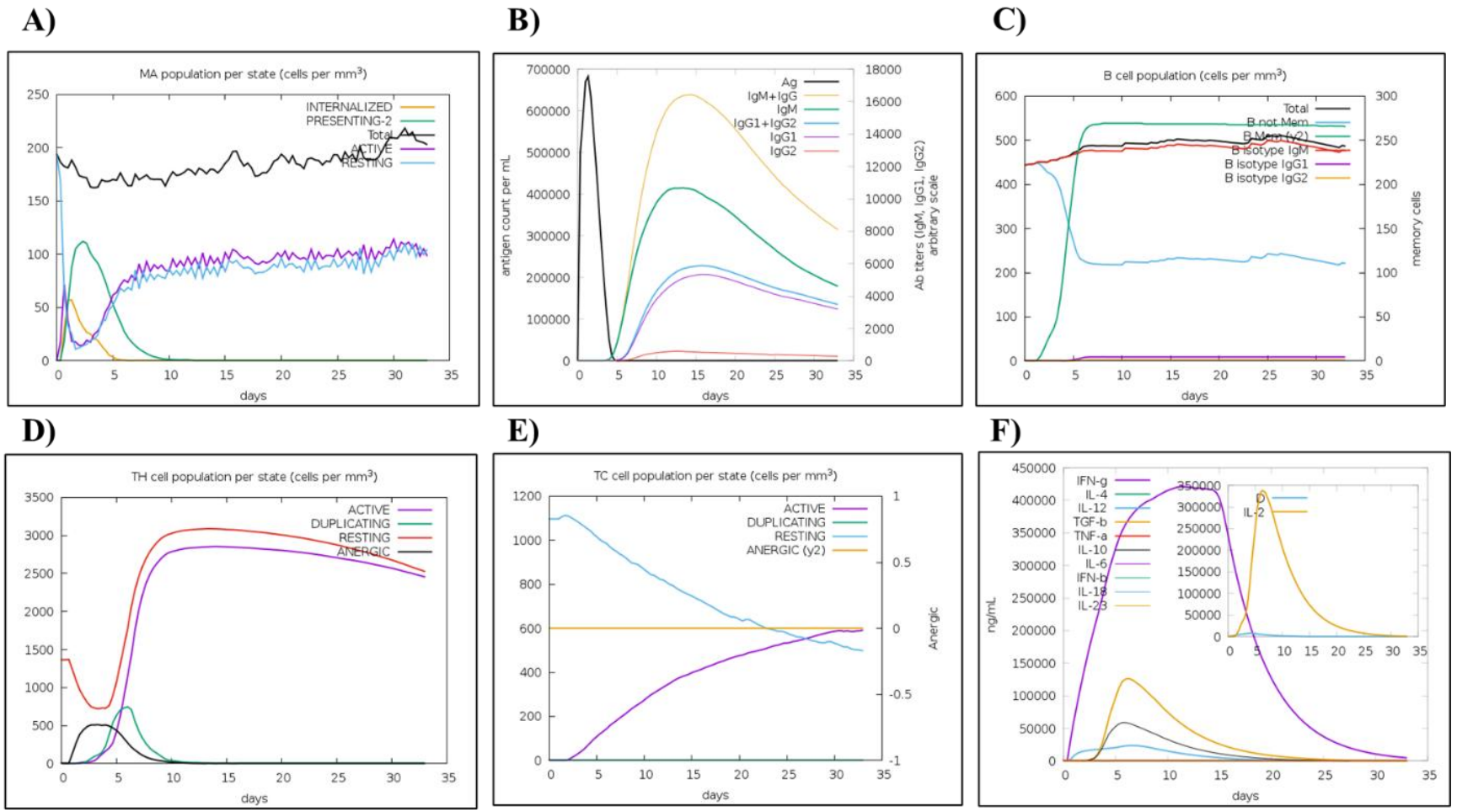

Fig. 3.13 ***In silico*** **immune simulation spectrum using C-ImmSim. A)** Activation of macrophages in response to antigen injection. **B)** Generation of immunoglobulin production and isotypes in response to OmpA exposure. **C)** Evolution of the B-cell population in response to OmpA injection. **D)** Evolution of the helper T-cell population per state (cells/mm^3) in response to OmpA injection. **E)** Evolution of the cytotoxic T-cell population per state (cells/mm^3) in response to OmpA injection. **F)** Production of cytokines (IFN-γ, TGF-β) and interleukins (IL-10, IL-2, and IL-18) upon exposure to OmpA.

3.3 Summary

In this chapter, the *in silico* and biophysical characterization of OmpA from *S.* Typhimurium was investigated. Initially, *in silico* analyses were performed to examine its structural features, including signal peptide prediction, secondary structure analysis, and tertiary structure modeling. Interestingly, computational analysis reveals a high conservation of OmpA within the *Enterobacteriaceae* family. Additionally, OmpA has features typical of β-barrel OMP, including a signal peptide at the N-terminal, a β-barrel structure, and a C-terminal domain located in the periplasmic space.

On the other hand, due to its β-sheet-rich structure, OmpA forms inclusion bodies during overexpression. To address this, we used a high pH buffer for solubilization and refolding with LDAO, which effectively preserves its native structure. OmpA forms a dimer, confirmed by semi-native SDS-PAGE and size exclusion chromatography. Additionally, secondary structures assessment via ATR-FTIR indicated a mixed α-helices, β-sheet, and coiled structures. In addition, CD spectroscopy confirmed that OmpA is rich in β-sheets. We also evaluated various detergents and lipids for refolding and revealed that LDAO is the most effective candidate, as demonstrated through tryptophan fluorimetry and CD spectroscopy. **Table 3.10** summarizes the biochemical and biophysical assays and their findings.

Additionally, we conducted an immunoinformatic analysis to identify B-cell and T-cell epitopes within the extracellular domain of OmpA, highlighting its potential as a vaccine candidate. Notably, immune simulations show that OmpA enhances both innate and adaptive immune responses, facilitating the generation of memory cells and contributing to the elimination of bacterial infections. Overall, this study provides a foundation for developing novel therapeutics against *S.* Typhimurium pathogenesis.

Table 3.10: Summary table of the biochemical and biophysical assays and their inferences.

Sr. no	Category	Assay and techniques used	Experimental readout	Key observation	Inference
1	Protein expression	SDS-PAGE	Expression profile	OmpA expressed as inclusion bodies	Typical behavior of β-barrel outer membrane proteins
	Protein solubilization	Chemical solubilization (Urea, GnHCl, SDS, high-pH buffer)	Solubilization efficiency and yield	High-pH buffer and 6–8 M Urea solubilized OmpA efficiently	High pH and 6–8 M Urea efficiently solubilize OmpA
	Protein purification	Ni-IMAC affinity chromatography	Purity and yield	~94–95% purity; highest yield with high-pH buffer solubilization	Efficient purification of recombinant His-tagged OmpA
	Protein identification	Western blot (anti-His)	Immunoreactive band (~38 kDa)	Single specific band detected	Confirms the identity of purified OmpA
2	Folding assessment	Heat modifiability assay	Mobility shift upon boiling	Unboiled protein migrates faster than boiled protein	Confirms native-like β-barrel folding
3	Oligomeric state	Size exclusion chromatography	Estimation of molecular weight and oligomerization	Major peak at ~72 kDa	OmpA predominantly exists as a dimer
		Semi-native SDS-PAGE	Dimer stability	Dimer is stable unless boiled with β-ME	
4	Protease accessibility	Trypsin digestion assay	Fragment pattern	Protease-resistant (~N- and C-terminal domain observed)	Prediction of domain organization
5	Secondary structure	ATR-FTIR (Amide-I region)	Peak deconvolution	Dominant β-sheet signatures	OmpA is rich in β-sheet structure
	Secondary structure	Far-UV CD spectroscopy	Ellipticity minima (~220 nm)	Restored β-sheet-rich secondary structure	Validates β-barrel refolding
6	Refolding optimization	CD with detergents/lipids	Secondary structure recovery	Best refolding with LDAO, DMPC, DOPC	Membrane-mimetic environments to stabilize OmpA
	Chemical stability	CD (Urea denaturation 0-6 M Urea)	Loss of ellipticity	Progressive unfolding with increasing urea	OmpA stability is urea-sensitive
	Thermal stability	CD (Temperature 10-90 °C)	Ellipticity changes	Stable up to ~60 °C	OmpA shows moderate thermal stability
	pH stability	CD (pH 3–10)	Structural retention	Stable between pH 7.0 and 10.0	Neutral to alkaline pH favors OmpA stability
7	Topology assessment	Tryptophan fluorescence spectroscopy	Emission maximum shift	Blue shift (~326 nm) in folded state	Tryptophan residues are buried in the hydrophobic core, indicating native-like topology
	Refolding efficiency	Fluorescence with detergents/lipids	Intensity enhancement	Highest fluorescence with LDAO and DDM	Membrane-mimetic environments to stabilize OmpA

Chapter 4

Results for Objective 2

Chapter 4
4. Unravelling the Role of OmpA from *S.* Typhimurium in Host TLR2 Interaction and Its Impact on Immune Modulation.

4.1 Introduction

To understand the complex interactions between pathogenic bacteria and the host immune system, it is crucial to study microbial pathogenesis and develop targeted therapeutic interventions. One significant pathogen is *Salmonella enterica* Typhimurium, a Gram-negative facultative intracellular bacterium that is a leading cause of foodborne diseases. This bacterium has evolved various mechanisms to evade the host immune system and establish chronic infections, primarily by manipulating host immune receptors and signaling pathways. A key factor in its pathogenicity is its ability to influence host immune responses, particularly through outer membrane proteins (OMPs) [2,9].

One of the most conserved and abundant OMPs in Gram-negative bacteria is OmpA. Besides contributing to membrane stability, OmpA plays a crucial role in important processes such as invasion, adhesion, and biofilm formation. Furthermore, it protects against oxidative and nitrosative stress [133,140]. Thus, given its potential immunogenic properties, along with its conservation across various bacterial species, OmpA is a significant target for therapeutic interventions and studies on host-pathogen interactions. However, the functional role of OmpA from *S.* Typhimurium in modulating the host immune response has yet to be explored.

Pattern recognition receptors (PRRs) such as Toll-like receptors (TLRs) are central to the first line of defense against pathogens. We hypothesize, based on existing literature, that OmpA is recognized by pathogen-associated molecular patterns (PAMPs) on host cells. We hypothesize that OmpA is recognized by TLRs as a PAMP, particularly TLR2, TLR4, and TLR9, which sense bacterial components [141]. Several studies have identified homologs of OmpA from various bacteria that act as ligands for TLR2. Notably, Yumei Li et al. reported that OmpA from *Acinetobacter baumannii* activates the TLR2-NF-κB signaling pathway, which acts as an initiating signal for the

activation of the NOD-, LRR-, and pyrin domain-containing protein 3 (NLRP3) inflammasome. They also confirmed that silencing TLR2 or NLRP3 inhibited the expression of inflammasome-associated proteins and genes [142]. Moreover, findings from He et al. reported that 43K OMP from *Fusobacterium necrophorum were* involved in the production of inflammatory cytokines such as TNFα through NF-κB activation [143]. Interestingly, findings from Duan et al. revealed that pro-inflammatory cytokines like TNFα are not only critical to the inflammatory process but also induce the expression of activation-induced cytidine deaminase (AID) through NF-κB signaling [93]. AID is a crucial enzyme that belongs to the cytidine deaminase family, responsible for converting cytosine nucleotides into uracil in RNA. It is predominantly expressed in the germinal centers of activated B-cells and plays a pivotal role in inducing somatic hypermutation (SHM) and class switch recombination (CSR). These processes are essential for improving antibody affinity and helping the immune system combat a variety of pathogens [80,85].

Investigating the interaction between *S.* Typhimurium OmpA and host TLR2 is crucial for understanding how bacteria modulate host immunity. To achieve this, we employed an integrated approach to validate the interaction between OmpA and TLR2. To investigate the interaction of OmpA from *S.* Typhimurium with TLR2, we initially conducted an *in silico* docking analysis focused on the extracellular domain of OmpA and selected TLR2 for this study. We have experimentally validated this interaction and explored OmpA-mediated interactions with host cells using two distinct cell line models. The HEp-2 cell line, which is derived from human laryngeal carcinoma, serves as a model for studying pathogen-epithelial interactions. Meanwhile, Raji cells, a B-cell line derived from human Burkitt lymphoma, were used to investigate immune modulation. We validated this interaction using pulldown assays, co-immunoprecipitation, and co-localization studies. Additionally, we analyzed the mRNA and protein expression levels of TLR2 to assess its potential role in activating host cell receptors and initiating downstream signaling events. Furthermore, we investigated OmpA's ability to induce an immune response in B-cells and analyzed the activation of NF-κB expression, which is crucial for the production of inflammatory cytokines such as TNFα and for the induction of AID expression.

In conclusion, these findings provide an insight into how *S.* Typhimurium OmpA interacts with TLR2 to affect host immune signaling. This research not only enhances our understanding of *Salmonella's* virulence strategies but also suggests the potential for targeting OmpA-TLR2 interactions in developing novel therapeutic approaches to combat *Salmonella* infections.

4.2 Results

4.2.1 Interaction between OmpA with TLR2 using *In Silico* Analysis

To investigate the interaction of OmpA and host cell receptors, we conducted an interaction analysis of OmpA with the TLR2 receptor. In our docking analysis, we screened the top OmpA-TLR2 complexes based on their maximum binding energies **(Fig. 4.1A-D)**. Among these complexes, we selected a model that primarily interacts with the extracellularly exposed loop regions of OmpA and demonstrates a favorable maximum binding energy of -10.6 kcal/mol. This indicates a significant interaction between the external loop of OmpA and TLR2, and this model was used for further analysis **(Fig. 4.1B)**.

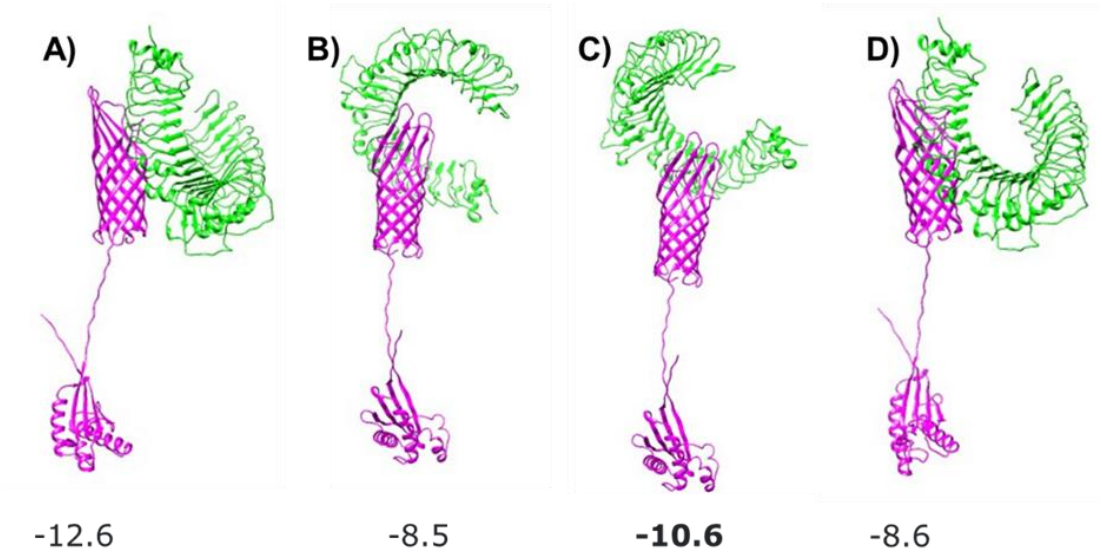

Fig. 4.1 Interaction between OmpA with TLR2 using *In Silico* Analysis. A docking study of the OmpA protein with TLR2 was performed using the HawkDock server V2, and the binding energy of the interaction was calculated using the Prodigy web server, from which the top model was selected.

Additionally, we utilized the iMOD server to perform Normal Mode Analysis (NMA) to evaluate the stability of the OmpA complexed with TLR-2. The iMOD analyzed the structure by adjusting the complex force field at different time intervals. These findings are shown in **Fig. 4.2A-G.** In NMA, B-factor values are proportional to the root mean square. The eigenvalue for the OmpA-TLR2 complex was 3.96×10^{-7}, indicating the energy required to deform the structure. The covariance matrix shows residue correlations, and the elastic network model depicts connections between atoms as springs. These results suggest that the OmpA-TLR2 complex has stable interactions.

4.2.2 Biochemical and Cellular Validation of OmpA-TLR2 Interaction in HEp-2 and Raji Human B-cells

Interestingly, *in silico* studies suggested that OmpA interacts with TLR2. To validate this interaction, we performed an *in vitro* pull-down assay. Whole cell lysate was incubated with OmpA overnight, followed by a pull-down using a Ni-NTA column. The interaction was then analyzed through Western blotting with anti-His and anti-TLR2 antibodies. As anticipated, our *in vitro* pull-down assay confirmed the interaction between OmpA and TLR2 **(Fig. 4.3A-B)**. Additionally, we performed a co-immunoprecipitation assay, immunoprecipitating TLR2 from HEp-2 and Raji human B-cells using an anti-TLR2 antibody. The presence of the OmpA-His protein was detected using an anti-His antibody. Likewise, we immunoprecipitated OmpA from HEp-2 and Raji human B-cells using an anti-His antibody, and the presence of the TLR2 protein was detected with the anti-TLR2 antibody **(Fig. 4.3C)**.

Furthermore, we performed a co-localization assay of OmpA and TLR2 proteins using immunofluorescence staining. This involved the use of an anti-His tag mouse monoclonal antibody alongside an anti-TLR2 rabbit monoclonal antibody in HEp-2 and Raji human B-cells. In Hep2 cells, the control group shows minimal background green signal, while TLR2 exhibits constitutive red signal expression with a cytoplasmic distribution. When stimulated with OmpA, TLR2 relocates to the peripheral membrane, resulting in a change in distribution. This stimulation causes a distinct co-localization of OmpA and TLR2 at the periphery of the cell membrane, leading to a yellow-orange merged signal **(Fig. 4.4A)**.

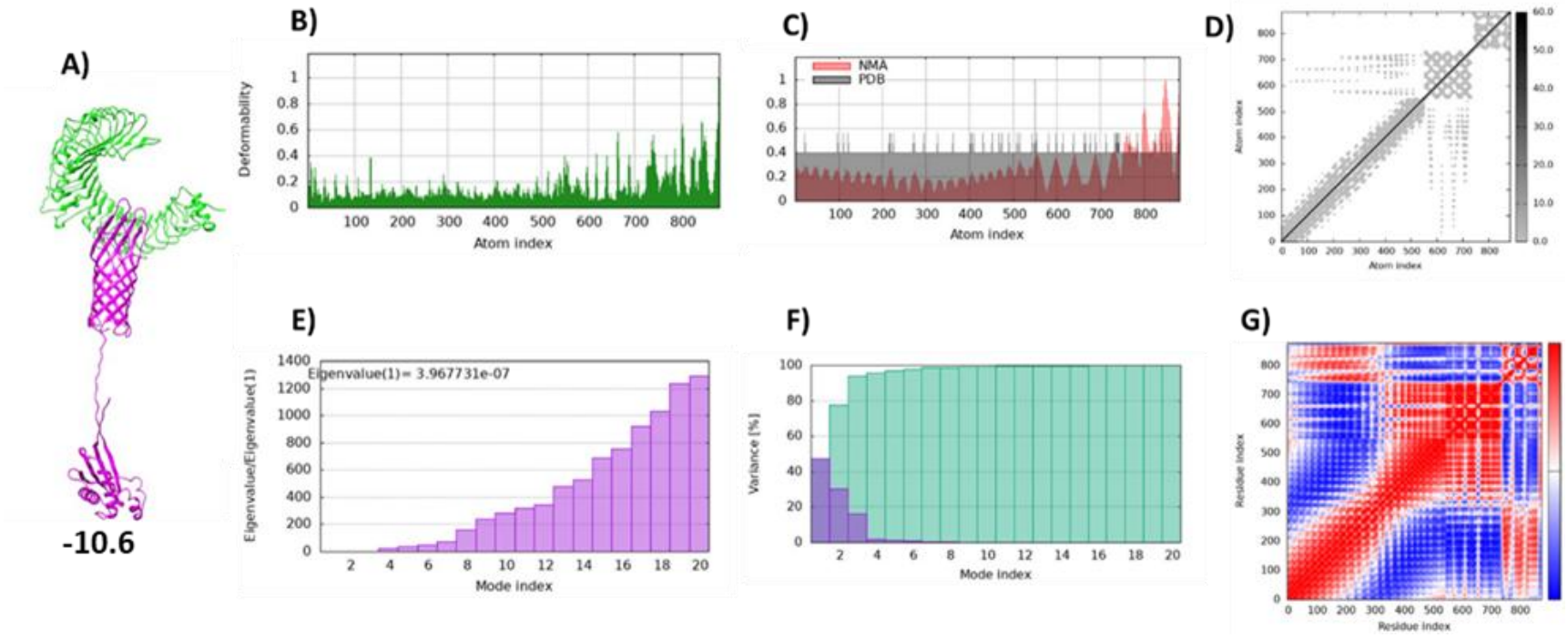

Fig. 4.2 Molecular dynamics simulation of OmpA-TLR2 complex by the iMODs server. **A)** OmpA-TLR2 complex. **B)** Deformability of complex. **C)** B-factor of the complex. **D)** shows an elastic network (stiffer region indicated by a darker grey color). **E)** Eigenvalue of the complex. **F)** Cumulative variance is shown in green and variance in red. **G)** Correlated, anti-correlated, and noncorrelated variance maps indicated by red, blue, and white colors, respectively.

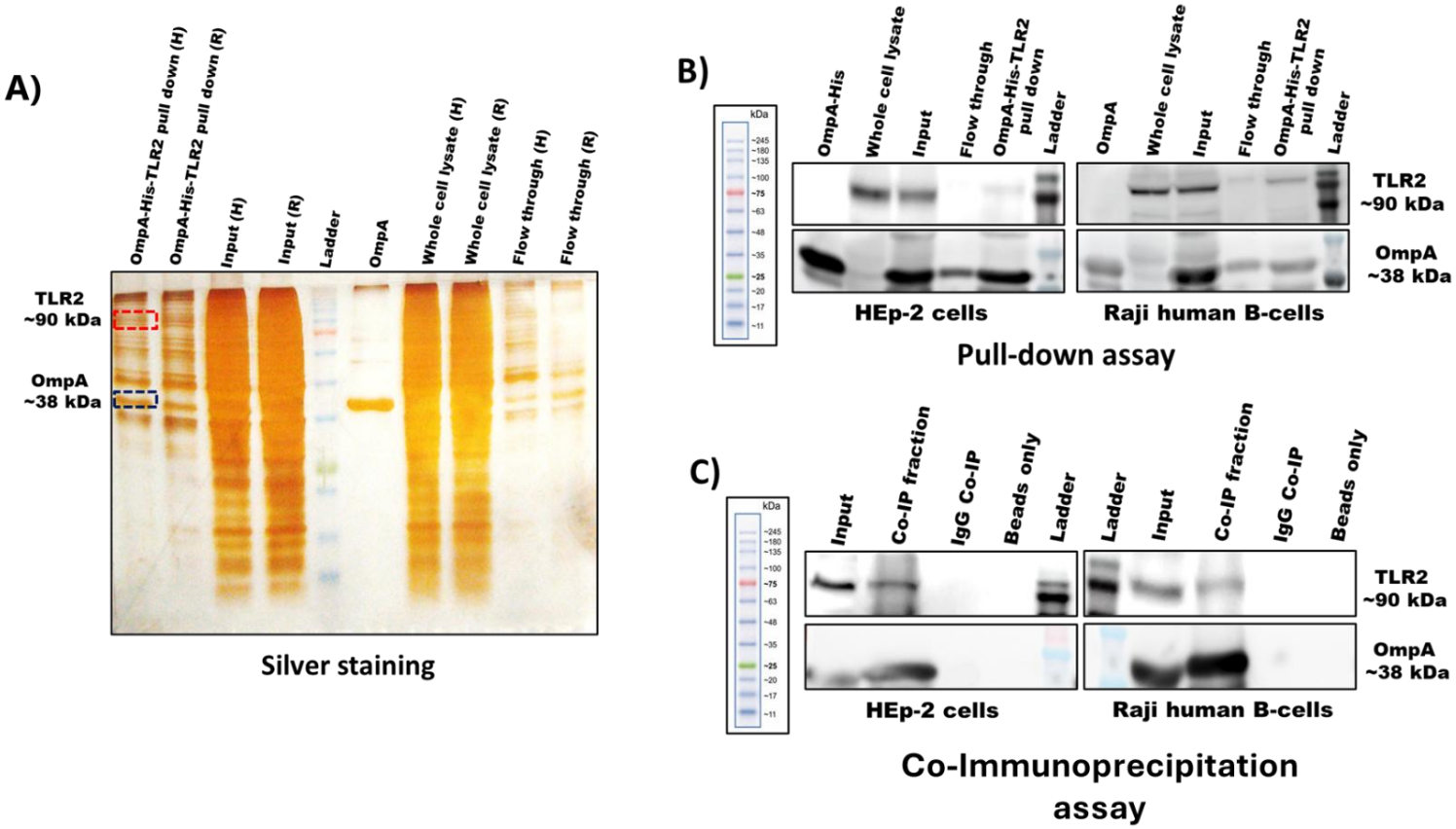

Fig. 4.3 Analysis of the interaction between OmpA and TLR2 in HEp-2 and Raji human B-cells. A) Silver-stained SDS-PAGE shows fractions from a pull-down assay illustrating HEp-2 cells (H) and Raji human B-cells (R). **B)** His-tagged pull-down assay for OmpA interaction with TLR2. His-tagged OmpA was immobilized on Ni-NTA beads, followed by incubation with whole cell lysate from HEp-2 and Raji human B-cells, and analyzed by Western immunoblotting using anti-His or anti-TLR2 antibodies. **C)** Co-immunoprecipitation of His-tagged OmpA with whole-cell lysates was performed using anti-His antibodies in conjunction with protein A/G agarose beads. The resulting precipitated complexes were subsequently analyzed by Western immunoblotting, utilizing anti-TLR2 to detect TLR2. In a similar approach, Co-immunoprecipitation of His-tagged OmpA was conducted with whole-cell lysates using anti-TLR2 antibodies alongside protein A/G agarose beads. The resulting precipitated complexes were then analyzed via Western immunoblotting, employing anti-His antibodies to identify the OmpA protein.

In Raji human B-cells, TLR2 expression, indicated by fluorescence intensity, is minimal in control cells, displaying heterogeneous expression. However, in OmpA-stimulated cells, OmpA is primarily localized on the cell surface and shows an interaction with TLR2. Additionally, the fluorescence intensity levels of TLR2 are significantly higher in samples stimulated with OmpA compared to the control samples **(Fig. 4.4B)**.

4.2.3 OmpA Stimulation Enhances TLR2 Expression and Activates the NF-κB–AID axis in B-cells

To investigate the expression of TLR2 in response to OmpA interaction in HEp-2 and Raji human B-cells, we performed analyses using RT-PCR and Western immunoblotting. The mRNA expression using RT-PCR results indicated that OmpA stimulation upregulated TLR2 expression in HEp-2 and Raji human B-cells. Notably, HEp-2 cells exhibited a considerable increase in TLR2 mRNA expression up to 8 h post-OmpA stimulation, whereas Raji human B-cells reached their peak expression at 24 h **(Fig. 4.5A-C)**. Additionally, Western immunoblotting results showed that OmpA stimulation also enhanced TLR2 protein expression in both HEp-2 and Raji human B-cells. Specifically, HEp-2 cells showed a notable increase in TLR2 protein expression up to 8 h, while Raji human B-cells notably higher expression level at 4 h following OmpA stimulation **(Fig. 4.5D-G)**.

We further investigated host cell activation and gene expression changes following OmpA stimulation in Raji human B-cells, which demonstrated that the interaction between OmpA and TLR2 may trigger NF-κB activation, which in turn upregulates the expression of downstream genes such as AID, a key enzyme involved in the CSR and SHM, and pro-inflammatory cytokines like TNFα **(Fig. 4.6A)**. Interestingly, OmpA stimulation significantly upregulated NF-κB-p65 expression at 8 h post-stimulation (1.44-fold), and this elevated level was maintained up to 24 h (1.35-fold) **(Fig. 4.6B)**. Additionally, TNFα expression markedly increased at 8 h (2.27-fold) before declining to 1.27-fold at 24 h **(Fig. 4.6C)**. Furthermore, AID expression significantly increased, reaching 3.03-fold at 24 h **(Fig. 4.6D)**.

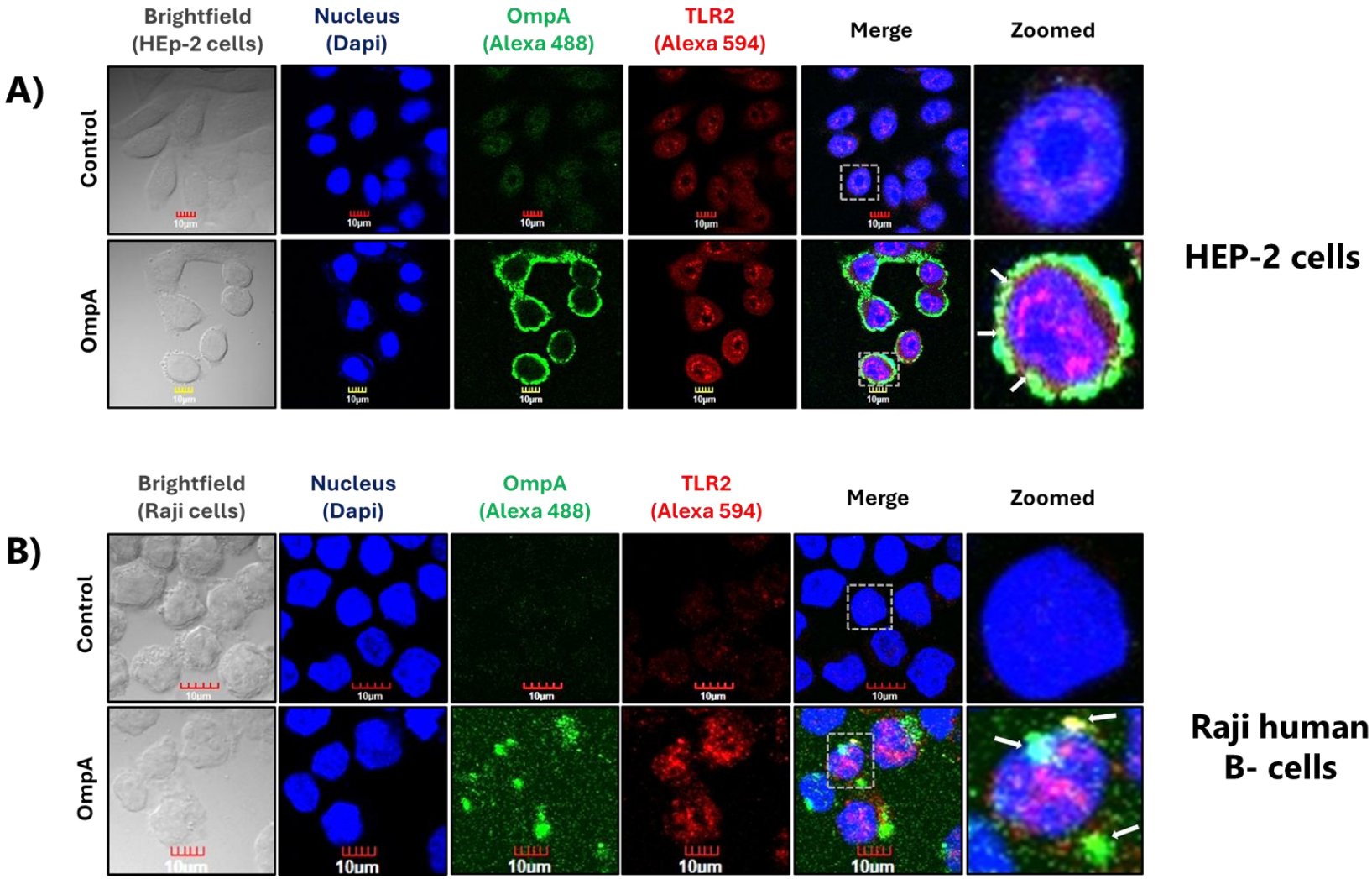

Fig. 4.4 Analysis of the interaction between OmpA and TLR2 in HEp-2 and Raji human B-cells. A) Co-localization of OmpA with TLR2 in HEp-2 cells was observed. The cells were fixed and stained using anti-His and anti-TLR2 antibodies. OmpA and TLR2 are predominantly localized at the cell surface. Yellow spots indicate the co-localization of OmpA with TLR2. **B)** Co-localization of OmpA with TLR2 in Raji human B-cells was observed. The cells were fixed and stained using anti-His and anti-TLR2 antibodies. OmpA and TLR2 are predominantly localized at the cell surface. Yellow spots indicate the co-localization of OmpA with TLR2.

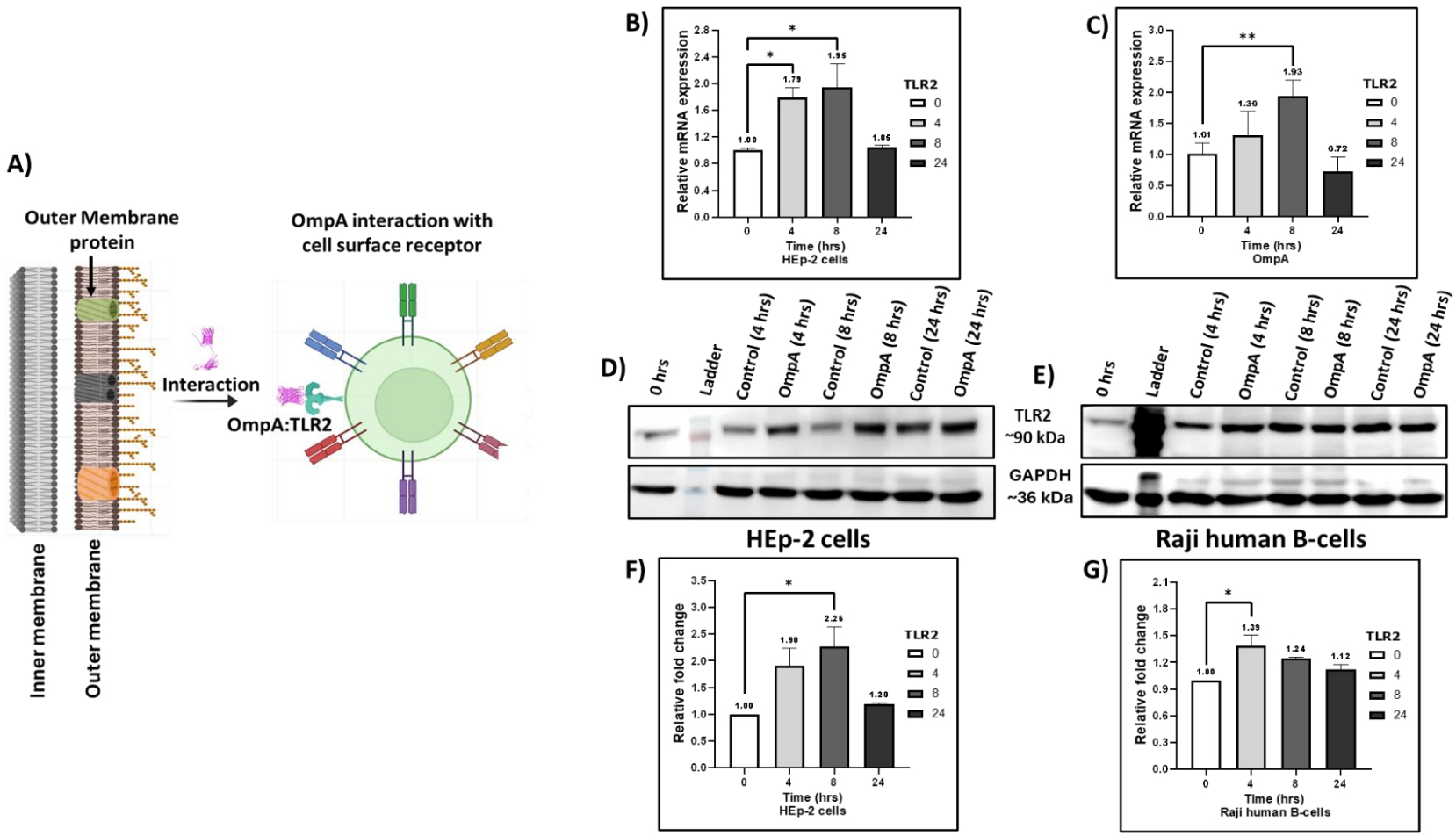

Fig. 4.5 OmpA-induced TLR2-mediated cell activation in HEp-2 and Raji human B-cells. A) Schematic illustration of OmpA's interaction with TLR2. **B)** mRNA expression levels of TLR2 in HEp-2 cells treated with OmpA were assessed at various time intervals. **C)** Similarly, TLR2 mRNA expression in Raji human B-cells was evaluated at different time points. **D)** Immunoblot analysis was conducted to determine TLR2 expression in OmpA-stimulated HEp-2 cells at multiple time intervals. **E)** Additionally, immunoblot analysis of TLR2 expression was performed in OmpA-stimulated Raji human B-cells across various time points. GAPDH served as a housekeeping gene for normalization purposes. Data indicating significant differences ($p < 0.05$) from the control group are marked with an "∗." Statistical significance was determined using analysis of variance (ANOVA) with the following designations: (*$p \leq 0.05$; **$p \leq 0.01$; *** $p \leq 0.001$), analyzed using PRISM 8.0.

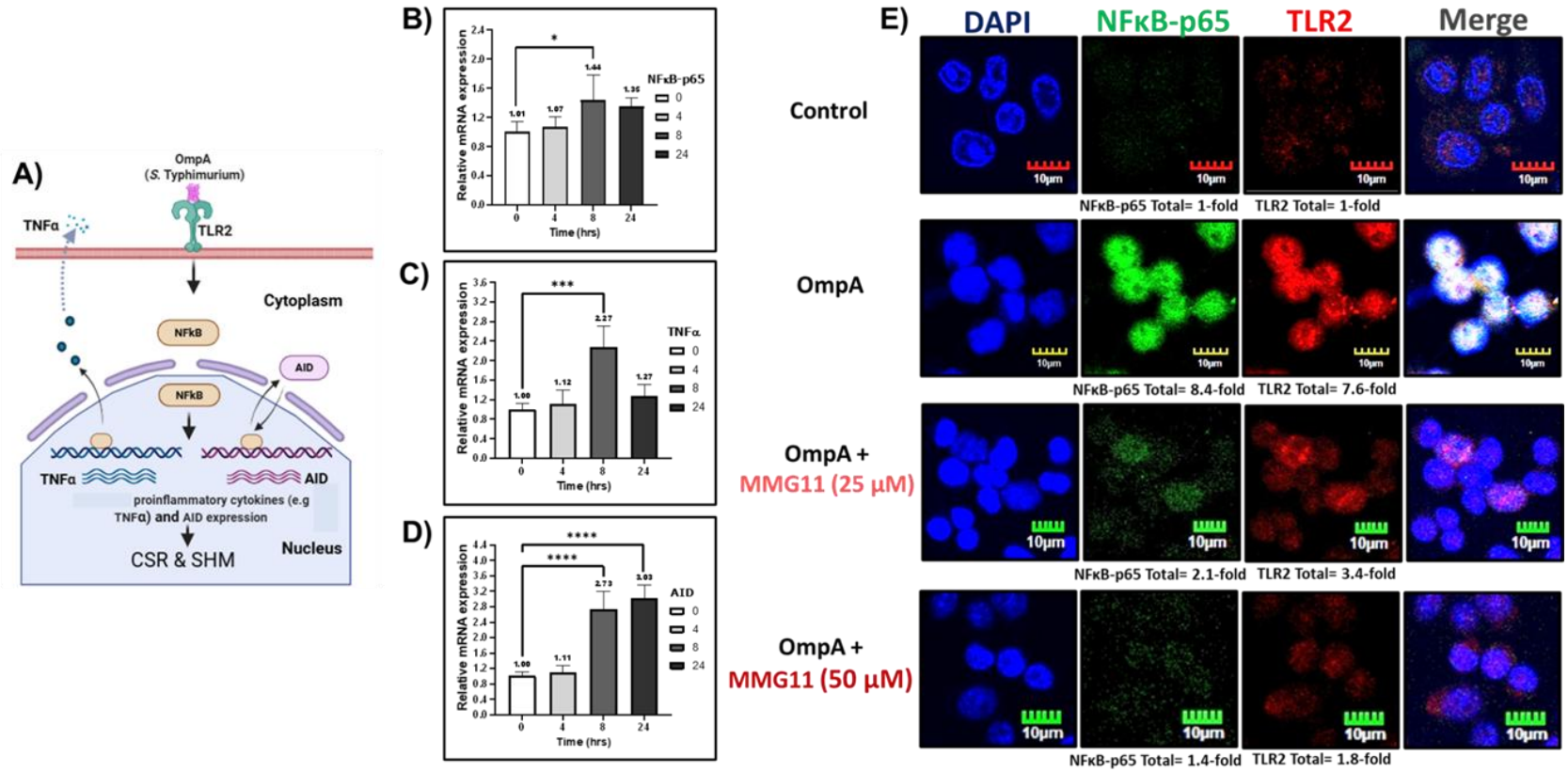

Fig. 4.6 TLR2-mediated NF-κB activation induces TNFα and AID expression, which is inhibited by MMG11 in Raji human B-cells. A) Schematic representation shows OmpA interacts with TLR2 on B-cells, activating NF-κB and inducing proinflammatory cytokines like TNFα, as well as upregulating AID, promoting CSR and SHM. **B-D)** Relative mRNA expression levels of NF-κB-p65, TNFα, and AID in Raji human B-cells treated with OmpA were evaluated at different time points. GAPDH served as a housekeeping gene for normalization purposes. **E)** Immunofluorescence showed an increased expression of NF-κB-p65 (green), indicating enhanced nuclear translocation, as well as increased TLR2 (red) expression in Raji human B-cells following OmpA stimulation. DAPI (blue) was used to stain the nuclei. Treatment with the TLR2 inhibitor MMG11 at concentrations of 25 μM and 50 μM reduced NF-κB expression in a dose-dependent manner, suggesting a decrease in nuclear translocation. Scale bar: 10 μm. Data indicating significant differences ($p < 0.05$) from the control group are marked with an "∗." Statistical significance was determined using analysis of variance (ANOVA) with the following designations: (*$p \leq 0.05$; **$p \leq 0.01$; *** $p \leq 0.001$), analyzed using PRISM 8.0.

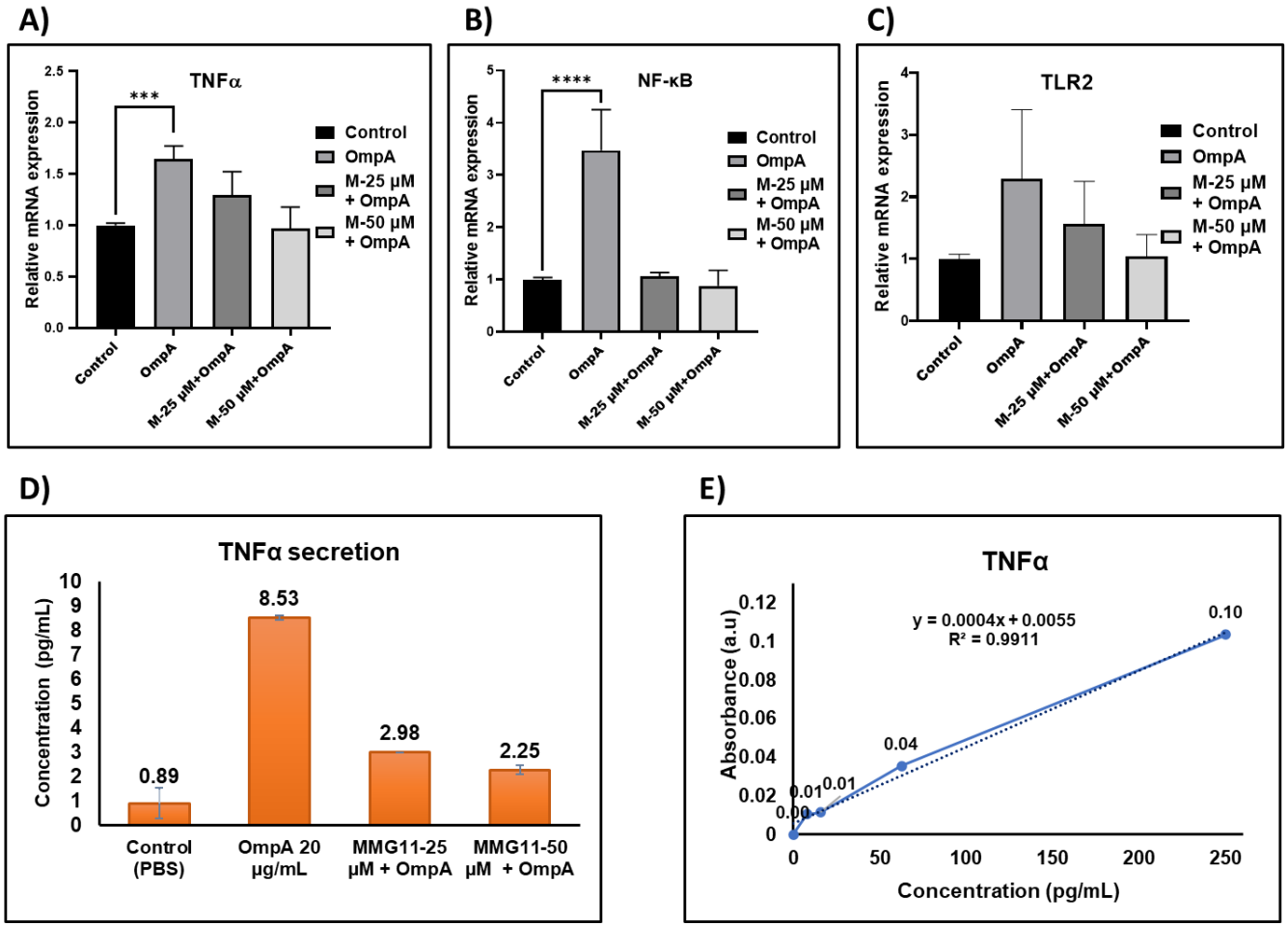

Fig. 4.7 Effect of OmpA and TLR2 inhibitor on TLR2, NF-κB, and TNF-α expression in Raji human B-cells. Cells were treated with OmpA alone or in combination with the pretreated TLR2 inhibitor MMG11 (25 µM and 50 µM). **A)** Relative mRNA expression of TLR2. **B)** Relative mRNA expression of NF-κB-p65. **C)** Relative mRNA expression of TNF-α. Data represents the mean ± SD of two independent experiments. Statistical significances were calculated by analysis of variance (*p ≤ 0.05; **p ≤ 0.01; ***p ≤ 0.001; ****p ≤ 0.0001). Quantification of TNF-α secretion in Raji human B-cells by ELISA. **D)** TNF-α levels measured in Raji human B-cells stimulated with OmpA, with or without pretreatment using the TLR2 inhibitor MMG11 (25 µM and 50 µM). **E)** Standard curve generated for TNF-α quantification.

Furthermore, the role of TLR2 in OmpA-mediated NF-κB activation was validated using immunofluorescence and RT-PCR analyses. OmpA stimulation led to an increase in TLR2 expression and NF-κB-p65 activation, indicating that OmpA engages TLR2 to initiate downstream signaling. This mechanism was further confirmed using the TLR2 inhibitor MMG11. Pre-treatment with MMG11 (25 μM and 50 μM) resulted in a dose-dependent reduction in both TLR2 expression and NF-κB-p65 activation at the mRNA **(Fig. 4.7A-C)** and protein levels **(Fig. 4.6E)**. demonstrating that OmpA-induced signaling is TLR2 dependent.

Consistent with NF-κB-p65 activation, OmpA stimulation significantly increased TNF-α secretion, as quantified by ELISA. Notably, MMG11 pre-treatment at both concentrations (25 μM and 50 μM) substantially reduced TNF-α secretion (**Fig. 4.7D, E)**, further confirming that the pro-inflammatory response increased by OmpA occurs through TLR2-driven NF-κB signaling. Collectively, these findings suggest that OmpA may involve and activate the TLR2–NF-κB-p65 signaling in B-cells, resulting in the induction of pro-inflammatory cytokine responses.

4.3 Summary

To investigate the interaction of OmpA from *S*. Typhimurium with the host cells, we explored its interaction with TLR2, a receptor involved in recognizing bacterial outer membrane components and mediating immune responses. We initially conducted an *in silico* docking analysis focused on the extracellular domain of OmpA and selected TLR2 for this study. The analysis revealed that the extracellular region of OmpA plays a crucial role in interacting with the host cell surface receptor.

Furthermore, we experimentally validated the interaction between OmpA and TLR2 and investigated how OmpA interacts with host cells using two different cell line models. The HEp-2 cell line, which is derived from human laryngeal carcinoma, serves as a model for studying pathogen-epithelial interactions. Meanwhile, Raji cells, a B-cell line derived from human Burkitt lymphoma, were used to investigate immune modulation. We validated this interaction using pulldown assays, co-immunoprecipitation, and co-localization studies. Furthermore, our findings revealed that OmpA stimulation enhances TLR2 expression and induces pro-inflammatory

cytokine production, such as TNFα, through NF-κB activation in Raji human B-cells, contributing to inflammation. Additionally, we observed that OmpA plays a role in inducing AID expression, which is essential for generating antibody diversity in immunoglobulins.

Notably, pre-treatment with MMG11, a TLR2 inhibitor, significantly decreased the expression levels of both TLR2 and NF-κB in a dose-dependent manner. This confirms the essential role of TLR2 in mediating these immune responses. Overall, our findings suggest that OmpA interacts with and activates TLR2, resulting in increased expression of NF-κB-p65. Therefore, in this study, OmpA serves a dual function; it connects innate immune activation through TLR2/NF-κB signaling to an adaptive immune response via AID expression. These findings enhance our comprehension of OmpA as an immunomodulatory agent and indicate its potential as a therapeutic or vaccine target for *Salmonella* infections.

Chapter 5

Results for Objective 3

Chapter 5

5. Unraveling the Impact of Outer Membrane Protein, OmpA, from *S.* Typhimurium on Aberrant AID Expression and IgM to IgA Class Switching in Human B-cells.

5.1 Introduction

Salmonella enterica serovar Typhimurium (*S.* Typhimurium), a Gram-negative bacterium, is known to cause gastrointestinal infection globally, significantly worsened by antibiotic resistance [2,144]. The pathogenic nature of *Salmonella* is driven by its capacity to interact with host cells, manipulate immune responses, and persist within its human and animal hosts [139]. Long-lasting infections with *Salmonella* may increase the risk of developing colon cancer [145]. Mirzarazi et al, conducted a study comparing the proteomics of isolated *Escherichia coli* from colorectal cancer (CRC) and healthy individuals. Their findings showed increased expression of OmpA protein in CRC patients, impacting the colon cancer apoptosis pathway by significantly reducing the expression of pro-apoptotic genes Bax and Bak, as well as expression of p53, driving the metastasis phenomenon [146].

At the forefront of this pathogenic event, *Salmonella* uses the family of outer membrane proteins (OMPs), which serve as a critical interface between the bacterium and the host. Among these OMPs, OmpA is highly conserved and remarkably abundant in various *Salmonella* serovars [147]. Structurally, OmpA is a porin protein characterized by a unique β-barrel integrated into the outer membrane of Gram-negative bacteria. It also possesses externally exposed loops and periplasmic turns [43]. These features give OmpA various functions, including aiding in biofilm formation, regulating outer membrane permeability in response to environmental stress, and causing disease when it invades host cells [43,148,149].

While studies on OmpA and its interactions with B-cell surface receptors (BCR) are limited, we hypothesize, based on existing literature, that OmpA is recognized by pathogen-associated molecular patterns (PAMPs) on B-cells. This recognition occurs particularly through toll-like receptors (TLRs) such as TLR2, TLR4, and TLR9, which

are known to sense bacterial components, as reported by Bekeredjian-Ding and Jego [141]. Interestingly, Yumei Li et al. reported that OmpA from *Acinetobacter baumannii* activates the TLR2-NF-κB signaling pathway, which acts as an initiating signal for the activation of the NOD-, LRR-, and pyrin domain-containing protein 3 (NLRP3) inflammasome. They also confirmed that silencing TLR2 or NLRP3 inhibited the expression of inflammasome-associated proteins and genes [142].

During infection, naive B-cells initially differentiate in secondary lymphoid organs upon antigen recognition, rapidly becoming short-lived plasmacytes that produce bursts of short-lived IgM antibodies with low affinity. Once activated, most B-cells move into the germinal center, where they undergo somatic hypermutation (SHM) and class switch recombination (CSR) [80,150]. A key player in immune interactions is activation-induced cytidine deaminase (AID), mainly expressed in B-lymphocytes within the germinal center. AID deaminates deoxycytidines to deoxyuridines, introducing mutations and DNA breaks, which are essential for generating antibody diversity and class switching in B-cells [80,151]. SHM introduces single-point mutations in the immunoglobulin gene's variable region to enhance antigen affinity maturation. CSR replaces the heavy chain constant region Iμ with Cγ, Cα, or Cε, modulating antibody function and promoting high-affinity B-cell proliferation [152,153]. These processes are crucial for immunity but need tight regulation to avoid off-target effects that can impair affinity maturation, cause genomic instability, and promote cancer progression [79,80,86]. In B-cells, a lack of AID expression leads to hyper-IgM syndrome. For example, mutations in AID expression in humans cause hyper-IgM syndrome type 2, marked by high IgM levels, decreased SHM, and impaired CSR [87]. Similarly, a study by Tamrakar and Kodgire showed that OMPs from *Helicobacter pylori*, specifically HomA and HomB, reduce AID expression and modulate B-cell responses.

In this research, we aimed to uncover the secrets of how OmpA affects AID expression in B-cells will provide valuable insight into the interplay between *Salmonella* infection and the antibody diversification mechanism. We cloned the *ompA* gene to purify recombinant OmpA and characterized the refolded protein by using

various biophysical techniques such as size exclusion chromatography (SEC), heat modifiability assay, CD spectroscopy, and tryptophan fluorescence spectroscopy. These methods confirmed the secondary structure rich in β-sheets and the structural arrangement of the folded state, as described in **Chapter 3**. Next, we examined the impact of OmpA on B-cell viability using the MTT assay and the trypan blue exclusion method. Additionally, we conducted a cell proliferation study utilizing Ki-67 and PCNA (Proliferating Cell Nuclear Antigen). We focused on the regulation of AID expression, particularly analyzing transcription factors such as PAX5, cMYC, STAT6, and SMAD3, which act as activator, and cMYB and E2F1 act as repressors in driving AID expression regulation. Additionally, we also assessed the effect of aberrant AID expression on CSR activity. Interestingly, we observed that OmpA-stimulated B-cells upregulate AID expression at both mRNA and protein levels, and this upregulation of AID expression promotes an increased CSR activity.

In conclusion, this research not only helps us understand *Salmonella* infection but also sets the foundation for developing targeted therapies and preventive strategies to address the pathological consequences of *Salmonella* infection.

5.2 Results

5.2.1 Cell Morphology, Cell Viability, Proliferation Marker Expression, and Cell Surface Receptor Activation in Response to OmpA-Stimulation

To investigate the impact of OmpA on B-cell viability, we used Raji human B-cells and stimulated them with varying concentrations of endotoxin-free OmpA (>0.01 EU/mL). The observations revealed notable effects on cell morphology, including the formation of proliferating cell clusters as the OmpA concentration increased from 0 to 40 μg/mL (**Fig. 5.1A**). Subsequently, we conducted cell viability assessments using both the MTT assay and the trypan blue exclusion method. The MTT assay showed a maximum reduction of 49.2% at 40 μg/mL and 45.1% at 80 μg/mL of OmpA concentration, respectively (**Fig. 5.1B**). At the same time, the trypan blue exclusion method demonstrated a maximum cell death rate of 47.9% and 43.7% at 40 and 80 μg/mL of OmpA concentration, respectively (**Fig. 5.1C**). Consequently, OmpA concentrations up to 20 μg were selected for further investigation.

Furthermore, we analyzed the cell proliferation response to OmpA stimulation in B-cells by examining the expression of these proliferation markers. **Fig. 5.1D-E** illustrates the relative mRNA expression of Ki-67 and PCNA in B-cells treated with increasing concentrations of OmpA (0–40 μg/mL) after 24 h of stimulation. The results indicate a dose-dependent decrease in the expression of these proliferation markers, suggesting that higher concentrations of OmpA may induce cellular stress or other inhibitory effects, leading to the downregulation of proliferation-related genes at this time point. This decline may be due to cellular stress or other downstream signaling processes.

5.2.2 OmpA Upregulates AID Expression

We explored the effect of OmpA stimulation on AID expression in Raji human B-cells. Interestingly, exposure to OmpA at various concentrations (0, 5, 10, and 20 μg/mL) and different time durations (2, 4, 8, and 24 h) resulted in elevated AID expression, with the highest expression observed at 20 μg/mL. This increase in AID expression was confirmed at both the mRNA **(Fig. 5.2A-B)** and protein levels **(Fig. 5.3A-B)**, setting the stage for future experiments to understand how AID expression is controlled.

5.2.3 Involvement of AID Transcription Regulators in Response to OmpA Stimulation

The regulation of AID expression and activity is intricately managed at multiple levels, encompassing transcription, post-transcriptional processes, post-translational modifications (including nuclear/cytoplasmic distribution and stability), and enzymatic functionality. Additionally, the regulation of AID is influenced by transcription factors, including enhancers and repressors **(Fig. 5.4 E)**. Notably, cMYC, PAX, SMAD3, and STAT6 act as positive modulators of AID expression, while cMYB and E2F1 function as negative regulators [154,155].

In our study, OmpA upregulated AID expression, confirmed by studying transcription factors at the mRNA level. This upregulation of AID expression was accompanied by increased recruitment of enhancers, such as Pax5, cMYC, and STAT6, to the promoter region of the AID locus **(Fig. 5.4A-C)**.

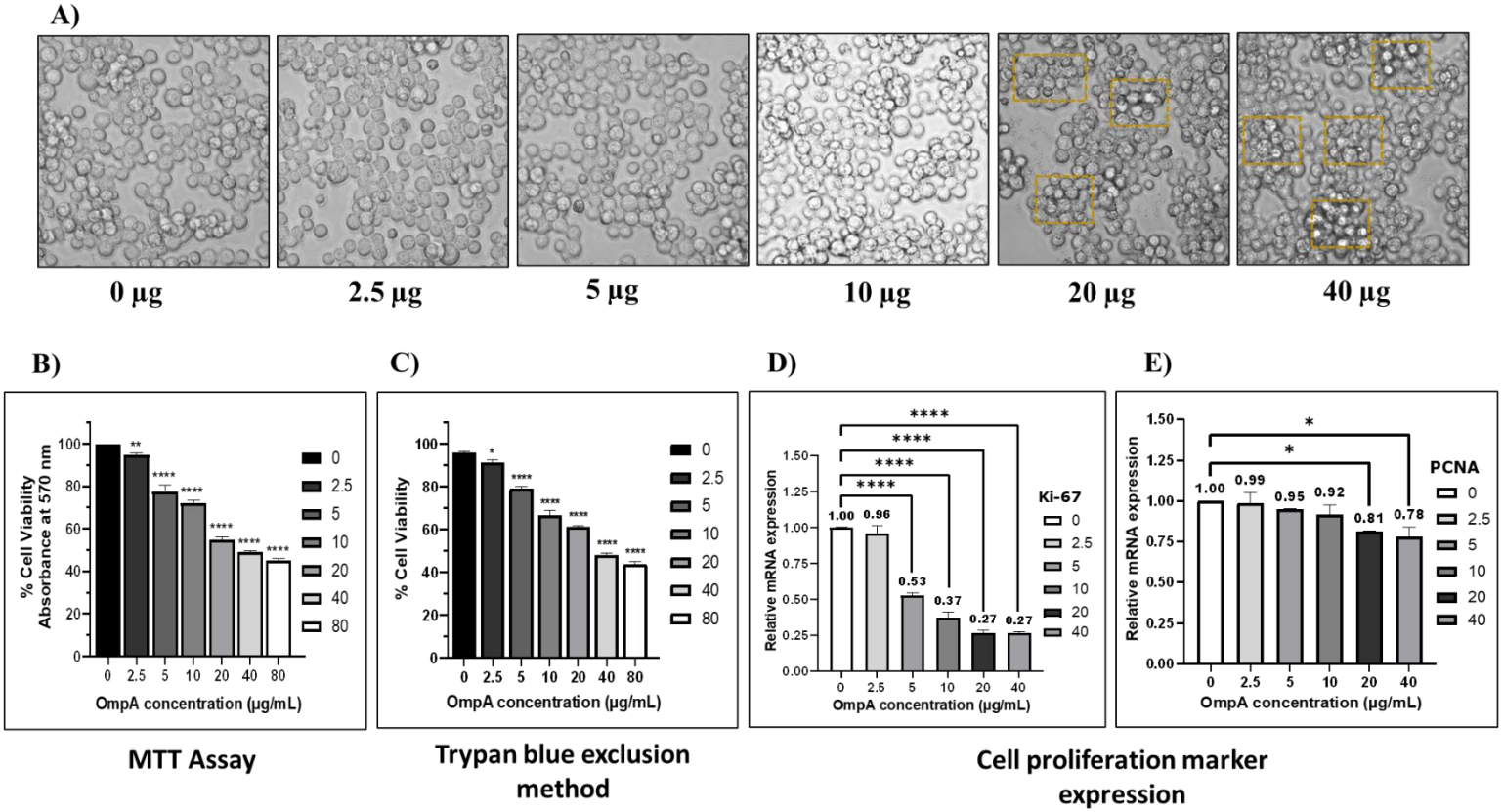

Fig. 5.1 Cell morphology, cell viability, and cell proliferation marker expression in OmpA-stimulated B-cells. **A)** The cell morphology of stimulated B-cells at different concentrations of OmpA after 24 h reveals proliferating cells characterized by cluster formation. **B)** Cell viability of OmpA-stimulated B-cells assessed using the MTT method. Cell viability was measured after treatment with various concentrations of OmpA. The results indicate a maximum cell death of 49.2% at 40 µg/mL and 45.1% at 80 µg/mL of OmpA concentration, respectively. **C)** Cell viability of OmpA-stimulated B-cells was determined by the trypan blue exclusion method, indicating a maximum cell death rate of 47.9% and 43.7% at 40 and 80 µg/mL of OmpA concentration, respectively. **D)** The relative mRNA expression levels of Ki-67 in B-cells treated with OmpA were measured at various concentrations. **E)** The relative mRNA expression levels of PCNA in B-cells treated with OmpA were measured at various concentrations. Data represent the mean ± SD of two independent experiments as biological duplicates. Statistical significances were calculated by analysis of variance (ANOVA) (*$p \leq 0.05$; **$p \leq 0.01$; ***$p \leq 0.001$; ****$p \leq 0.0001$).

A)

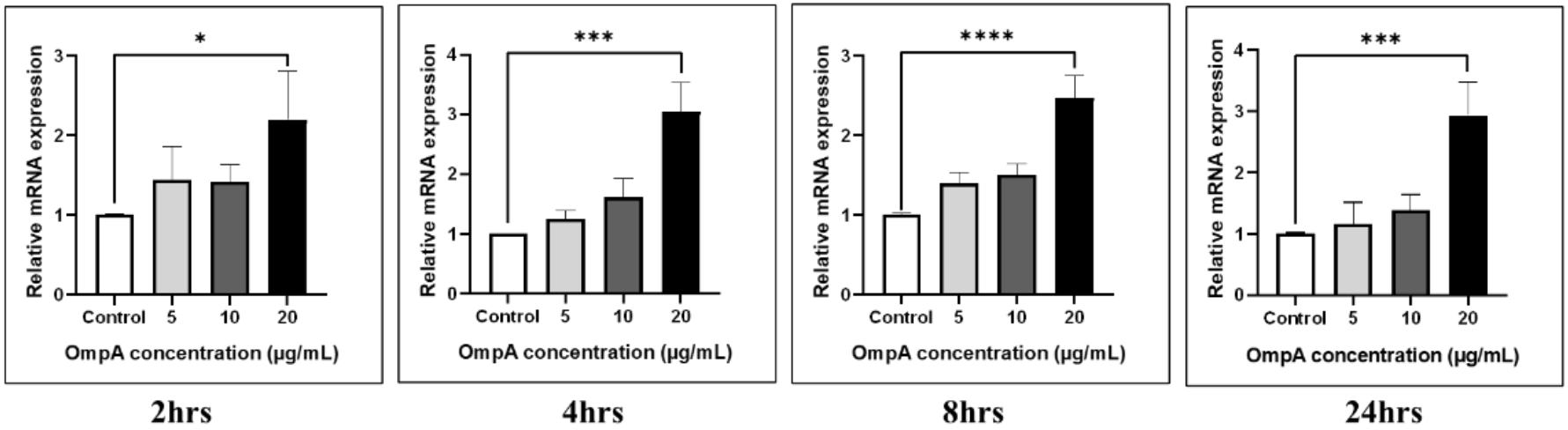

B)

OmpA concentration (µg/mL)	Time (hrs)			
	2	4	8	24
0	1.00	1.00	1.01	1.01
5	1.45	1.25	1.40	1.16
10	1.42	1.61	1.51	1.38
20	2.20	3.04	2.48	2.94

Min.
Max.

Fig. 5.2 AID mRNA expression in OmpA-treated B-cells analyzed using RT-qPCR. A) The relative mRNA expression levels of AID in B-cells treated with OmpA were measured at various concentrations and time points for stimulation. **B)** Heat map showing the relative AID expression in OmpA-stimulated B-cells. Data represent the mean ± SD of three independent experiments. Statistical significances were calculated by analysis of variance (ANOVA) (*$p \leq 0.05$; **$p \leq 0.01$; ***$p \leq 0.001$; ****$p \leq 0.0001$).

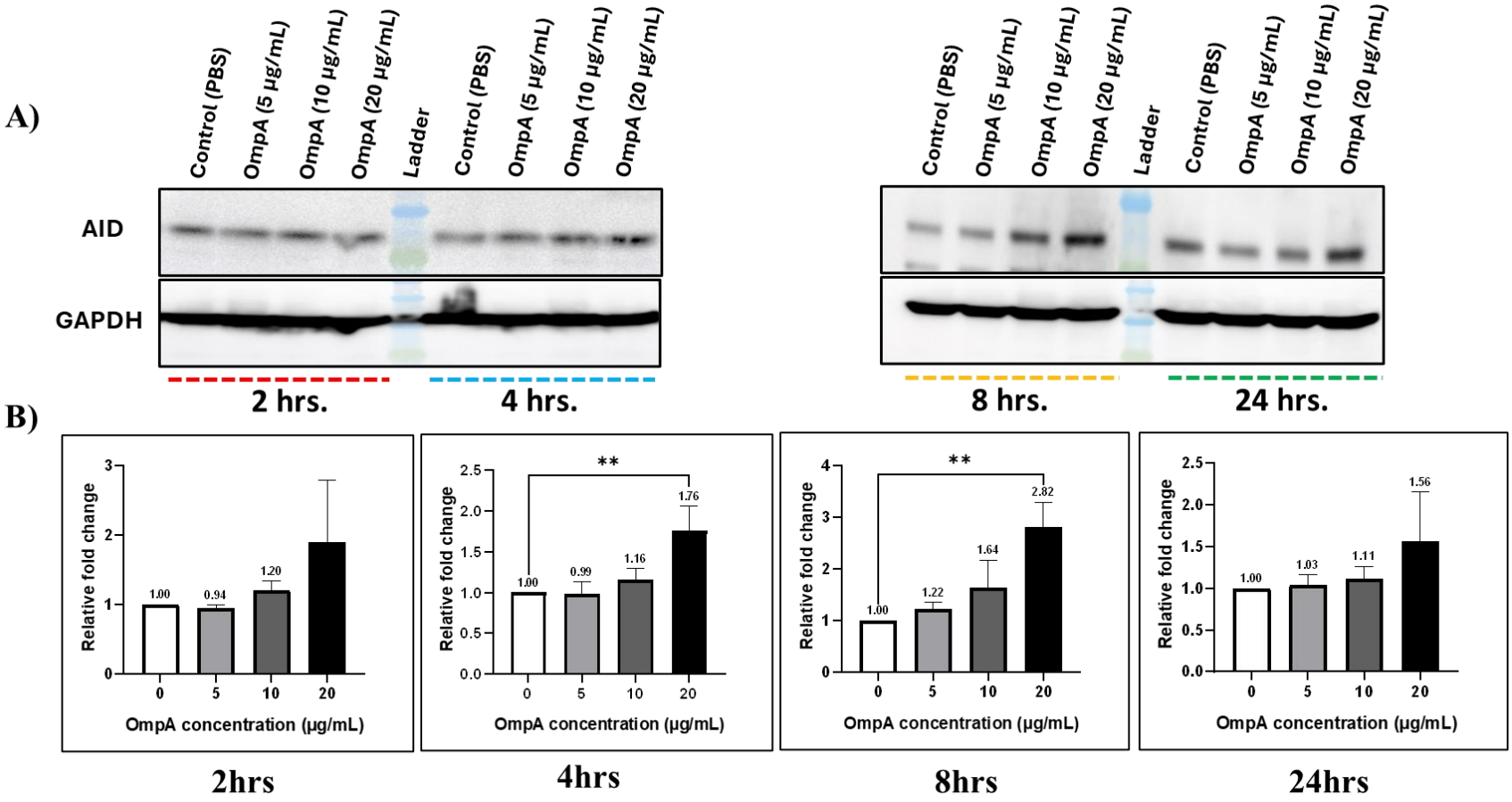

Fig. 5.3 AID protein expression in OmpA-treated B-cells was analyzed using Western immunoblotting. A) Immunoblot analysis of AID in OmpA-treated B-cells at various concentrations and time intervals for stimulation. **B)** Densitometric graph representing the immunoblot of AID expression. Data represent the mean ± SD of three independent experiments. Statistical significances were calculated by analysis of variance (ANOVA) *$p \leq 0.05$; **$p \leq 0.01$).

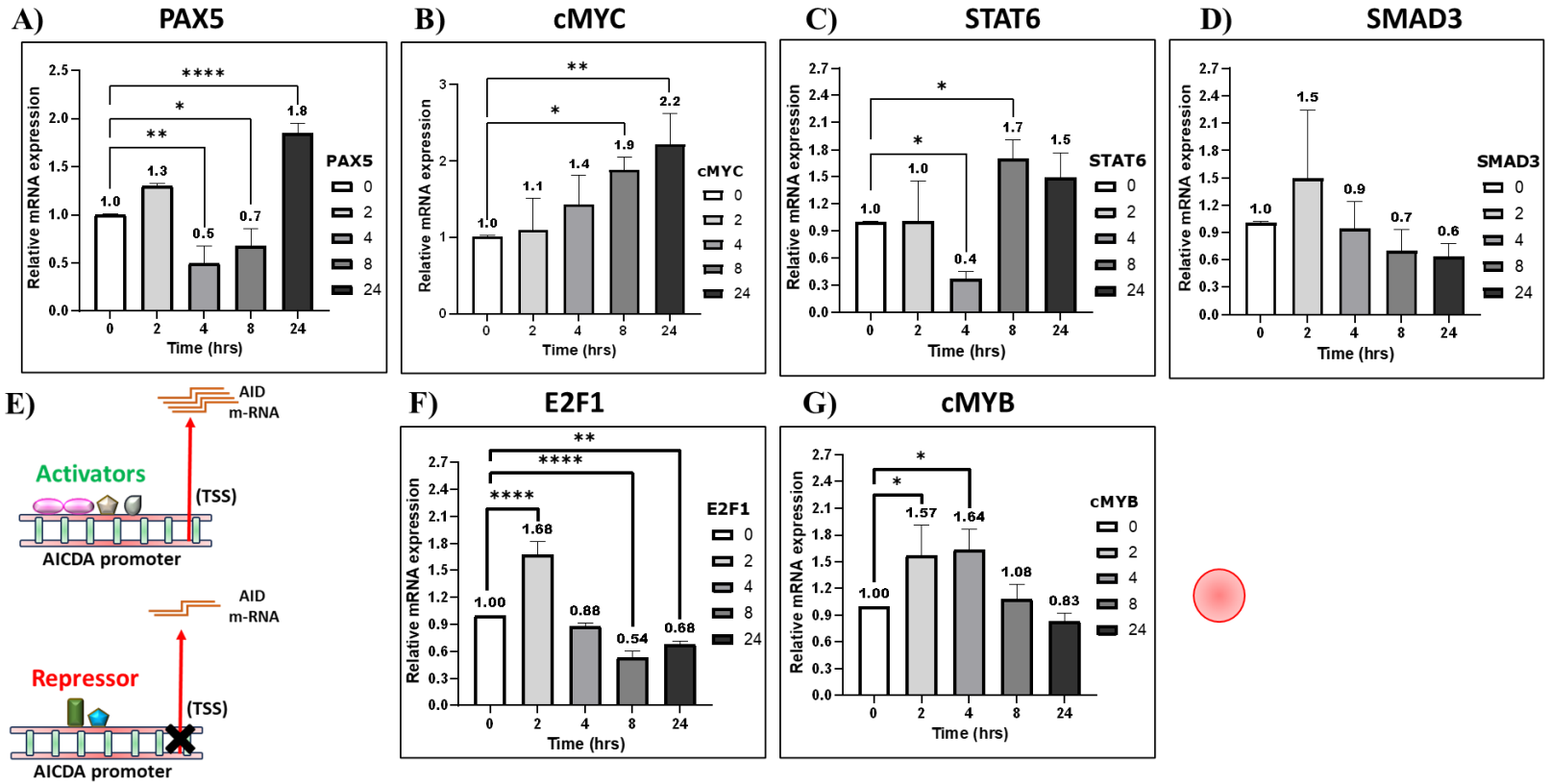

Fig. 5.4 Analysis of AID transcription activator and repressor expression. (**A-D**) mRNA expression analysis of AID transcription activators, namely cMYC, STAT6, and SMAD3, at various time points (2, 4, 8, and 24 hours) in B-cells treated with OmpA. **E)** Schematic representation of AID transcription activator and repressor expression. (**F-G**) mRNA expression analysis of AID transcription repressors, specifically cMYB and E2F1, under similar treatment conditions and time points. Data represent the mean ± SD of two independent experiments. Statistical significances were calculated by analysis of variance (ANOVA) (*$p \leq 0.05$; **$p \leq 0.01$; ***$p \leq 0.001$).

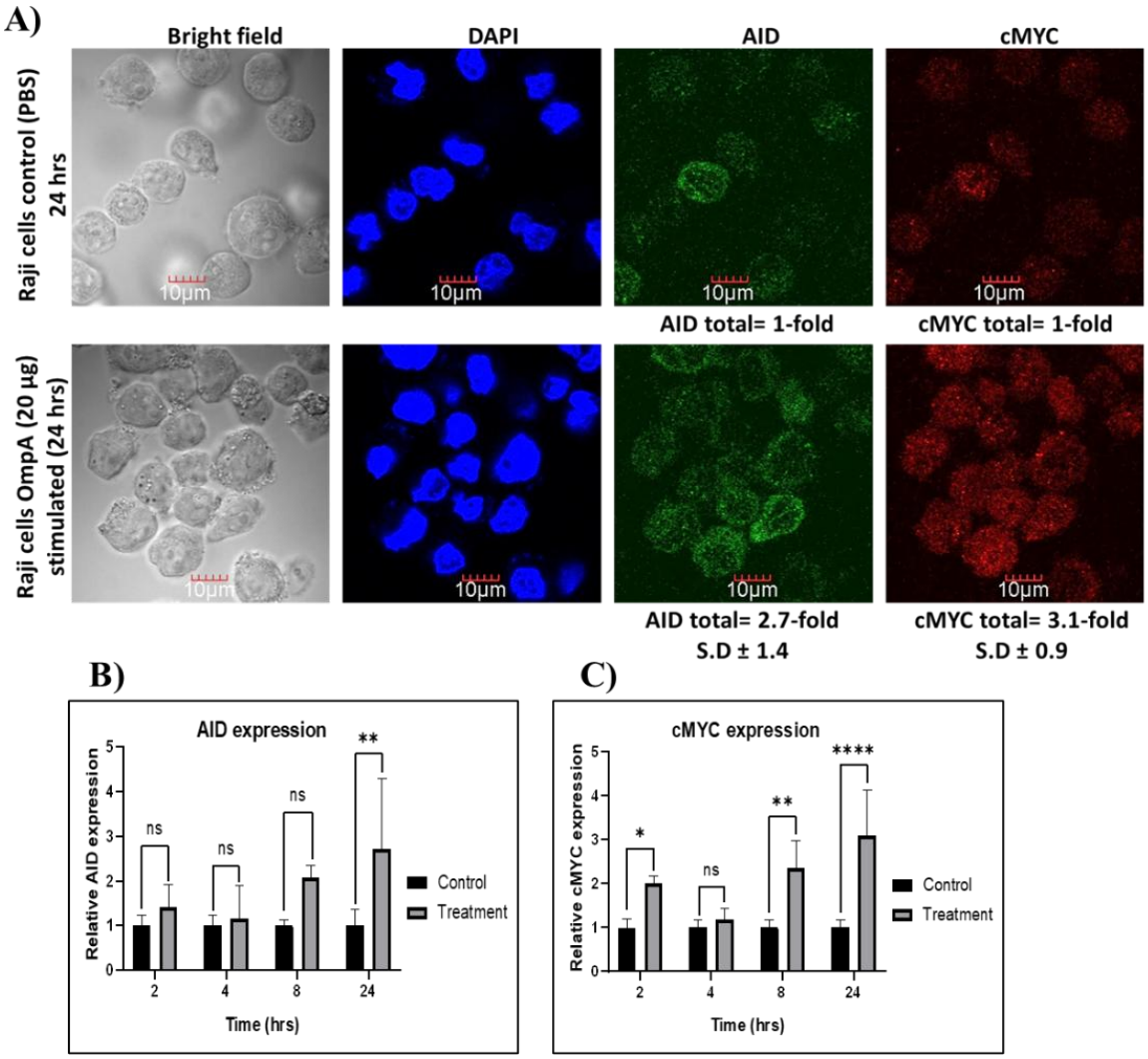

Fig. 5.5 AID transcription activator expression analysis. A) AID and cMYC expression were assessed through an immunofluorescence assay at 24 h. The sequence of images from left to right illustrates the observation of B-cells using bright field microscopy, DNA visualization through DAPI staining, AID detection through Alexa Fluor 488 staining, and cMYC identification via Alexa Fluor 594 staining. The confocal microscopy data are provided as technical duplicates. The presented data for confocal microscopy were represented as technical duplicates. **B)** AID expression analysis by quantification of fluorescence measure using ImageJ software, the result of quantification of 5 images per time point. **C)** cMYC expression analysis by quantification of fluorescence measure using ImageJ software, the result of quantification of 5 images per time point. Statistical significances were calculated by analysis of variance (ANOVA) (*$p \leq 0.05$; **$p \leq 0.01$; ***$p \leq 0.001$; ****$p \leq 0.0001$).

In contrast, the expression level of SMAD3 remained unchanged until the 8-hour mark **(Fig. 5.4D)**. Simultaneously, the expression levels of repressors increase in E2F1 at 2 h and in cMYB at 2 and 4 h, followed by a decrease in expression, indicating their reduced binding to the AID promoter region **(Fig. 5.4F-G)**. These findings provide insights into the transcriptional regulation of AID by OmpA. To further reinforce our observation of the relationship between AID and cMYC expression in stimulated B-cells, we conducted immunofluorescence analysis of AID and cMYC. Notably, a substantial increase in the expression of both AID and cMYC was observed **(Fig. 5.5A-C).**

Upon detecting the increase in expression of cMYC following OmpA stimulation, we explored cMYC occupancy at the *aicda* regulatory locus **(Fig. 5.6A)**. Interestingly, we noted a significant rise in cMYC occupancy correlated with the duration of the time interval **(Fig. 5.6B)**. In conclusion, these results suggest that the overexpression of the cMYC activator in stimulated B-cells is responsible for aberrant AID expression in B-cells.

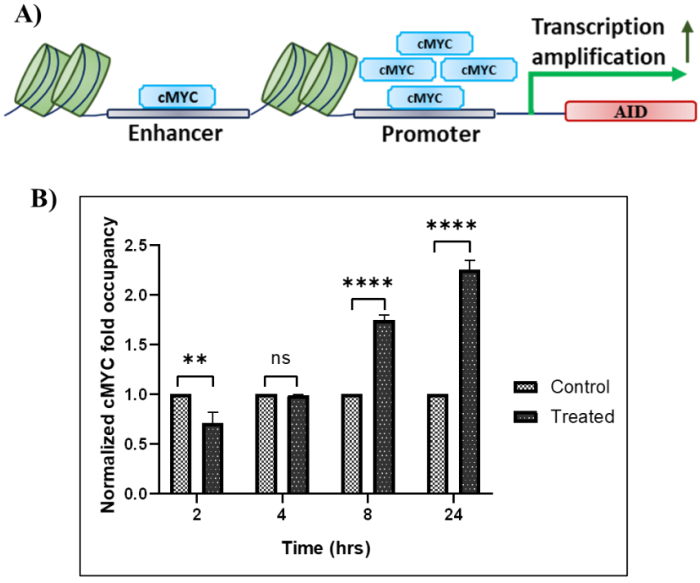

Fig. 5.6 Chromatin immunoprecipitation (ChIP) assay showing c-MYC occupancy at the promoter region in B-cells. A) Schematic representation of cMYC occupancy at the AID cis-regulatory region. **B)** The graph represents the cMYC fold occupancy on the AID cis-regulatory region. Data represent the mean ± SD of two independent experiments as biological duplicates. Statistical significances were calculated by analysis of variance (ANOVA) (*p ≤ 0.05; **p ≤ 0.01; ***p ≤ 0.001; ****p ≤ 0.0001).

5.2.4 OmpA affects the CSR of the immunoglobulin gene

During pathogenic infection, mature B-cells are activated to generate specific neutralizing antibodies via the process of SHM and CSR. CSR is a crucial process for the expression of different immunoglobulin isotypes, allowing B-cells to produce antibodies with various effector functions **(Fig. 5.7A)** [79]. B-cells undergo spontaneous CSR from IgM to IgA or IgG. In our study, we investigated whether the incubation of OmpA affects CSR activity in B-cells by measuring the mRNA expression level of the mature transcript of the immunoglobulin gene. First, we examined the expression of mature IgV-Cμ transcript, which is typically expressed in mature B-cells before class switching occurs. We observed that the B-cells stimulated with OmpA initially showed an increase in IgM expression at 2 h, followed by a decrease in mature transcript compared to the control B-cells **(Fig. 5.7B)**. Similarly, we checked the mRNA expression of the mature transcript product of IgV-Cα, and we observed that the OmpA-stimulated B-cells showed 2.0-fold higher expression of IgA at 24 h in the mature transcript as compared with the control B-cells **(Fig. 5.7C)**. Given the higher expression level of IgM and IgA mature transcripts, we further analyze the effect of OmpA on the CSR process in B-cells by examining the ratio of IgM and IgA. Interestingly, we found that the IgA ratio was approximately 1.9-fold higher at 24 h as compared to control B-cells **(Fig. 5.7D)**.

In conclusion, the observed aberrant expression of AID in stimulated B-cells enhances class switch recombination (CSR) activity and may suggest a potential link to B-cell lymphoma **(Fig. 5.8)**, unveils a novel dimension of *Salmonella*-host interactions, emphasizing the central role played by OmpA in modulating host immune responses. The multifaceted approach employed here offers a comprehensive view of OmpA's functional attributes, laying the groundwork for future investigations into the precise molecular mechanisms governing this interaction. Ultimately, this research opens new avenues for combating *Salmonella* infections and advancing our understanding of microbial pathogenesis within the context of the host immune system.

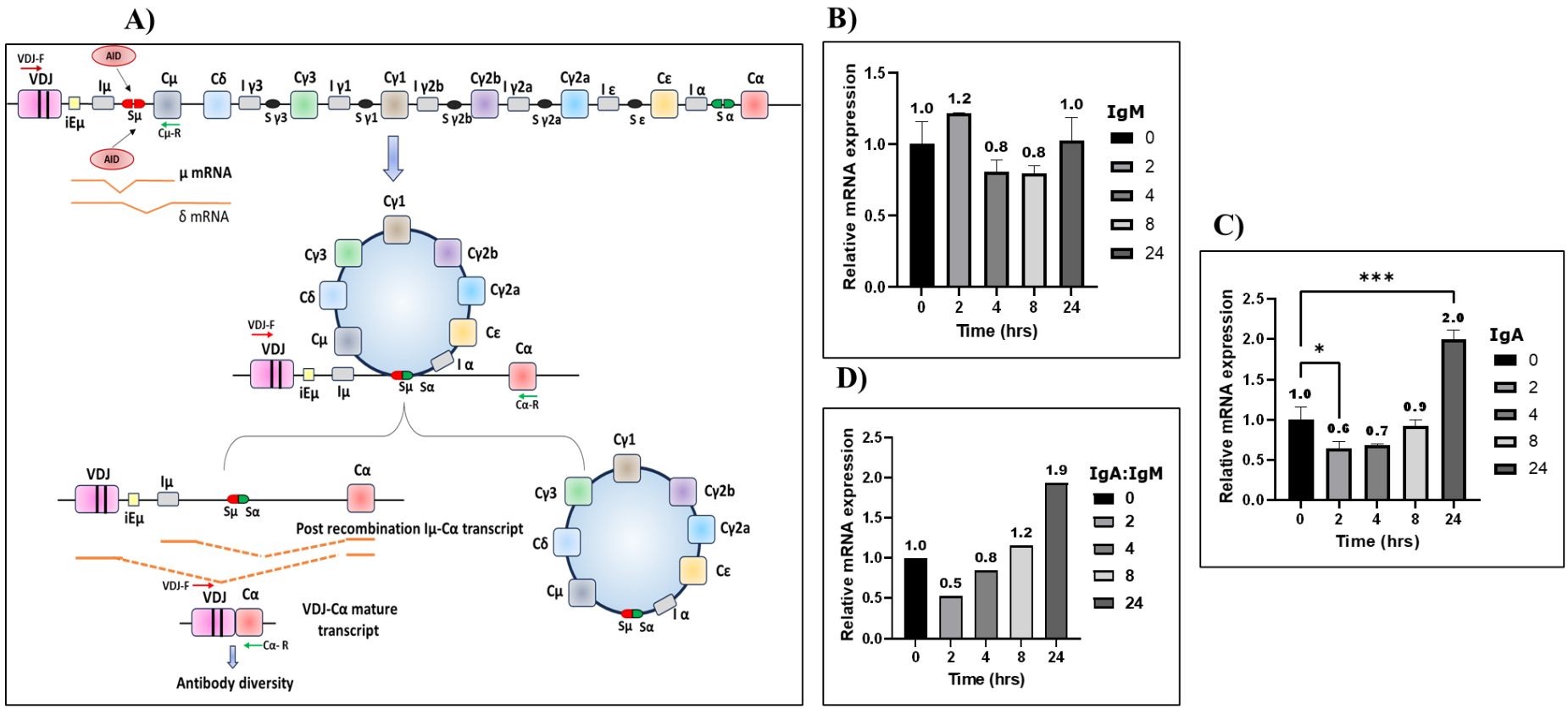

Fig. 5.7. OmpA increases the induction of class switching to IgA. A) Schematic representation of the class switching recombinant process in a B-cell. **B)** mRNA expression analysis of IgM mature transcript of OmpA-treated B-cells. **C)** mRNA expression analysis of IgA mature transcript of OmpA-treated B-cells. **D)** IgA to IgM ratio analysis in OmpA-treated B-cells. Data represent the mean ± SD of two independent experiments as biological duplicates. Statistical significances were calculated by analysis of variance (ANOVA) (*$p \leq 0.05$; **$p \leq 0.01$; ***$p \leq 0.001$).

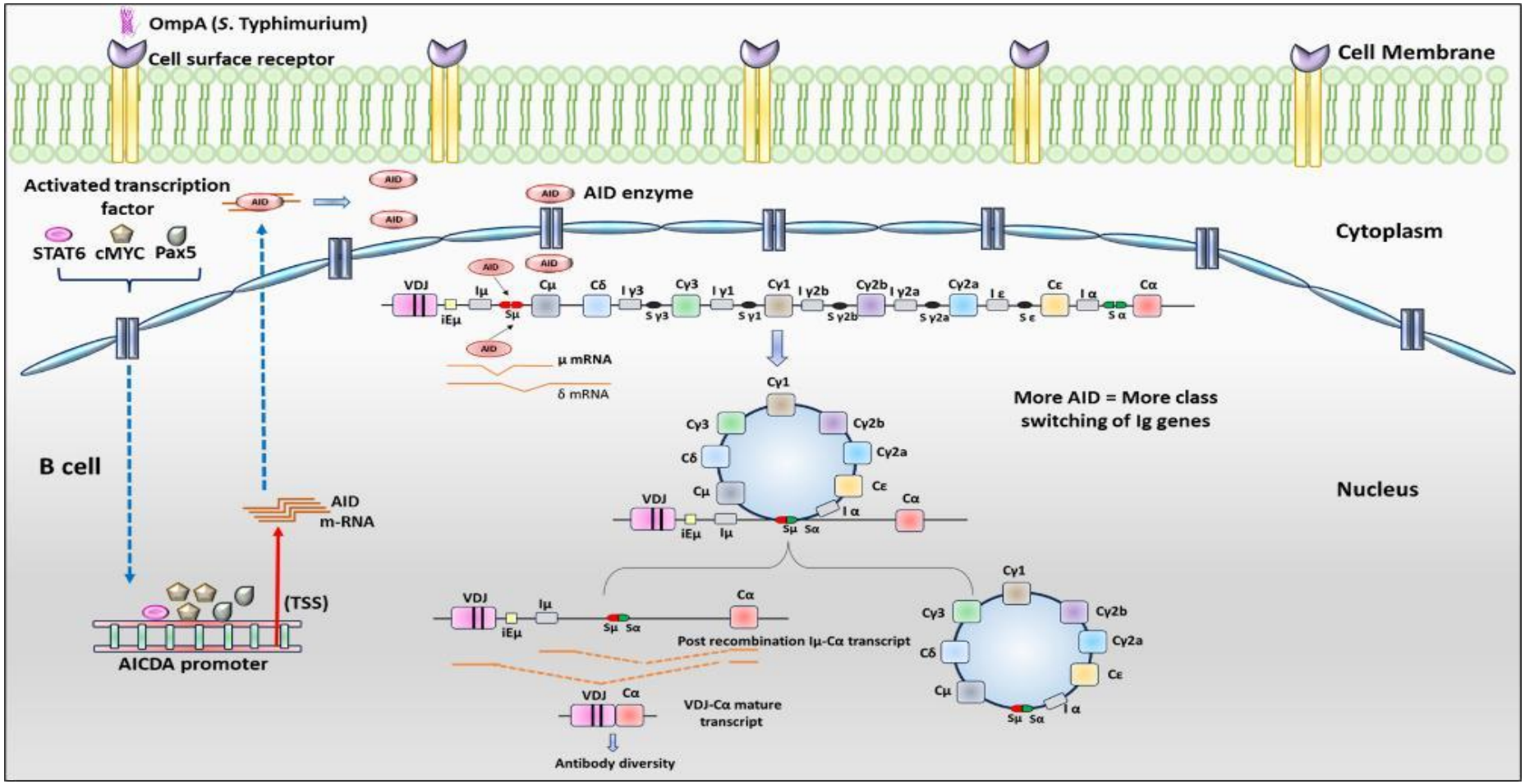

Fig. 5.8 Schematic representation of stimulation of OmpA in B-cells, resulting in increased AID expression within B-cells participating in SHM and CSR.

5.3 Summary

In this study, we investigated the impact of OmpA on AID expression in B-cells, which are essential for the class switching of immunoglobulins by initiating the process of CSR. We purified and characterized recombinantly cloned OmpA and ensured endotoxin removal. Stimulation of B-cells with endotoxin-free OmpA resulted in altered cell morphology and reduced viability, as confirmed by MTT and Trypan blue exclusion assays. Our findings show that OmpA activates TLR2 and enhances AID expression at both mRNA and protein levels within 24 h. Several transcription factors, including cMYC, Pax5, SMAD3, and STAT6, promote AID expression, while cMYB and E2F1 inhibit it.

In our study, OmpA enhances the expression of activators such as cMYC, Pax5, and STAT6. Concurrently, OmpA reduces the binding of repressors like E2F1 and cMYB to the AID promoter. This suggests that OmpA transcriptionally regulates AID by enhancing the recruitment of activators and decreasing the binding of repressors. Interestingly, in our study, we found that increased AID expression was likely due to cMYC overexpression, which acts as an activator for AID. ChIP assays confirmed elevated cMYC occupancy at the *aicda* locus. Additionally, we found that increased AID expression is involved in CSR events, specifically in switching to IgA. In summary, our study suggests that OmpA may modulate B-cell regulation and the adaptive immune system, highlighting its potential as a therapeutic target against *S.* Typhimurium pathogenesis.

Chapter 6

Results for Objective 4

Chapter 6

6. Engineering Outer Membrane Vesicles (OMVs) Carrying OmpA from *S.* Typhimurium for Targeted Modulation of Human B-cell Function through AID Expression and Class Switch Recombination.

6.1 Introduction

Salmonella enterica Typhimurium (*S.* Typhimurium) is a facultative intracellular, Gram-negative bacterium, known for causing foodborne gastroenteritis, which poses serious threats to human health and animals, resulting in global economic losses [2,64,144]. As a result, vaccination has become increasingly important in controlling and preventing *Salmonella* infections worldwide by emphasizing the need for protective efficacy and safety. Outer membrane vesicles (OMVs) have gained attention in the fields of immunology and vaccine development for their potential to provide this protective efficacy and safety [156].

OMVs are closed, spherical lipid bilayer nanoparticles, typically ranging from 10 to 300 nm in diameter, that are constitutively secreted by Gram-negative bacteria through multiple mechanisms, including outer membrane budding, peptidoglycan remodeling, and bacterial stress responses [64–66]. OMVs naturally contain adjuvant-specific cargo molecules, including outer membrane proteins (OMPs), lipopolysaccharides (LPS), flagellin, and peptidoglycans. Pathogenic bacteria use OMVs as a secretion and delivery system for various functions. Functionally, OMVs facilitate several bacterial processes, including virulence factors, horizontal gene transfer, biofilm formation, toxin delivery, and immune evasion [19,67].

Traditionally, OMVs have been used in homologous vaccination approaches to protect against the pathogenic strain of the bacteria that produce these vesicles. Notable examples include approved vaccines designed to protect against the *Neisseria meningitidis* serogroup B (MenB) and *Haemophilus influenzae* type b (Hib) [157]. In recent years, there has been growing interest in recombinant OMVs that incorporate heterologous targets, where OMVs are used as carriers for diverse antigens [158]. Interestingly, one of the key components of OMVs is OMPs, including OmpA, OmpV,

OmpC, OmpD, OmpF, and OmpW. These proteins play significant roles in the pathogenesis of *Salmonella*. Among them, OmpA is highly conserved, has a beta-barrel structure, and is abundant across various *Salmonella* serovars. It is involved in essential processes such as invasion, adhesion, and biofilm formation. Additionally, OmpA offers protection against oxidative and nitrosative stress [133,140]. Thus, given its potential to elicit an immune response, OmpA represents a promising target for therapeutic interventions.

In addition to their role as antigen carriers, OMVs also exhibit intrinsic adjuvant properties due to the presence of pathogen-associated molecular patterns (PAMPs). These PAMPs engage pattern recognition receptors (PRRs), including Toll-like receptors (TLRs) and B-cell receptors (BCRs). This activation occurs through PRR-mediated signalling pathways, ultimately enhancing B-cell activation and modulating immune responses [116,159–161]. Similarly, a study by Perez Vidakovics et al. reported that OMVs have the potential to interact with and activate B-cells. Additionally, they found that TLR2 and TLR9 were involved in the activation of B-cells [161].

In our previous study, we demonstrated that the OmpA protein from *S.* Typhimurium plays a vital role in B-cell modulation. We used purified and refolded OmpA to stimulate human B-cells and found that OmpA was involved in the increased AID expression and class switching in these cells [162]. However, the use of isolated purified OmpA may not fully reflect how the immune system encounters the protein during an actual infection. Therefore, in this study, we are utilizing recombinant OMVs that carry OmpA from *S.* Typhimurium. This approach is advantageous due to the nano-structural size of the OMVs and the preservation of OmpA's native conformation within the lipid bilayer of the OMVs, which may enhance receptor recognition and downstream signaling. As a result, using OmpA-OMVs not only provides physiologically relevant antigen presentation but also represents an effective strategy to enhance class switching in B-cells.

In this study, we investigated how OMVs influence B-cell activity, specifically focusing on the involvement of OmpA-containing OMVs in CSR by regulating AID expression, which is essential for class switching in immunoglobulin genes. Initially,

we assessed B-cell activation by analyzing the expression of TLR2, a PRR that recognizes bacterial components through PAMPs and triggers NF-κB signaling. We then explored whether OmpA-containing OMVs exert their effects through the TLR2–NF–κB axis. Furthermore, we analyzed the impact of OMVs on AID expression and supported our conclusions by exploring transcriptional regulation through the activation of transcription factors such as cMYC, PAX5, SMAD3, and STAT6. We also examined cMYB expression, which is known to repress AID expression. To delve deeper into this interaction, we performed chromatin immunoprecipitation analysis to track cMYC occupancy in the chromatin over time. Based on our findings regarding AID expression, we further analyzed its role in the CSR process. By exploring the comprehensive mechanisms of recombinant OmpA-containing OMVs in B-cell modulation, this research enhances our understanding of *Salmonella* pathogenesis and contributes to the development of novel immunotherapies or vaccines against *Salmonella* infections.

6.2 Results

6.2.1 Construction and Characterization of Recombinant OMVs

In our study, we successfully cloned the *ompA* gene from *S.* Typhimurium, including its native signal peptide sequence, into the pET43a vector to facilitate the localization of OmpA to the outer membrane and its incorporation into OMVs. The resultant recombinant OmpA clone was transformed into *E. coli* BL21(DE3) cells to facilitate the expression of OmpA, which was used to isolate OMVs. The total protein and phosphate content of the OMVs were quantified **(Fig. 6.1A-C)**. SDS-PAGE analysis of the isolated OmpA-OMVs revealed a distinct protein band of approximately 38 kDa, corresponding to OmpA, with purified OmpA serving as a positive control and OMVs from BL21(DE3) as a negative control. Furthermore, immunoblot analysis using an anti-His antibody confirmed the presence of His-tagged OmpA in the OMVs **(Fig. 6.2A-B)**.

We analysed the OMV samples using ATR-FTIR, a rapid and label-free technique that analyses samples without disturbing their native state. This method allows for the characterization of intact OMV samples. In Figures **6.2C-D**, the ATR-FTIR spectra of BL21-OMVs and OmpA-OMVs reveal characteristic bands associated

with proteins, lipids, and polysaccharides. To enhance the resolution of overlapping spectral bands, we utilized second derivative analysis, which allowed for a more precise interpretation of the results. Both types of OMVs exhibited peaks corresponding to amide I (1639–1635 cm^{-1}), indicating a protein content in the membrane. Additionally, a peak for amide II (1520–1530 cm^{-1}) was observed, representing N-H bending vibrations of the peptide bond in proteins. A peak associated with C–O–C stretching vibrations related to lipopolysaccharides was also detected in the range of 1000–1150 cm^{-1}, while C–H stretching was identified between 2845–2930 cm^{-1}, reflecting the lipid components of the membrane [118,119].

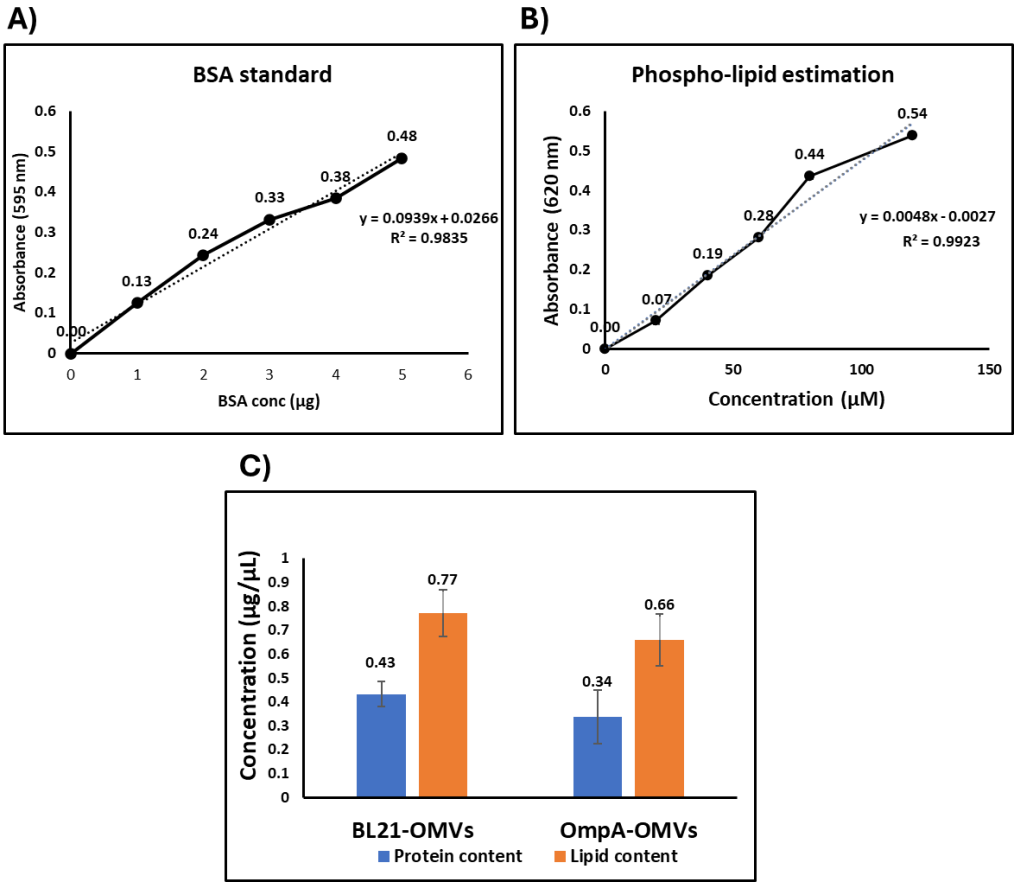

Fig. 6.1 Analysis of protein content and phosphate levels in lipids extracted from isolated OMVs. A) Standard BSA graph for estimation of total protein content using Bradford assay. **B)** Standard phosphate graph for estimating total phosphate content by a malachite green phosphate assay. **C)** Analysis of total protein content from isolated OMVs using Bradford assay and malachite green assay for total phosphate content.

Additionally, we deconvoluted the absorbance spectra of the amide I region (1580–1720 cm^{-1}) to evaluate the protein membrane components from the BL21-OMVs and OmpA-OMVs **(Fig. 6.2E-F)**. Our analysis revealed that the secondary derivatives of the absorbance spectra within the amid I region correspond to the proteins' secondary structures. The signals at around 1623 and 1639 cm^{-1} indicate β-sheet structures, while those in the 1675–1695 cm^{-1} range signify antiparallel β-sheets. Signals between 1647–1664 cm^{-1} suggest α-helices, and bands at around 1645–1647 cm^{-1} and 1662–1678 cm^{-1} correspond to turns, loops, and random coils. Furthermore, the signal ranging from 1590 to 1623 cm^{-1} indicates the presence of aggregated protein structures. This analysis was conducted according to the guidelines presented by Tamm and Tatulian [163].

Furthermore, we conducted the size distribution analysis of OMVs using the DLS and SEM. The characterization of OMVs using DLS, which measures the hydrodynamic diameter, indicated that the average diameter of OMVs ranged from 50-150 nm **(Fig. 6.3A-B)**. Similarly, the zeta potential measurements revealed that the isolated BL21-OMVs were -12.66 mV and OmpA-OMVs were -14.05 mV **(Fig. 6.3C)**. Furthermore, SEM was used to assess the structure and size distribution of OMVs. The SEM analysis confirmed their spherical shape, with an average diameter of 140 nm for BL21-OMVs and 168 nm for OmpA-OMVs **(Fig. 6.3D-G)**.

6.2.2 Cell Cytotoxicity and Cell Surface Receptor Activation in Response to OMV Stimulation

To assess the cytotoxic effect of OMVs on Raji human B-cells, we employed phase-contrast microscopy, MTT assay, and the Trypan blue exclusion method. The phase-contrast microscopic images **(Fig. 6.4A-B)** revealed a concentration-dependent decrease in cell viability upon stimulation with BL21-OMVs and OmpA-OMVs. At lower concentrations of OMVs, specifically between 0.08 and 0.62 μg/mL, we observed minimal morphological effects in both OMV groups. However, the cells exhibited significant shrinkage and aggregation at higher concentrations ≥1.25 μg/mL, indicating a cytotoxic effect. Furthermore, extensive cell death was observed at even higher concentrations of 2.5 and 5 μg/mL. Likewise, the MTT assay revealed a dose-dependent decrease in B-cell viability **(Fig. 6.4C-D).**

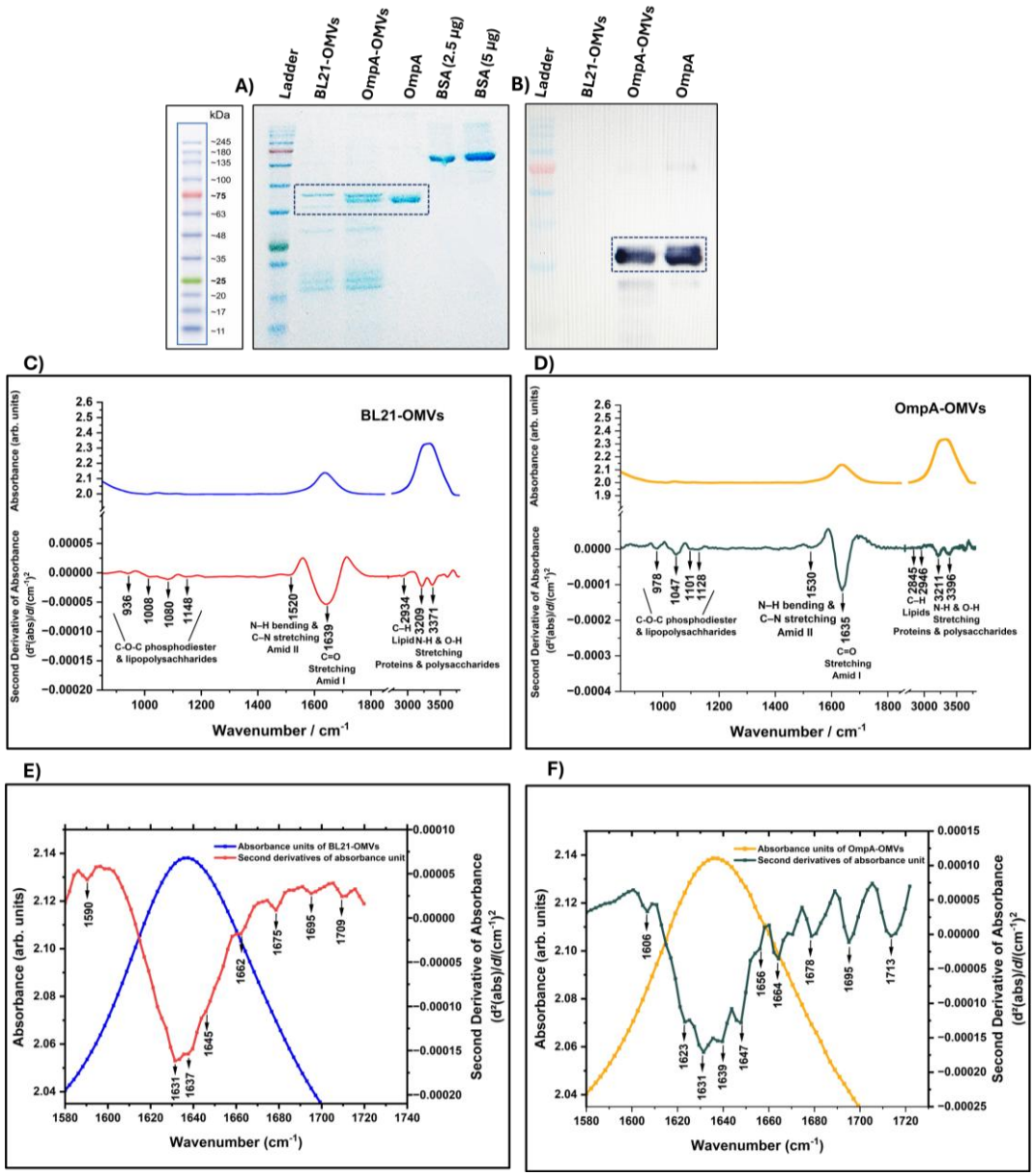

Fig. 6.2 Characterization of OMVs by SDS-PAGE, Western Blot, and ATR-FTIR spectroscopy: A) The Protein content of OMVs was analyzed using SDS-PAGE. Lane 1: protein marker; Lane 2: BL21-OMVs; Lane 3: OmpA-OMVs; Lane 4: Purified OmpA; Lane 5: BSA (2.5 µg); Lane 6: BSA (5 µg). **B)** Western immunoblotting of OMVs was performed using a His-tag antibody. Lane 1: protein marker; Lane 2: BL21-OMVs; Lane 3: OmpA-OMVs; Lane 4: Purified OmpA. **C-D)** The IR spectrum of the BL21-OMVs and OmpA-OMVs was recorded, and to improve spectral resolution, second derivative spectra were generated for specific wavenumber regions, including the amide I and amide II bands (1800–1500 cm^{-1}), lipid and polysaccharide-associated regions (3200–3500 cm^{-1}), and the fingerprint region (1300–800 cm^{-1}).

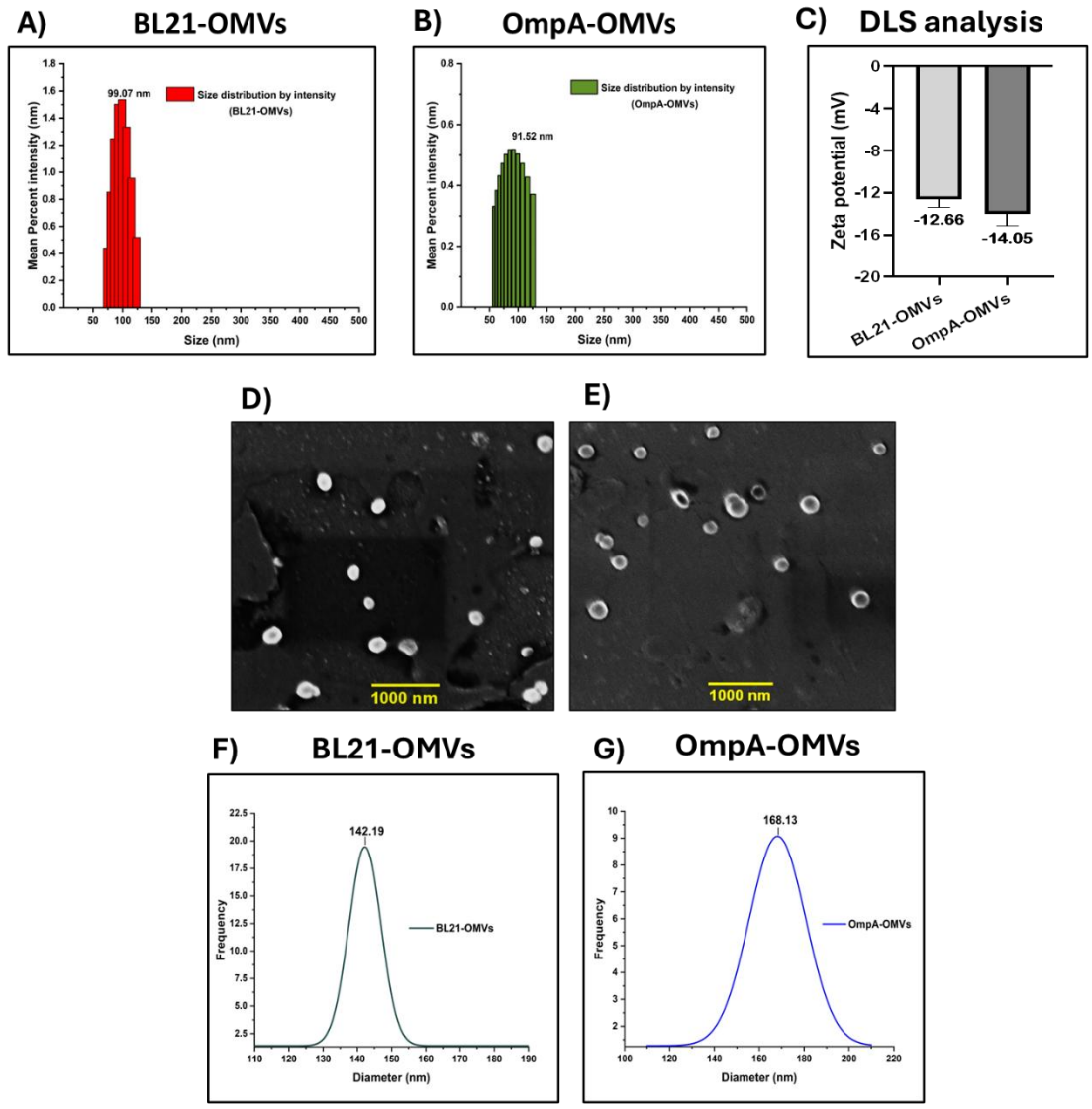

Fig. 6.3 Morphological characterization of OMVs by DLS, Zeta Potential, and SEM: A-B) Size distribution analysis of BL21-OMVs and OmpA-OMVs was conducted using DLS. The scale bar represents 200 nm. **B)** Size distribution analysis of OmpA-OMVs was conducted using DLS. The scale bar represents 200 nm. **C)** Zeta potential analysis of OMVs was performed using DLS. **D)** Morphological analysis of BL21-OMVs was evaluated using SEM. **E)** Morphological analysis of OmpA-OMVs was evaluated using SEM. **F)** Size distribution analysis of BL21-OMVs was conducted using SEM. **G)** Size distribution analysis of OmpA-OMVs was conducted using SEM.

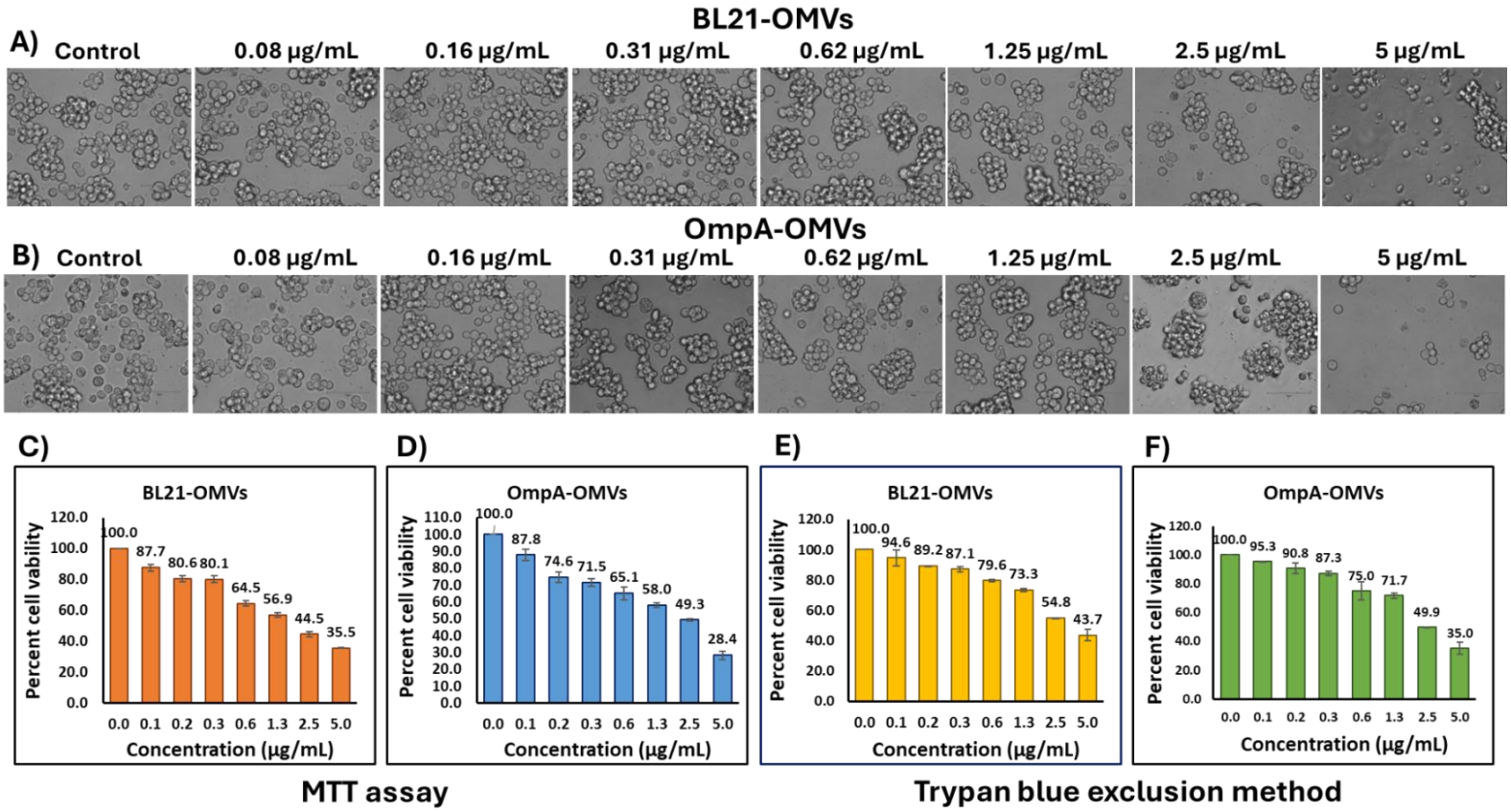

Fig. 6.4 Cell morphology and cell cytotoxicity in response to OMVs stimulated Raji human B-cells: A) Examination of the morphology of stimulated B-cells after 24 h at various concentrations of BL21-OMVs shows an increase in morphological changes as the concentration of BL21-OMVs rises. **B)** Examination of the morphology of stimulated B-cells after 24 h at various concentrations of OmpA-OMVs shows an increase in morphological changes as the concentration of OmpA-OMVs rises. **C-D)** The cytotoxicity of OMV-stimulated B-cells was assessed using the MTT assay, revealing a decrease in cell viability from 100% in the control group to 35.5% at a concentration of 5 µg/mL for BL21-OMVs. In contrast, cell viability for OmpA-OMVs decreased from 100% in the control to 28.4% at the same concentration. Data is represented as mean ± SD from technical duplicates. **E-F)** Additional assessment of cell viability using the trypan blue exclusion method indicated a decrease from 100% in the control group to 43.7% at 5 µg/mL for BL21-OMVs. In contrast, for OmpA-OMVs, viability dropped from 100 % to 35.0% at this concentration. Data is represented as mean ± SD from technical duplicates.

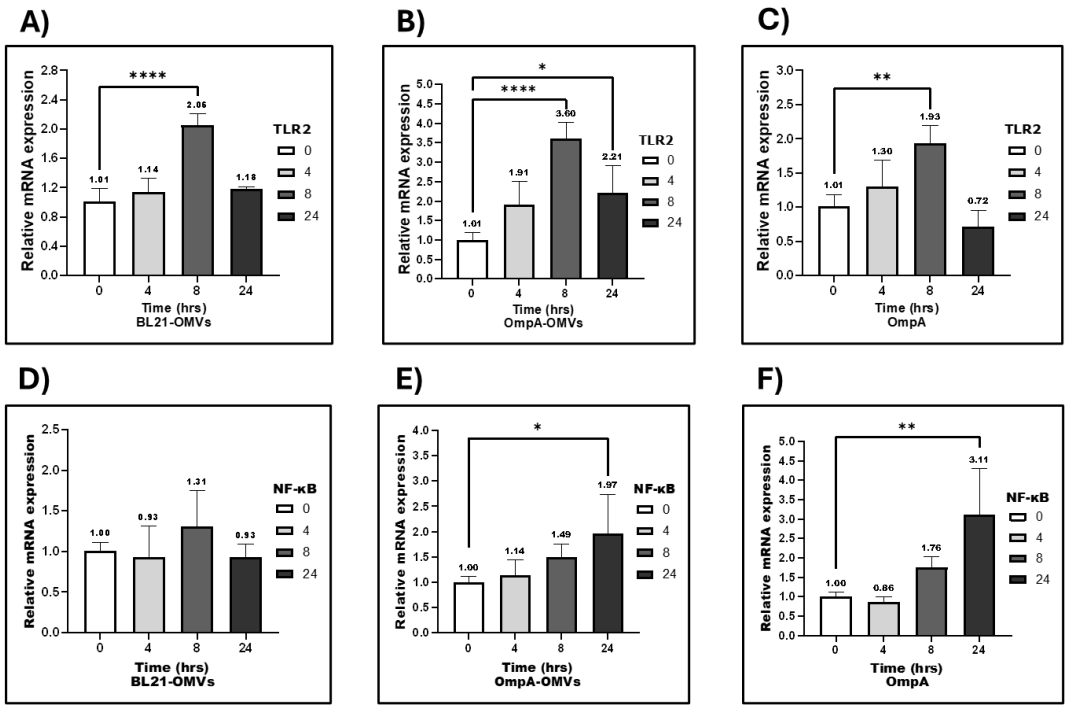

Fig 6.5 Cell surface receptor expression in response to OMVs stimulated Raji human B-cells: A-C) The relative mRNA expression levels of TLR2 in B-cells treated with OMVs and OmpA were measured at different time intervals. **D-F)** The relative mRNA expression levels of NF-κB in B-cells treated with OMVs and OmpA were measured at different time intervals. Data are presented as mean ± SD from two independent experiments conducted as biological duplicates. Statistical significance was determined using analysis of variance (ANOVA) with the following p-values: *p ≤ 0.05; **p ≤ 0.01; ***p ≤ 0.001; ****p ≤ 0.0001.

The BL21-OMVs demonstrated toxicity, with cell viability decreasing from 100% in the control to 35.5% at a concentration of 5 µg/mL. The OmpA-OMVs also exhibited toxicity, reducing B-cell viability to 28.4% at the highest concentration of 5 µg/mL. Additionally, consistent with the MTT assay, trypan blue exclusion results **(Fig. 6.4E-F)** also reflected decreased cell viability as OMV concentration increased. For BL21-OMVs, cell viability dropped from 94.6% at 0.08 µg/mL to 43.7% at 5 µg/mL, while OmpA-OMVs decreased from 95.3% to 35 %. Based on the comprehensive results from cell cytotoxicity, we selected the OMV concentration up to 1.25 µg/mL for further investigation.

Furthermore, we investigated TLR2 expression, a key PRR for bacterial lipoproteins, to determine its role in OMV-induced signaling in human B-cells [161]. Our findings showed that both OMVs and OmpA significantly upregulate TLR2 expression for up to 8 h **(Fig. 6.5 A-C)**. This observation suggests that OMVs trigger

TLR2-mediated signaling at the cell surface. We found that BL21-OMVs induce NF-κB expression for up to 8 h, while OmpA-OMVs and purified OmpA increase it for up to 24 h **(Fig. 6.5D-F)**.

6.2.3 OmpA-OMVs Mediated Upregulation of AID Expression in B-cells

We investigated the impact of OMVs on AID expression in Raji human B-cells. Our findings showed that stimulating these cells with OMVs for 4, 8, and 24 h increased AID expression, peaking at 24 h, as seen at both mRNA **(Fig. 6.6A-C)** and protein levels **(Fig. 6.6D-G)**. These results provide a basis for future studies on the mechanisms regulating AID expression.

6.2.4 OmpA-OMV Influences the Transcriptional Regulation of AID Expression

In our study, we found that OmpA-OMVs upregulate AID expression. This upregulation is due to an increase in the recruitment of enhancers in the promoter region of the AID locus. To investigate the transcription factors involved in regulating AID expression, we examined the expression levels of key transcriptional activators, including cMYC, PAX5, SMAD3, and STAT6, as well as transcriptional repressors such as E2F1 and cMYB. This analysis was conducted at various time intervals (0, 4, 8, and 24 h) upon stimulation of BL21-OMVs, OmpA-OMVs, and purified OmpA.

Interestingly, we noted that the expression of cMYC, one of the activators of AID, significantly increased after 4 h of treatment with OmpA-OMVs and OmpA, compared to the BL21-OMVs **(Fig. 6.7A)**. Similarly, PAX5 expression showed a significant increase at up to 8 h, particularly with OmpA-OMVs treatment, in comparison to both BL21-OMVs and OmpA **(Fig. 6.7B)**. Notably, while SMAD3 expression remained relatively stable, there was an increase at the 24 h mark with OmpA-OMVs stimulation **(Fig. 6.7C)**. Furthermore, the STAT6 expression was significantly higher at 24 h with OmpA-OMVs compared to BL21-OMVs and OmpA **(Fig. 6.7D)**.

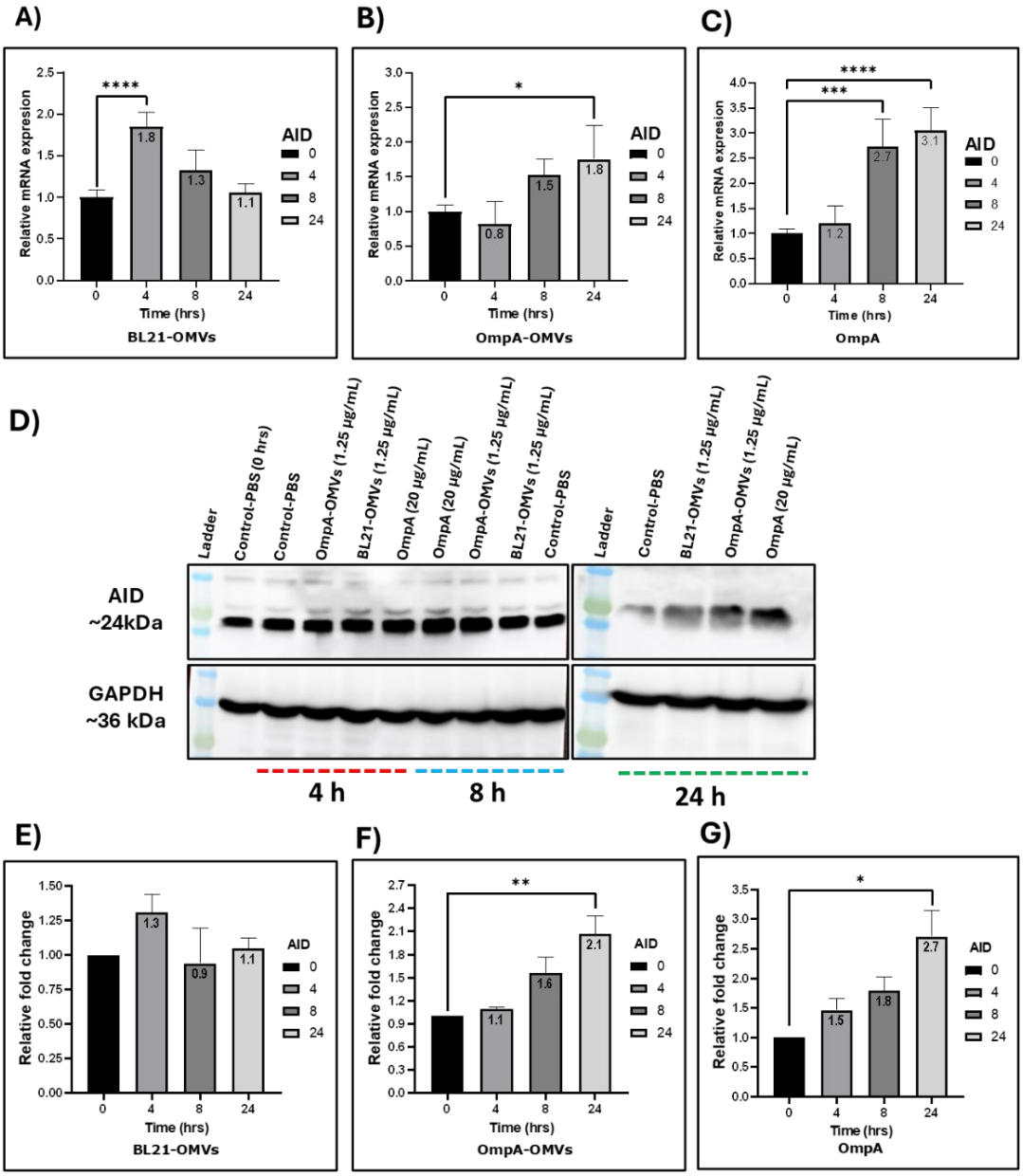

Fig. 6.6 AID expression in stimulated Raji human B-cells. A-C) Relative mRNA expression analysis through RT-PCR represents the transcriptional levels of genes in response to BL21-OMVs (A), OmpA-OMVs (B), and OmpA (C) over the time points of 0, 4, 8, and 24 h. **D)** Western blot analysis was performed to assess the expression levels of AID (~24 kDa), using GAPDH (~36 kDa) as an internal control. The analysis utilized cell lysates from Raji human B-cells treated with Control-PBS, BL21-OMVs, OmpA-OMVs, and OmpA at time points of 4, 8, and 24 h. **E–G)** Densitometric quantification of relative fold changes in AID protein expression corresponding to BL21-OMVs (E), OmpA-OMVs (F), and OmpA (G) treatments over time. Data represent the mean ± SD of two independent experiments as biological duplicates. Statistical significance was determined using ANOVA with the following p-values: *p ≤ 0.05; **p ≤ 0.01; ***p ≤ 0.001; ****p ≤ 0.0001.

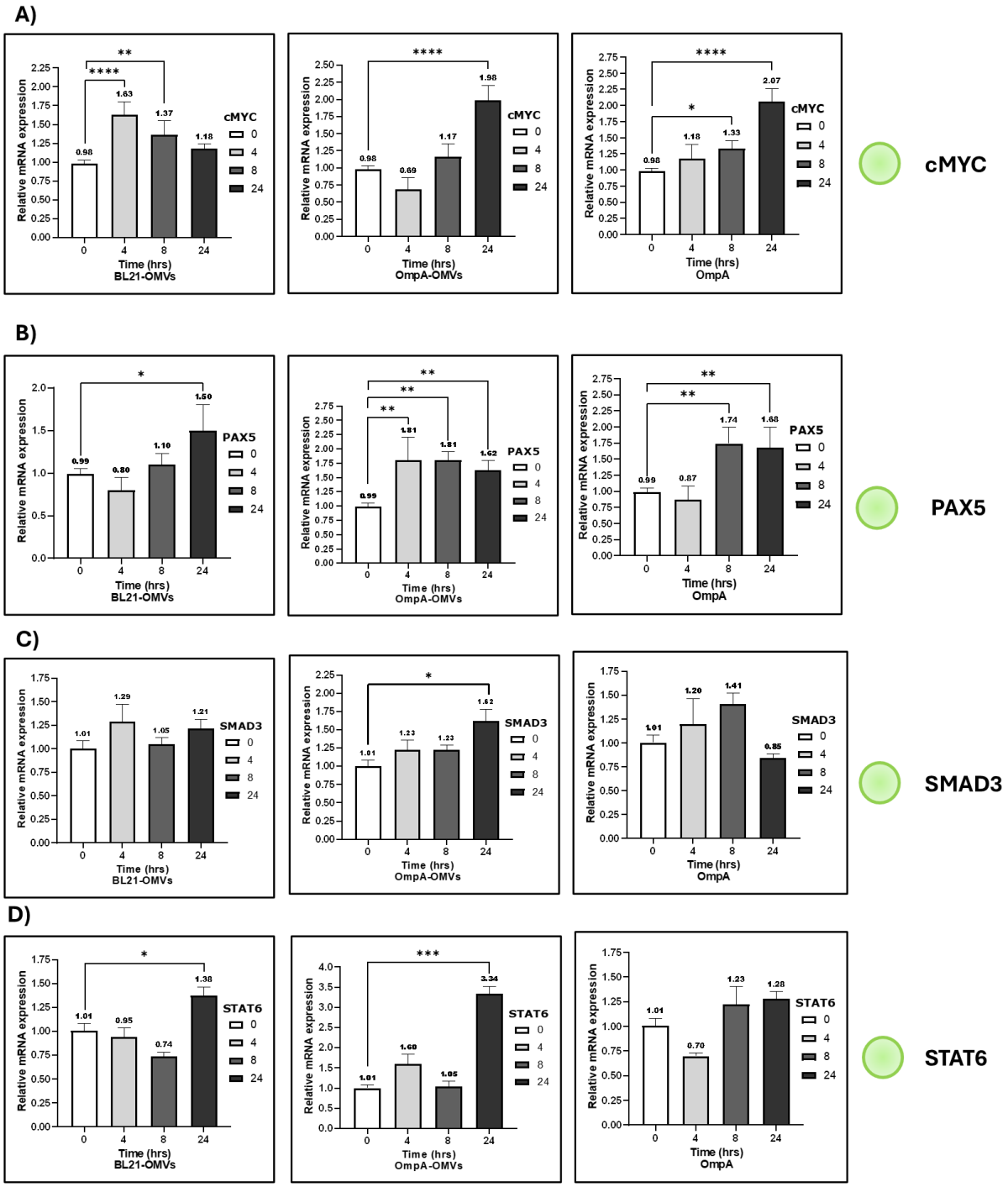

Fig. 6.7 Examine the mRNA expression analysis of the AID transcription activator over 0, 4, 8, and 24 h. A) Relative cMYC expression was analyzed as a transcription activator of AID in response to BL21-OMVs, OmpA-OMVs, and OmpA treatments. Similarly, **B)** Relative mRNA expression of PAX5 was analyzed. **C)** Relative mRNA expression of SMAD3 was also assessed. **D)** The relative mRNA expression was analyzed. Data are presented as the mean ± SD from two independent experiments. Statistical significance was evaluated using ANOVA, with p-values defined as follows: *$p \leq 0.05$; **$p \leq 0.01$; ***$p \leq 0.001$; ****$p \leq 0.0001$.

These results indicate that OmpA-OMVs elicit stronger transcriptional responses in activating genes than BL21-OMVs. We further analyzed cMYB and E2F1 mRNA expression, finding that BL21-OMVs significantly increased cMYB expression at 24 h. In contrast, OmpA-OMVs and OmpA treatments reduced cMYB expression after 8 and 4 h, respectively **(Fig. 6.8A)**. Furthermore, BL21-OMVs showed a moderate increase in E2F1 expression at 24 h. In contrast, OmpA-OMVs had a transient decrease at 4 h but recovered, while OmpA treatment led to significant downregulation after 4 h **(Fig. 6.8B)**. Overall, these findings highlight the OmpA-OMVs' role in downregulating repressors, aiding AID expression induction.

Furthermore, we evaluated the effect of OMVs on cMYC and PAX5 expression through Western blotting and immunofluorescence assays. Western blot analysis, using densitometry, showed a time-dependent increase in cMYC expression in Raji human B-cells treated with OmpA-OMVs and OmpA. The highest increase was observed at 24 h, with increases of 2.2-fold and 2.3-fold, respectively. In contrast, BL21-OMVs showed no significant effect **(Fig. 6.9A-B)**. Similarly, immunofluorescence image analysis indicated significantly enhanced nuclear localization of cMYC and AID in cells treated with OmpA-OMVs and purified OmpA compared to the BL21-OMVs and PBS controls. The merged images depicted the colocalization of DAPI-stained nuclei (blue), cMYC (red), and AID (green). Additionally, the quantification of normalized fold occupancy using fluorescence intensity indicated an increase in cMYC levels after 24 h. The treatment with OmpA-OMVs showed a 2.06-fold increase, while the purified OmpA treatment demonstrated a 2.77-fold increase. Additionally, AID expression levels after 24 h for OmpA-OMVs exhibited a 4.0-fold increase, whereas the purified OmpA treatment showed a 9.87-fold increase **(Fig. 6.9C)**. A ChIP assay was also performed to confirm cMYC occupancy at the nuclear level, where the quantification of normalized cMYC fold occupancy demonstrated upregulation of cMYC expression at 24 h for both OmpA-OMVs and purified OmpA treatments **(Fig. 6.9D)**.

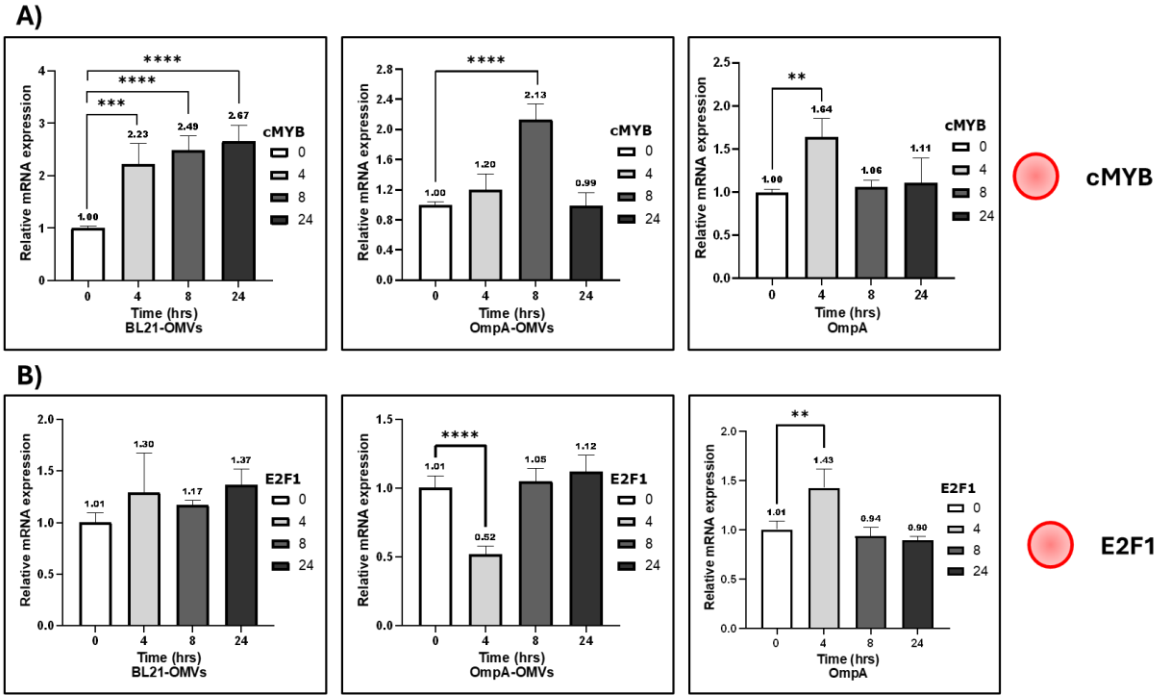

Fig. 6.8 Examine the mRNA expression analysis of the AID transcription repressor over 0, 4, 8, and 24 h. A) Relative cMYB expression was analyzed as a transcription activator of AID in response to BL21-OMVs, OmpA-OMVs, and OmpA treatments. Similarly, **B)** Relative mRNA expression of E2F1 was analyzed. Data are presented as the mean ± SD from two independent experiments. Statistical significance was evaluated using ANOVA, with p-values defined as follows: *p ≤ 0.05; **p ≤ 0.01; ***p ≤ 0.001; ****p ≤ 0.0001.

These findings suggest that OmpA-OMVs effectively induce cMYC and AID expression, highlighting their crucial role in modulating cellular processes associated with these proteins. Furthermore, to assess the impact of OmpA-OMVs on B-cell modulation, we analysed PAX5 expression. Western blot analysis, utilizing densitometry, revealed that both OmpA-OMVs and OmpA significantly upregulated PAX5 expression over time. The highest increases were noted at 24 h, with OmpA-OMVs showing a 1.9-fold increase and purified OmpA demonstrating a 2.5-fold increase. In contrast, BL21-OMVs did not show any significant effect **(Fig. 6.10A-B)**. Immunofluorescence image analysis supported these findings, displaying a significantly enhanced expression of PAX5 in cells treated with OmpA-OMVs and purified OmpA, compared to those treated with BL21-OMVs and PBS controls.

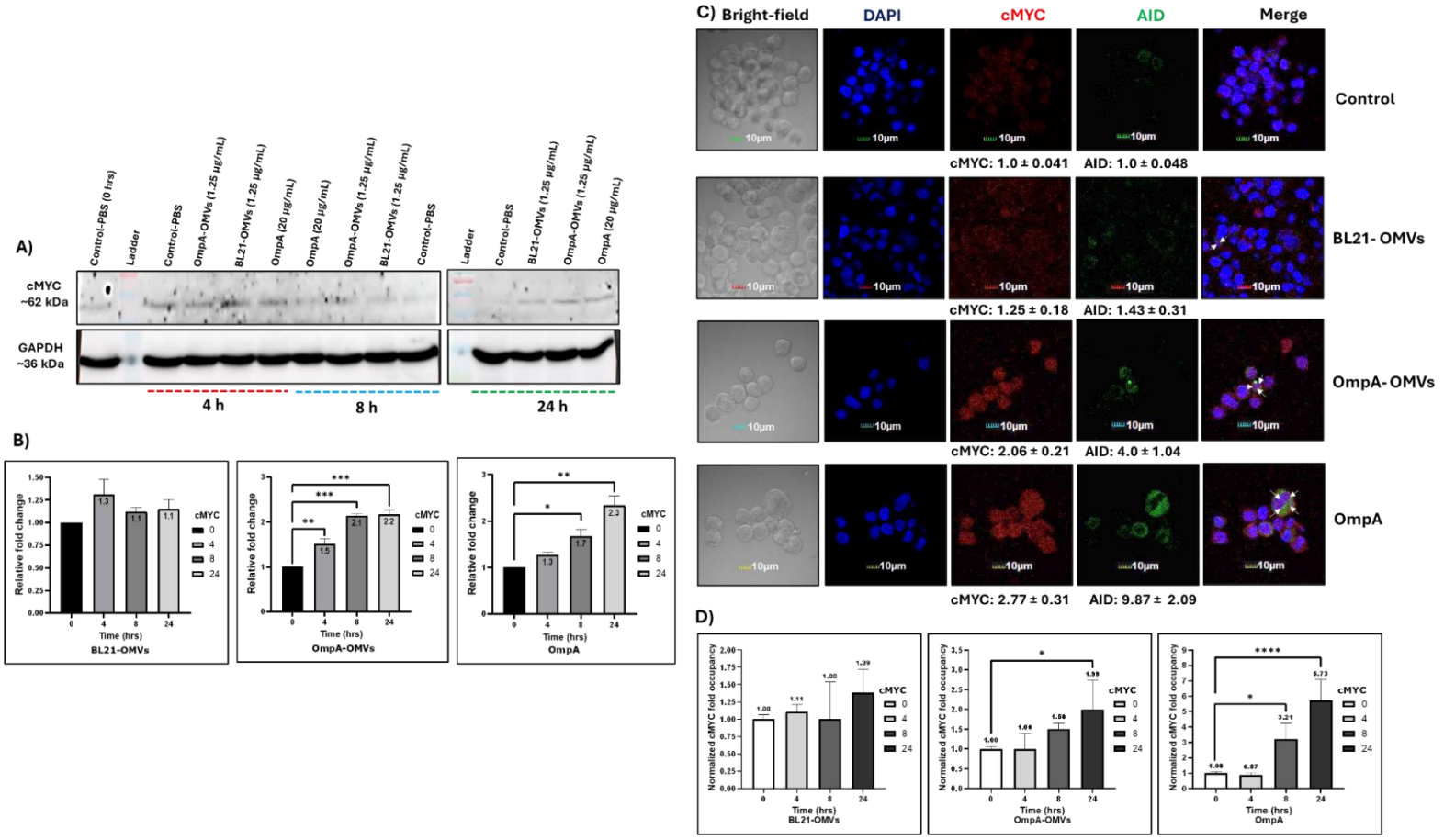

Fig. 6.9 Evaluation of cMYC expression as a transcriptional activator for AID using Western blotting, confocal microscopy, and ChIP analysis. A) Western blot analysis assessed cMYC (~62 kDa) levels with GAPDH (~36 kDa) as a control, using Raji human B-cell lysates treated with Control-PBS, BL21-OMVs, OmpA-OMVs, and OmpA at 4, 8, and 24 h. **B)** Densitometric quantification evaluated fold changes in cMYC protein expression in response to treatments over time. **C)** Confocal images displayed cMYC (red) and AID (green) in stimulated Raji B-cells after 24 h, with nuclei stained by DAPI (blue; scale bar: 10 µm). **D)** ChIP analysis demonstrated cMYC occupancy on target promoters after treatments at various time points. Data represent mean ± SD for two independent biological duplicates. Statistical significance was assessed using ANOVA with p-values: *p ≤ 0.05; **p ≤ 0.01; ***p ≤ 0.001; ****p ≤ 0.0001.

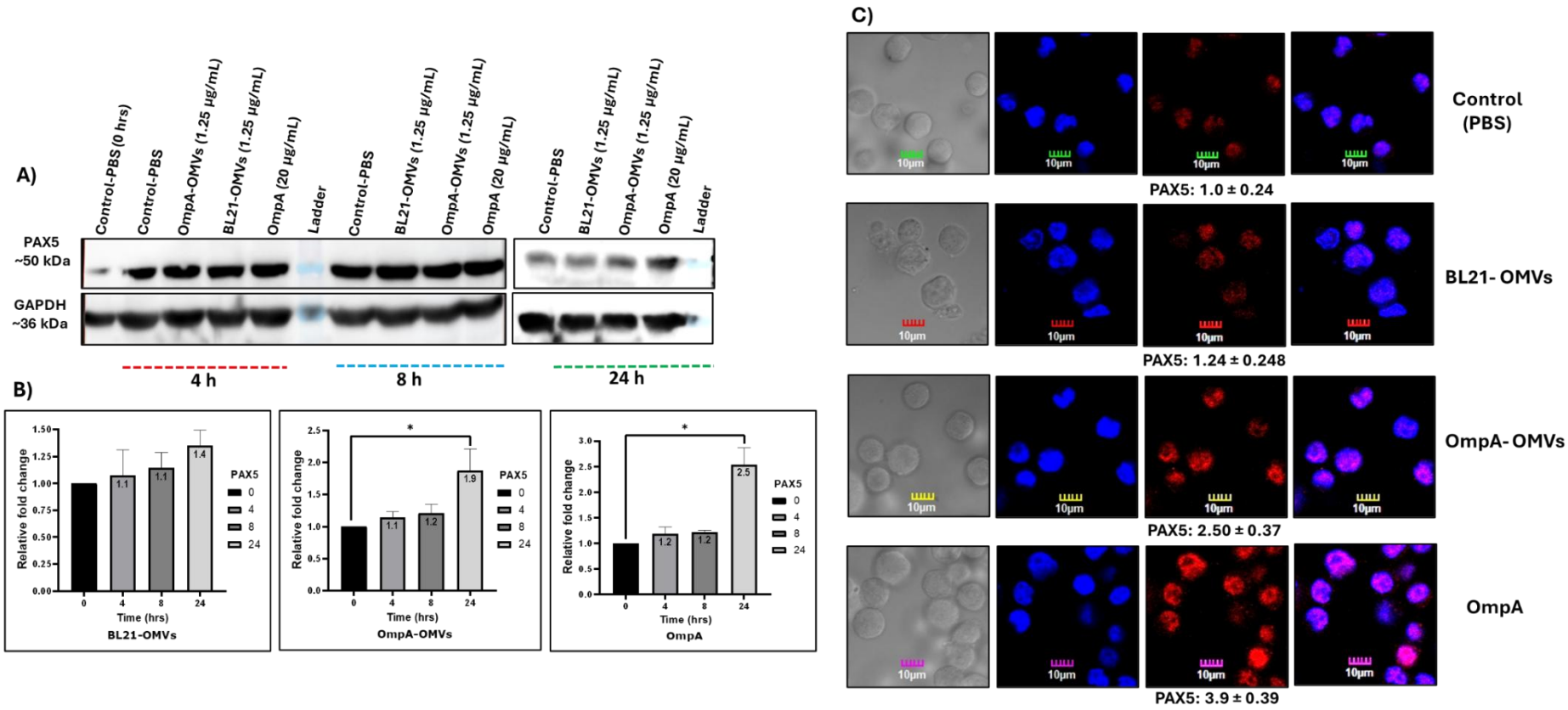

Fig. 6.10 Evaluation of PAX5 expression as a transcriptional activator for AID using Western blotting and confocal microscopy. A) Western blot analysis assessed PAX5 (~50 kDa) levels with GAPDH (~36 kDa) as a control, using Raji human B-cell lysates treated with Control-PBS, BL21-OMVs, OmpA-OMVs, and OmpA at 4, 8, and 24 h. **B)** Densitometric quantification evaluated fold changes in PAX5 protein expression in response to treatments over time. **C)** Confocal images displayed PAX5 (red) in stimulated Raji B-cells after 24 h, with nuclei stained by DAPI (blue; scale bar: 10 µm). Data represent mean ± SD for two independent biological duplicates. Statistical significance was assessed using ANOVA with p-values: *p ≤ 0.05; **p ≤ 0.01; ***p ≤ 0.001; ****p ≤ 0.0001.

Quantification of the normalized fold change in fluorescence intensity indicated a notable increase in PAX5 expression levels at the 24 h mark for both OmpA-OMVs and purified OmpA treatments, with increases of up to 2.5-fold and 3.9-fold, respectively, compared to control samples, while BL21-OMVs showed no significant effect **(Fig. 6.10C)**.

6.2.5 OmpA-OMV Enhances the CSR of Ig Genes

In our research, we investigated the effects of OMV incubation on the CSR activity in Raji human B-cells by measuring the mRNA expression levels of Ig genes at the mature transcript stage. We initially analysed the expression of the mature IgV-Cμ transcript, which is typically present in mature B-cells before class switching occurs. Our findings revealed that B-cells exposed to OMVs and OmpA exhibited an initial increase in IgM expression at the 4 h mark. However, this was followed by a decrease in IgM expression levels compared to the control cells. Interestingly, we also observed mRNA expression of the mature IgV-Cα transcript, with B-cells stimulated by OmpA-OMVs and OmpA exhibiting 1.48-fold and 1.95-fold increases, respectively, in IgA expression at the 24 h mark compared to the control B-cells **(Fig. 6.11A-B)**. Due to the elevated expression levels of both IgM and IgA mature transcripts, we conducted a further analysis of the impact of OmpA on the CSR process in B-cells by assessing the ratios of IgM to IgA. Notably, we found that B-cells treated with OmpA-OMVs and OmpA had IgA ratios approximately 1.78-fold and 2.48-fold higher, respectively, at the 24-hour mark compared to control B-cells. **(Fig. 6.11C)**. Similarly, we also analysed the mRNA expression levels of IgG. We observed that while there was a minimal increase in IgG expression in BL21-OMVs, B-cells stimulated with OmpA-OMVs, and OmpA showed a decrease in IgG expression at the 24 h mark **(Fig. 6.11D)**.

In conclusion, our results indicate that OmpA-containing OMVs effectively enhance B-cell activity by increasing AID expression and CSR function **(Fig. 6.12)**. This underscores their potential as modulators of the immune system and as candidates for therapeutic interventions. These OMVs may act as natural adjuvants to enhance humoral immunity, while recombinant OmpA-OMVs with specific antigens could serve as next-generation vaccine platforms against *Salmonella* and other bacterial infections.

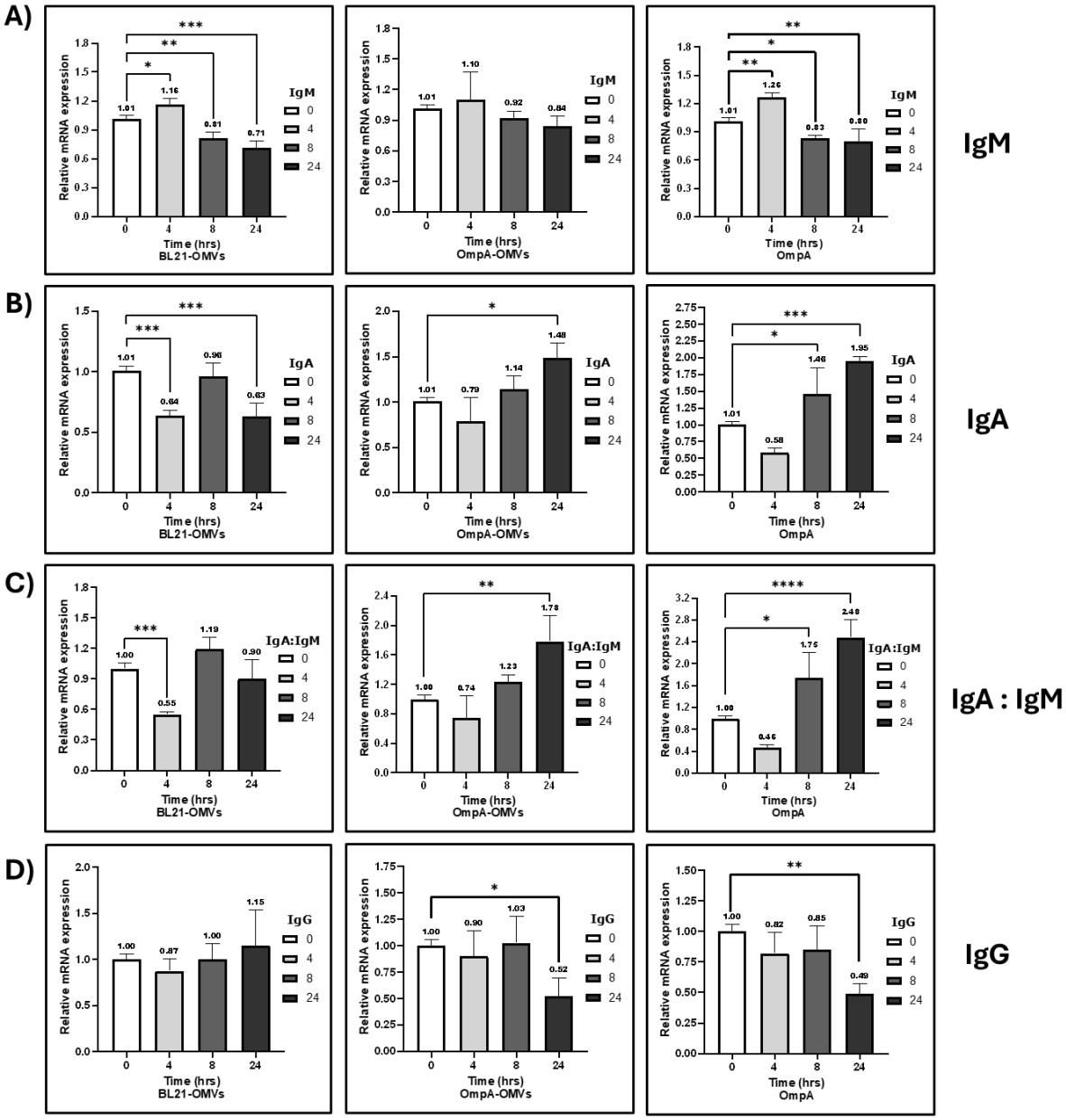

Fig. 6.11 Evaluation of CSR dynamics in stimulated Raji human B-cells. A) mRNA expression of IgM in B-cells treated with BL21-OMVs, OmpA-OMVs, and OmpA at 0, 4, 8, and 24 h shows initial upregulation at 4 h, followed by significant downregulation for BL21-OMVs and OmpA treatments, while OmpA-OMVs show minimal changes. **B)** IgA expression analysis reveals significant upregulation at 24 h for OmpA-OMVs and OmpA, while BL21-OMVs downregulate IgA. **C)** Analysis of the IgA to IgM ratio. **D)** IgG mRNA expression analysis at the same time points. Data are presented as mean ± SD from two independent experiments. Statistical significance was assessed using ANOVA with p-values: *$p \leq 0.05$; **$p \leq 0.01$; ***$p \leq 0.001$; ****$p \leq 0.0001$.

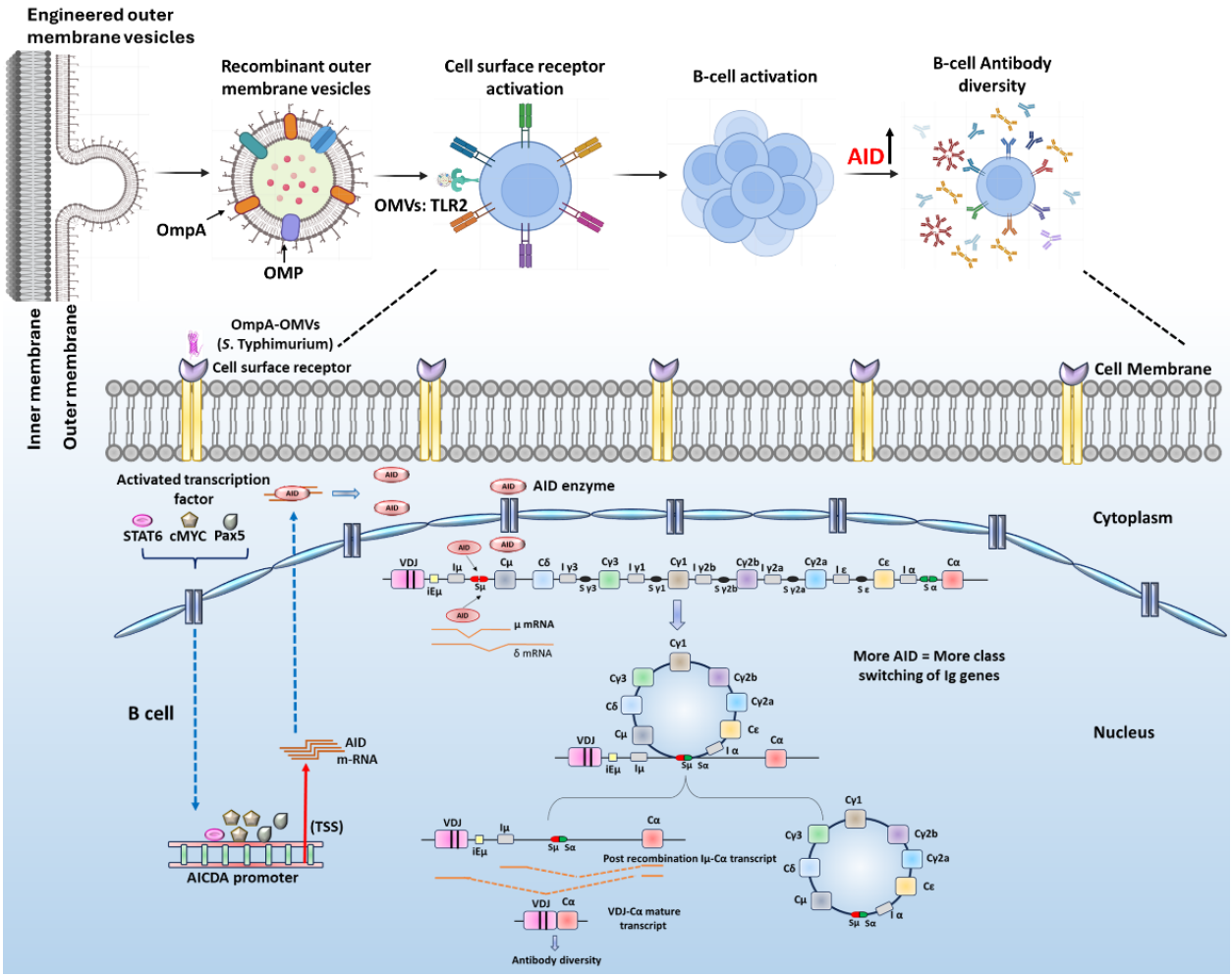

Fig. 6.12 A graphical illustration depicting the activation of OmpA-OMVs in B-cells, leading to abnormal AID expression in B-cells involved in SHM and CSR.

6.3 Summary

In this study, we examined the role of rOmpA-OMVs in modulating B-cell immune responses. Before conducting functional assays, we characterized the isolated rOmpA-OMVs to determine their structural and physicochemical properties. ATR-FTIR analysis confirmed the presence of characteristic protein and lipid functional groups in the OMVs. SEM analysis verified their roughly spherical shape, and DLS analysis indicated a uniform size distribution, with an average diameter of 90-100 nm.

Furthermore, we found that OMVs enriched with rOmpA-OMVs activate TLR2 and induce NF-κB expression, resulting in the activation of downstream signaling. Notably, this B-cell activation by OmpA-OMVs significantly upregulated AID expression, a key enzyme in CSR and antibody diversification **(Fig. 6.12)**. This upregulation is accompanied by transcription activators of AID, such as cMYC, PAX5, STAT6, and SMAD3. At the same time, there was a downregulation of the repressor cMYB, as analyzed at the mRNA level. Protein-level confirmation via immunoblotting showed elevated expression of cMYC and PAX5. Moreover, we also observed increased cMYC occupancy at the nuclear level over time through chromatin immunoprecipitation analysis. This indicates that OmpA transcriptionally regulates AID by enhancing the recruitment of activators and reducing the binding of repressors.

Functionally, OmpA-OMVs promoted IgA expression within 24 h, indicating active isotype switching from IgM. This suggests that OmpA-OMVs enhance the immunogenic properties of OmpA and improve vesicular-mediated delivery, boosting immune activation compared to purified OmpA protein. These findings support the potential use of OmpA-OMVs in targeted immunotherapies or vaccines against *Salmonella* infections.

Chapter 7

Conclusion and Scope of Future Prospects

Chapter 7
7. Conclusion and Scope of Future Prospects

7.1 Introduction

The Gram-negative bacteria are known to have outer membranes and act as the first line of defense against bactericidal agents or toxic compounds. The Outer membrane proteins (OMPs) are components of the outer membrane of Gram-negative bacteria involved in maintaining cell integrity, facilitating nutrient absorption, mediating import and export processes, promoting cell adhesion and invasion, and participating in cell signaling [21,43]. It has been suggested that OmpA is the highly conserved and most abundant OMP in *Salmonella enterica* Typhimurium, and it plays a crucial role in pathogenesis, serving a pivotal role in survival, adhesion, invasion, and immune modulation [43].

Beyond their structural roles, OMPs are also known to adhere to host cells and modulate the immune response. For instance, the porins of *S.* Typhimurium have been found to activate the complement system through both classical and alternative pathways. This highlights their role in immune modulation and bacterial virulence [164]. Additionally, the rapid development of antibiotic resistance in *S. Typhimurium* infections remains a major clinical challenge. Studies have demonstrated that OmpA plays an important role in the resistance to antibiotics like ceftazidime and meropenem. Notably, a study by Chaudhary et al. found that an OmpA-deficient strain of *S.* Typhimurium (STM ΔompA) exhibited reduced proliferation within macrophages [43].

The antigenic properties, surface-exposed loop, and structural conservation of OmpA make it an attractive target for therapeutic potential [20]. In addition, emerging evidence suggests that outer membrane vesicles (OMVs) containing OmpA are involved in the increased immunogenic potential and enhanced drug delivery, making them ideal for vaccine development and diagnostic applications [61,62,165]. Thus, given the rising antibiotic resistance in *Salmonella*, it is crucial to understand the roles of OmpA. This thesis investigates the structural and functional aspects of OmpA from *S.* Typhimurium, focusing on the immunomodulatory effects of recombinant OmpA and OmpA-decorated outer membrane vesicles (OMVs) on B-cells. Specifically, it

examines how OmpA influences the expression of activation-induced cytidine deaminase (AID), which modulates class switch recombination. The findings from this study contribute not only to our understanding of OmpA as a virulence factor but also highlight its potential as a target for therapeutic intervention. In this chapter, we discuss our key findings with existing research and provide conclusions along with future prospects for this study.

7.2 Computational and biophysical characterization of OmpA, a major outer membrane protein from *S.* Typhimurium.

Among the OMPs, OmpA is the most abundant protein in Gram-negative bacteria, with typically 100,000 copies per cell, and is highly conserved across multiple species of Gram-negative bacteria. It plays a multifaceted role in bacterial structural integrity and pathogenicity [37]. In *S.* Typhimurium, the N-terminal domain of OmpA contains 8 transmembrane β-barrel motifs residing within the outer membrane, while the C-terminal domain resides within the periplasm region. A 15-amino-acid residue linker region that connects the β-barrel protein to the soluble C-terminal domain [37]. While the crystal structure of the C-terminal domain of OmpA is available in *S.* Typhimurium 14028s (PDB ID: 5VES), the three-dimensional structure of the N-terminal domain of OmpA in *S.* Typhimurium has not yet been solved. This structural gap is significant because β-barrel domains are essential for membrane integration and immune recognition.

In this study, we conducted computational analysis to predict the subcellular localization, signal peptide, and secondary and tertiary structure of the OmpA, thereby confirming its classification as a membrane protein. Despite the availability of the N-terminal domain structure in *E. coli* with 90% sequence similarity, the detailed biophysical characterization of OmpA in *S.* Typhimurium is limited. Thus, these findings elucidate its significance in *S.* Typhimurium pathogenesis and contribute to its potential as a target for developing therapeutic targets. Additionally, OmpA's structural flexibility in the loop region of the beta-barrel may facilitate *S.* Typhimurium's survival under diverse host environments. This adaptability enhances resistance to adverse

circumstances by altering peptidoglycan interactions and pore dimensions for selective permeability [166,167].

Visualization of the OmpA protein using the PoreWalker tool reveals a structure comprising a β-barrel-protein, forming a pore-like cavity within the barrel. Thus, upon visualization of the OmpA pore, cavity features, diameter, and shape, it was observed that the pore diameter of OmpA varied from 22 to 3 Å. The narrowest region likely acts as a selective filter, restricting the passage of larger molecules. This characteristic aligns with OmpA's role as a low-permeability porin, allowing only small solute diffusion. Thus, OmpA is identified as a porin with low permeability, facilitating the passage of small solutes. A study by Sugawara and Nikaido demonstrated that OmpA forms a diffusion channel with an approximate diameter of 10 Å, allowing the passage of small molecules up to 600 Da *in E. coli* [168]. This suggests its involvement in pathogenesis through facilitating diffusion and permeability, which aid in transporting essential nutrients and toxins and potentially play a crucial role in bacterial infections.

Utilizing different solubilization, purification, and refolding strategies has provided valuable insights into preserving the structural integrity of OmpA. Singh and Panda emphasize that refolding the inclusion body into a bioactive form is crucial to avoid poor recovery and major production costs of recombinant proteins. Their approach involves solubilizing the inclusion body in a mild solubilizing agent containing an alkaline pH in the presence of 2M urea. This method results in recovering bioactive protein while maintaining its native structural integrity, compared to utilizing a high concentration of a chaotropic agent [1]. Notably, solubilizing OmpA in a high-pH buffer has proven effective in preventing complete denaturation and retaining its native-like secondary structure in a solubilized state.

Characterization of OmpA through biophysical techniques by employing refolding dynamics studies has provided valuable insights into its structural attributes and functional properties. OmpA plays a crucial role in maintaining the structural integrity of the outer membrane through interaction with peptidoglycans. Interestingly, a study by Park *et al*. indicated that OmpA from *A. baumannii* is a key protein that anchors the outer membrane to peptidoglycans. They found that the C-terminal domain

of OmpA binds to diaminopimelate, a unique amino acid present in peptidoglycan, which is essential for linking and anchoring [166]. In our study, we observed that OmpA forms a dimer, as confirmed by SEC and semi-native SDS-PAGE. SEC-based methods are widely recognized for determining protein oligomeric states and are employed in protein characterization. For example, Chandravanshi et al. reported that the S9bs peptidase from *Bacillus subtilis* eluted as a ~293 kDa species in SEC while migrating as a ~75 kDa monomer on SDS-PAGE, thereby confirming its tetrameric assembly through SEC alone [169]. Nevertheless, as this observation could be influenced by detergent micelles, further validation using techniques such as SEC-MALS or native mass spectrometry would be necessary to confirm dimerization of OmpA.

Among OMPs, OmpA tends to form dimers that contribute to membrane stability and function [38]. Importantly, dimerization plays a key role in maintaining the structural integrity of OmpA by preventing the collapse of the flexible linker that connects its transmembrane and periplasmic domains. This stabilization enhances both the structural integrity and mechanical strength of the outer membrane [37,170]. Furthermore, the dimeric form of OmpA may facilitate interactions with host factors that enhance the virulence of *Salmonella*. Similarly, a study by Ortiz-Suarez proposed that the dimerization of OmpA from *E. coli* is involved in pore formation, peptidoglycan binding, and host adhesion, supporting its multifunctional role beyond just being a porin [37]. Moreover, the oligomerization of OMPs profoundly influences organismal pathogenesis, such as HomA and HomB shed light on their potential roles in bacterial colonization, persistent infection, and biofilm formation [114]. OmpA's role in biofilm formation and distinct dimerization patterns further enhances bacterial persistence, making it an essential part of pathogenesis and a potential target for therapy [171]. This process leads to the formation of pore structures in the outer membrane, facilitating functions like nutrient uptake, toxin efflux, and secretion of virulence factors [172]. Heat modifiability is a distinctive feature of β-barrel proteins, which demonstrates migration differences in semi-native SDS-PAGE [115,173–175], while trypsin digestion has confirmed the presence of distinct domains within the protein. The analysis of OmpA's secondary structure using FTIR spectroscopy and circular

dichroism spectroscopy has revealed a predominance of β-sheet structures, consistent with its role as a β-barrel protein.

The ATR-FTIR is a useful technique for determining the relative amounts of different secondary structures in proteins. This information can be obtained in the amide-I band of protein in the IR spectrum, ranging from 1600 to 7600 cm^{-1} [176]. In our study, we conducted the IR study, which revealed that the generated spectra contained the sum of α-helix, rich in β-sheets, turns, and coil structures [114,177]. Similarly, in the CD spectra, a broad negative peak around 220 nm is more prominent, which corresponds to β-sheets, indicating that the protein has a high level of structural integrity [178,179]. However, when we unfold the protein in the presence of urea denaturant, it loses its secondary structural integrity, and a strong negative peak vanishes. The stability of OmpA under different environmental conditions, such as varying pH and temperature, has underscored its robustness and potential suitability for therapeutic applications. We have also investigated how the OMPs interact with detergents and lipids, providing a membrane-like amphipathic environment that imparts unique properties compared to aqueous solutions. For instance, the dielectric constant of the hydrophobic core of micelles, in which OMP is embedded, is believed to be lower than that of proteins present in aqueous solutions, such as water [180]. Consequently, the refolding of denatured protein in the presence of detergent and lipids leads to the restoration of its native structure, as verified by CD spectra analysis.

Tryptophan fluorescence spectroscopy further confirmed the maintenance of the tertiary structure, with native OmpA exhibiting fluorescence maximum at 326 nm, which shifted to 342 nm in the denatured state with a loss of fluorescent intensity. Similar shifts in λmax in the presence of urea have been reported previously [114,181]. Notably, when the denatured protein was refolded with detergents and lipids, the structural integrity of the β-barrel protein was restored, accompanied by an increase in fluorescence intensity compared to the unfolded OMP.

In this study, we present an initial biophysical characterization of *S. Typhimurium* OmpA, including analyses of its secondary structure, folding, and size-exclusion behavior, to begin addressing the lack of structural data. However, high-

resolution studies like cryo-EM, X-ray crystallography, or NMR spectroscopy are needed for detailed insights into the N-terminal domain of OmpA. Future studies will use these methods to define OmpA's β-barrel structure in membrane-mimetic systems, such as lipopolysaccharide (LPS)-containing asymmetric bilayers, OMVs, and supported phospholipid bilayers. This will enhance our understanding of OmpA's folding, membrane integration, and immune recognition [61,182,183].

Vaccines are a safe and effective means of controlling the spread of infectious diseases, playing an important role in immune system activation. The use of surface antigenic epitopes is essential for designing effective vaccines. Conventional vaccine development faces several challenges, including being labor-intensive, time-consuming, and costly [184]. In this study, OmpA protein was utilized to screen the multi-epitopes for vaccine development using an immunoinformatic approach, demonstrating a high potential for binding with MHC class-I, MHC class-II, and B-cells. Overall, our results suggested that OmpA is a promising vaccine target against antibiotic-resistant *S. Typhimurium*. Interestingly, the immune simulation results indicated that OmpA has the potential to trigger both cellular and humoral immune reactions. The immune simulation predicted that OmpA activates macrophages, T-cells, and B-cells for antigen clearance. Additionally, it induces IFN-γ, TGF-β, and IL-10 during immune simulation validations. In summary, the epitopes derived from OmpA as a vaccine candidate are likely to be antigenic, non-toxic, and to stimulate innate and adaptive immune responses, suggesting it is a strong vaccine candidate for *S*. Typhimurium infection. However, further studies, including biologically relevant *in vitro* and *in vivo* models, are essential to validate the immunogenicity, safety, and protective efficacy of these epitopes before translational application.

In conclusion, this study signifies a substantial step forward in our understanding of the structural and functional properties of OmpA, providing a foundation for future investigation into its therapeutic significance.

7.3 Unravelling the role of OmpA from *S*. Typhimurium in host TLR2 interaction and its impact on immune modulation.

OmpA plays a significant role in bacterial interaction with host cells [185,186]. A study conducted by Kim *et al*. demonstrated that *in vitro* studies using human laryngeal epithelial HEp-2 cells in response to OmpA from *A. boumannii* have shown the induction of pathogen-associated molecular patterns (PAMP) and immune responses. Notably, there was a significant surface expression of TLR2 and activation of iNOS, both of which are crucial for the host-defense mechanism [187].

To investigate the interaction of OmpA from *S*. Typhimurium with TLR2, we initially performed an *in silico* docking analysis, focusing on the extracellular domain of OmpA and selecting TLR2 for the study. The analysis revealed that the extracellular region of OmpA plays a crucial role in interacting with the host cell surface receptor. Two distinct cell models were utilized to experimentally validate this interaction and investigate OmpA-mediated host cell interactions. The HEp-2 cell line, derived from human laryngeal carcinoma, serves as a model for studying pathogen–epithelial interactions. It was utilized to simulate the initial contact site of *Salmonella* at the mucosal barrier, reflecting the natural epithelial entry point during infection. HEp-2 cells exhibit epithelial-like morphology and retain characteristics resembling mucosal surfaces, making them suitable for investigating bacterial adhesion, invasion, and interaction dynamics [188–190]. In contrast, Raji cells, a human Burkitt lymphoma-derived B-cell line, were employed as a model to explore immune modulation, B-cell surface receptors, immunoglobulin expression, and CSR studies [191–194]. Together, these cell lines provide a complementary *in vitro* system to mimic both the epithelial invasion and immune modulation phases of *Salmonella* pathogenesis.

In our study, stimulation of HEp-2 cells and Raji human B-cells with OmpA led to not only interaction but also upregulation of TLR-2 expression at mRNA and protein levels, indicating activation of cell surface receptors on the cells, which allows TLR2 to aid in the recognition of PAMP that expressed on infectious agents and mediates the cytokine production necessary for the development of effective immunity. In our research, we validated this interaction using pulldown assays, co-immunoprecipitation, and co-localization studies. While the biochemical evidence

supports the OmpA-TLR2 interaction, we recognize that complementary biophysical methods such as surface plasmon resonance (SPR), isothermal titration calorimetry (ITC), and targeted mutagenesis could provide additional refinement and strengthen the mechanistic understanding of this interaction. Furthermore, our findings indicated that OmpA stimulation enhances TLR2 expression, contributing to the induction of pro-inflammatory cytokine production such as TNFα through the activation of NF-κB, which plays a crucial role in immune activation [195]. However, inclusion of TLR-2 agonists, such as Pam3CSK4 and Pam2CSK4, as positive controls would enhance the interpretation of OmpA-mediated effects and validate TLR-2-dependent signaling [196].

Interestingly, Zhang *et al*. reported that OmpA from *A. baumannii* disrupts the pulmonary epithelial barrier through the induction of TLR2/NF-kB activation, resulting in the production of pro-inflammatory cytokines such as IL-6 and TNFα, which play a crucial role in epithelial permeability dysfunction [195]. Likewise, in our study, we found that stimulation with OmpA resulted in the upregulation of NF-κB-p65 and TNF-α expression in Raji human B-cells, which is further involved in the inflammation process. In gastric carcinogenesis, *Helicobacter pylori* CagA-positive strains significantly increase the expression of NF-κB-p65 and its target genes (c-Myc, Cyclin D1, and Bcl-xL) in conditions such as intestinal metaplasia (IM), dysplasia (DYS), and intestinal-type gastric carcinoma (GC), thereby facilitating carcinogenesis [197]. In this context, CagA also facilitates the aberrant expression of AID, an enzyme vital for DNA/RNA editing that contributes to SHM and CSR of immunoglobulin genes, through the activation of NF-κB via the type IV secretion system [198].

Importantly, a study conducted by Tamrakar *et al*. demonstrated that OMPs such as HomA and HomB modulate B-cell responses by suppressing AID expression and CSR in B-cells, reducing the IgA/IgG expression while enhancing the expression of immunosuppressive markers (IL10, IL35, and PD-L1), thereby aiding in immune evasion. The reduction in NF-κB expression, a key regulator of AID expression, may contribute to this immunosuppression [79]. In contrast, a recent report from our group revealed that OmpA from *S*. Typhimurium is involved in the aberrant AID expression,

which leads to class switching of immunoglobulin from IgM to IgA in B-cells [20]. This increased abnormal AID expression may further promote carcinogenesis. Thus, in this study, OmpA serves a dual purpose: it links innate immune activation through TLR2/NF-κB signaling and facilitates an adaptive immune response via AID expression. While class switching is essential for antibody diversity, aberrant AID expression can lead to genomic instability and contribute to inflammation-associated carcinogenesis.

In summary, studying the molecular mechanism of OmpA's modulation in host cells is pivotal for understanding *Salmonella* pathogenesis. Targeting OmpA to disrupt its interaction with TLR2 and the activation of NF-κB could help mitigate inflammatory damage and AID-mediated mutagenesis. Thus, utilizing OmpA emerges as a critical therapeutic strategy against *Salmonella*-related diseases. Moreover, this research is significant for developing vaccine candidates utilizing OMPs.

7.4 Unraveling the impact of Outer Membrane Protein, OmpA, from *S.* Typhimurium on aberrant AID expression and IgM to IgA class switching in human B-cells.

In this study, we delved into the influence of OmpA from *S.* Typhimurium in modulating the aberrant AID expression in B-cells, shedding light on the mechanism by which bacterial components influence host cellular processes. Our findings highlight the novel interaction between OmpA and the host immune system, revealing that OmpA potentially induces aberrant AID expression in B-cells. This aberrant AID expression in B-cells leads to significant changes in B-cell activities, notably SHM and CSR, which play pivotal roles in antibody diversification within antigen-specific B-cells and contribute significantly to the adaptive immune system [20].

The interaction of *S.* Typhimurium and the host immune system is complex, involving both innate and adaptive immune responses. During the initial stage of infection, PAMPs are recognized by the pathogen recognition receptors (PRRs), triggering acute intestinal inflammation. *Salmonella* has evolved strategies to withstand neutrophil attacks in intestinal tissues and exploit the inflamed environment to enhance

its survival and proliferation [199,200]. Regarding the adaptive immune response, CD4 T-helper (Th) cells produce cytokines that influence the immune profile, with Th1 responses characterized by pro-inflammatory effects and activation of antimicrobial mechanisms, while Th2 responses have anti-inflammatory properties [201]. Maintaining the balance between these responses is crucial during persistent *Salmonella* infections.

In the context of *S.* Typhimurium infection, OmpA plays an important role in intracellular virulence, facilitating adhesion and invasion processes. A study by Choudhary *et al.* emphasizes that an OmpA-deficient strain of *S.* Typhimurium exhibited decreased proliferation in macrophages and increased susceptibility to nitrosative stress [43]. Additionally, OmpA contributes to antibiotic resistance, thereby protecting *S.* Typhimurium from broad-spectrum β-lactam antibiotics, such as ceftazidime and meropenem, by stabilizing the outer membrane [133]. Souwer et al. reported that *Salmonella* disseminates systemically by exploiting primary human antigen-specific B-cells. When these B-cells recognize *Salmonella* through B-cell receptors, they internalize the bacteria, facilitating its entry and interaction within the host immune system for infection spread [202]. However, the impact of *Salmonella* infection on B-cells, particularly on the antibody response, remains largely unexplored.

In our study, we investigated the impact of OmpA from *S.* Typhimurium on AID expression, which is crucial for CSR and affinity maturation, processes specific to B-cells. Recombinantly cloned and expressed OmpA was characterized to ensure proper refolding and to make it endotoxin-free after its purification. Furthermore, we aimed to elucidate the intricate regulation of AID expression. AID is a crucial enzyme responsible for antibody diversity and plays a significant role in CSR. In this study, we utilized the Raji human B-cell line, which is derived from human Burkitt lymphoma, as a model for our hypothesis regarding the role of OmpA in inducing aberrant AID expression and regulating the CSR process. However, Raji human B-cells carry some properties of human primary B-cells, including mutations, MYC translocation, aberrant expression patterns, and genetic modifications across various genes. Raji human B-cells have been one of the choices of researchers for studying immune modulation,

BCR signaling, and immunoglobulin expression studies [93,191–194]. However, additional validation of these findings is needed through the use of human primary B-cells, particularly those with an induced germinal center phenotype B-cells (iGB cells) [203], as well as clinical samples like peripheral blood mononuclear cells (PBMCs) from infected patients or animal models. This will contribute to the development of therapeutics for *Salmonella* infections and the exploration of OmpA as a potential virulence factor.

Initially, we conducted cell viability assays by stimulating B-cells with OmpA, which revealed notable effects on cell morphology. This was further assessed by measuring the expression of proliferative markers, which indicated that both Ki-67 and PCNA were downregulated. Additionally, we observed the formation of clusters of proliferating cells, suggesting that their development is not solely dependent on the upregulation of Ki-67 or PCNA. Other factors, such as cell stress, cell adhesion, the presence of small B-cell receptor clusters, and differentiation signals from B-cell activators, may also play a significant role [204–206]. Furthermore, we noted a decrease in cell viability, which we quantified using the MTT assay and the trypan blue exclusion method.

Moreover, we have found that OmpA functionally activates TLR2-mediated cell surface receptor activation. Our findings also indicated that stimulation of B-cells with increasing concentrations of OmpA leads to upregulation of AID expression. Interestingly, we observed a significant increase in the mRNA expression of AID at various time intervals. However, when examining AID expression at the protein level, we found that this increase was not sustained at the 24-hour mark. This discrepancy could be due to post-transcriptional regulatory mechanisms, as AID is known to be a tightly regulated enzyme with a relatively short half-life of approximately 8 h [207,208].

Various transcription factors regulate the expression and activity of AID at multiple levels. Factors such as cMYC, NF-κB, Pax5, SMAD3, and STAT6 enhance AID expression, while others, such as cMYB and E2F1, inhibit its expression [79,154]. Our findings indicated that on stimulation of B-cells with increasing concentrations of

OmpA, there is an upregulation of AID expression. We noted that OmpA upregulates the expression of enhancers such as cMYC, Pax5, and STAT6. These enhancers may recruit to the AID promoter region, facilitating the increase in AID expression. Concurrently, OmpA diminishes the binding of repressors such as E2F1 and cMYB to the AID promoter region. This suggests that OmpA transcriptionally regulates AID by enhancing the recruitment of transcriptional activators and reducing the binding of transcriptional repressors. Furthermore, our study unveiled a direct relationship between AID and cMYC expression, evident at both protein and mRNA levels, as supported by immunoblotting and RT-qPCR analyses. Additionally, through immunofluorescence studies, we observed increased expression and nuclear localization of both AID and cMYC in stimulated B-cells. Further investigation of cMYC occupancy at the *aicda* regulatory locus demonstrated a significant increase over time. Based on these findings, it can also be suggested that overexpression of the cMYC, Pax5, and STAT6 in stimulated B-cells leads to aberrant AID expression, which may progress toward dysregulated CSR.

Our study not only shows a possible connection between aberrant AID expression and antibody diversity, but it also raises the possibility that OmpA may have an impact on mechanisms involved in B-cell lymphoma. These mechanisms are crucial in producing a broad repertoire of antibodies to combat pathogens. The mechanisms underlying adaptive immunity are in the variable region of the heavy and light chain immunoglobulin loci. CSR and AID are greatly dependent on the transcription of the immunoglobulin gene [79]. Transcription of the immunoglobulin gene provides a single-stranded DNA sequence for the AID enzyme, which deaminates the cytosine to uracil. AID is a crucial factor required to trigger both CSR and SHM when DNA breaks are introduced into the variable or switched regions of immunoglobulin genes, resulting in isotype switching of the constant region from Cμ to Cγ, Cα, and Cε [79,209].

AID is essential for CSR and SHM and generates antibody diversity to enhance pathogen immunity. However, when AID expression is dysregulated, it can lead to suboptimal class switching, altering the balance of protective versus non-protective antibodies [153]. In our study, we observed that B-cells stimulated by OmpA exhibited

aberrant AID expression. This induced AID expression may further contribute to the high frequency of malignancies [89,90].

Beyond the immune evasion, *Salmonella* spp. is recognized for its ability to cause chronic inflammation of the bile ducts and produce toxins with carcinogenic potential, which may contribute to the development of extrahepatic biliary tract cancer [210]. Among its serovars, *S.* Typhi has been specifically linked to an increased risk of gallbladder cancer, as it can persist in the gallbladder and induce prolonged inflammation. This creates a microenvironment that is conducive to carcinogenesis [211]. Furthermore, *Salmonella* infections have also been implicated in colorectal cancer. Chronic infections with non-typhoidal *Salmonella*, especially *S*. Typhimurium and *S*. Enteritidis, have been associated with an increased risk of developing colon cancer. This risk is significantly elevated in individuals who have suffered from severe salmonellosis, suggesting that these infections may play a major role in the development of colorectal tumorigenesis [145,212]. Mechanistically, *Salmonella* influences cancer progression by modulating host cell signaling pathways. According to Liu et al., *Salmonella* effector proteins (AvrA) can activate the Wnt/β-catenin pathway, which plays a crucial role in regulating cell proliferation and differentiation. This activation can result in cellular transformation and the development of tumors [213]. Similarly, Duan *et al*. demonstrated that TNF-α could elevate the expression of AID via the NF-κB signaling pathway. This increase in AID expression consequently enhances the Igα heavy chain expression and its binding ability to the Sα region. Their finding strongly suggests that the involvement of TNF-α induced AID expression in the process of CSR within cancer [93]. Our findings suggest that OmpA-driven AID upregulation and increased CSR may contribute to oncogenic transformation by inducing genomic instability in B-cells, a process that has been linked to lymphoma development. The intersection between *Salmonella*-induced immune modulation and oncogenesis underscores the need for further research into its long-term effects on host immunity and cancer risk. Our research provides a foundation for future therapeutic strategies targeting immune modulation.

In summary, this study uses a comprehensive strategy to investigate the functional features of OmpA, which answers fundamental issues about its role in AID control and suggests fascinating possibilities regarding its involvement in other critical immunological processes. As a result, this study's findings provide useful insights that could aid in the development of novel therapeutic techniques for *Salmonella* infections. Researchers may develop ways to mitigate *Salmonella* and other diseases by focusing on important players such as OmpA.

7.5 Engineering Outer Membrane Vesicles (OMVs) carrying OmpA from *S.* Typhimurium for targeted modulation of human B-cell function through AID expression and class switch recombination.

OMVs are gaining attention due to their immunogenic properties, self-adjuvants, and components such as OMPs, LPS, flagellin, and peptidoglycan that elicit both humoral and cell-mediated immune responses [67,214]. Tan et al. suggested that OMVs represent a new era in adjuvant development, providing a safer and more effective alternative to traditional adjuvants, along with multifunctional vaccine delivery capabilities [215]. Notably, Liu et al. have investigated engineered OMVs as adjuvants to enhance immunity against *H. pylori* infection. These OMVs are designed to carry plasmids that encode immunomodulatory cytokines, such as IL-12 and IFN-γ. When administered alongside *H. pylori*, they generate stronger humoral and mucosal immune responses in mice and significantly reduce bacterial colonization in the gastric mucosa compared to standard adjuvants or OMVs that do not contain cytokine plasmids [216]. Similarly, OMVs can also potentiate *H. pylori* vaccine efficacy by promoting robust mucosal immunity and Th1/Th17 responses, highlighting their potential as next-generation adjuvant platforms [217,218]. Thus, these OMVs are promising candidates for vaccine development. OMVs have been extensively studied, particularly in relation to *Neisseria meningitidis*, leading to the approval of the meningococcal vaccine (MenB) and the *Haemophilus influenzae* type b (Hib) vaccine [157].

Interestingly, Harrell et al. conducted a study in which they developed an oral vaccine against *Salmonella*, utilizing OMVs from *Burkholderia pseudomallei* as an adjuvant. They found that a combination of heat-killed *S.* Typhimurium and OMVs

protects against lethal *Salmonella* infections in mice by inducing CD4 T-cell and B-cell responses through the production of neutralizing systemic and mucosal antibodies, which enhance overall immunity [219]. Likewise, Alaniz et al. reported that membrane vesicles secreted by *S*. Typhimurium play an important role in stimulating both innate and adaptive immune responses. Specifically, researchers have demonstrated that OMVs can activate dendritic cells, leading to the production of signaling molecules known as cytokines, such as TNF-α and IL-12. These cytokines help recruit and prime B-cells and T-cells, which contribute to the development of a specific immune response against *Salmonella* infection. Overall, their findings suggest that OMVs may open up new possibilities for developing effective vaccines against *Salmonella* pathogenesis [220].

Traditionally, the study of OMPs has relied on solubilized or reconstituted proteins. However, these methods may not fully replicate the cellular membrane and often lack key features, such as lipid diversity and specific membrane compositions. Additionally, they do not account for how the immune system interacts with the proteins during actual infections. In contrast, using OMVs is advantageous because they naturally carry a lipid bilayer and preserve OMPs within it, providing a more accurate representation of the protein's environment. For example, a study by Thoma et al. investigated the folding, structure, and assembly of OmpG, FhuA, Tsx, and BamA in the native membrane environment of OMVs. Their findings revealed that comparing OMPs in OMVs with those in reconstituted artificial lipid membranes demonstrates that OMVs serve as a more biologically relevant platform for understanding the structure-function relationship of OMPs in their natural state [221]. Additionally, OMVs have potential advantages for vaccine development, including the absence of replication, enhanced safety, increased immunogenicity, and intrinsic adjuvant properties due to components like LPS, OMPs, and immune-stimulating molecules [214,222]. As compared with the previous study, it indicates that the OmpA from *Shigella flexneri* 2a can induce protective innate and adaptive immunity through TLR2 in mice by inducing IgA and IgG in systemic and mucosal compartments by activating Th1 cells, leading to enhanced cellular immunity, offering a novel approach to developing a Shigellosis vaccine [223]. Similarly, in our previous study **Chapter 5**, we

reported that the OmpA protein from *S*. Typhimurium plays a role in B-cell modulation. We used purified and refolded OmpA (20 μg/mL) to stimulate human B-cells and found that OmpA was involved in the increased AID expression and class switching in these cells [20]. However, the use of isolated purified OmpA may not fully reflect how the immune system encounters the protein during an actual infection. Therefore, in this work, we utilized OmpA-OMVs as a delivery platform to explore their immunomodulatory potential that mimics natural membrane environments, allowing for enhanced receptor engagement and downstream signaling [43,224]. Additionally, we included BL21-OMVs as a control. These vesicles are derived from *E. coli* BL21(DE3) and contain various OMPs, such as OmpA, OmpF, OmpC, and LamB, which may contribute to the activation of the immune system [221]. Although OmpA is conserved among the Gram-negative bacteria, including *E. coli* BL21(DE3), species-specific variation may also influence their ability to modulate immune responses in the B-cells. Notably, a study from Won et al. noted that mass-produced *E. coli* BL21(DE3) ΔmsbB-derived OMVs exhibit immunostimulatory properties by activating and recruiting antigen-specific and stem-like $CD8^+$ T cells [225]. Similarly, a study by Skerniškytė et al. showed that OMVs lacking OmpA from *A. baumannii* resulted in reduced inflammatory gene expression in macrophages [226]. Given these findings, our study aims to conduct a comparative analysis to elucidate the immunomodulatory activity of OmpA in B-cells. We have included recombinant purified endotoxin-free OmpA, engineered OMVs carrying OmpA, and the control BL21-OMVs in our analysis.

In our study, we hypothesized to investigate the role of recombinant OmpA-containing OMVs in B-cell modulation and their impact on Ig gene regulation, specifically by assessing AID expression, which is crucial for the CSR events and affinity maturation in the Ig gene locus. This suggests a potential mechanism through which bacteria may manipulate host immune responses. Additionally, we sought to explore the intricate regulation of AID expression. AID is a potent mutator enzyme that can influence mutagenesis not only in Ig loci but also in non-Ig loci, leading to genomic instability in both B-cells and non-B-cells and contributing to tumorigenesis. The expression of AID is triggered by signals from activated B-cells in the germinal center

through T-dependent and T-independent pathways, particularly from BCRs, TLRs, and factors like IL-4 produced by T-cells, which enhance AID expression. Thus, AID expression and its activity must be tightly regulated to maintain genomic integrity and prevent harmful effects from its dysregulation [227–229]. Importantly, recombinant OMVs may emerge as potential modulators of AID expression in B-cells, presenting a novel strategy for controlling its activity. OMVs derived from bacterial sources have been shown to engage with immune cells, thereby influencing B-cell responses. In this study, we used the Raji human B-cell line, which originates from human Burkitt lymphoma, as a model to test our hypothesis regarding the role of OmpA in promoting abnormal AID expression and regulating the CSR process. However, Raji human B-cells exhibit certain characteristics typical of primary human B-cells, including mutations, MYC translocation, irregular expression patterns, and genetic alterations in various genes. Researchers have widely chosen Raji human B-cells for investigations related to immune modulation, BCR signaling, and studies of immunoglobulin expression [93,191–194].

Our findings indicate that OmpA-containing OMVs derived from BL21(DE3) cells can modulate human Raji B-cells. We initially noted that these OMVs induced the expression of TLR2, indicating an interaction with this pattern recognition receptor on B-cells. This interaction may initiate a signaling cascade that contributes to the activation of B-cells. Likewise, a study by Nadalian et al. demonstrates that OMVs from adherent-invasive *E. coli* can enhance the inflammatory response by enhancing TLR2 and TLR4 expression in the human epithelial Caco-2 cell line [230]. Furthermore, engagement of TLR2 initiates the downstream signaling cascade via activating the NF-κB transcription factor, which plays a crucial role in regulating multiple aspects of B-cell lineage development and function. This includes the generation and maturation of B-cells from early progenitors in the bone marrow and spleen, as well as their proliferation and differentiation into plasma blasts [231]. In our study, we noted that OmpA-OMVs and OmpA induce NF-κB expression, which may subsequently trigger downstream effects leading to the upregulation of AID expression and modulation of B-cell function [232].

Importantly, the most significant finding in our study is the upregulation of AID expression in B-cells stimulated with the OmpA-OMVs; a similar effect was observed with the purified OmpA. AID plays a crucial role by initiating the SHM and CSR, which are essential for antibody diversity and enabling class switching in the humoral immune response, contributing to long-term immunity [80]. In comparison to OmpA, we found that stimulating Raji human B-cells with purified OmpA at a concentration of 20 µg/mL resulted in a significant increase in AID expression and promoted the class switching of immunoglobulin from IgM to IgA [20]. To further explore this, we used recombinant OmpA-OMVs at a concentration of 1.25 µg/mL. This concentration was chosen based on cytotoxicity assessments, which indicated ~60–70% cell viability. It is important to note that this concentration might induce moderate cytotoxicity. Consequently, there is a potential for immune activation and cellular stress responses to occur concurrently.

Additionally, we aimed to evaluate its impact on B-cell modulation through AID expression. Our analysis revealed that stimulating B-cells with purified OmpA at a concentration of 20 µg/mL resulted in a 3.1-fold increase in AID expression at the mRNA level and a 2.7-fold increase at the protein level after 24 h. In comparison, treatment with OmpA-OMVs at the lower concentration of 1.25 µg/mL led to a 1.8-fold increase in AID expression at the mRNA level and a 2.1-fold increase at the protein level after 24 h. When normalized, OmpA-OMVs showed a 1.4-fold/µg increase in AID mRNA expression, compared to 0.155-fold/µg for purified OmpA. At the protein level, OmpA-OMVs had a 1.68-fold/µg increase, while purified OmpA had 0.135-fold/µg. These findings suggest that OmpA-OMVs show greater potency than purified OmpA, effectively modulating B-cell function at lower concentrations and providing a natural delivery mechanism that enhances biological relevance. However, further studies are needed to validate the relative efficacy of purified OmpA versus OmpA-OMVs.

The molecular mechanism underlying the upregulation of AID expression involves a complex interplay between activators and repressors that function as transcriptional regulators. We observed that induction in the expression of key

transcriptional activators of AID, such as cMYC, PAX5, SMAD3, and STAT6, occurred upon stimulation with OmpA-OMVs treatment. Additionally, we noted a downregulation of transcriptional repressors of AID, such as cMYb, after stimulation with OmpA-OMVs. These findings illustrate how OmpA-OMVs modulate the transcriptional activity in B-cells, creating a favorable environment for the induction of AID expression, which is further involved in the process. Additionally, the increased nuclear localization of cMYC and its occupancy at the chromatin level, as demonstrated by the ChIP assay, further strengthens our hypothesis and suggests its role as a transcriptional activator mediating OmpA-OMVs-based AID induction in the B-cells. These findings align with previous reports that identify cMYC as a key regulator of AID expression [80].

Furthermore, our investigation revealed that OmpA-OMVs treatment in B-cells dynamically changes the immunoglobulin expression profile. The initial increase in IgM expression at 4 h was followed by a downregulation by 24 h. Similarly, there was a significant increase in IgA expression after 4 h, indicating that OmpA-OMVs play a role in promoting class switching from IgM to IgA in B-cells. This conclusion is further supported by the observed increase in the IgA:IgM ratio in OmpA-OMV-treated B-cells, which was 1.78-fold higher than that of the control sample at 24 h. Notably, the expression of IgG in OmpA-OMV-treated B-cells showed minimal changes up to 8 h but was downregulated at 24 h. This varied regulation of immunoglobulin isotypes suggests that OmpA-OMVs specifically promote class switching towards IgA rather than IgG.

Our study offers valuable insights into the immunomodulatory effects of OmpA-OMVs on B-cells. However, further validation of these findings is essential, particularly through the examination of human primary B-cells, especially induced germinal center B-cells [203]. Additionally, it would be beneficial to utilize clinical samples such as peripheral blood mononuclear cells (PBMCs) from infected patients and relevant animal models. Furthermore, we identified TLR2 as a potential receptor involved in B-cell activation, but other PRRs may also play a role. This research will provide valuable insights into the role of OMVs in host-pathogen interactions.

Although our study demonstrates that the engineered OmpA carrying OMVs and OmpA can induce AID expression and promote CSR in B-cells. However, it is also important to consider the potential risk associated with the induced AID expression, as it is a potential mutagenic enzyme known to induce SHM and CSR. However, upon its dysregulation, it can cause genomic instability, including chromosomal translocations, DNA double-strand breaks, and further contribute to cancer progression [79,80,86].

For instance, a study by Kim et al. reported that AID expression, when activated via the NF-κB pathway, induces TP53 mutations in gastric epithelial cells, contributing to *H. pylori*-associated gastric carcinogenesis [91]. Similarly, aberrant AID expression has been identified in various tumors originating from germinal centers, including Burkitt lymphomas, diffuse large B-cell lymphomas (DLBCLs), and follicular lymphomas [80]. Additionally, a study by Shinmura et al. indicates that induced AID expression raises mutation rates, especially in the p53 gene, thereby contributing to lung cancer [92]. Given the oncogenic potential of dysregulated AID expression, the therapeutic application of OmpA-OMVs must be approached with caution. While our study provides promising insights into the immunomodulatory effects of OmpA-OMVs on B-cells, it is crucial to conduct thorough biosafety evaluations using animal models. Additionally, long-term monitoring is necessary to assess their safety profile and to mitigate the risk of genotoxicity.

In conclusion, our study demonstrates that OmpA-OMVs significantly modulate B-cell function by enhancing AID expression and directing the CSR towards IgA**.** This reveals a new aspect of the interactions between OMVs and hosts, highlighting the key role of OmpA-OMVs in shaping host immune responses. These findings improve our understanding of bacterial pathogenesis and immunomodulation, potentially leading to new therapeutic approaches for *Salmonella* infections through OMV-based vaccines and immunotherapies.

7.6 Conclusion

This thesis examines the structural-functional relationship of OmpA and its impact on human B-cells. The research was conducted using an integrated approach that included *in silico* analysis, biophysical characterization, and functional immunological assays.

The initial chapter focuses on the computational and biophysical characterization of OmpA, involving its cloning, expression, purification, and refolding. SEC and semi-native SDS-PAGE revealed that OmpA exists in a dimeric form. Additionally, results from CD spectroscopy and tryptophan fluorescence analysis confirmed the proper folding and stability of OmpA.

Subsequent experiments explored the role of OmpA in B-cell modulation. The findings revealed that OmpA is involved in the activation of TLR2 signaling, which leads to the activation of NF-kB signaling and the production of TNF-α. Furthermore, purified OmpA was shown to upregulate the expression of AID, a key enzyme involved in antibody diversification through SHM and CSR [80]. This upregulation of AID expression was regulated by increased levels of transcription activators such as c-MYC and PAX5, resulting in enhanced IgA class switching [162]. These results suggest that OmpA can modulate B-cell function, potentially influencing host immune responses during infection.

In recent years, there has been growing interest in recombinant OMVs that incorporate heterologous targets, where OMVs are used as carriers for diverse antigens [158]. In our study, we used OMVs as a delivery system to present OmpA within its native membrane environment. We engineered, isolated, and characterized the OmpA-OMVs. Functionally, the OmpA-OMVs induced AID expression and CSR activity at lower concentrations compared to purified OmpA. This shows that OmpA-OMVs have better delivery efficiency and biological relevance than purified OmpA alone.

This thesis highlights the crucial role of OmpA and OmpA-OMVs **(Fig. 7.1)** in shaping B-cell responses, providing insights into bacterial pathogenesis and potential applications in *Salmonella* vaccine development and immunotherapies.

7.7 Future directions

This study provides critical insights into the structural and functional roles of OmpA; however, several aspects remain to be explored. High-resolution structural elucidation through X-ray crystallography or cryo-electron microscopy could offer detailed insights into OmpA's β-barrel and extracellular domains from *S.* Typhimurium.

Investigating the interaction between TLR2 in host cells and OmpA through mutagenesis studies would help delineate the signaling mechanisms involved. Additionally, exploring the downstream signaling pathways related to TLR2-mediated NF-κB activation could enhance our understanding of OmpA's role in the inflammatory process within host cells. Furthermore, beyond investigating the OmpA-TLR2 interaction, it is important to examine the impact of other PAMPs such as flagellins and lipoproteins, as well as their interactions with PRRs like other TLRs and BCRs. This will help build a broader understanding of B-cell sensing and adaptive modulation.

Moreover, a comprehensive analysis of transcriptomics (RNA-sequencing) and proteomics data from stimulated B-cells using OmpA or OmpA-containing OMVs could reveal novel pathways and regulatory networks influenced by these bacterial OMPs. This may uncover a novel biomarker for infection. Since OMVs contain natural endotoxins, future studies should investigate standard OMVs alongside endotoxin-free OMVs to determine OmpA's specific contribution to modulating responses against lipopolysaccharides (LPS) in B-cells, as this is crucial for clinical translation.

In addition, detailed work is needed to validate *in vitro* studies regarding the immunomodulatory role of OmpA or OmpA-OMVs through *in vivo* studies that assess their potential as vaccine candidates or therapeutic immunomodulators. Evaluating their immunogenicity and protective efficacy in animal models is crucial for translating these findings into next-generation nano-vaccine platforms or targeted immunotherapies against *Salmonella* infections. Since the AID expression is a potential mutator, detailed long-term biosafety analyses are crucial, including studies on genotoxicity and oncogenic potential, before therapeutic applications.

Overall, advancing this research will not only deepen our understanding of OmpA’s role in *Salmonella* pathogenesis but also open doors for its strategic application in the development of vaccines and immunotherapies interventions.

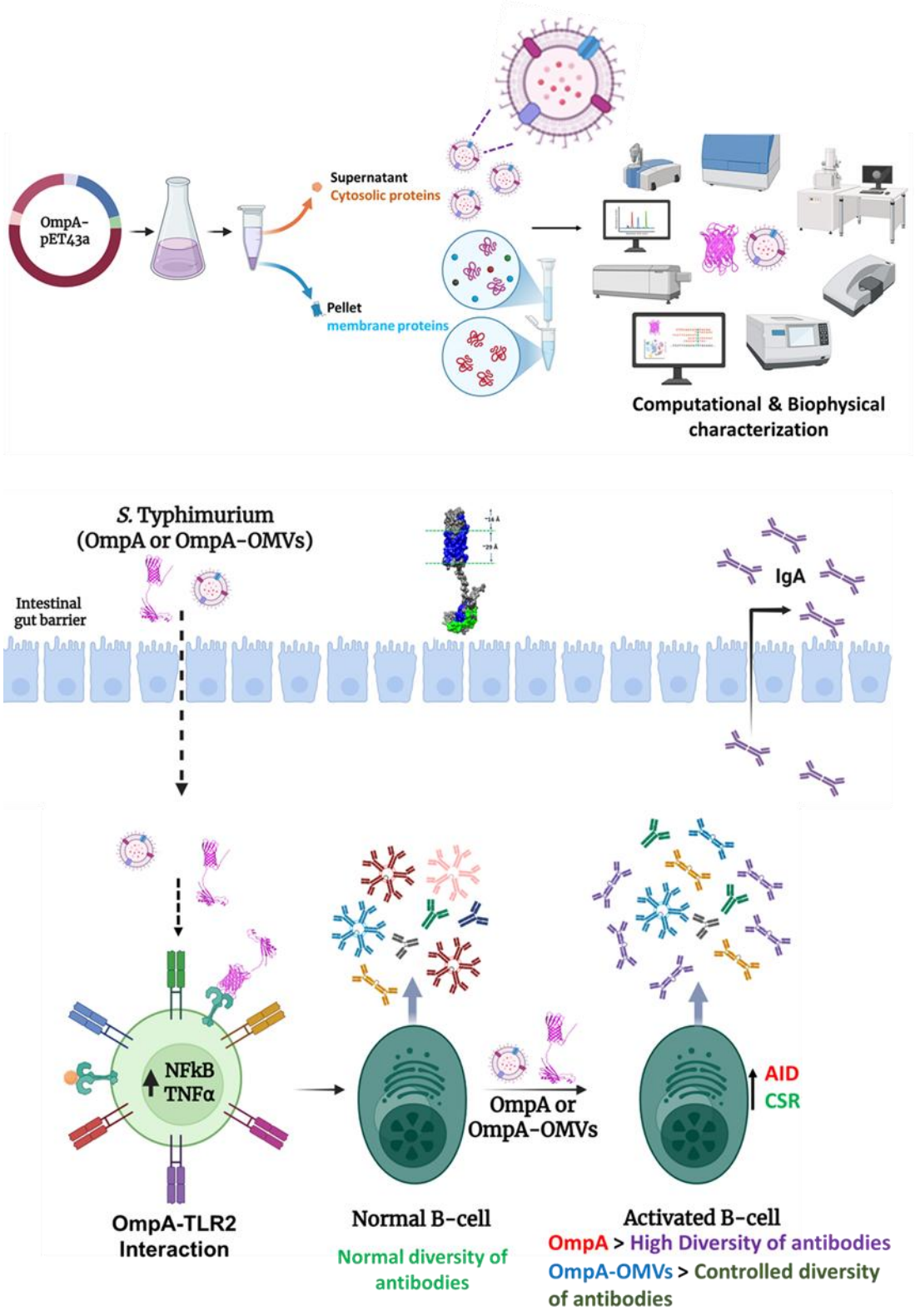

Fig. 7.1 Schematic overview summarizing the chapters 3, 4, 5, and 6 of the research work.

Appendix A

pET43a vector map

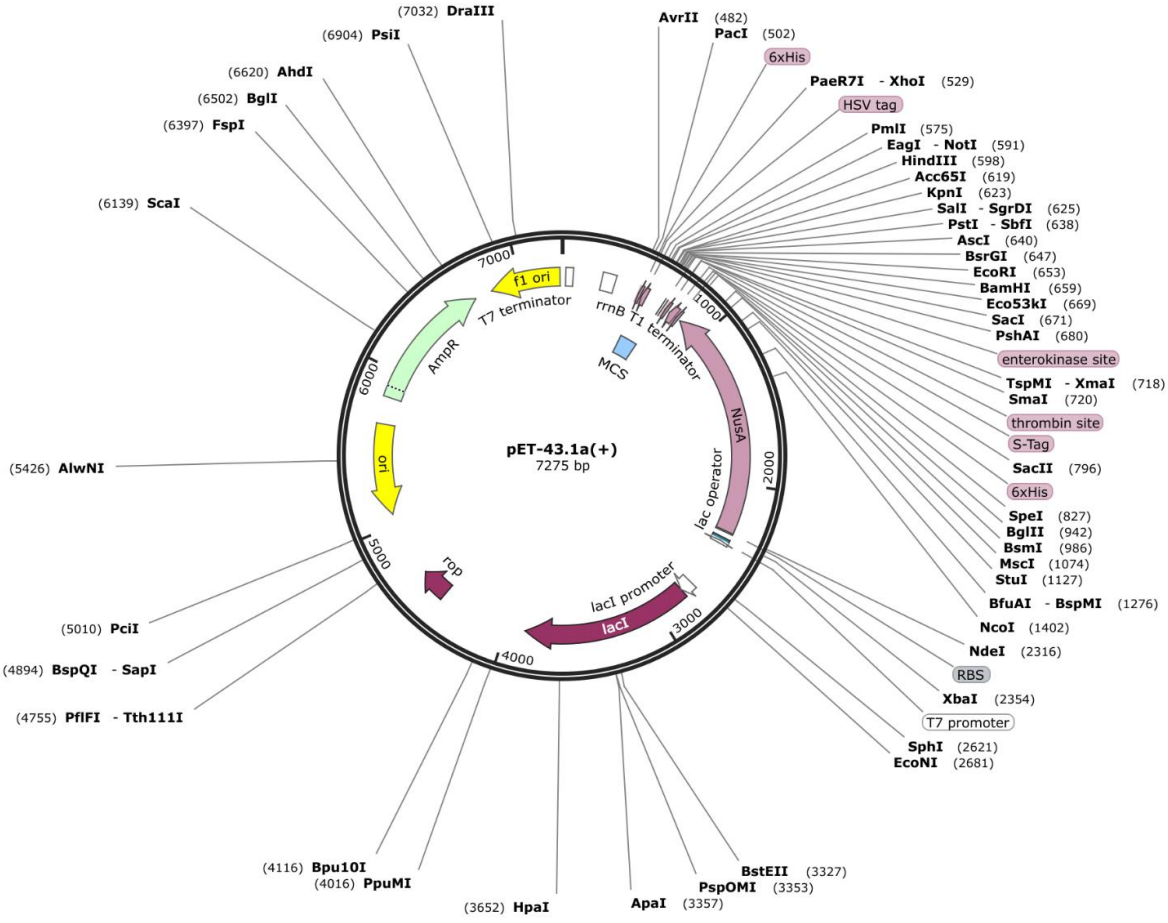

Appendix B

List of primers used in the study

Sr no	Primer Name	Gene	Primer Sequence 5' to 3’
1	PK929	OmpA FP	GTAGCATATGAAAAAGACAGCTATCGCGATTGC
2	PK930	OmpA RP	GAACTCGAGAGCCTGCGGCTGAGTTACC
3	PK1007	Ki-67 Sense	ATAAACACCCCAACACACACAA
4	PK1008	Ki-67 Antisense	GCCACTTCTTCATTCCAGTTACA
5	PK1009	PCNA Sense	TCCTCCTTCCCGCCTGCCTGTAGC
6	PK10010	PCNA Antisense	CGCGTTATCTTCGGCCCTTAGTGTA
7	PK1012	TLR2 Sense	GGCCAGCAAATTACCTGTGTG
8	PK1013	TLR2 Antisense	AGGCGGACATCCTGAACCT
9	PK1060	NF-κB (P65) Sense	TGAACCGAAACTCTGGCAGCTG
10	PK1061	NF-κB (P65) Antisense	CATCAGCTTGCGAAAAGGAGCC
11	PK1070	TNF-α Sense	CTCTTCTGCCTGCTGCACTTTG
12	PK1071	TNF-α Antisense	ATGGGCTACAGGCTTGTCACTC
13	PK632	AID Sense	AAATGTCCGCTGGGCTAAG
14	PK633	AID Antisense	GAGGAAGAGCAATTCCACGT
15	PK646	GAPDH Sense	GAGTCAACGGATTTGGTCGT
16	PK647	GAPDH Antisense	GAGGTCAATGAAGGGGTCAT
17	PK728	cMYB Sense	TACAATGCGTCGGAAGGTCG
18	PK729	cMYB Antisense	GCGGAGCCTGAGCAAAACC
19	PK730	E2F1Sense	GTGTAGGACGGTGAGAGCAC
20	PK731	E2F1 Antisense	TCAAGGGTAGAGGGAGTTGG
21	PK734	PAX5 Sense	GACCTGAATGCTGTGCGGC
22	PK735	PAX5 Antisense	GCACCGGAGACTCCTGAATAC
23	PK738	cMYC Sense	AAAGGCCCCCAAGGTAGTTA
24	PK739	cMYC Antisense	GCACAAGAGTTCCGTAGCTG
25	PK746	STAT6 Sense	AGTGCAGCGGCTCTATGTCGAC
26	PK747	STAT6 Antisense	CACCGAGGCCTGAAGGTGC
27	PK748	SMAD3 Sense	ATGTCAACAGGAATGCAGCAGTGG
28	PK749	SMAD3 Antisense	ATAGCGCTGGTTACAGTTGGGAGA

List of primers used in the study

Sr no	Primer Name	Gene	Primer Sequence 5' to 3’
29	PK960	cMYC Sense (ChIP)	GGACGACGAGACCTTCATCAA
30	PK961	cMYC Antisense (ChIP)	CCAGCTTCTCTCAGACGAGCTT
31	PK781	VHDJH sense	GACACGGCTGTGTATTACTGTGCG
32	PK782	Cμ Antisense	CCGAATTCAGACGAGGGGGAAAAGGGTT
33	PK784	Cα Antisense	GGGTGGCGGTTAGCGGGGTCTTGG
34	PK1016	IgG1 Sense	ACGGCGTGGAGGTGCATAATG
35	PK1017	IgG1 Antisense	CGGGAGGCGTGGTCTTGTAGTT

Appendix C

List of antibodies used in the study

Sr no.	Type	Protein	Antibody details
1	Primary antibody	AID	Anti-AID Monoclonal antibody (ZA001), Invitrogen
2		cMYC	c-Myc Recombinant Rabbit Monoclonal Antibody (27H46L35), Invitrogen
3		GAPDH	Anti-GAPDH (0411, sc-47724), Santa Cruz Biotechnology
4		TLR2	TLR2 Recombinant Rabbit Monoclonal Antibody (JM22-41), Invitrogen
5		NF-kB-p65	Phospho-NFkB p65 (Ser536) Monoclonal Antibody, (MA5-15181), Invitrogen
6	Secondary antibody	Rabbit IgG (H+L)	Goat anti-Rabbit IgG (H+L) Secondary Antibody, HRP, (31430), Invitrogen
7		Mouse IgG (H+L)	Goat anti-Mouse IgG (H+L) Secondary Antibody, HRP, (31460), Invitrogen
8		Rabbit IgG (H+L)	Alexa Fluor 594, A21207, Invitrogen
9		Mouse IgG (H+L)	Alexa Fluor 488, A11001, Invitrogen

References

[1] D. Kaur, A. Mukhopadhaya, Outer membrane protein OmpV mediates *Salmonella enterica* serovar *typhimurium* adhesion to intestinal epithelial cells via fibronectin and α1β1 integrin, Cell. Microbiol. 22 (2020) e13172. https://doi.org/10.1111/cmi.13172.

[2] R. Chaudhari, K. Singh, P. Kodgire, Biochemical and molecular mechanisms of antibiotic resistance in *Salmonella* spp, Res. Microbiol. 174 (2023) 103985. https://doi.org/10.1016/j.resmic.2022.103985.

[3] D.C. Bay, K.L. Rommens, R.J. Turner, Small multidrug resistance proteins: A multidrug transporter family that continues to grow, Biochim. Biophys. Acta BBA - Biomembr. 1778 (2008) 1814–1838. https://doi.org/10.1016/j.bbamem.2007.08.015.

[4] M. Hancuh, Typhoid Fever Surveillance, Incidence Estimates, and Progress Toward Typhoid Conjugate Vaccine Introduction — Worldwide, 2018–2022, MMWR Morb. Mortal. Wkly. Rep. 72 (2023). https://doi.org/10.15585/mmwr.mm7207a2.

[5] D. Acheson, E.L. Hohmann, Nontyphoidal Salmonellosis, Clin. Infect. Dis. 32 (2001) 263–269. https://doi.org/10.1086/318457.

[6] J.D. Stanaway, A. Parisi, K. Sarkar, B.F. Blacker, R.C. Reiner, S.I. Hay, M.R. Nixon, C. Dolecek, S.L. James, A.H. Mokdad, G. Abebe, E. Ahmadian, F. Alahdab, B.T.T. Alemnew, V. Alipour, F. Allah Bakeshei, M.D. Animut, F. Ansari, J. Arabloo, E.T. Asfaw, M. Bagherzadeh, Q. Bassat, Y.M.M. Belayneh, F. Carvalho, A. Daryani, F.M. Demeke, A.B.B. Demis, M. Dubey, E.E. Duken, S.J. Dunachie, A. Eftekhari, E. Fernandes, R. Fouladi Fard, G.A. Gedefaw, B. Geta, K.B. Gibney, A. Hasanzadeh, C.L. Hoang, A. Kasaeian, A. Khater, Z.T. Kidanemariam, A.M. Lakew, R. Malekzadeh, A. Melese, D.T. Mengistu, T. Mestrovic, B. Miazgowski, K.A. Mohammad, M. Mohammadian, A. Mohammadian-Hafshejani, C.T. Nguyen, L.H. Nguyen, S.H. Nguyen, Y.L. Nirayo, A.T. Olagunju, T.O. Olagunju, H. Pourjafar, M. Qorbani, M. Rabiee, N. Rabiee, A. Rafay, A. Rezapour, A.M. Samy, S.G. Sepanlou, M.A. Shaikh, M. Sharif, M. Shigematsu, B. Tessema, B.X. Tran, I. Ullah, E.M. Yimer, Z. Zaidi, C.J.L. Murray, J.A. Crump, The global burden of non-typhoidal *Salmonella* invasive disease: a systematic analysis for the Global Burden of Disease Study 2017, Lancet Infect. Dis. 19 (2019) 1312–1324. https://doi.org/10.1016/S1473-3099(19)30418-9.

[7] A.A. Al kraiem, Yang ,Guang, Al kraiem ,Fahd, T. and Chen, Challenges associated with ceftriaxone resistance in *Salmonella*, Front. Life Sci. 11 (2018) 26–34. https://doi.org/10.1080/21553769.2018.1491427.

[8] M.R. Wilmes-Riesenberg, B. Bearson, J.W. Foster, 3rd R Curtis, Role of the acid tolerance response in virulence of *Salmonella typhimurium*, Infect. Immun. 64 (1996) 1085. https://doi.org/10.1128/iai.64.4.1085-1092.1996.

[9] J.E. Galán, *Salmonella* Typhimurium and inflammation: a pathogen-centric affair, Nat. Rev. Microbiol. 19 (2021) 716–725. https://doi.org/10.1038/s41579-021-00561-4.

[10] A. Haraga, M.B. Ohlson, S.I. Miller, *Salmonella*e interplay with host cells, Nat. Rev. Microbiol. 6 (2008) 53–66. https://doi.org/10.1038/nrmicro1788.

[11] M.I. Hutchings, A.W. Truman, B. Wilkinson, Antibiotics: past, present and future, Curr. Opin. Microbiol. 51 (2019) 72–80. https://doi.org/10.1016/j.mib.2019.10.008.
[12] G. Lancini, F. Parenti, G.G. Gallo, The Antibiotics, in: G. Lancini, F. Parenti, G.G. Gallo (Eds.), Antibiot. Multidiscip. Approach, Springer US, Boston, MA, 1995: pp. 1–14. https://doi.org/10.1007/978-1-4757-9200-3_1.
[13] S.M. Jajere, A review of *Salmonella enterica* with particular focus on the pathogenicity and virulence factors, host specificity and antimicrobial resistance including multidrug resistance, Vet. World 12 (2019) 504–521. https://doi.org/10.14202/vetworld.2019.504-521.
[14] S. Argimón, G. Nagaraj, V. Shamanna, D. Sravani, A.K. Vasanth, A. Prasanna, A. Poojary, A.K. Bari, A. Underwood, M. Kekre, S. Baker, D.M. Aanensen, R.K. Lingegowda, Circulation of Third-Generation Cephalosporin Resistant *Salmonella* Typhi in Mumbai, India, Clin. Infect. Dis. (2021) ciab897. https://doi.org/10.1093/cid/ciab897.
[15] E.J. Klemm, S. Shakoor, A.J. Page, F.N. Qamar, K. Judge, D.K. Saeed, V.K. Wong, T.J. Dallman, S. Nair, S. Baker, G. Shaheen, S. Qureshi, M.T. Yousafzai, M.K. Saleem, Z. Hasan, G. Dougan, R. Hasan, Emergence of an Extensively Drug-Resistant *Salmonella enterica* Serovar Typhi Clone Harboring a Promiscuous Plasmid Encoding Resistance to Fluoroquinolones and Third-Generation Cephalosporins, mBio 9 (2018) e00105-18. https://doi.org/10.1128/mBio.00105-18.
[16] P.F. McDermott, R.D. Walker, D.G. White, Antimicrobials: modes of action and mechanisms of resistance, Int. J. Toxicol. 22 (2003) 135–143. https://doi.org/10.1080/10915810305089.
[17] X.-B. Wu, L.-H. Tian, H.-J. Zou, C.-Y. Wang, Z.-Q. Yu, C.-H. Tang, F.-K. Zhao, J.-Y. Pan, Outer membrane protein OmpW of *Escherichia coli* is required for resistance to phagocytosis, Res. Microbiol. 164 (2013) 848–855. https://doi.org/10.1016/j.resmic.2013.06.008.
[18] U. Choi, C.-R. Lee, Distinct Roles of Outer Membrane Porins in Antibiotic Resistance and Membrane Integrity in *Escherichia coli*, Front. Microbiol. 10 (2019) 953. https://doi.org/10.3389/fmicb.2019.00953.
[19] N. Furuyama, M.P. Sircili, Outer Membrane Vesicles (OMVs) Produced by Gram-Negative Bacteria: Structure, Functions, Biogenesis, and Vaccine Application, BioMed Res. Int. 2021 (2021) 1490732. https://doi.org/10.1155/2021/1490732.
[20] R. Chaudhari, M. Dasgupta, P. Kodgire, Unravelling the Impact of Outer Membrane Protein, OmpA, From *S.* Typhimurium on Aberrant AID Expression and IgM to IgA Class Switching in Human B-Cells, Immunology 175 (2025) 359–372. https://doi.org/10.1111/imm.13938.
[21] S.E. Rollauer, M.A. Sooreshjani, N. Noinaj, S.K. Buchanan, Outer membrane protein biogenesis in Gram-negative bacteria, Philos. Trans. R. Soc. B Biol. Sci. 370 (2015) 20150023. https://doi.org/10.1098/rstb.2015.0023.
[22] S. Galdiero, A. Falanga, M. Cantisani, R. Tarallo, M.E.D. Pepa, V. D'Oriano, M. Galdiero, Microbe-Host Interactions: Structure and Role of Gram-Negative Bacterial Porins, Curr. Protein Pept. Sci. 13 (2012) 843–854.

https://doi.org/10.2174/138920312804871120.
[23] O.D. Novikova, T.F. Solovyeva, Nonspecific porins of the outer membrane of Gram-negative bacteria: Structure and functions, Biochem. Mosc. Suppl. Ser. Membr. Cell Biol. 3 (2009) 3–15. https://doi.org/10.1134/S1990747809010024.
[24] W.C. Wimley, The versatile β-barrel membrane protein, Curr. Opin. Struct. Biol. 13 (2003) 404–411. https://doi.org/10.1016/S0959-440X(03)00099-X.
[25] M.T. Doyle, H.D. Bernstein, Bacterial outer membrane proteins assemble via asymmetric interactions with the BamA β-barrel, Nat. Commun. 10 (2019) 3358. https://doi.org/10.1038/s41467-019-11230-9.
[26] M.V. Belousov, A.O. Kosolapova, H. Fayoud, M.I. Sulatsky, A.I. Sulatskaya, M.N. Romanenko, A.G. Bobylev, K.S. Antonets, A.A. Nizhnikov, OmpC and OmpF Outer Membrane Proteins of *Escherichia coli* and *Salmonella enterica* Form Bona Fide Amyloids, Int. J. Mol. Sci. 24 (2023) 15522. https://doi.org/10.3390/ijms242115522.
[27] M. Masi, J.-M. Pagès, Structure, Function and Regulation of Outer Membrane Proteins Involved in Drug Transport in Enterobactericeae: the OmpF/C – TolC Case, Open Microbiol. J. 7 (2013) 22–33. https://doi.org/10.2174/1874285801307010022.
[28] V. Baldwin, M. Bhatia, M. Luckey, Folding studies of purified LamB protein, the maltoporin from the *Escherichia coli* outer membrane: Trimer dissociation can be separated from unfolding, Biochim. Biophys. Acta BBA - Biomembr. 1808 (2011) 2206–2213. https://doi.org/10.1016/j.bbamem.2011.05.013.
[29] N. Ruiz, D. Kahne, T.J. Silhavy, Advances in understanding bacterial outer-membrane biogenesis, Nat. Rev. Microbiol. 4 (2006) 57–66. https://doi.org/10.1038/nrmicro1322.
[30] J.E. Horne, D.J. Brockwell, S.E. Radford, Role of the lipid bilayer in outer membrane protein folding in Gram-negative bacteria, J. Biol. Chem. 295 (2020) 10340–10367. https://doi.org/10.1074/jbc.REV120.011473.
[31] S. Chetri, The culmination of multidrug-resistant efflux pumps vs. meager antibiotic arsenal era: Urgent need for an improved new generation of EPIs, Front. Microbiol. 14 (2023) 1149418. https://doi.org/10.3389/fmicb.2023.1149418.
[32] G. Zhou, Q. Wang, Y. Wang, X. Wen, H. Peng, R. Peng, Q. Shi, X. Xie, L. Li, Outer Membrane Porins Contribute to Antimicrobial Resistance in Gram-Negative Bacteria, Microorganisms 11 (2023) 1690. https://doi.org/10.3390/microorganisms11071690.
[33] J.P. Park, M.-J. Choi, S.H. Kim, S.H. Lee, H. Lee, Preparation of Sticky *Escherichia coli* through Surface Display of an Adhesive Catecholamine Moiety, Appl. Environ. Microbiol. 80 (2014) 43–53. https://doi.org/10.1128/AEM.02223-13.
[34] L. Wan, Y. Guo, C.-Y. Hui, X.-L. Liu, W.-B. Zhang, H. Cao, H. Cao, The surface protease ompT serves as *Escherichia coli* K1 adhesin in binding to human brain micro vascular endothelial cells, Pak. J. Pharm. Sci. 27 (2014) 617–624.
[35] A. Isibasi, V. Ortiz, J. Moreno, J. Paniagua, M. Vargas, C. González, J. Kumate, The Role of Outer Membrane Proteins From Gram-Negative Bacteria as VACCINES with Special Emphasis in Typhoid Fever: Monoclonal antibodies

against S. typhi porins, in: L.E. Cañedo, L.E. Todd, L. Packer, J. Jaz (Eds.), Cell Funct. Dis., Springer US, Boston, MA, 1988: pp. 281–292. https://doi.org/10.1007/978-1-4613-0813-3_25.

[36] M. Pérez-Toledo, N. Valero-Pacheco, R. Pastelin-Palacios, C. Gil-Cruz, C. Perez-Shibayama, M.A. Moreno-Eutimio, I. Becker, S.M. Pérez-Tapia, L. Arriaga-Pizano, A.F. Cunningham, A. Isibasi, L.C. Bonifaz, C. López-Macías, *Salmonella* Typhi Porins OmpC and OmpF Are Potent Adjuvants for T-Dependent and T-Independent Antigens, Front. Immunol. 8 (2017) 230. https://doi.org/10.3389/fimmu.2017.00230.

[37] M.L. Ortiz-Suarez, F. Samsudin, T.J. Piggot, P.J. Bond, S. Khalid, Full-Length OmpA: Structure, Function, and Membrane Interactions Predicted by Molecular Dynamics Simulations, Biophys. J. 111 (2016) 1692–1702. https://doi.org/10.1016/j.bpj.2016.09.009.

[38] J. Marcoux, A. Politis, D. Rinehart, D.P. Marshall, M.I. Wallace, L.K. Tamm, C.V. Robinson, Mass spectrometry defines the C-terminal dimerization domain and enables modeling of the structure of full-length OmpA, Struct. Lond. Engl. 1993 22 (2014) 781–790. https://doi.org/10.1016/j.str.2014.03.004.

[39] M.S. Beketskaia, D.C. Bay, R.J. Turner, Outer Membrane Protein OmpW Participates with Small Multidrug Resistance Protein Member EmrE in Quaternary Cationic Compound Efflux, J. Bacteriol. 196 (2014) 1908–1914. https://doi.org/10.1128/jb.01483-14.

[40] A.C. Briones, D. Lorca, A. Cofre, C.E. Cabezas, G.I. Krüger, C. Pardo-Esté, M.S. Baquedano, C.R. Salinas, M. Espinoza, J. Castro-Severyn, F. Remonsellez, A.A. Hidalgo, E.H. Morales, C.P. Saavedra, Genetic regulation of the ompX porin of *Salmonella* Typhimurium in response to hydrogen peroxide stress, Biol. Res. 55 (2022) 8. https://doi.org/10.1186/s40659-022-00377-3.

[41] H. Hirakawa, K. Suzue, A. Takita, W. Kamitani, H. Tomita, Roles of OmpX, an Outer Membrane Protein, on Virulence and Flagellar Expression in Uropathogenic *Escherichia coli*, Infect. Immun. 89 (2021). https://doi.org/10.1128/iai.00721-20.

[42] M.J. Jang, J.-E. Kim, Y.H. Chung, W.B. Lee, Y.K. Shin, J.S. Lee, D. Kim, Y.-M. Park, Dendritic cells stimulated with outer membrane protein A (OmpA) of *Salmonella typhimurium* generate effective anti-tumor immunity, Vaccine 29 (2011) 2400–2410. https://doi.org/10.1016/j.vaccine.2011.01.036.

[43] A.R. Chowdhury, S. Sah, U. Varshney, D. Chakravortty, *Salmonella* Typhimurium outer membrane protein A (OmpA) renders protection from nitrosative stress of macrophages by maintaining the stability of bacterial outer membrane, PLOS Pathog. 18 (2022) e1010708. https://doi.org/10.1371/journal.ppat.1010708.

[44] J. XU, K. SUITA, K. OKUNO, A. TAKAYA, T. YAMAMOTO, E. ISOGAI, Membrane vesicle protein PagC as a novel biomarker for detecting pathogenic *Salmonella* in the viable but not culturable state, J. Vet. Med. Sci. 80 (2018) 133–137. https://doi.org/10.1292/jvms.17-0164.

[45] H. Ej, H. J, F. J, G. D, The *Salmonella typhimurium* virulence plasmid complement resistance gene *rck* is homologous to a family of virulence-related outer membrane protein genes, including pagC and ail, PubMed (n.d.).

https://pubmed.ncbi.nlm.nih.gov/1729227/ (accessed July 24, 2025).
[46] M. Rosselin, I. Virlogeux-Payant, C. Roy, E. Bottreau, P.-Y. Sizaret, L. Mijouin, P. Germon, E. Caron, P. Velge, A. Wiedemann, Rck of *Salmonella* enterica, subspecies *enterica* serovar Enteritidis, mediates Zipper-like internalization, Cell Res. 20 (2010) 647–664. https://doi.org/10.1038/cr.2010.45.
[47] A.A.-K. Jawad, A.H. Al-Charrakh, Outer Membrane Protein C (*ompC*) Gene as the Target for Diagnosis of *Salmonella* Species Isolated from Human and Animal Sources, Avicenna J. Med. Biotechnol. 8 (2016) 42–45.
[48] N. Valero-Pacheco, J. Blight, G. Aldapa-Vega, P. Kemlo, M. Pérez-Toledo, I. Wong-Baeza, A. Kurioka, C. Perez-Shibayama, C. Gil-Cruz, L.E. Sánchez-Torres, R. Pastelin-Palacios, A. Isibasi, A. Reyes-Sandoval, P. Klenerman, C. López-Macías, Frontiers | Conservation of the OmpC Porin Among Typhoidal and Non-Typhoidal *Salmonella* Serovars, (n.d.). https://doi.org/10.3389/fimmu.2019.02966.
[49] S. K, B. R, LamB (maltoporin) of *Salmonella typhimurium*: isolation, purification and comparison of sugar binding with LamB of *Escherichia coli*, PubMed (n.d.). https://pubmed.ncbi.nlm.nih.gov/1693746/ (accessed July 24, 2025).
[50] S.M.L. Baghal, S.L.M. Gargari, I. Rasooli, Production and immunogenicity of recombinant ferric enterobactin protein (FepA), Int. J. Infect. Dis. 14 (2010) e166–e170. https://doi.org/10.1016/j.ijid.2009.12.009.
[51] Y. Wang, X. Chen, Y. Hu, G. Zhu, A.P. White, W. Köster, Evolution and Sequence Diversity of FhuA in *Salmonella* and *Escherichia*, Infect. Immun. 86 (2018) e00573-18. https://doi.org/10.1128/IAI.00573-18.
[52] M. Bonhivers, L. Plançon, A. Ghazi, P. Boulanger, M. le Maire, O. Lambert, J.L. Rigaud, L. Letellier, FhuA, an *Escherichia coli* outer membrane protein with a dual function of transporter and channel which mediates the transport of phage DNA, Biochimie 80 (1998) 363–369. https://doi.org/10.1016/s0300-9084(00)80004-8.
[53] W. By, B. C, K. Rj, Conserved structural and regulatory regions in the *Salmonella typhimurium btuB* gene for the outer membrane vitamin B12 transport protein, PubMed (n.d.). https://pubmed.ncbi.nlm.nih.gov/1448622/ (accessed July 24, 2025).
[54] R. S, A. Di, Vitamin B12 repression of the *btuB* gene in *Salmonella typhimurium* is mediated via a translational control which requires leader and coding sequences, PubMed (n.d.). https://pubmed.ncbi.nlm.nih.gov/9004218/ (accessed July 24, 2025).
[55] D.K. J, M.J. C, S.V. B, S.S. E, K.A. K, G. M, P.O. Cl, O. De, P. Js, Low-resolution structures of OmpA·DDM protein-detergent complexes, PubMed (2014). https://pubmed.ncbi.nlm.nih.gov/25138961/ (accessed July 22, 2025).
[56] R.N. Reusch, Insights into the structure and assembly of *Escherichia coli* outer membrane protein A, FEBS J. 279 (2012) 894–909. https://doi.org/10.1111/j.1742-4658.2012.08484.x.
[57] D. Nie, Y. Hu, Z. Chen, M. Li, Z. Hou, X. Luo, X. Mao, X. Xue, Outer membrane protein A (OmpA) as a potential therapeutic target for *Acinetobacter baumannii* infection, J. Biomed. Sci. 27 (2020) 26.

https://doi.org/10.1186/s12929-020-0617-7.
[58] W. Jn, G. Ec, Outer membrane protein A (OmpA) contributes to serum resistance and pathogenicity of *Escherichia coli* K-1, PubMed (n.d.). https://pubmed.ncbi.nlm.nih.gov/1646768/ (accessed July 22, 2025).
[59] S. C, B. T, A. Jp, D. Y, B. N, C. G, R. T, B. Jy, J. P, Outer membrane protein A (OmpA) binds to and activates human macrophages, PubMed (2000). https://pubmed.ncbi.nlm.nih.gov/10946255/ (accessed July 22, 2025).
[60] A. H, T.-B. M, B. M, D. A, K. M, Study of the immunogenicity of outer membrane protein A (ompA) gene from *Acinetobacter baumannii* as DNA vaccine candidate *in vivo*, PubMed (n.d.). https://pubmed.ncbi.nlm.nih.gov/31231495/?dopt=Abstract (accessed July 22, 2025).
[61] R. Chaudhari, M. Dasgupta, D. Nigam, P. Kodgire, Engineering outer membrane vesicles (OMVs) carrying OmpA from *S.* Typhimurium for targeted modulation of human B-cell function through AID expression and class switch recombination, Microb. Pathog. 207 (2025) 107918. https://doi.org/10.1016/j.micpath.2025.107918.
[62] V. Tiku, E.M. Kofoed, D. Yan, J. Kang, M. Xu, M. Reichelt, I. Dikic, M.-W. Tan, Outer membrane vesicles containing OmpA induce mitochondrial fragmentation to promote pathogenesis of *Acinetobacter baumannii*, Sci. Rep. 11 (2021) 618. https://doi.org/10.1038/s41598-020-79966-9.
[63] J.Y. Kim, J.W. Suh, J.S. Kang, S.B. Kim, Y.K. Yoon, J.W. Sohn, Gram-Negative Bacteria's Outer Membrane Vesicles, Infect. Chemother. 55 (2023) 1–9. https://doi.org/10.3947/ic.2022.0145.
[64] Q. Liu, Q. Liu, J. Yi, K. Liang, B. Hu, X. Zhang, R. Curtiss, Q. Kong, Outer membrane vesicles from flagellin-deficient *Salmonella enterica* serovar Typhimurium induce cross-reactive immunity and provide cross-protection against heterologous *Salmonella* challenge, Sci. Rep. 6 (2016) 34776. https://doi.org/10.1038/srep34776.
[65] G. Dhurve, A.K. Madikonda, M.V. Jagannadham, D. Siddavattam, Outer Membrane Vesicles of *Acinetobacter baumannii* DS002 Are Selectively Enriched with TonB-Dependent Transporters and Play a Key Role in Iron Acquisition, Microbiol. Spectr. 10 (n.d.) e00293-22. https://doi.org/10.1128/spectrum.00293-22.
[66] A. Kulp, M.J. Kuehn, Biological Functions and Biogenesis of Secreted Bacterial Outer Membrane Vesicles, Annu. Rev. Microbiol. 64 (2010) 163–184. https://doi.org/10.1146/annurev.micro.091208.073413.
[67] L. Fantappiè, M. de Santis, E. Chiarot, F. Carboni, G. Bensi, O. Jousson, I. Margarit, G. Grandi, Antibody-mediated immunity induced by engineered *Escherichia coli* OMVs carrying heterologous antigens in their lumen, J. Extracell. Vesicles 3 (2014) 24015. https://doi.org/10.3402/jev.v3.24015.
[68] M.D. Balhuizen, E.J.A. Veldhuizen, H.P. Haagsman, Frontiers | Outer Membrane Vesicle Induction and Isolation for Vaccine Development, (n.d.). https://doi.org/10.3389/fmicb.2021.629090.
[69] D. Li, L. Zhu, Y. Wang, X. Zhou, Y. Li, Bacterial outer membrane vesicles in cancer: Biogenesis, pathogenesis, and clinical application, Biomed.

Pharmacother. 165 (2023) 115120. https://doi.org/10.1016/j.biopha.2023.115120.
[70] S.I. Kim, S. Kim, E. Kim, S.Y. Hwang, H. Yoon, Secretion of *Salmonella* Pathogenicity Island 1-Encoded Type III Secretion System Effectors by Outer Membrane Vesicles in *Salmonella enterica* Serovar Typhimurium, Front. Microbiol. 9 (2018) 2810. https://doi.org/10.3389/fmicb.2018.02810.
[71] H. Yoon, C. Ansong, J.N. Adkins, F. Heffron, Discovery of *Salmonella* Virulence Factors Translocated via Outer Membrane Vesicles to Murine Macrophages, Infect. Immun. 79 (2011) 2182–2192. https://doi.org/10.1128/iai.01277-10.
[72] B. C, S. Jm, B. S, M. Y, U. Be, W. Sn, Release of the type I secreted alpha-haemolysin via outer membrane vesicles from *Escherichia coli*, PubMed (n.d.). https://pubmed.ncbi.nlm.nih.gov/16359321/ (accessed July 23, 2025).
[73] Z. Zhu, F. Antenucci, K.R. Villumsen, A.M. Bojesen, Bacterial Outer Membrane Vesicles as a Versatile Tool in Vaccine Research and the Fight against Antimicrobial Resistance, mBio 12 (2021) 10.1128/mbio.01707-21. https://doi.org/10.1128/mbio.01707-21.
[74] A. Mr, S. As, S. Sm, J. F, M. A, V. R, Z. R, M. A, S. Sd, Application of outer membrane vesicle of *Neisseria meningitidis* serogroup B as a new adjuvant to induce strongly Th1-oriented responses against HIV-1, PubMed (2011). https://pubmed.ncbi.nlm.nih.gov/22211657/ (accessed July 23, 2025).
[75] V. Sk, R. Aj, B. B, B. I, Y. M, D. Sd, R. Vak, Bacterial Outer Membrane Vesicles Mediate Cytosolic Localization of LPS and Caspase-11 Activation, PubMed (2016). https://pubmed.ncbi.nlm.nih.gov/27156449/ (accessed July 23, 2025).
[76] A.-C. Ed, L.-M. A, J. N, P. H, L.-V. Eo, S. N, B. Sm, W. S, C.-R. A, Characterization of outer membrane vesicles from *Brucella melitensis* and protection induced in mice, PubMed (n.d.). https://pubmed.ncbi.nlm.nih.gov/22242036/ (accessed July 23, 2025).
[77] K.B. Weyant, A. Oloyede, S. Pal, J. Liao, M.R.-D. Jesus, T. Jaroentomeechai, T.D. Moeller, S. Hoang-Phou, S.F. Gilmore, R. Singh, D.C. Pan, D. Putnam, C. Locher, L.M. de la Maza, M.A. Coleman, M.P. DeLisa, A modular vaccine platform enabled by decoration of bacterial outer membrane vesicles with biotinylated antigens, Nat. Commun. 14 (2023) 464. https://doi.org/10.1038/s41467-023-36101-2.
[78] K. Pieper, B. Grimbacher, H. Eibel, B-cell biology and development, J. Allergy Clin. Immunol. 131 (2013) 959–971. https://doi.org/10.1016/j.jaci.2013.01.046.
[79] A. Tamrakar, P. Kodgire, HomA and HomB, outer membrane proteins of *Helicobacter pylori* down-regulate activation-induced cytidine deaminase (AID) and Ig switch germline transcription and thereby affect class switch recombination (CSR) of Ig genes in human B-cells, Mol. Immunol. 142 (2022) 37–49. https://doi.org/10.1016/j.molimm.2021.12.014.
[80] M. Choudhary, A. Tamrakar, A.K. Singh, M. Jain, A. Jaiswal, P. Kodgire, AID Biology: A pathological and clinical perspective, Int. Rev. Immunol. 37 (2018) 37–56. https://doi.org/10.1080/08830185.2017.1369980.
[81] N.S. De Silva, U. Klein, Dynamics of B cells in germinal centres, Nat. Rev. Immunol. 15 (2015) 137–148. https://doi.org/10.1038/nri3804.

[82] A. Jaiswal, R. Roy, A. Tamrakar, A.K. Singh, P. Kar, P. Kodgire, Activation-induced cytidine deaminase an antibody diversification enzyme interacts with chromatin modifier UBN1 in B-cells, Sci. Rep. 13 (2023) 19615. https://doi.org/10.1038/s41598-023-46448-7.
[83] R. C, W. Gt, N. H, B. De, L. T, N. Ms, Immunoglobulin isotype switching is inhibited and somatic hypermutation perturbed in UNG-deficient mice, PubMed (2002). https://pubmed.ncbi.nlm.nih.gov/12401169/ (accessed July 24, 2025).
[84] J. Stavnezer, J.E.J. Guikema, C.E. Schrader, Mechanism and Regulation of Class Switch Recombination, (2008). https://doi.org/10.1146/annurev.immunol.26.021607.090248.
[85] T. Honjo, K. Kinoshita, M. Muramatsu, Molecular mechanism of class switch recombination: linkage with somatic hypermutation, Annu. Rev. Immunol. 20 (2002) 165–196. https://doi.org/10.1146/annurev.immunol.20.090501.112049.
[86] C.R. Ruprecht, A. Lanzavecchia, Toll-like receptor stimulation as a third signal required for activation of human naive B cells, Eur. J. Immunol. 36 (2006) 810–816. https://doi.org/10.1002/eji.200535744.
[87] P. Revy, T. Muto, Y. Levy, F. Geissmann, A. Plebani, O. Sanal, N. Catalan, M. Forveille, R. Dufourcq-Lagelouse, A. Gennery, I. Tezcan, F. Ersoy, H. Kayserili, A.G. Ugazio, N. Brousse, M. Muramatsu, L.D. Notarangelo, K. Kinoshita, T. Honjo, A. Fischer, A. Durandy, Activation-Induced Cytidine Deaminase (AID) Deficiency Causes the Autosomal Recessive Form of the Hyper-IgM Syndrome (HIGM2), Cell 102 (2000) 565–575. https://doi.org/10.1016/S0092-8674(00)00079-9.
[88] S. Fagarasan, M. Muramatsu, K. Suzuki, H. Nagaoka, H. Hiai, T. Honjo, Critical roles of activation-induced cytidine deaminase in the homeostasis of gut flora, Science 298 (2002) 1424–1427. https://doi.org/10.1126/science.1077336.
[89] L. Pasqualucci, P. Neumeister, T. Goossens, G. Nanjangud, R.S. Chaganti, R. Küppers, R. Dalla-Favera, Hypermutation of multiple proto-oncogenes in B-cell diffuse large-cell lymphomas, Nature 412 (2001) 341–346. https://doi.org/10.1038/35085588.
[90] E. Edry, D. Melamed, Class switch recombination: A friend and a foe, Clin. Immunol. 123 (2007) 244–251. https://doi.org/10.1016/j.clim.2007.02.008.
[91] C.J. Kim, J.H. Song, Y.G. Cho, Z. Cao, S.Y. Kim, S.W. Nam, J.Y. Lee, W.S. Park, Activation-Induced Cytidine Deaminase Expression in Gastric Cancer, Tumor Biol. 28 (2008) 333–339. https://doi.org/10.1159/000124239.
[92] K. Shinmura, H. Igarashi, M. Goto, H. Tao, H. Yamada, S. Matsuura, M. Tajima, T. Matsuda, A. Yamane, K. Funai, M. Tanahashi, H. Niwa, H. Ogawa, H. Sugimura, Aberrant Expression and Mutation-Inducing Activity of AID in Human Lung Cancer, Ann. Surg. Oncol. 18 (2011) 2084–2092. https://doi.org/10.1245/s10434-011-1568-8.
[93] Z. Duan, H. Zheng, H. Liu, M. Li, M. Tang, X. Weng, W. Yi, A.M. Bode, Y. Cao, AID expression increased by TNF-α is associated with class switch recombination of Igα gene in cancers, Cell. Mol. Immunol. 13 (2016) 484–491. https://doi.org/10.1038/cmi.2015.26.
[94] X. Robert, P. Gouet, Deciphering key features in protein structures with the new ENDscript server, Nucleic Acids Res. 42 (2014) W320-324.

https://doi.org/10.1093/nar/gku316.
[95] M.S. Klausen, M.C. Jespersen, H. Nielsen, K.K. Jensen, V.I. Jurtz, C.K. Sønderby, M.O.A. Sommer, O. Winther, M. Nielsen, B. Petersen, P. Marcatili, NetSurfP-2.0: Improved prediction of protein structural features by integrated deep learning, Proteins 87 (2019) 520–527. https://doi.org/10.1002/prot.25674.
[96] M.H. Høie, E.N. Kiehl, B. Petersen, M. Nielsen, O. Winther, H. Nielsen, J. Hallgren, P. Marcatili, NetSurfP-3.0: accurate and fast prediction of protein structural features by protein language models and deep learning, Nucleic Acids Res. 50 (2022) W510–W515. https://doi.org/10.1093/nar/gkac439.
[97] J. Jumper, R. Evans, A. Pritzel, T. Green, M. Figurnov, O. Ronneberger, K. Tunyasuvunakool, R. Bates, A. Žídek, A. Potapenko, A. Bridgland, C. Meyer, S.A.A. Kohl, A.J. Ballard, A. Cowie, B. Romera-Paredes, S. Nikolov, R. Jain, J. Adler, T. Back, S. Petersen, D. Reiman, E. Clancy, M. Zielinski, M. Steinegger, M. Pacholska, T. Berghammer, S. Bodenstein, D. Silver, O. Vinyals, A.W. Senior, K. Kavukcuoglu, P. Kohli, D. Hassabis, Highly accurate protein structure prediction with AlphaFold, Nature 596 (2021) 583–589. https://doi.org/10.1038/s41586-021-03819-2.
[98] M. Mirdita, K. Schütze, Y. Moriwaki, L. Heo, S. Ovchinnikov, M. Steinegger, ColabFold - Making protein folding accessible to all, (2022) 2021.08.15.456425. https://doi.org/10.1101/2021.08.15.456425.
[99] M. Pellegrini-Calace, T. Maiwald, J.M. Thornton, PoreWalker: A Novel Tool for the Identification and Characterization of Channels in Transmembrane Proteins from Their Three-Dimensional Structure, PLoS Comput. Biol. 5 (2009) e1000440. https://doi.org/10.1371/journal.pcbi.1000440.
[100] E. Gasteiger, C. Hoogland, A. Gattiker, S. Duvaud, M.R. Wilkins, R.D. Appel, A. Bairoch, Protein Identification and Analysis Tools on the ExPASy Server, in: J.M. Walker (Ed.), Proteomics Protoc. Handb., Humana Press, Totowa, NJ, 2005: pp. 571–607. https://doi.org/10.1385/1-59259-890-0:571.
[101] R.V. Honorato, P.I. Koukos, B. Jiménez-García, A. Tsaregorodtsev, M. Verlato, A. Giachetti, A. Rosato, A.M.J.J. Bonvin, Structural Biology in the Clouds: The WeNMR-EOSC Ecosystem, Front. Mol. Biosci. 8 (2021). https://doi.org/10.3389/fmolb.2021.729513.
[102] A. Vangone, A.M. Bonvin, Contacts-based prediction of binding affinity in protein–protein complexes, eLife 4 (2015) e07454. https://doi.org/10.7554/eLife.07454.
[103] L.C. Xue, J.P. Rodrigues, P.L. Kastritis, A.M. Bonvin, A. Vangone, PRODIGY: a web server for predicting the binding affinity of protein–protein complexes, Bioinformatics 32 (2016) 3676–3678. https://doi.org/10.1093/bioinformatics/btw514.
[104] J.R. López-Blanco, J.I. Aliaga, E.S. Quintana-Ortí, P. Chacón, iMODS: internal coordinates normal mode analysis server, Nucleic Acids Res. 42 (2014) W271–W276. https://doi.org/10.1093/nar/gku339.
[105] H. Motamedi, A. Alvandi, M. Fathollahi, M.M. Ari, S. Moradi, J. Moradi, R. Abiri, *In silico* designing and immunoinformatics analysis of a novel peptide vaccine against metallo-beta-lactamase (VIM and IMP) variants, PLOS ONE 18 (2023) e0275237. https://doi.org/10.1371/journal.pone.0275237.

[106] Q. Yousafi, H. Amin, S. Bibi, R. Rafi, M.S. Khan, H. Ali, A. Masroor, Subtractive Proteomics and Immuno-informatics Approaches for Multi-peptide Vaccine Prediction Against *Klebsiella oxytoca* and Validation Through *In Silico* Expression, Int. J. Pept. Res. Ther. 27 (2021) 2685–2701. https://doi.org/10.1007/s10989-021-10283-z.
[107] M.V. Larsen, C. Lundegaard, K. Lamberth, S. Buus, O. Lund, M. Nielsen, Large-scale validation of methods for cytotoxic T-lymphocyte epitope prediction, BMC Bioinformatics 8 (2007) 424. https://doi.org/10.1186/1471-2105-8-424.
[108] S. Paul, J. Sidney, A. Sette, B. Peters, TepiTool: A Pipeline for Computational Prediction of T Cell Epitope Candidates, Curr. Protoc. Immunol. 114 (2016) 18.19.1-18.19.24. https://doi.org/10.1002/cpim.12.
[109] M.C. Jespersen, B. Peters, M. Nielsen, P. Marcatili, BepiPred-2.0: improving sequence-based B-cell epitope prediction using conformational epitopes, Nucleic Acids Res. 45 (2017) W24–W29. https://doi.org/10.1093/nar/gkx346.
[110] J.J.A. Calis, M. Maybeno, J.A. Greenbaum, D. Weiskopf, A.D. De Silva, A. Sette, C. Keşmir, B. Peters, Properties of MHC class I presented peptides that enhance immunogenicity, PLoS Comput. Biol. 9 (2013) e1003266. https://doi.org/10.1371/journal.pcbi.1003266.
[111] I.A. Doytchinova, D.R. Flower, VaxiJen: a server for prediction of protective antigens, tumour antigens and subunit vaccines, BMC Bioinformatics 8 (2007) 4. https://doi.org/10.1186/1471-2105-8-4.
[112] S. Gupta, P. Kapoor, K. Chaudhary, A. Gautam, R. Kumar, Open Source Drug Discovery Consortium, G.P.S. Raghava, *In silico* approach for predicting toxicity of peptides and proteins, PloS One 8 (2013) e73957. https://doi.org/10.1371/journal.pone.0073957.
[113] N. Rapin, O. Lund, M. Bernaschi, F. Castiglione, Computational Immunology Meets Bioinformatics: The Use of Prediction Tools for Molecular Binding in the Simulation of the Immune System, PLOS ONE 5 (2010) e9862. https://doi.org/10.1371/journal.pone.0009862.
[114] A. Tamrakar, R. Singh, A. Kumar, R.D. Makde, Ashish, P. Kodgire, Biophysical characterization of the homodimers of HomA and HomB, outer membrane proteins of *Helicobacter pylori*, Sci. Rep. 11 (2021) 24471. https://doi.org/10.1038/s41598-021-04039-4.
[115] N. Noinaj, A.J. Kuszak, S.K. Buchanan, Heat Modifiability of Outer Membrane Proteins from Gram-Negative Bacteria, Methods Mol. Biol. Clifton NJ 1329 (2015) 51–56. https://doi.org/10.1007/978-1-4939-2871-2_4.
[116] Delivery of Yersinia pestis antigens via *Escherichia coli* outer membrane vesicles offered improved protection against plague, mSphere 9 (2024). https://doi.org/10.1128/msphere.00330-24.
[117] S.L. Reimer, D.R. Beniac, S.L. Hiebert, T.F. Booth, P.M. Chong, G.R. Westmacott, G.G. Zhanel, D.C. Bay, Comparative Analysis of Outer Membrane Vesicle Isolation Methods With an *Escherichia coli* tolA Mutant Reveals a Hypervesiculating Phenotype With Outer-Inner Membrane Vesicle Content, Front. Microbiol. 12 (2021) 628801. https://doi.org/10.3389/fmicb.2021.628801.

[118] J. Płaczkiewicz, K. Gieczewska, M. Musiałowski, M. Adamczyk-Popławska, P. Bącal, A. Kwiatek, Availability of iron ions impacts physicochemical properties and proteome of outer membrane vesicles released by *Neisseria gonorrhoeae*, Sci. Rep. 13 (2023) 18733. https://doi.org/10.1038/s41598-023-45498-1.
[119] D. Szöllősi, P. Hajdrik, H. Tordai, I. Horváth, D.S. Veres, B. Gillich, K.D. Shailaja, L. Smeller, R. Bergmann, M. Bachmann, J. Mihály, A. Gaál, B. Jezsó, B. Barátki, D. Kövesdi, S. Bősze, I. Szabó, T. Felföldi, E. Oszwald, P. Padmanabhan, B.Z. Gulyás, N. Hamdani, D. Máthé, Z. Varga, K. Szigeti, Molecular imaging of bacterial outer membrane vesicles based on bacterial surface display, Sci. Rep. 13 (2023) 18752. https://doi.org/10.1038/s41598-023-45628-9.
[120] M. Potter, C. Hanson, A.J. Anderson, E. Vargis, D.W. Britt, Abiotic stressors impact outer membrane vesicle composition in a beneficial rhizobacterium: Raman spectroscopy characterization, Sci. Rep. 10 (2020) 21289. https://doi.org/10.1038/s41598-020-78357-4.
[121] A. Maity, D. Bagchi, H. Tabassum, P. Nath, S. Sinha, A. Chakraborty, Diverse Role of Buffer Mediums and Protein Concentrations to Mediate the Multimodal Interaction of Phenylalanine-Functionalized Gold Nanoparticle and Lysozyme Protein at Same Nominal pH, J. Phys. Chem. B 128 (2024) 10625–10635. https://doi.org/10.1021/acs.jpcb.4c05463.
[122] W. Strober, Trypan Blue Exclusion Test of Cell Viability, Curr. Protoc. Immunol. 111 (2015) A3.B.1-A3.B.3. https://doi.org/10.1002/0471142735.ima03bs111.
[123] N.T.H. Nga, T.T.B. Ngoc, N.T.M. Trinh, T.L. Thuoc, D.T.P. Thao, Optimization and application of MTT assay in determining density of suspension cells, Anal. Biochem. 610 (2020) 113937. https://doi.org/10.1016/j.ab.2020.113937.
[124] M. Nikbakht, B. Pakbin, G. Nikbakht Brujeni, Evaluation of a new lymphocyte proliferation assay based on cyclic voltammetry; an alternative method, Sci. Rep. 9 (2019) 4503. https://doi.org/10.1038/s41598-019-41171-8.
[125] J.A. Dahl, P. Collas, A rapid micro chromatin immunoprecipitation assay (microChIP), Nat. Protoc. 3 (2008) 1032–1045. https://doi.org/10.1038/nprot.2008.68.
[126] M.F. Carey, C.L. Peterson, S.T. Smale, Chromatin Immunoprecipitation (ChIP), Cold Spring Harb. Protoc. 2009 (2009) pdb.prot5279. https://doi.org/10.1101/pdb.prot5279.
[127] X. Lin, L. Tirichine, C. Bowler, Protocol: Chromatin immunoprecipitation (ChIP) methodology to investigate histone modifications in two model diatom species, Plant Methods 8 (2012) 48. https://doi.org/10.1186/1746-4811-8-48.
[128] X. Hu, H. Yan, K. Liu, J. Hu, C. Qi, J. Yang, Y. Liu, J. Zhao, J. Liu, Identification and characterization of a novel stress-responsive outer membrane protein Lip40 from *Actinobacillus pleuropneumoniae*, BMC Biotechnol. 15 (2015) 106. https://doi.org/10.1186/s12896-015-0199-8.
[129] J. Mambu, I. Virlogeux-Payant, S. Holbert, O. Grépinet, P. Velge, A. Wiedemann, An Updated View on the Rck Invasin of *Salmonella*: Still Much to Discover, Front. Cell. Infect. Microbiol. 7 (2017) 500. https://doi.org/10.3389/fcimb.2017.00500.

[130] A. Pautsch, G.E. Schulz, Structure of the outer membrane protein A transmembrane domain, Nat. Struct. Biol. 5 (1998) 1013–1017. https://doi.org/10.1038/2983.
[131] Y. Wang, The function of OmpA in *Escherichia coli*, Biochem. Biophys. Res. Commun. 292 (2002) 396–401. https://doi.org/10.1006/bbrc.2002.6657.
[132] A.W. Confer, S. Ayalew, The OmpA family of proteins: Roles in bacterial pathogenesis and immunity, Vet. Microbiol. 163 (2013) 207–222. https://doi.org/10.1016/j.vetmic.2012.08.019.
[133] A.R. Chowdhury, D. Mukherjee, A.K. Singh, D. Chakravortty, Loss of outer membrane protein A (OmpA) impairs the survival of *Salmonella* Typhimurium by inducing membrane damage in the presence of ceftazidime and meropenem, J. Antimicrob. Chemother. 77 (2022) 3376–3389. https://doi.org/10.1093/jac/dkac327.
[134] M. Mouhib, A. Benediktsdottir, C.S. Nilsson, C.N. Chi, Influence of Detergent and Lipid Composition on Reconstituted Membrane Proteins for Structural Studies, ACS Omega 6 (2021) 24377–24381. https://doi.org/10.1021/acsomega.1c02542.
[135] A.M. Seddon, P. Curnow, P.J. Booth, Membrane proteins, lipids and detergents: not just a soap opera, Biochim. Biophys. Acta BBA - Biomembr. 1666 (2004) 105–117. https://doi.org/10.1016/j.bbamem.2004.04.011.
[136] W. Chumjan, P. Wiboongun, K. Muangcham, A. Yimyuan, A. Tankrathok, Cloning, expression and purification of the outer membrane protein N from Gram-negative bacterial strains, Process Biochem. 131 (2023) 19–31. https://doi.org/10.1016/j.procbio.2023.05.033.
[137] S. Sukumaran, K. Hauser, E. Maier, R. Benz, W. Mäntele, Tracking the Unfolding and Refolding Pathways of Outer Membrane Protein Porin from *Paracoccus denitrificans*, Biochemistry 45 (2006) 3972–3980. https://doi.org/10.1021/bi052198b.
[138] A.P. Heuck, A.E. Johnson, Pore-forming protein structure analysis in membranes using multiple independent fluorescence techniques, Cell Biochem. Biophys. 36 (2002) 89–101. https://doi.org/10.1385/CBB:36:1:89.
[139] P. Broz, M.B. Ohlson, D.M. Monack, Innate immune response to *Salmonella typhimurium*, a model enteric pathogen, Gut Microbes 3 (2012) 62–70. https://doi.org/10.4161/gmic.19141.
[140] J. van der Heijden, L.A. Reynolds, W. Deng, A. Mills, R. Scholz, K. Imami, L.J. Foster, F. Duong, B.B. Finlay, *Salmonella* Rapidly Regulates Membrane Permeability To Survive Oxidative Stress, mBio 7 (2016) 10.1128/mbio.01238-16. https://doi.org/10.1128/mbio.01238-16.
[141] I. Bekeredjian-Ding, G. Jego, Toll-like receptors--sentries in the B-cell response, Immunology 128 (2009) 311–323. https://doi.org/10.1111/j.1365-2567.2009.03173.x.
[142] Y. Li, L. Liu, C. Xiao, B. Sun, S. Luo, D. Yang, X. Zhang, T. Huang, Z. Yu, X. Li, Outer membrane protein A of *Acinetobacter baumannii* regulates pulmonary inflammation through the TLR2-NF-κB pathway, Vet. Microbiol. 284 (2023) 109812. https://doi.org/10.1016/j.vetmic.2023.109812.
[143] X. He, J. Liu, K. Jiang, S. Lian, Y. Shi, S. Fu, P. Zhao, J. Xiao, D. Sun, D. Guo,

The outer membrane protein of *Fusobacterium necrophorum*, 43K OMP, stimulates inflammatory cytokine production through nuclear factor kappa B activation, Anaerobe 82 (2023) 102768. https://doi.org/10.1016/j.anaerobe.2023.102768.
[144] A.M.P. dos Santos, R.G. Ferrari, C.A. Conte-Junior, Virulence Factors in *Salmonella* Typhimurium: The Sagacity of a Bacterium, Curr. Microbiol. 76 (2019) 762–773. https://doi.org/10.1007/s00284-018-1510-4.
[145] E.B. Shanker, J. Sun, *Salmonella* infection acts as an environmental risk factor for human colon cancer, Cell Insight 2 (2023) 100125. https://doi.org/10.1016/j.cellin.2023.100125.
[146] M. Mirzarazi, S. Bashiri, A. Hashemi, M. Vahidi, B. Kazemi, M. Bandehpour, The OmpA of commensal *Escherichia coli* of CRC patients affects apoptosis of the HCT116 colon cancer cell line, BMC Microbiol. 22 (2022) 139. https://doi.org/10.1186/s12866-022-02540-y.
[147] H. Choi, M. Kim, J. Jeon, J.K. Han, K. Kim, Overexpression of MicA induces production of OmpC-enriched outer membrane vesicles that protect against *Salmonella* challenge, Biochem. Biophys. Res. Commun. 490 (2017) 991–996. https://doi.org/10.1016/j.bbrc.2017.06.152.
[148] M.-H. Tsai, Y.-H. Liang, C.-L. Chen, C.-H. Chiu, Characterization of *Salmonella* resistance to bile during biofilm formation, J. Microbiol. Immunol. Infect. 53 (2020) 518–524. https://doi.org/10.1016/j.jmii.2019.06.003.
[149] J. van der Heijden, L.A. Reynolds, W. Deng, A. Mills, R. Scholz, K. Imami, L.J. Foster, F. Duong, B.B. Finlay, *Salmonella* Rapidly Regulates Membrane Permeability To Survive Oxidative Stress, mBio 7 (2016) 10.1128/mbio.01238-16. https://doi.org/10.1128/mbio.01238-16.
[150] E.J. Pone, H. Zan, J. Zhang, A. Al-Qahtani, Z. Xu, P. Casali, Toll-like Receptors and B-cell Receptors Synergize to Induce Immunoglobulin Class Switch DNA Recombination: Relevance to Microbial Antibody Responses, Crit. Rev. Immunol. 30 (2010) 1–29.
[151] E. Çakan, G. Gunaydin, Activation induced cytidine deaminase: An old friend with new faces, Front. Immunol. 13 (2022). https://www.frontiersin.org/articles/10.3389/fimmu.2022.965312 (accessed September 26, 2023).
[152] R. Nakagawa, D.P. Calado, Positive Selection in the Light Zone of Germinal Centers, Front. Immunol. 12 (2021) 661678. https://doi.org/10.3389/fimmu.2021.661678.
[153] E.E. Crouch, Z. Li, M. Takizawa, S. Fichtner-Feigl, P. Gourzi, C. Montaño, L. Feigenbaum, P. Wilson, S. Janz, F.N. Papavasiliou, R. Casellas, Regulation of AID expression in the immune response, J. Exp. Med. 204 (2007) 1145–1156. https://doi.org/10.1084/jem.20061952.
[154] H. Zan, P. Casali, Regulation of Aicda expression and AID activity, Autoimmunity 46 (2013) 83–101. https://doi.org/10.3109/08916934.2012.749244.
[155] S.-R. Park, P.-H. Kim, K.-S. Lee, S.-H. Lee, G.-Y. Seo, Y.-C. Yoo, J. Lee, P. Casali, APRIL stimulates NF-κB-mediated HoxC4 induction for AID expression in mouse B cells, Cytokine 61 (2013) 608–613.

https://doi.org/10.1016/j.cyto.2012.10.018.
[156] X. Jiang, C. Chu, Z. Wang, J. Gu, Y. Hong, Q. Li, X. Jiao, Preclinical evaluation of OMVs as potential vaccine candidates against *Salmonella enterica* serovar Enteritidis infection, Front. Cell. Infect. Microbiol. 12 (2022) 1037607. https://doi.org/10.3389/fcimb.2022.1037607.
[157] F. Micoli, R. Adamo, U. Nakakana, Outer Membrane Vesicle Vaccine Platforms, Biodrugs 38 (2024) 47–59. https://doi.org/10.1007/s40259-023-00627-0.
[158] A.L. Carvalho, S. Fonseca, A. Miquel-Clopés, K. Cross, K.-S. Kok, U. Wegmann, K. Gil-Cardoso, E.G. Bentley, S.H.M. Al Katy, J.L. Coombes, A. Kipar, R. Stentz, J.P. Stewart, S.R. Carding, Bioengineering commensal bacteria-derived outer membrane vesicles for delivery of biologics to the gastrointestinal and respiratory tract, J. Extracell. Vesicles 8 (2019) 1632100. https://doi.org/10.1080/20013078.2019.1632100.
[159] M. Toyofuku, N. Nomura, L. Eberl, Types and origins of bacterial membrane vesicles, Nat. Rev. Microbiol. 17 (2019) 13–24. https://doi.org/10.1038/s41579-018-0112-2.
[160] E. Bartolini, E. Ianni, E. Frigimelica, R. Petracca, G. Galli, F. Berlanda Scorza, N. Norais, D. Laera, F. Giusti, A. Pierleoni, M. Donati, R. Cevenini, O. Finco, G. Grandi, R. Grifantini, Recombinant outer membrane vesicles carrying *Chlamydia muridarum* HtrA induce antibodies that neutralize chlamydial infection *in vitro*, J. Extracell. Vesicles 2 (2013) 20181. https://doi.org/10.3402/jev.v2i0.20181.
[161] M.L.A. Perez Vidakovics, J. Jendholm, M. Mörgelin, A. Månsson, C. Larsson, L.-O. Cardell, K. Riesbeck, B Cell Activation by Outer Membrane Vesicles—A Novel Virulence Mechanism, PLoS Pathog. 6 (2010) e1000724. https://doi.org/10.1371/journal.ppat.1000724.
[162] Rahul Chaudhari, Mallar Dasgupta, Prashant Kodgire, Unraveling the impact of Outer Membrane Protein, OmpA, from *S.* Typhimurium on aberrant AID expression and IgM to IgA class switching in human B-cells, Immunology (2025). https://doi.org/10.1111/imm.13938.
[163] L. Tamm, S. Tatulian, Infrared Spectroscopy of Proteins and Peptides in Lipid Bilayers, Q. Rev. Biophys. 30 (1997) 365–429. https://doi.org/10.1017/S0033583597003375.
[164] G. F, T. Ma, S. L, F. A, T. F, Activation of complement system by porins extracted from *Salmonella typhimurium*, PubMed (n.d.). https://pubmed.ncbi.nlm.nih.gov/6094352/ (accessed July 19, 2025).
[165] R. Richter, M.A.M. Kamal, M. Koch, B. Niebuur, A. Huber, A. Goes, C. Volz, J. Vergalli, T. Kraus, R. Müller, N. Schneider-Daum, G. Fuhrmann, J. Pagès, C. Lehr, An Outer Membrane Vesicle-Based Permeation Assay (OMPA) for Assessing Bacterial Bioavailability, Adv. Healthc. Mater. 11 (2022) 2101180. https://doi.org/10.1002/adhm.202101180.
[166] J.S. Park, W.C. Lee, K.J. Yeo, K.-S. Ryu, M. Kumarasiri, D. Hesek, M. Lee, S. Mobashery, J.H. Song, S.I. Kim, J.C. Lee, C. Cheong, Y.H. Jeon, H.-Y. Kim, Mechanism of anchoring of OmpA protein to the cell wall peptidoglycan of the gram-negative bacterial outer membrane, FASEB J. 26 (2012) 219–228.

https://doi.org/10.1096/fj.11-188425.
[167] E. Sugawara, H. Nikaido, Pore-forming activity of OmpA protein of *Escherichia coli*., J. Biol. Chem. 267 (1992) 2507–2511. https://doi.org/10.1016/S0021-9258(18)45908-X.
[168] E. Sugawara, H. Nikaido, OmpA protein of *Escherichia coli* outer membrane occurs in open and closed channel forms, J. Biol. Chem. 269 (1994) 17981–17987.
[169] K. Chandravanshi, R. Singh, A. Kumar, G.N. Bhange, A. Kumar, R.D. Makde, Structural adaptations for carboxypeptidase activity in putative S9 acylaminoacyl peptidase from *Bacillus subtilis*, Int. J. Biol. Macromol. 282 (2024) 136734. https://doi.org/10.1016/j.ijbiomac.2024.136734.
[170] M. J, P. A, R. D, M. Dp, W. Mi, T. Lk, R. Cv, Mass spectrometry defines the C-terminal dimerization domain and enables modeling of the structure of full-length OmpA, PubMed (2014). https://pubmed.ncbi.nlm.nih.gov/24746938/ (accessed July 22, 2025).
[171] B. H, F. Z, J.N. M, R. I, Anti-OmpA antibodies as potential inhibitors of *Acinetobacter baumannii* biofilm formation, adherence to, and proliferation in A549 human alveolar epithelial cells, PubMed (n.d.). https://pubmed.ncbi.nlm.nih.gov/38048840/ (accessed July 27, 2025).
[172] S. Galdiero, A. Falanga, M. Cantisani, R. Tarallo, M.E.D. Pepa, V. D'Oriano, M. Galdiero, Microbe-Host Interactions: Structure and Role of Gram-Negative Bacterial Porins, Curr. Protein Pept. Sci. 13 (2012) 843–854. https://doi.org/10.2174/138920312804871120.
[173] F. Jacob-Dubuisson, C. El-Hamel, N. Saint, S. Guédin, E. Willery, G. Molle, C. Locht, Channel Formation by FhaC, the Outer Membrane Protein Involved in the Secretion of the *Bordetella pertussis* Filamentous Hemagglutinin*, J. Biol. Chem. 274 (1999) 37731–37735. https://doi.org/10.1074/jbc.274.53.37731.
[174] S. Conlan, H. Bayley, Folding of a monomeric porin, OmpG, in detergent solution, Biochemistry 42 (2003) 9453–9465. https://doi.org/10.1021/bi0344228.
[175] N.K. Burgess, T.P. Dao, A.M. Stanley, K.G. Fleming, β-Barrel Proteins That Reside in the *Escherichia coli* Outer Membrane *in vivo* Demonstrate Varied Folding Behavior *in Vitro*, J. Biol. Chem. 283 (2008) 26748–26758. https://doi.org/10.1074/jbc.M802754200.
[176] J. Kong, S. Yu, Fourier transform infrared spectroscopic analysis of protein secondary structures, Acta Biochim. Biophys. Sin. 39 (2007) 549–559. https://doi.org/10.1111/j.1745-7270.2007.00320.x.
[177] N. Nagaratnam, J.M. Martin-Garcia, J.-H. Yang, M.R. Goode, G. Ketawala, F.M. Craciunescu, J.D. Zook, M. Sonowal, D. Williams, T.D. Grant, R. Fromme, D.T. Hansen, P. Fromme, Structural and biophysical properties of FopA, a major outer membrane protein of *Francisella tularensis*, PloS One 17 (2022) e0267370. https://doi.org/10.1371/journal.pone.0267370.
[178] A. Tamrakar, A. Singh, Fighting with Gram-negative enemy: Can outer membrane proteins aid in the rescue?, Chem. Biol. Lett. 2017,4(1) (2016) 9–19.
[179] E.J. Danoff, K.G. Fleming, The soluble, periplasmic domain of OmpA folds as an independent unit and displays chaperone activity by reducing the self-

association propensity of the unfolded OmpA transmembrane β-barrel, Biophys. Chem. 159 (2011) 194–204. https://doi.org/10.1016/j.bpc.2011.06.013.
[180] A. J. Miles, B. A. Wallace, Circular dichroism spectroscopy of membrane proteins, Chem. Soc. Rev. 45 (2016) 4859–4872. https://doi.org/10.1039/C5CS00084J.
[181] G. Rabbani, J. Kaur, E. Ahmad, R.H. Khan, S.K. Jain, Structural characteristics of thermostable immunogenic outer membrane protein from *Salmonella enterica* serovar Typhi, Appl. Microbiol. Biotechnol. 98 (2014) 2533–2543. https://doi.org/10.1007/s00253-013-5123-3.
[182] Z.O. Shenkarev, E.N. Lyukmanova, I.O. Butenko, L.E. Petrovskaya, A.S. Paramonov, M.A. Shulepko, O.V. Nekrasova, M.P. Kirpichnikov, A.S. Arseniev, Lipid–protein nanodiscs promote *in vitro* folding of transmembrane domains of multi-helical and multimeric membrane proteins, Biochim. Biophys. Acta BBA - Biomembr. 1828 (2013) 776–784. https://doi.org/10.1016/j.bbamem.2012.11.005.
[183] C.L. Hagan, S. Kim, D. Kahne, Reconstitution of Outer Membrane Protein Assembly from Purified Components, Science 328 (2010) 890–892. https://doi.org/10.1126/science.1188919.
[184] M. Alizadeh, H. Amini-Khoei, S. Tahmasebian, M. Ghatrehsamani, K. Ghatreh Samani, Y. Edalatpanah, S. Rostampur, M. Salehi, M. Ghasemi-Dehnoo, F. Azadegan-Dehkordi, S. Sanami, N. Bagheri, Designing a novel multi-epitope vaccine against Ebola virus using reverse vaccinology approach, Sci. Rep. 12 (2022) 7757. https://doi.org/10.1038/s41598-022-11851-z.
[185] J.A. Gaddy, A.P. Tomaras, L.A. Actis, The *Acinetobacter baumannii* 19606 OmpA Protein Plays a Role in Biofilm Formation on Abiotic Surfaces and in the Interaction of This Pathogen with Eukaryotic Cells, Infect. Immun. 77 (2009) 3150. https://doi.org/10.1128/IAI.00096-09.
[186] P. Jeannin, G. Magistrelli, L. Goetsch, J.-F. Haeuw, N. Thieblemont, J.-Y. Bonnefoy, Y. Delneste, Outer membrane protein A (OmpA): a new pathogen-associated molecular pattern that interacts with antigen presenting cells-impact on vaccine strategies, Vaccine 20 Suppl 4 (2002) A23-27. https://doi.org/10.1016/s0264-410x(02)00383-3.
[187] S.A. Kim, S.M. Yoo, S.H. Hyun, C.H. Choi, S.Y. Yang, H.J. Kim, B.C. Jang, S.I. Suh, J.C. Lee, Global gene expression patterns and induction of innate immune response in human laryngeal epithelial cells in response to *Acinetobacter baumannii* outer membrane protein A, FEMS Immunol. Med. Microbiol. 54 (2008) 45–52. https://doi.org/10.1111/j.1574-695X.2008.00446.x.
[188] L.L. Nesse, K. Berg, L.K. Vestby, I. Olsaker, B. Djønne, *Salmonella* Typhimurium invasion of HEp-2 epithelial cells *in vitro* is increased by N-acylhomoserine lactone quorum sensing signals, Acta Vet. Scand. 53 (2011) 44. https://doi.org/10.1186/1751-0147-53-44.
[189] C.H. Choi, E.Y. Lee, Y.C. Lee, T.I. Park, H.J. Kim, S.H. Hyun, S.A. Kim, S.-K. Lee, J.C. Lee, Outer membrane protein 38 of *Acinetobacter baumannii* localizes to the mitochondria and induces apoptosis of epithelial cells, Cell. Microbiol. 7 (2005) 1127–1138. https://doi.org/10.1111/j.1462-5822.2005.00538.x.

[190] H.S. You, S.H. Lee, S.S. Kang, S.H. Hyun, OmpA of *Klebsiella pneumoniae* ATCC 13883 induces pyroptosis in HEp-2 cells, leading to cell-cycle arrest and apoptosis, Microbes Infect. 22 (2020) 432–440. https://doi.org/10.1016/j.micinf.2020.06.002.
[191] P.A. Singer, A.R. Williamson, Cell surface immunoglobulin μ and γ chains of human lymphoid cells are of higher apparent molecular weight than their secreted counterparts, Eur. J. Immunol. 10 (1980) 180–186. https://doi.org/10.1002/eji.1830100305.
[192] M. Gururajan, C.D. Jennings, S. Bondada, Cutting Edge: Constitutive B Cell Receptor Signaling Is Critical for Basal Growth of B Lymphoma1, J. Immunol. 176 (2006) 5715–5719. https://doi.org/10.4049/jimmunol.176.10.5715.
[193] K. Van Belle, J. Herman, L. Boon, M. Waer, B. Sprangers, T. Louat, Comparative *In Vitro* Immune Stimulation Analysis of Primary Human B Cells and B Cell Lines, J. Immunol. Res. 2016 (2016) 5281823. https://doi.org/10.1155/2016/5281823.
[194] R. Caeser, M. Di Re, J.A. Krupka, J. Gao, M. Lara-Chica, J.M.L. Dias, S.L. Cooke, R. Fenner, Z. Usheva, H.F.P. Runge, P.A. Beer, H. Eldaly, H.-K. Pak, C.-S. Park, G.S. Vassiliou, B.J.P. Huntly, A. Mupo, R.J.M. Bashford-Rogers, D.J. Hodson, Genetic modification of primary human B cells to model high-grade lymphoma, Nat. Commun. 10 (2019) 4543. https://doi.org/10.1038/s41467-019-12494-x.
[195] W. Zhang, H. Zhou, Y. Jiang, J. He, Y. Yao, J. Wang, X. Liu, S. Leptihn, X. Hua, Y. Yu, *Acinetobacter baumannii* Outer Membrane Protein A Induces Pulmonary Epithelial Barrier Dysfunction and Bacterial Translocation Through The TLR2/IQGAP1 Axis, Front. Immunol. 13 (2022) 927955. https://doi.org/10.3389/fimmu.2022.927955.
[196] J. Holze, F. Lauber, S. Soler, E. Kostenis, G. Weindl, Label-free biosensor assay decodes the dynamics of Toll-like receptor signaling, Nat. Commun. 15 (2024) 9554. https://doi.org/10.1038/s41467-024-53770-9.
[197] G.-F. Yang, C.-S. Deng, Y.-Y. Xiong, L.-L. Gong, B.-C. Wang, J. Luo, Expression of nuclear factor-kappa B and target genes in gastric precancerous lesions and adenocarcinoma: Association with *Helicobactor pylori cagA* (+) infection, World J. Gastroenterol. 10 (2004) 491–496. https://doi.org/10.3748/wjg.v10.i4.491.
[198] A. Takahashi-Kanemitsu, C.T. Knight, M. Hatakeyama, Molecular anatomy and pathogenic actions of *Helicobacter pylori* CagA that underpin gastric carcinogenesis, Cell. Mol. Immunol. 17 (2020) 50–63. https://doi.org/10.1038/s41423-019-0339-5.
[199] C.V. Srikanth, B.J. Cherayil, Intestinal Innate Immunity and the Pathogenesis of *Salmonella* Enteritis, Immunol. Res. 37 (2007) 61–78.
[200] A. Takaya, T. Yamamoto, K. Tokoyoda, Humoral Immunity vs. *Salmonella*, Front. Immunol. 10 (2020) 3155. https://doi.org/10.3389/fimmu.2019.03155.
[201] R.V. Luckheeram, R. Zhou, A.D. Verma, B. Xia, CD4+T Cells: Differentiation and Functions, Clin. Dev. Immunol. 2012 (2012) 925135. https://doi.org/10.1155/2012/925135.
[202] Y. Souwer, A. Griekspoor, J. de Wit, C. Martinoli, E. Zagato, H. Janssen, T.

Jorritsma, Y.E. Bar-Ephraïm, M. Rescigno, J. Neefjes, S.M. van Ham, Selective Infection of Antigen-Specific B Lymphocytes by *Salmonella* Mediates Bacterial Survival and Systemic Spreading of Infection, PLOS ONE 7 (2012) e50667. https://doi.org/10.1371/journal.pone.0050667.

[203] T. Nojima, K. Haniuda, T. Moutai, M. Matsudaira, S. Mizokawa, I. Shiratori, T. Azuma, D. Kitamura, In-vitro derived germinal centre B cells differentially generate memory B or plasma cells *in vivo*, Nat. Commun. 2 (2011) 465. https://doi.org/10.1038/ncomms1475.

[204] Y. Takahama, S. Ono, K. Ishihara, T. Hamaoka, Cluster formation among small resting B lymphocytes leading to B cell activation, Int. Immunol. 1 (1989) 36–42. https://doi.org/10.1093/intimm/1.1.36.

[205] B. Hat, B. Kazmierczak, T. Lipniacki, B Cell Activation Triggered by the Formation of the Small Receptor Cluster: A Computational Study, PLOS Comput. Biol. 7 (2011) e1002197. https://doi.org/10.1371/journal.pcbi.1002197.

[206] N. Kushnir, L. Liu, G.G. MacPherson, Dendritic Cells and Resting B Cells Form Clusters *In Vitro* and *In Vivo*: T Cell Independence, Partial LFA-1 Dependence, and Regulation by Cross-Linking Surface Molecules1, J. Immunol. 160 (1998) 1774–1781. https://doi.org/10.4049/jimmunol.160.4.1774.

[207] J. Stavnezer, Complex regulation and function of activation-induced cytidine deaminase, Trends Immunol. 32 (2011) 194–201. https://doi.org/10.1016/j.it.2011.03.003.

[208] T.H. Tran, M. Nakata, K. Suzuki, N.A. Begum, R. Shinkura, S. Fagarasan, T. Honjo, H. Nagaoka, B cell–specific and stimulation-responsive enhancers derepress Aicda by overcoming the effects of silencers, Nat. Immunol. 11 (2010) 148–154. https://doi.org/10.1038/ni.1829.

[209] D. Mechtcheriakova, M. Svoboda, A. Meshcheryakova, E. Jensen-Jarolim, Activation-induced cytidine deaminase (AID) linking immunity, chronic inflammation, and cancer, Cancer Immunol. Immunother. CII 61 (2012) 1591–1598. https://doi.org/10.1007/s00262-012-1255-z.

[210] L. Marcano-Bonilla, E.A. Mohamed, T. Mounajjed, L.R. Roberts, Biliary tract cancers: epidemiology, molecular pathogenesis and genetic risk associations, Chin. Clin. Oncol. 5 (2016) 61. https://doi.org/10.21037/cco.2016.10.09.

[211] L. Zha, S. Garrett, J. Sun, *Salmonella* Infection in Chronic Inflammation and Gastrointestinal Cancer, Diseases 7 (2019) 28. https://doi.org/10.3390/diseases7010028.

[212] L. Mughini-Gras, M. Schaapveld, J. Kramers, S. Mooij, E.A. Neefjes-Borst, W. van Pelt, J. Neefjes, Increased colon cancer risk after severe *Salmonella* infection, PloS One 13 (2018) e0189721. https://doi.org/10.1371/journal.pone.0189721.

[213] X. Liu, R. Lu, S. Wu, J. Sun, *Salmonella* regulation of intestinal stem cells through the Wnt/β-catenin pathway, FEBS Lett. 584 (2010) 911–916. https://doi.org/10.1016/j.febslet.2010.01.024.

[214] T.N. Ellis, M.J. Kuehn, Virulence and immunomodulatory roles of bacterial outer membrane vesicles, Microbiol. Mol. Biol. Rev. MMBR 74 (2010) 81–94. https://doi.org/10.1128/MMBR.00031-09.

[215] K. Tan, R. Li, X. Huang, Q. Liu, Outer Membrane Vesicles: Current Status and Future Direction of These Novel Vaccine Adjuvants, Front. Microbiol. 9 (2018) 783. https://doi.org/10.3389/fmicb.2018.00783.
[216] Q. Liu, B. Li, J. Lu, Y. Zhang, Y. Shang, Y. Li, T. Gong, C. Zhang, Recombinant outer membrane vesicles delivering eukaryotic expression plasmid of cytokines act as enhanced adjuvants against *Helicobacter pylori* infection in mice, Infect. Immun. 91 (2023) e0031323. https://doi.org/10.1128/iai.00313-23.
[217] H. Zhang, Z. Liu, Y. Li, Z. Tao, L. Shen, Y. Shang, X. Huang, Q. Liu, Adjuvants for *Helicobacter pylori* vaccines: Outer membrane vesicles provide an alternative strategy, Virulence 15 (2024) 2425773. https://doi.org/10.1080/21505594.2024.2425773.
[218] Z. Song, B. Li, Y. Zhang, R. Li, H. Ruan, J. Wu, Q. Liu, Outer Membrane Vesicles of *Helicobacter pylori* 7.13 as Adjuvants Promote Protective Efficacy Against *Helicobacter pylori* Infection, Front. Microbiol. 11 (2020) 1340. https://doi.org/10.3389/fmicb.2020.01340.
[219] J.E. Harrell, J.R. Kurtz, D.L. Bauer, J.T. Prior, P.S. Gellings, L.A. Morici, J.B. McLachlan, An Outer Membrane Vesicle-Adjuvanted Oral Vaccine Protects Against Lethal, Oral *Salmonella* Infection, Pathogens 10 (2021) 616. https://doi.org/10.3390/pathogens10050616.
[220] R.C. Alaniz, B.L. Deatherage, J.C. Lara, B.T. Cookson, Membrane Vesicles Are Immunogenic Facsimiles of *Salmonella typhimurium* That Potently Activate Dendritic Cells, Prime B and T Cell Responses, and Stimulate Protective Immunity *In Vivo*1, J. Immunol. 179 (2007) 7692–7701. https://doi.org/10.4049/jimmunol.179.11.7692.
[221] J. Thoma, S. Manioglu, D. Kalbermatter, P.D. Bosshart, D. Fotiadis, D.J. Müller, Protein-enriched outer membrane vesicles as a native platform for outer membrane protein studies, Commun. Biol. 1 (2018) 1–9. https://doi.org/10.1038/s42003-018-0027-5.
[222] M.J. Kuehn, N.C. Kesty, Bacterial outer membrane vesicles and the host-pathogen interaction, Genes Dev. 19 (2005) 2645–2655. https://doi.org/10.1101/gad.1299905.
[223] D. Pore, N. Mahata, A. Pal, M.K. Chakrabarti, Outer Membrane Protein A (OmpA) of *Shigella flexneri* 2a, Induces Protective Immune Response in a Mouse Model, PLoS ONE 6 (2011) e22663. https://doi.org/10.1371/journal.pone.0022663.
[224] S. Krishnan, N.V. Prasadarao, Outer membrane protein A and OprF: versatile roles in Gram-negative bacterial infections, FEBS J. 279 (2012) 919–931. https://doi.org/10.1111/j.1742-4658.2012.08482.x.
[225] S. Won, C. Lee, S. Bae, J. Lee, D. Choi, M. Kim, S. Song, J. Lee, E. Kim, H. Shin, A. Basukala, T.R. Lee, D. Lee, Y.S. Gho, Mass-produced gram-negative bacterial outer membrane vesicles activate cancer antigen-specific stem-like CD8+ T cells which enables an effective combination immunotherapy with anti-PD-1, J. Extracell. Vesicles 12 (2023) 12357. https://doi.org/10.1002/jev2.12357.
[226] J. Skerniškytė, E. Karazijaitė, A. Lučiūnaitė, E. Sužiedėlienė, OmpA Protein-Deficient *Acinetobacter baumannii* Outer Membrane Vesicles Trigger Reduced

Inflammatory Response, Pathogens 10 (2021) 407. https://doi.org/10.3390/pathogens10040407.
[227] A.K. Singh, A. Tamrakar, A. Jaiswal, N. Kanayama, P. Kodgire, SRSF1-3, a splicing and somatic hypermutation regulator, controls transcription of *Ig*V genes via chromatin regulators SATB2, UBN1 and histone variant H3.3, Mol. Immunol. 119 (2020) 69–82. https://doi.org/10.1016/j.molimm.2020.01.005.
[228] H. Zan, P. Casali, Regulation of Aicda expression and AID activity, Autoimmunity 46 (2013) 83–101. https://doi.org/10.3109/08916934.2012.749244.
[229] Z. Xu, E.J. Pone, A. Al-Qahtani, S.-R. Park, H. Zan, P. Casali, Regulation of aicda expression and AID activity: Relevance to somatic hypermutation and class switch DNA recombination, Crit. Rev. Immunol. 27 (2007) 367–397.
[230] B. Nadalian, B. Nadalian, M.R. Zali, A. Yadegar, Outer Membrane Vesicles Derived from Adherent-Invasive *Escherichia coli* Induce Inflammatory Response and Alter the Gene Expression of Junction-Associated Proteins in Human Intestinal Epithelial Cells, Can. J. Infect. Dis. Med. Microbiol. 2024 (2024) 2701675. https://doi.org/10.1155/2024/2701675.
[231] A. Merino-Vico, J.P. van Hamburg, P. Tuijnenburg, G. Frazzei, A. Al-Soudi, C.G. Bonasia, B. Helder, A. Rutgers, W.H. Abdulahad, C.A. Stegeman, J.-S. Sanders, L. Bergamaschi, P.A. Lyons, T. Bijma, L. van Keep, K. Wesenhagen, A. Jongejan, H. Olsson, N. de Vries, T.W. Kuijpers, P. Heeringa, S.W. Tas, Targeting NF-κB signaling in B cells as a potential new treatment modality for ANCA-associated vasculitis, J. Autoimmun. 142 (2024) 103133. https://doi.org/10.1016/j.jaut.2023.103133.
[232] Y. Endo, H. Marusawa, K. Kinoshita, T. Morisawa, T. Sakurai, I.-M. Okazaki, K. Watashi, K. Shimotohno, T. Honjo, T. Chiba, Expression of activation-induced cytidine deaminase in human hepatocytes via NF-κB signaling, Oncogene 26 (2007) 5587–5595. https://doi.org/10.1038/sj.onc.1210344.